



National Library  
of Canada

Bibliothèque nationale  
du Canada

Canadian Theses Service

Service des thèses canadiennes

Ottawa, Canada  
K1A 0N4

## NOTICE

The quality of this microform is heavily dependent upon the quality of the original thesis submitted for microfilming. Every effort has been made to ensure the highest quality of reproduction possible.

If pages are missing, contact the university which granted the degree.

Some pages may have indistinct print especially if the original pages were typed with a poor typewriter ribbon or if the university sent us an inferior photocopy.

Reproduction in full or in part of this microform is governed by the Canadian Copyright Act, R.S.C. 1970, c. C-30, and subsequent amendments.

## AVIS

La qualité de cette microforme dépend grandement de la qualité de la thèse soumise au microfilmage. Nous avons tout fait pour assurer une qualité supérieure de reproduction.

S'il manque des pages, veuillez communiquer avec l'université qui a conféré le grade.

La qualité d'impression de certaines pages peut laisser à désirer, surtout si les pages originales ont été dactylographiées à l'aide d'un ruban usé ou si l'université nous a fait parvenir une photocopie de qualité inférieure.

La reproduction, même partielle, de cette microforme est soumise à la Loi canadienne sur le droit d'auteur, SRC 1970, c. C-30, et ses amendements subséquents.

UNIVERSITY OF ALBERTA

PARAMETRIC SENSITIVITY OF TUBULAR REACTORS:  
AN EXPERIMENTAL STUDY INVOLVING THE OXIDATION OF SODIUM SULFITE  
BY HYDROGEN PEROXIDE

BY

Luigi Ciro Boccanfuso



A THESIS

SUBMITTED TO THE FACULTY OF GRADUATE STUDIES AND RESEARCH  
IN PARTIAL FULFILLMENT OF THE REQUIREMENTS FOR THE DEGREE  
OF MASTER OF SCIENCE

DEPARTMENT OF CHEMICAL ENGINEERING

EDMONTON, ALBERTA

FALL 1990



**National Library  
of Canada**

**Bibliothèque nationale  
du Canada**

**Canadian Theses Service    Service des thèses canadiennes**

**Ottawa, Canada:  
K1A 0N4**

**The author has granted an irrevocable non-exclusive licence allowing the National Library of Canada to reproduce, loan, distribute or sell copies of his/her thesis by any means and in any form or format, making this thesis available to interested persons.**

**The author retains ownership of the copyright in his/her thesis. Neither the thesis nor substantial extracts from it may be printed or otherwise reproduced without his/her permission.**

**L'auteur a accordé une licence irrévocable et non exclusive permettant à la Bibliothèque nationale du Canada de reproduire, prêter, distribuer ou vendre des copies de sa thèse de quelque manière et sous quelque forme que ce soit pour mettre des exemplaires de cette thèse à la disposition des personnes intéressées.**

**L'auteur conserve la propriété du droit d'auteur qui protège sa thèse. Ni la thèse ni des extraits substantiels de celle-ci ne doivent être imprimés ou autrement reproduits sans son autorisation.**

**ISBN 0-315-65084-2**

UNIVERSITY OF ALBERTA

RELEASE FORM

NAME OF AUTHOR: Luigi Ciro Boccanfuso

TITLE OF THESIS: PARAMETRIC SENSITIVITY OF TUBULAR  
REACTORS: AN EXPERIMENTAL STUDY  
INVOLVING THE OXIDATION OF SODIUM  
SULFITE BY HYDROGEN PEROXIDE

DEGREE: MASTER OF SCIENCE

YEAR THIS DEGREE GRANTED: FALL 1990

PERMISSION IS HEREBY GRANTED TO THE UNIVERSITY OF ALBERTA LIBRARY  
TO REPRODUCE SINGLE COPIES OF THIS THESIS AND TO LEND OR SELL SUCH  
COPIES FOR PRIVATE, SCHOLARLY OR SCIENTIFIC RESEARCH PURPOSES ONLY.

THE AUTHOR RESERVES OTHER PUBLICATION RIGHTS, AND NEITHER THE  
THESIS NOR EXTENSIVE EXTRACTS FROM IT MAY BE PRINTED OR OTHERWISE  
REPRODUCED WITHOUT THE AUTHOR'S WRITTEN PERMISSION.

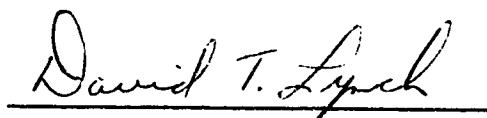
Luigi Boccanfuso  
#306, 10101 Saskatchewan Dr  
Edmonton, Alta  
T6E 4R6

Date: October 12th, 1990

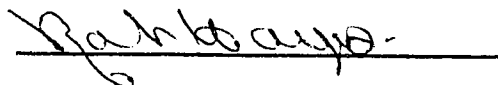


UNIVERSITY OF ALBERTA  
FACULTY OF GRADUATE STUDIES AND RESEARCH

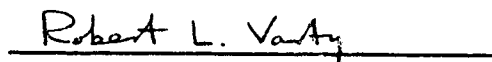
The undersigned certify that they have read, and recommend to the Faculty of Graduate Studies and Research, for acceptance, a thesis entitled PARAMETRIC SENSITIVITY OF TUBULAR REACTORS: AN EXPERIMENTAL STUDY INVOLVING THE OXIDATION OF SODIUM SULFITE BY HYDROGEN PEROXIDE, submitted by Luigi Ciro Boccanfuso in partial fulfillment of the requirements for the degree of MASTER OF SCIENCE in CHEMICAL ENGINEERING



Dr. D.T. Lynch



Dr. R.E. Hayes



Dr. R.L. Varty

Date : October 9, 1990

### ABSTRACT

The oxidation of sodium sulfite ( $\text{Na}_2\text{SO}_3$ ) by hydrogen peroxide ( $\text{H}_2\text{O}_2$ ) was studied using a 0.175 cm diameter tubular reactor. The reactor was constructed of type 304 stainless steel tubing with type J thermocouples inserted at 29 cm intervals for temperature monitoring. For cooling purposes, the reactor was immersed in an isothermal water bath. The observed axial temperature profiles were compared with both an ODPH (One Dimensional Pseudo Homogeneous) and TDPH (Two Dimensional Pseudo Homogeneous) reactor model. It was determined that, although both models predicted the basic features of the temperature profiles, they overestimated the value of the observed hot-spot. The ODPH model, with an appropriate fine tuning of the Arrhenius parameters, was found to be able to predict accurately the value of the hot-spot for those temperature profiles which were both heat transfer and reaction rate controlled.

Parametric sensitivity of the hot-spot temperature with respect to three operating parameters was examined. These parameters were the inlet feed temperature, the coolant temperature and the inlet sulfite concentration. A qualitative examination of the effect of changes in value of the overall heat transfer coefficient was also performed. The data obtained were used to evaluate five existing parametric sensitivity criteria (Barkelew (1959), Van Welsenaere and Froment (1970), Oroskar and Stern (1979), Morbidelli and Varma (1982) and Akella and Lee (1983)). The criteria were found to be generally quite

conservative. The criterion developed by Barkelew, which is illustrated in the form of sensitivity diagrams, was found to be the most useful.

An experimental study of the kinetic parameters of the oxidation of sodium sulfite by hydrogen peroxide in a phosphate buffer (pH = 10.0) was also performed. The values determined for the Arrhenius parameters were 64,268 J/mol for the activation energy and  $3.56 \cdot 10^{10}$  L/(mol·s) for the pre-exponential factor.

### ACKNOWLEDGEMENTS

To acknowledge everyone who helped me out in any way would take quite some time. However, to say simply, "thanks to everyone who helped", would be a disservice to each of them. Therefore, thank you ---

To my parents - for their patience, love and support during these last three years

To the rest of my family - for just keeping in touch and being there when I was home for a visit

To Jane - for being my first friend in Alberta

To Andrew, Doug and Ian - for keeping in touch (with E-Mail it was just like the good ol days at U of T!)

To Don - for helping me find that little "off-the-wall" part of me that I always suspected I had

To Paul - for putting up with me under the same roof for one year and for making sure my car always worked

To Lyle - for helping me move (how many times was it?) and teaching me the importance of taking computer bridge breaks

To Dave - for introducing me to the cuisine of chicken wings (my stomach may never be the same again!)

To Keith, Ron, Bob and John - for building my equipment for me and showing a lot of patience when I requested successively shorter lengths of tubing

To Laurie - for always lending an ear when I needed someone to talk to

To Don, Alan and Walter - for making sure that I could always get by with my "I don't know, I just turn it on and it works" knowledge of electricity

To Greg - for introducing me to a "real" (i.e., one that is played in the rain and the cold) American game

To Andrée - for obtaining all my chemicals for me and for not flinching when I asked for 150 kg of sodium sulfite

To Paula - for letting me borrow countless pieces of lab equipment (I hope you didn't keep track and expect them all returned)

To Bob - for keeping Curly alive just long enough for me to acquire all my data and plot all my figures

To Wendy - for showing me the importance of being your own person

To Shelley - for showing me that life is not just what you are given, it's also what you decide to do with it

To Dr Reid - for cimetidine (my stomach and I both thank you)

To Audrey, Mildred and Bev - for sharing extra pieces of birthday cake and other assorted goodies (read Cookie Day!)

To Christine - for teaching me that true happiness is: a peanut butter and vegemite sandwich, a stuffed tiger and a good *Calvin and Hobbes* comic book (and for being such a sweetheart and putting up with me the last few weeks)

To Paul & Wendy & Rayna - for being my substitute family whenever I needed one

To Bob, Chris, Henry, Don, Dave and everyone else who was part of the  
"Get Luigi's Thesis Finished By Fall Convocation Deadline" project -  
(\$)400 thank-yous!!!

To my supervisor, David Lynch - for all his help and encouragement  
throughout these three years (and for not once ever mentioning that it  
actually took me three years to finish!)

## TABLE OF CONTENTS

Chapter	Page
1.0 Introduction.....	1
2.0 Literature Survey.....	4
3.0 Selection of Reaction System.....	14
3.1 Reaction Selection.....	14
3.2 Reactor Design.....	17
3.3 Computer Simulation of Proposed Reactor.....	19
3.4 Determination of Kinetic Parameters.....	32
3.4.1 Adiabatic Batch Reactor System.....	37
3.4.2 Adiabatic Batch Reactor Results.....	38
4.0 Experimental Tubular Reactor System.....	45
4.1 Experimental Procedure.....	49
4.2 Experimental Heat Transfer Evaluation.....	52
5.0 Experimental Tubular Reactor-Characterization of Heat Transfer	55
5.1 Heat Transfer Coefficient Determination.....	55
6.0 Experimental Tubular Reactor - Results and Discussion.....	67
6.1 Experimental Tubular Reactor - Transient Data.....	67
6.2 Experimental Tubular Reactor - Variation of Inlet Temperature.....	69
6.3 Experimental Tubular Reactor - Variation of Sulfite Concentration.....	74
6.4 Experimental Tubular Reactor - Variation of Overall Heat Transfer Coefficient.....	90

7.0 Comparison of Experimental Data With Reactor Models.....	98
7.1 Comparison of Experimental Data With Reactor Models- Determination of Most Appropriate Parameter Fit.....	124
8.0 Experimental Tubular Reactor - Evaluation of Parametric Sensitivity.....	134
8.1 Parametric Sensitivity - Extraction of Critical Conditions.....	141
9.0 Parametric Sensitivity - Evaluation of Existing Criteria.....	154
9.1 Evaluation of the Criterion of Barkelew.....	154
9.2 Evaluation of the Criterion of Van Welsenaere and Froment.....	157
9.3 Evaluation of the Criterion of Oroskar and Stern....	162
9.4 Evaluation of the Criterion of Morbidelli and Varma.	163
9.5 Evaluation of the Criterion of Akella and Lee.....	164
9.6 Criterion Selection.....	165
Conclusions.....	169
References.....	171
Appendix A.....	176
Appendix B.....	198
Appendix C.....	204
Appendix D.....	280
Appendix E.....	304
Appendix F.....	313
Appendix G.....	344



## LIST OF TABLES

Table	Page
3.1 Arrhenius Parameters For the Reaction $\text{Na}_2\text{SO}_3 + \text{H}_2\text{O}_2$ .....	44
4.1 List of Experimental Conditions.....	53
4.2 List of Heat Transfer Experiments.....	54
5.1 Overall Heat Transfer Coefficients.....	62
5.2 Bath Side Heat Transfer Coefficients Determined From ODPH Model.....	64
8.1 Parametrically Sensitive Conditions (Experimental).....	148
9.1 Parameter Values for Experimental Tubular Reactor.....	154
9.2 Summary of Barkelew Criterion.....	155
9.3 Summary of Barkelew Criterion with $T_c \neq T_o$ .....	156
9.4 Summary of Van Welsenaere and Froment Criterion.....	158
9.5 Summary of Results Using Van Welsenaere and Froment Criterion as Applied to all Experimental Conditions.....	160
9.6 Summary of Oroskar and Stern Criterion.....	163
9.7 Summary of Morbidelli and Varma Criterion.....	164

## LIST OF FIGURES

Figure	Page
3.1 Comparison of Adiabatic Profiles for Sulfite and Peroxide Reactions.....	22
3.2 Comparison of Tubing Sizes for Sulfite Reaction.....	24
3.3 Comparison of Inlet Peroxide Concentrations (Sulfite Reaction).	27
3.4 Determination of Sensitive Operating Conditions (Simulation)...	29
3.5 Effect of Arrhenius Parameters on Temperature Profile.....	30
3.6 Adiabatic Batch Reactor.....	36
3.7 Adiabatic Batch Reactor Data.....	39
3.8 Adiabatic Batch Reactor Data.....	40
3.9 Adiabatic Batch Reactor Data.....	41
3.10 Typical Arrhenius Plot with Adiabatic Batch Reactor Data.....	42
4.1 Experimental Apparatus Schematic.....	46
4.2 Top and Front Views of Tubular Reactor.....	47
5.1 Experimental Heat Transfer Data.....	58
5.2 Comparison of Heat Transfer Data with ODPH Model.....	59
5.3 Comparison of Heat Transfer Data with TDPH Model.....	60
6.1 Tubular Reactor - Transient Experimental Data.....	68
6.2 Tubular Reactor - Experimental Data.....	75
6.3 Experimental Data.....	76
6.4 Experimental Data.....	77
6.5 Experimental Data.....	78
6.6 Experimental Data.....	79
6.7 Experimental Data.....	80

6.8	Experimental Data.....	81
6.9	Experimental Data.....	82
6.10	Experimental Data.....	83
6.11	Temperature Readings at Reactor Inlet.....	84
6.12	Experimental Data.....	87
6.13	Experimental Data.....	88
6.14	Experimental Data.....	89
6.15	Experimental Data.....	95
6.16	Experimental Data.....	96
6.17	Experimental Data.....	97
7.1	Experimental Data Comparison with ODPH Model.....	101
7.2	Experimental Data Comparison with TDPH Model.....	102
7.3	Experimental Data Comparison with ODPH Model.....	103
7.4	Experimental Data Comparison with TDPH Model.....	104
7.5	Experimental Data Comparison with ODPH and TDPH Models.....	106
7.6	Experimental Data Comparison with ODPH and TDPH Models.....	107
7.7	Experimental Data Comparison with ODPH and TDPH Models.....	108
7.8	Experimental Data Comparison with ODPH and TDPH Models.....	109
7.9	Experimental Data Comparison with ODPH and TDPH Models.....	110
7.10	Experimental Data Comparison with ODPH and TDPH Models.....	111
7.11	Experimental Data Comparison with ODPH and TDPH Models.....	112
7.12	Experimental Data Comparison with ODPH and TDPH Models.....	113
7.13	Experimental Data Comparison with ODPH and TDPH Models.....	114
7.14	Experimental Data Comparison with ODPH and TDPH Models.....	115
7.15	Experimental Data Comparison with ODPH and TDPH Models.....	116

7.16	Experimental Data Comparison with ODPH and TDPH Models.....	117
7.17	Experimental Data Comparison with ODPH Model.....	120
7.18	Experimental Data Comparison with ODPH Model.....	121
7.19	Experimental Data Comparison with ODPH Model.....	122
7.20	Experimental Data Comparison with TDPH Model.....	123
7.21	Determination of Optimal Arrhenius Parameters.....	126
7.22	Arrhenius Plot using all Adiabatic Batch Reactor Data.....	127
7.23	Experimental Data Comparison with ODPH Model using Optimal Arrhenius Parameters.....	128
7.24	Experimental Data Comparison with ODPH Model using Optimal Arrhenius Parameters.....	129
7.25	Experimental Data Comparison with ODPH Model using Optimal Arrhenius Parameters.....	130
8.1	Experimental Data.....	135
8.2	Experimental Data.....	136
8.3	Experimental Data.....	137
8.4	Experimental Data.....	138
8.5	Experimental Data.....	139
8.6	Experimental Data.....	140
8.7	Sensitivity Analysis.....	143
8.8	Sensitivity Analysis.....	144
8.9	Sensitivity Analysis.....	145
8.10	Experimentally Determined Critical Points.....	149
8.11	Experimentally Determined Critical Points.....	150
8.12	Sensitivity Plot for Fixed Inlet Concentration.....	152
9.1	Phase Plane Analysis for Sulfite Reaction As Per Akella and Lee.....	166

## NOMENCLATURE

- A - Arrhenius pre-exponential factor ( $L^{n-1}/(\text{mol}^{n-1}\cdot\text{s})$ ), also parameter grouping as defined by Van Welsenaere and Froment
- $a_1, a_2, a_3$  and  $a_4$  - parameter groupings as defined by Akella and Lee
- $a$  -  $-E_A/T$  ( $J/(\text{mol}\cdot K)$ )
- B - parameter grouping as defined by Van Welsenaere and Froment
- $b$  -  $\ln(A)$
- C - parameter grouping as defined by Van Welsenaere and Froment
- $C^*$  - adjusted sodium sulfite concentration ( $= 89\cdot C_{Ao}$ ) ( $^{\circ}\text{C}$ )
- $C_A, C_B$  - concentrations of species A and B ( $\text{mol/L}$ )
- $C_A(t)$  - concentration of species A at time=t ( $\text{mol/L}$ )
- $C_A(0)$  - concentration of species A at time=0 ( $\text{mol/L}$ )
- $C_p$  - heat capacity ( $J/(\text{kg}\cdot K)$ )
- C.I. - confidence interval
- CSTR - continuous stirred tank reactor
- D - reactor diameter (m)
- $D_e$  - effective diffusivity ( $\text{m}^2/\text{s}$ )
- $E_A$  - activation energy ( $J/\text{mol}$ )
- ESS - Error Sum of Squares for linear regression
- f - Fanning friction factor
- g - acceleration due to gravity ( $\approx 9.81 \text{ m/s}^2$ )
- h - heat transfer coefficient ( $\text{W}/(\text{m}^2\cdot K)$ )
- k - reaction rate constant ( $L^{n-1}/(\text{mol}^{n-1}\cdot\text{s})$ )
- $k_f$  - thermal conductivity of reaction fluid ( $\text{W}/(\text{m}\cdot K)$ )
- $k_t$  - thermal conductivity of tubing material ( $\text{W}/(\text{m}\cdot K)$ )

$L_e$  - equivalent length of tubing (m)  
 $L$  - total length of reactor (m)  
 $mC_p$  - thermal capacity (J/K)  
 $N$  - parameter grouping as defined by Barkelew  
 $n$  - reaction order  
 $Nu$  - Nusselt number =  $h \cdot D / k_f$   
 $ODPH$  - one dimensional pseudo homogeneous reactor model  
 $ODHT$  - one dimensional heterogeneous reactor model  
 $O.D.$  - outside diameter (m)  
 $P$  - pressure (Pa)  
 $Pr$  - Prandtl number =  $C_p \cdot \mu / k_f$   
 $Q$  - flow rate (L/s)  
 $R_A$  - rate of reaction with respect to species A (mol/(L·s))  
 $Re$  - Reynolds number =  $(\rho \cdot u \cdot D) / \mu$   
 $R$  - universal gas constant  
 $r$  - radial coordinate (m)  
 $RTD$  - residence time distribution  
 $S$  - parameter grouping as defined by Barkelew  
 $T(t)$  - temperature at time =  $t$  ( $^{\circ}C$ )  
 $T(0)$  - temperature at time = 0 ( $^{\circ}C$ )  
 $T$  - temperature ( $^{\circ}C$ )  
 $TDPH$  - two dimensional pseudo homogeneous reactor model  
 $u$  - velocity (m/s)  
 $U$  - overall heat transfer coefficient ( $W/(m^2 \cdot K)$ )  
 $V$  - volume (L)

$W_f$  - energy loss due to friction (J/kg)

$X$  - reactant conversion

$x$  - rotameter tube scale reading

$z$  - axial coordinate (m)

### Subscripts

$c$  - coolant

$cr$  - critical

$f$  - final condition

$i$  - "inside", as in  $D_i$  = inside diameter, when used in finite difference equations it refers to the radial grid coordinate

$in$  - inlet

$j$  - axial grid coordinate

$lm$  - log mean

$max$  - maximum

$o$  - initial condition, when used with  $U$  or  $D$  it refers to the term "outside", as in  $D_o$  = outside diameter

$rxn$  - reaction

$T$  - total

$w$  - water

### Greek Symbols

$\alpha$  - parameter grouping as defined by Oroskar and Stern and Morbidelli and Varma, kinetic parameter =  $C_{Ac}/C_{Bo}$  as defined by Barkelew

$\beta$  - parameter grouping as defined by Oroskar and Stern and Morbidelli

and Varma

$$\gamma = E_A / (R \cdot T_c)$$

$\Delta H$  - heat of reaction (J/mol)

$\Delta P$  - pressure drop (Pa)

$\Delta r$  - radial step size

$\Delta t$  - wall thickness (m), or time increment (s)

$\Delta z$  - change in elevation of fluid (m), when used in finite difference equations it refers to the axial step size

$\mu$  - viscosity (Pa·s)

$\rho$  - density (kg/m<sup>3</sup>)

$$\tau = (T_o - T_c) / (T_c \cdot \gamma)$$



## 1.0 INTRODUCTION

Tubular fixed-bed catalytic reactors are used quite extensively in the chemical industry. These reactors, which consist of a long narrow tube filled with porous catalyst, are usually chosen to carry out catalytic, gas-phase, exothermic reactions (i.e., the hydrogenation of acetylene, the epoxidation of ethylene, the synthesis of vinyl acetate and the oxidation of orthoxylene). Because the reactions are exothermic, the temperature profile along the length of the reactor exhibits a maximum, commonly referred to as a "hot-spot". It has been noted that, under certain conditions, this "hot-spot" becomes very sensitive to small changes in the operating parameters of the system. For example, in some instances, a one degree increase in the value of the inlet temperature of the reactants can result in a ten or twenty degree increase in the value of the "hot-spot" temperature. This is sometimes referred to as "thermal runaway" because the temperature profile rapidly shifts from one steady-state to another.

This phenomenon is more accurately called "Parametric Sensitivity". It is related in nature to the problem of thermal explosion of solids, as well as to the entire field of stability theory. It is important to note, however, the distinction between instability and parametric sensitivity.

Instability refers to a steady state at which operation is not possible. At an unstable steady state at least one eigenvalue of the

Jacobian matrix has a positive real part. (The Jacobian matrix is the matrix defined by the partial derivatives  $[\partial F_i / \partial x_j]$ , for  $i=1, I$  and  $j=1, J]$  where  $F_i$  are the dependent variables of the system and  $x_j$  are the independent variables.) Thus any perturbation from the steady state results in divergence from the steady state. The system then either moves to another steady state or, begins to oscillate. It is important to note that in the usual sense, instability refers to a situation where the operating conditions (the system parameters) are constant. Tubular reactors which are parametrically sensitive are not unstable in this sense. Instead, the temperature profile merely shifts from one steady state to another in response to a change in one or more of the operating parameters. Thus, the reactor is always stable, although the final steady state may not be desirable.

Parametric sensitivity still presents a problem because the increase in the value of the hot-spot temperature can be dramatic. This increased temperature can have serious effects on the reactor. For example, a catalyst can be damaged if the temperature increase is excessive. In some cases the increased temperature can result in the onset of an undesired side reaction or, cause a liquid-phase reaction to become suddenly gaseous. For this reason it is important for the reactor designer to know under what circumstances the system will exhibit parametric sensitivity. If the onset of sensitivity can be predetermined, then the reactor can either be designed to operate in a region of insensitivity, or, it can be designed to accommodate the

possibility of these temperature excursions.

The problem of determining which conditions give rise to parametric sensitivity has been examined for the past 30 years. Numerous studies have attempted to predict, *a priori* or otherwise, what these exact conditions are. Although these studies have established various criteria for evaluating the sensitivity of a given set of operating conditions, there have been very few studies to date that have actually tested these criteria with experimental data.

The purpose of this project was to collect experimental data on parametric sensitivity and to use these data to evaluate these previously established sensitivity criteria. The work involved choosing a suitable reaction (as well as a reactor design), collecting the data, evaluating the data, and then testing the various criteria. The final goal was to arrive at a conclusion as to which criterion was most accurate, and most useful.

It is important to note here that the decision was made to use a liquid-phase, homogeneous reaction. This choice was made because such a reaction is easier to work with physically, and to model mathematically, than a gas-phase, heterogeneous reaction. This did not create any problems when it came to criteria comparison as virtually all criteria are currently based on mathematical models in which it is assumed that homogeneous conditions exist inside the reactor.

## 2.0 LITERATURE SURVEY

Although the work of Barkelew (1959) is considered the first definitive study of parametric sensitivity, there were in fact contributions made prior to that time. Wilson (1946) observed that exothermic reactions in tubular reactors could result in temperature profiles which changed dramatically in response to changes in the operating conditions. Using a one dimensional pseudo homogeneous model, it was noted that the derivative of temperature with respect to concentration (at any point in the reactor) could become infinite under certain conditions. Chambré (1956) introduced the method of isoclines for analysis of plug-flow reactors. This method was used years later in determining criteria for parametric sensitivity. Bilous and Amundson (1956) illustrated the existence of parametric sensitivity using computer simulations based on a one dimensional pseudo homogeneous model. In the same study it was determined that reactor stability could be predicted by analyzing the frequency response of a linearized reactor model. This method, however, required that the steady-state profile be determined first.

Barkelew (1959) provided the first useful criterion for parametric sensitivity. This criterion was established by examining the results of over 750 computer simulations of a one dimensional pseudo homogeneous reactor model. The criterion itself was, quite naturally, empirical. It was, however, very simple to use. The conditions where parametric sensitivity could be expected were clearly delineated on a

simple plot of dimensionless overall heat transfer coefficient ( $U$ ) versus dimensionless heat of reaction parameter ( $\Delta H$ ).

Dente and Collina (1964a, 1964b) studied the stability of tubular reactors. Using a one dimensional pseudo homogeneous model, it was determined that the reactor would always be stable with respect to small perturbations. However, the reactor could become parametrically sensitive under certain conditions. Two criteria for parametric sensitivity were proposed. The first criterion stated that a sensitive reactor displayed a positive second derivative of temperature with respect to axial coordinate at a point somewhere before the hot-spot. The second criterion was more intuitive than observational. This criterion stated that insensitive reactors were characterized by temperature increases (upon changing an operating parameter, for example the inlet temperature) along the reactor which were smaller than the temperature increase observed at the reactor inlet. Using these criteria, sensitivity diagrams were produced which were similar in nature to those of Barkelew (i.e., the parameter groupings were the same). The proposed criteria were found to be in close agreement when it came to predicting sensitivity, although the second criterion was more conservative.

Agnew and Potter (1966) extended Barkelew's work by including axial and radial dispersion of mass and energy in their reactor model. Computer simulations of the two-dimensional cell network model of

Deans and Lapidus (1960) were used to obtain diagrams which illustrated under what conditions parametric sensitivity was likely to occur. These diagrams were similar to Barkelew's, differing only in the inclusion of an extra parameter which accounted for the number of radial cells in the two-dimensional model.

Van Welsenaere and Froment (1970) derived 2 new criteria for parametric sensitivity based on the intrinsic nature of the axial temperature profile in a tubular reactor (again, based on a one dimensional pseudo homogeneous model). The existence of an inflection point somewhere before the maximum temperature (i.e., the "hot-spot") in the axial temperature profile was found to be a sufficient condition for parametric sensitivity. Using this criterion it was possible to determine the value of the inlet reactant concentration which would give rise to a parametrically sensitive temperature profile (for a given set of reactor conditions). This method, however, required the use of trial and error.

Oroskar and Stern (1979) developed a parametric sensitivity diagram similar to Barkelew's by utilizing Chambré's method of isoclines. The results obtained were again based on a one dimensional pseudo homogeneous reactor model (ODPH). The diagram, however, was only applicable to first order reactions.

Morbidelli and Varma (1982), utilizing the method of isoclines and the existence of an inflection point before the hot spot as a criterion,

developed a method for determining parametrically sensitive operating conditions. This method did not require trial and error. The results obtained were used to produce diagrams which clearly distinguished regions of "safe" (i.e., non-sensitive) operation from those of "unsafe" (i.e., sensitive) operation. The effect of the various operating parameters on the regions of parametric sensitivity were qualitatively examined. It was determined that runaway was more likely for low reaction orders, large values of activation energy and high inlet temperatures.

The studies described so far were all based on kinetic formulations in which the Arrhenius expression for the temperature dependence of the reaction rate constant was linearized (usually about the value of the coolant temperature). This, of course, is an approximation of the actual temperature dependence of the rate constant (and hence the rate). Dente et al. (1966a) showed that such an approximation was not too severe as it resulted in conservative estimates of the critical (i.e., those which marked the onset of sensitive behavior) values of the operating parameters.

Soria Lopez et al. (1981) studied the effect of a co-currently flowing cooling medium on reactor behavior (all studies discussed so far were based on an isothermal cooling medium). The reactor configuration was that of a double pipe heat exchanger with the reaction fluid in the inner pipe and the coolant flowing through the outer pipe. It was determined that, under these conditions, the reactor could display

pseudo adiabatic behavior (i.e., a hot-spot occurring at the reactor outlet). A set of equations was derived to predict this occurrence. Parametric sensitivity with respect to flow rate of coolant was illustrated.

Hosten and Froment (1986) also studied co-current cooling flow, applying a criterion based on that of Van Welsenaere and Froment (1970) to determine critical conditions (i.e., those conditions which would lead to parametric sensitivity). The method involved trial and error, but did allow for the determination of the critical value for any parameter (as opposed to earlier work, such as that of Van Welsenaere and Froment, where only the critical value of the inlet concentration was determinable). A comparison with the critical conditions determined for a constant coolant temperature indicated that parametric sensitivity was more likely for co-current cooling than for a constant temperature coolant.

Akella and Lee (1983) developed a phase-plane analysis for reactors with a counter-current flow of coolant. Safe and "ignition" (i.e., sensitive) regions were mapped out as functions of the inlet feed and coolant temperatures. The criterion used to define "ignition" was the existence of a positive second derivative of temperature with respect to the axial coordinate at the reactor inlet.

Barkelew (1984) studied the sensitivity of adiabatic reactors. The



standard ODPH model and the continuous stirred tank reactor (CSTR) model were examined, as well as other models (i.e., the axial dispersion model and the imperfectly stirred tank model) which took into account non-ideal mixing. Criteria were established for both the maximum allowable reactor length and temperature rise. These criteria were found to be a function of only the variance and mean of the residence time distributions (RTD) of the models, and not of the particular form of the reactor models.

Westerterp and Ptasiński (1984a, 1984b), Westerterp et al. (1984c), and Westerterp and Overtoom (1985) extended the ODPH model to include multiple reactions (both parallel and consecutive). Criteria were established to limit the hot-spot temperature, thus ensuring the required yield or selectivity would be obtained. It was determined that these criteria also ensured that parametric sensitivity would be avoided.

The above described studies were based on various homogeneous reactor models. McGreavy and Adderly (1973, 1974) were the first to study parametric sensitivity using a one dimensional heterogeneous (ODHT) model (i.e., taking into account mass and heat transfer resistances in and around a catalyst particle in a fixed-bed reactor). For certain conditions, it was determined that local sensitivity could occur (i.e., particle temperature is parametrically sensitive whereas fluid temperature is insensitive). A criterion was established for

parametric sensitivity based on the behavior of the temperature difference between the fluid and the particle. McGreavy and Adderly also briefly examined the relationship between parametric sensitivity and catalyst steady-state multiplicity.

The work of Rajadhyaksha et al. (1975) continued the investigation of parametric sensitivity for the case of a one dimensional heterogeneous (ODHT) reactor model. Utilizing the criterion of Van Welsenaere and Froment (1970), critical inlet concentrations were determined for four different regimes (each characterized by the relative magnitudes of the transport limitations).

Morbidelli and Varma (1986a and 1987a) also considered an ODHT model. It was shown that parametric sensitivity would always precede multiplicity or ignition of the catalyst particle. Using the criterion of vanishing second and third derivatives of temperature with respect to conversion somewhere before the hot-spot, conditions leading to parametric sensitivity were determined. The results obtained were again presented in diagram form, clearly delineating sensitive regions from insensitive regions. A comparison with the experimental data of Emig et al. (1980) indicated that inclusion of heterogeneity into the determination of sensitive/insensitive conditions resulted in a much better agreement with the data (as compared with those conditions determined from a pseudo homogeneous model).

The concept of a sensitivity coefficient was introduced by Henning and Perez (1986). This coefficient was defined as the derivative of temperature (or conversion) with respect to an input parameter (i.e., inlet temperature). It was noted that the value of a sensitivity coefficient decreased monotonically as a function of reactor position for non-sensitive conditions. For sensitive conditions, the sensitivity coefficient profile displayed a minimum at some position.

Morbidelli and Varma (1986b) continued with the idea of using sensitivity coefficients and developed a generalized sensitivity criterion for parametric sensitivity. A normalized sensitivity coefficient, defined as the dimensionless rate of change of maximum temperature with respect to any input parameter, was introduced. It was observed that a plot of this sensitivity coefficient versus the heat of reaction parameter always yielded a maximum value (characterized by a sharp peak). Further, this peak occurred at the same value for the heat of reaction parameter, regardless of the input parameter used in calculating the normalized sensitivity. This observation tended to confirm the validity of using this approach. Chemburkar et al. (1986), Bauman et al. (1987, 1990) and Morbidelli and Varma (1989) applied this same idea of normalized sensitivity to other reactor configurations (i.e., CSTR, plug flow/ with co-current cooling, reaction networks) with similar results. Morbidelli and Varma (1988) extended its application to explosion theory. Tjahjadi et al. (1987) examined the parametric sensitivity of tubular polymerization

reactors using this same approach.

In reviewing the previous studies concerned with parametric sensitivity, it is also necessary to note the contributions made from explosion theory. For example, the existence of a positive second derivative somewhere before the hot-spot as a criterion for parametric sensitivity was actually first noted by Adler (1964). (In fact, it was noted that a more suitable criterion would be the existence of an inflection point in the temperature-conversion plane). As it turns out, the equations describing a tubular reactor (ODPH) are very similar to those describing ignition of a homogeneous solid. Hence, attempts have been made to modify stability criteria for ignition so as to use them for parametric sensitivity of tubular reactors. These criteria have been reviewed by Morbidelli and Varma (1985).

Surprisingly, the studies carried out so far have been almost exclusively theoretical. Emig et al. (1980), however, did collect experimental data on parametric sensitivity. The experimental study involved the synthesis of vinyl acetate in a fixed-bed catalytic reactor. The results seemed to confirm the validity of the criteria of Barkelew (1959) and McGreavy and Adderly (1973). A comparison of the data with Agnew's criteria indicated that sensitive conditions were observed in a region of predicted insensitivity. It was pointed out, however, that the discrepancy could have been due to the inappropriateness of Agnew's model for the system studied.

Bauman and Varma (1990) obtained experimental data for the catalytic (10% CuO on  $\gamma$ -alumina) oxidation of carbon monoxide (CO) in a fixed bed reactor. The observed parametrically sensitive conditions were in general agreement with those predicted using the generalized sensitivity criterion of Morbidelli and Varma (1986b).

### 3.0 SELECTION OF REACTION SYSTEM

The choice of a reaction system to study parametric sensitivity involved consideration of both the reaction and the reactor design. The factors considered in these selections are discussed in the following two sections.

#### 3.1 REACTION SELECTION

One of the objectives of this work was to obtain experimental data that could be used to compare criteria for parametric sensitivity. Therefore, the reaction to be used clearly had to have the capability of becoming parametrically sensitive (given the appropriate reactor conditions). In addition, it was desired to have a liquid-phase, homogeneous reaction so as to simplify reactor modeling and design of equipment. The other key consideration was that the reaction had to be "well-understood", i.e., the mechanism, the reaction order, and the kinetic parameters had to be known to a high degree of accuracy. Thus, the requirements for the reaction were:

- 1) large heat of reaction ( $\Delta H$ ),
- 2) large activation energy ( $E_A$ ),
- 3) mechanism and kinetics known,
- 4) kinetic (Arrhenius parameters) parameter values available,
- 5) liquid-phase, homogeneous and,
- 6) chemicals readily available and relatively inexpensive.

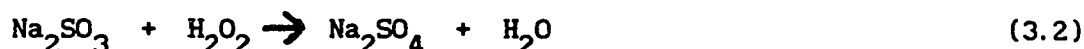
Two reactions were subjected to a detailed consideration. These reactions were:

the oxidation of sodium thiosulfate by hydrogen peroxide



and,

the oxidation of sodium sulfite by hydrogen peroxide



Reaction 3.1 had been used (Root and Schmitz (1969, 1970), Vejtasa and Schmitz (1970)) in studies of reactor multiplicity and stability and it therefore seemed natural that it could also be used in a study of parametric sensitivity. The Arrhenius parameters for the reaction were known, the activation energy being 76,410 (J/mol) and the pre-exponential factor having a value of  $6.85 \times 10^{11}$  (L/(mol·s)). However, as was noted by Vejtasa and Schmitz (1970), the reaction mechanism and distribution of products are complicated and seem to depend upon the reaction conditions. Further, the stoichiometric ratio of 2 moles peroxide per mole of thiosulfate is not necessarily constant for reaction conditions differing from those used in the above mentioned studies. Root and Schmitz (1969) also noted that the metal-catalyzed generation of hydrogen sulfide occurred under certain conditions. This reaction clearly had undesirable characteristics.

Reaction 3.2 was studied in depth by Mader (1957). Penkett et al. (1979) and Hoffman and Edwards (1975) also studied the reaction,

although not in as much detail. Mader confirmed that sulfate was indeed the product of the reaction (dithionate being the other possibility). It was shown that the reaction rate is dependent on the pH of the solution. Mader also noted that, for conditions where the pH was held constant by a buffer system, the buffer system itself had an effect on the reaction rate (i.e., deviation from simple kinetics was noted when a carbonate buffer was used, simple second order kinetics were observed when phosphate and carbonate buffers were used). For a pH above 8.0 (using a phosphate buffer), the reaction was determined to be second order (first order with respect to both reactants). For a pH range of 9.4 to 10.4 in a phosphate buffer, the rate constant was found to be independent of pH. Mader also reported values for the Arrhenius parameters. The activation energy was found to be 63,820 J/mol while the pre-exponential factor was calculated as  $3.08 \times 10^{10}$  L/(mol·s).

While the kinetics of the reaction 3.2 were certainly better understood than those of reaction 3.1, the reaction was still dependent on the experimental conditions, and in this sense, not much different than reaction 3.1. The decision as to which reaction was preferable was still not clear. The final choice, it was decided, would be based on computer simulations of the temperature profiles for each reaction. These simulations would, of necessity, have to involve some knowledge of the reactor design.



### 3.2 REACTOR DESIGN

The choice of an appropriate reactor design involved the following considerations. The reactor had to be tubular, with temperature measurement at points along its length. Cooling/heating, of some form, had to be possible. The design had to be such that the operating parameters (i.e., coolant temperature/flow, concentrations, inlet temperatures, flow rates, heat transfer coefficients, etc.) could be easily manipulated. Ideally, the reactor would also be easy to assemble/disassemble and modify as needed.

Two options were examined, with the key feature of each being small (an O.D. of 1.27 cm or less) metal tubing for the reactor core. The first system consisted of the reactor tubing running alongside a co-, or counter-currently flowing liquid (i.e., as in a double pipe heat exchanger) with thermocouples inserted at points along the reactor. The second arrangement involved the reactor being immersed in a bath, with the tubing cut into sections and joined together by tees. Thermocouples, one inserted in each tee, would provide the temperature measurements. The coolant in this case would be isothermal.

The first design would have been the easier of the two to assemble. However, it would not have had the flexibility of the second and would have required more elaborate modeling work later on. The second design appeared more promising, but it too had limitations. The inclusion of tees in the reactor created a potential modeling problem,

and the fact that the bath had to be maintained at a constant temperature throughout each experiment meant that some sort of cooling system would have to be employed.

In the end, the decision was made to use the second design. The reasons for this choice were:

- 1) Using precut lengths of tubing along with tees would allow for easy modification of the reactor. If it was necessary to change the length between temperature measurements, or insert another thermocouple in a certain spot, the reactor could be quickly disassembled and new tubing inserted.
- 2) A water bath, with a heating and refrigeration unit attached, was readily available. The cooling capacity appeared to be sufficient to maintain a constant bath temperature. A controller was also in place so that the bath temperature could be easily manipulated.
- 3) A smaller water bath (again with heating and cooling units) was also available. This bath could be used to preheat/cool the feed. Thus manipulation of the inlet temperature would be quite simple.
- 4) The water bath was large enough that an impeller could be inserted. This would ensure uniform mixing in the bath.

In addition, the decision was made to use pressurized storage vessels for the reactants. This would eliminate the use of pumps and allow for easy flow monitoring with rotameters. Independent control of the reactant flow rates could be used to adjust the inlet concentrations.

### 3.3 COMPUTER SIMULATION OF PROPOSED REACTOR

With the basic design of the reactor chosen, simulations of the temperature profiles in the reactor were then carried out. These simulations provided information about suitable operating conditions. They also helped determine which reaction was to be used. Using an ODPH model, axial temperature profiles were obtained for various operating conditions (i.e., inlet concentrations, inlet temperatures, reactor diameters).

The ODPH model equations are as follows:

$$\frac{dT}{dz} = \frac{\Delta H \cdot R_A \cdot \pi \cdot D^2}{4 \cdot Q \cdot C_p \cdot \rho} - \frac{U \cdot \pi \cdot D \cdot (T - T_c)}{Q \cdot C_p \cdot \rho} \quad (3.3)$$

$$\frac{dC_A}{dz} = \frac{-R_A \cdot \pi \cdot D^2}{4 \cdot Q} \quad (3.4)$$

where  $R_A$  = the rate of reaction with respect to species A

for a second order reaction  $R_A = k \cdot C_A \cdot C_B$ ;  $k = A \cdot \exp(-E_A/(R \cdot T))$

and  $C_B = C_{Bo} - (C_{Ao} - C_A)$  for the sulfite reaction

$C_B = C_{Bo} - 2 \cdot (C_{Ao} - C_A)$  for the thiosulfate reaction

The assumptions implicit in this model are:

- 1) plug flow conditions exist in the reactor,
- 2) temperature variations in the radial direction are negligible,
- 3) axial conduction of heat is negligible,

- 4) there is no radial or axial dispersion of mass,
- 5) heat transfer to the surrounding isothermal coolant can be characterized by an overall (U) convective heat transfer coefficient,
- 6) there is no reaction occurring, the kinetics of which are known,
- 7) steady-state conditions prevail, and
- 8) the temperature dependence of the reaction can be described by the Arrhenius expression for the rate constant.

It should be noted here that, although the model used to describe the reactor is called the "One Dimensional Pseudo Homogeneous" model, the reactor itself is actually homogeneous. There should be no confusion because of this. The reason why the term "pseudo" exists in the name of the model is because it is most often used in the study of catalytic (i.e., heterogeneous) reactors. When the assumption is made that the catalyst and fluid phase in such reactors can be modeled as a continuous medium (i.e., homogeneous), then the model is referred to as "pseudo" homogeneous. It is common to retain the term "pseudo" even when the model refers to an actual homogeneous system and thus, it is also retained here.

Although there is no analytical solution for equations 3.3 and 3.4, they can be readily solved using a standard 4th order Runge-Kutta routine. This routine is easily programmable on any computer and provides excellent results for any reasonable step size. The following results were all obtained using a step size of 0.01 m.

The simulated adiabatic temperature profiles for both reactions are illustrated in Figure 3.1. These profiles were used to make the final decision regarding the choice of reaction because, under adiabatic conditions, the temperature profiles would be as "steep" as possible (i.e.,  $dT/dz$  as large as possible). Since the adiabatic profile would be the profile approached as parametric sensitivity occurred, it was necessary to have as "steep" a profile as possible for adiabatic conditions so as to be able to distinguish the onset of parametric sensitivity under non adiabatic conditions.

In Figure 3.1 the concentrations of reactants in each case are in stoichiometric proportions. The concentrations of the limiting reactants were chosen so that the adiabatic temperature rise would be the same for each reaction. The reactor diameter and flow rate were chosen so as to obtain a Reynolds number of approximately 10,000. From the figure, it is obvious that the thiosulfate reaction requires a longer length of tubing for complete conversion than the sulfite reaction. The sulfite reaction requires only 2.5 meters for complete conversion and displays a steep temperature profile. Based on these profiles, the sulfite reaction appeared to be the reaction of choice. The fact that the thiosulfate reaction was not well understood only served to strengthen this conclusion. In the end the decision was made to use the sulfite reaction. It was felt that the pH dependence of the reaction would not create experimental problems, as the reaction could be carried out in a phosphate buffer at a pH of 10.0.

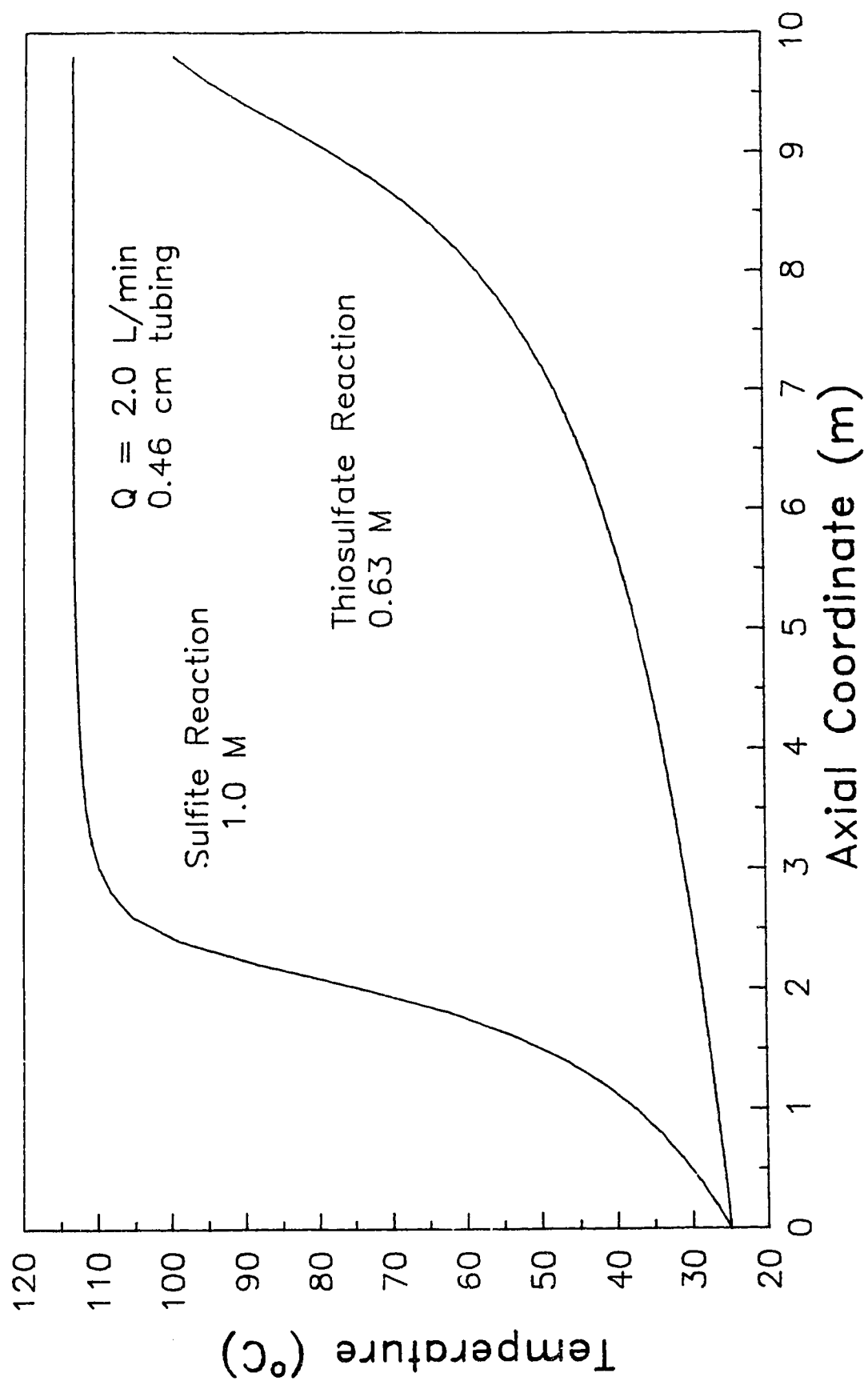


Figure 3.1 Comparison of Adiabatic Profiles

After choosing the reaction, the next step involved choosing the reactor dimensions. Although a flow rate of 2 L/min in a 0.46 cm diameter tube ensured a sufficiently high Reynolds number for turbulent flow (i.e., a Reynolds number of 10,000), the resulting heat output from this reactor would have been too large for the refrigeration unit to handle. With an available cooling capacity of only 2500 W, it was determined that the maximum flow rate could be approximately 400 mL/min. This reduced flow would result in the majority of the reaction taking place much closer to the inlet of the reactor. This is illustrated in Figure 3.2. From this figure, it became evident that the reactor diameter would have to be smaller so as to "stretch out", as it were, the temperature profile. This was necessary in order to obtain an adequate number of temperature measurements. Therefore, the decision was made to use a 0.175 cm diameter tube with a reduced flow rate. This reduced the Reynolds number to a value of approximately 5,000, indicating the flow could no longer be considered fully turbulent. This was not the ideal situation but, given the limitations of the refrigeration system, it was the best that could be achieved.

With the tubing size reduced, flow limitations due to the pressure drop through the reactor became a concern. A preliminary analysis indicated (see Appendix B) that a flow rate of 470 ml/min was possible. This calculation, however, was subject to error as there was no way of knowing the exact effect of the tees and thermocouples on

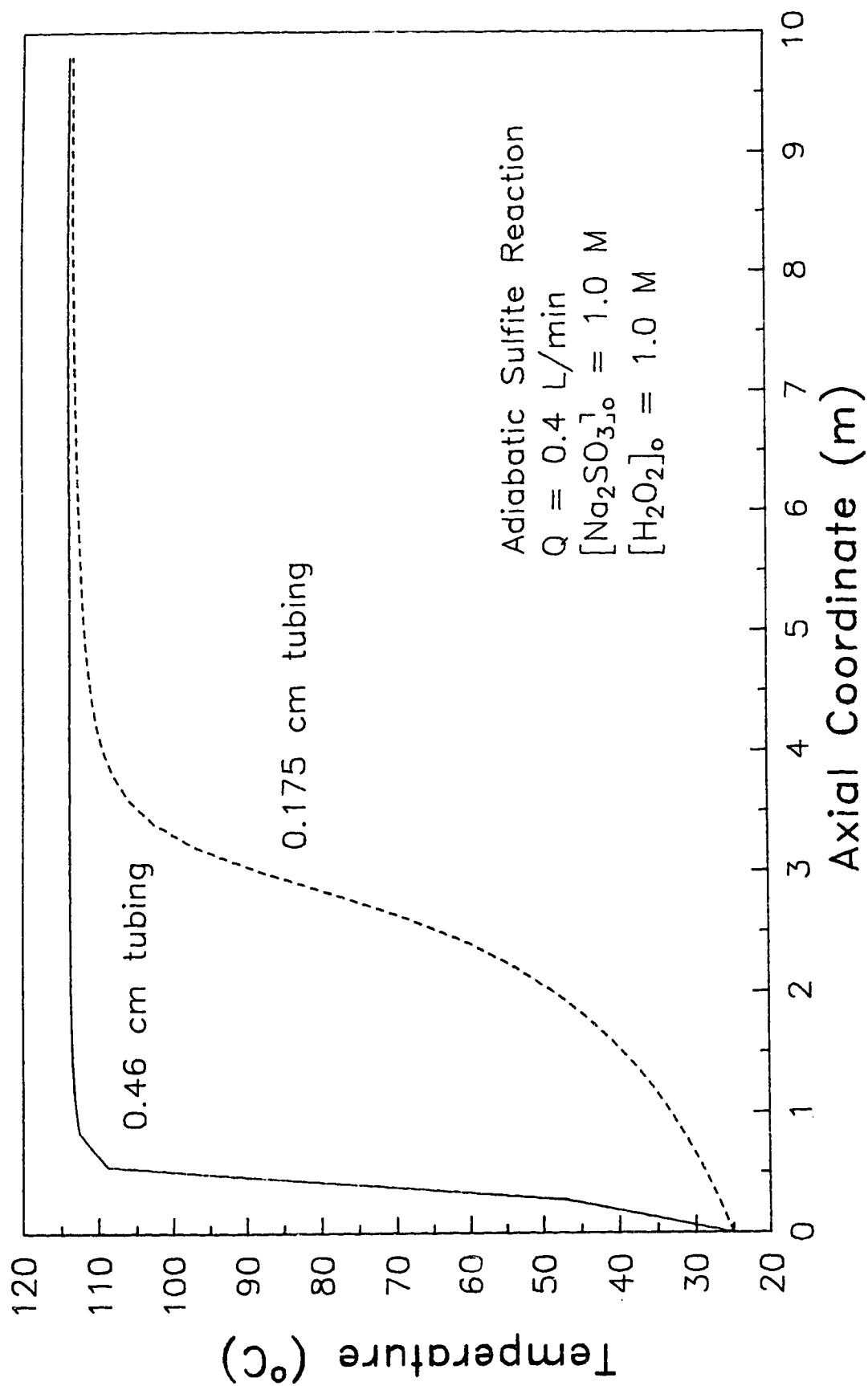


Figure 3.2 – Comparison of Tubing Sizes for Sulfite Reaction



the pressure drop. (Once the reactor was assembled it was found that a flow rate of approximately 400 ml/min was possible).

It is necessary to note here that the refrigeration system capacity was only a limiting factor for an inlet sulfite concentration of 1.0 M. Had a lower concentration been used, then the flow rate could have been increased and a larger Reynolds number would have been possible. However, as just noted, the flow rate could not have been increased much more due to the pressure drop limitation of the system.

It should also be noted that the solubility of sodium sulfite in water is approximately 1.1 moles/L at 0°C. Therefore, it was not possible to obtain a 1.0 M inlet concentration using a higher stock concentration of the sulfite and a lower overall flow rate. (The actual inlet sulfite concentration depended upon the stock concentration of the sulfite and the flow rate of the individual (both the sulfite and peroxide) feed streams). This would have alleviated the refrigeration capacity problem as well. Thus, it is perhaps more fitting to say that the final choice of flow rate and reactor diameter was a compromise, based on these factors:

- i) desire for turbulent flow (i.e., Reynolds number of 10,000),
- ii) refrigeration system capacity (2,500 W),
- iii) requirement for majority of the reaction to not take place in the front portion of the reactor,
- iv) pressure drop limitation of smaller reactor tubing,

v) sodium sulfite solubility in water limitations.

It should also be noted that the use of a smaller diameter tubing and a lower flow rate avoided some potential operational problems. For instance, radial temperature gradients (which were undesired) were more likely to occur in larger diameter tubes. Also, an increased flow rate would have meant an increase in the amount of chemicals required. This would have increased the cost of the project, as well as increasing the amount of waste for disposal. In addition, the size of the storage tanks for the solutions would have to have been much larger than the 40 L tanks that were eventually used. At a design pressure of 790 kPa, these tanks were already small pressure vessels. Any increase in the size would have resulted in even larger pressure vessels. For design purposes and safety considerations, this was something to be avoided.

One of the initial aims of this work was to study first order (pseudo, or actual) and second order reactions. Figure 3.3, however, showed this could not be done. For pseudo first order conditions (i.e. peroxide concentration 10 times greater than the sulfite), the majority of the reaction would take place extremely close to the reactor inlet. This would again make it difficult to obtain an adequate number of temperature measurements. The other two temperature profiles in Figure 3.3 indicated this problem would not occur if the initial reactant concentrations were of similar magnitude (i.e.,

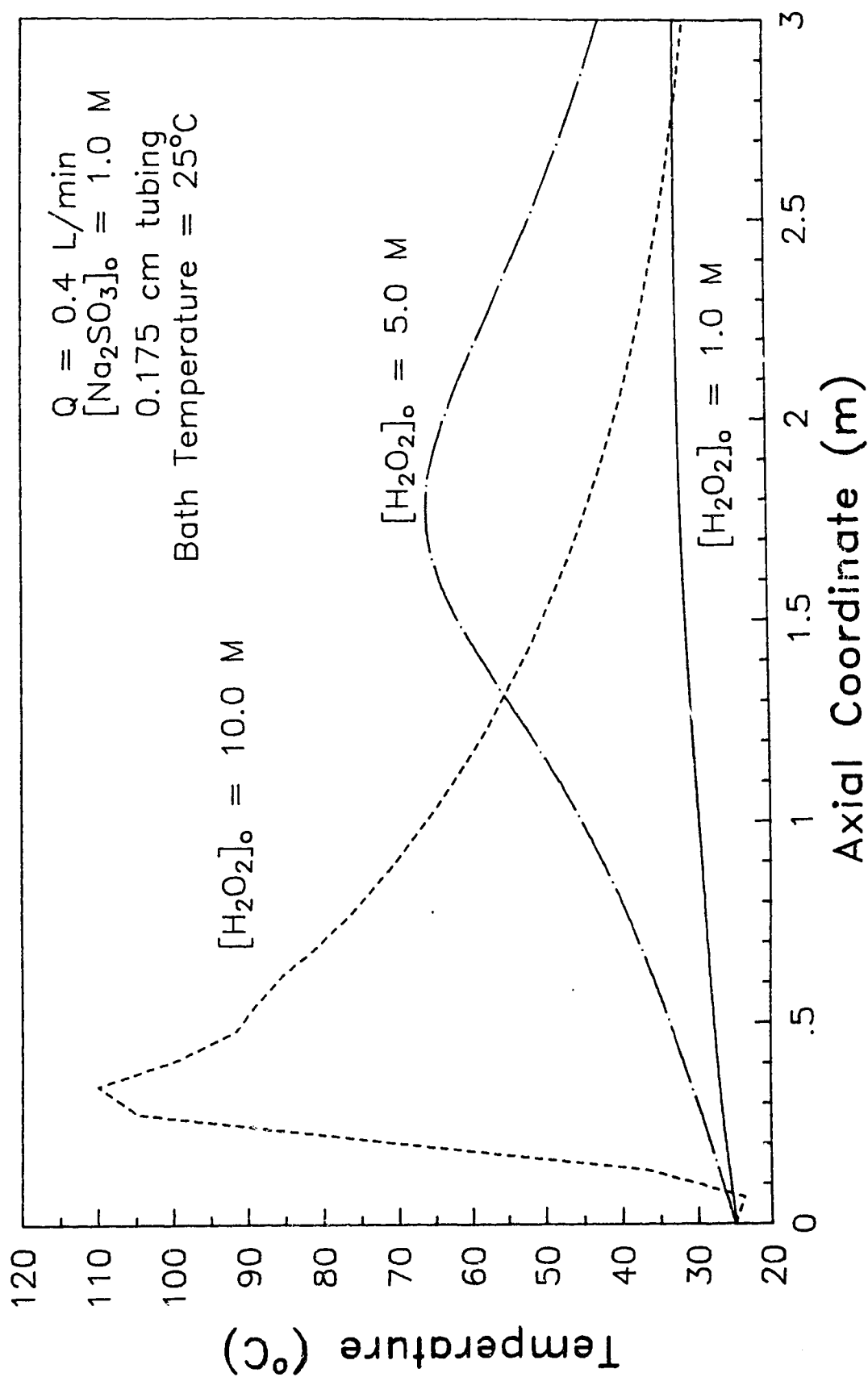


Figure 3.3 Comparison of Inlet Peroxide Concentrations

second order kinetics). Thus, the decision was made not to operate under pseudo first order conditions (large excess of peroxide). However, the profiles in Figure 3.3 also indicated that the inlet concentration ratio (peroxide to sulfite) had to be greater than 1 in order for an appreciable temperature rise to be observed. Thus, a true overall second order reaction could not be studied either. The kinetic conditions studied were thus somewhere between true first and true second order.

It is important to note here that the simulations in Figure 3.3 involved the use of an approximate value for the overall heat transfer coefficient. This was necessary because there was no way of knowing in advance the value of the heat transfer coefficient in the bath. For the purposes of these simulations, it was assumed that the entire resistance to heat transfer resided in the tube and the tube wall. The actual value for the heat transfer coefficient in the bath would be determined from the experimental equipment.

Further simulations centered on finding a set of conditions that would exhibit parametric sensitivity. The results obtained are illustrated in Figure 3.4. In this set of temperature profiles, the inlet temperature is varied while all the other parameters remain constant. At first, a change of 10 degrees in inlet temperature has little effect on the maximum temperature (i.e., the hot-spot). When the inlet temperature reaches 30 degrees however, a 10 degree change in inlet

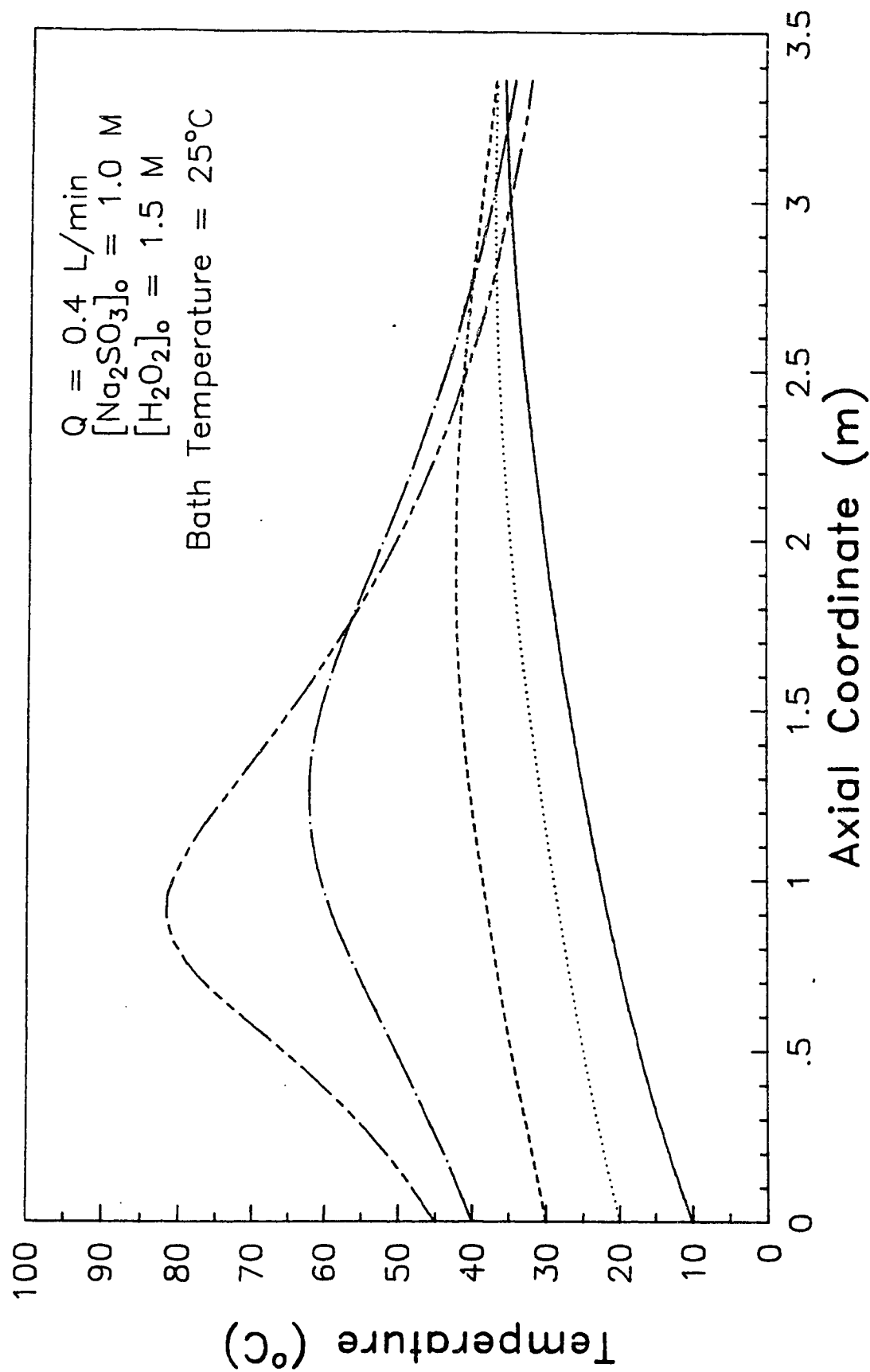


Figure 3.4 Determination of Sensitive Operating Conditions

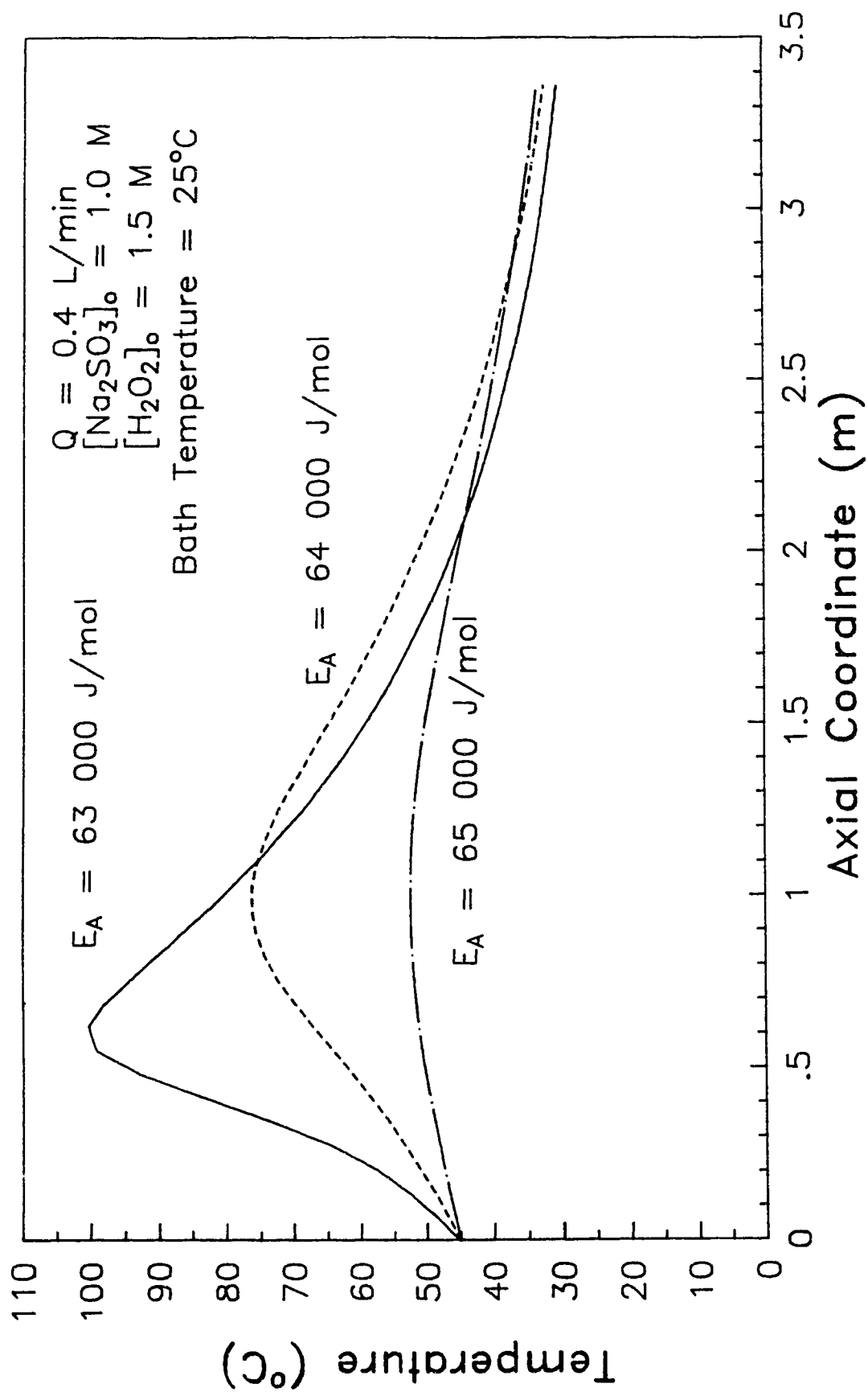


Figure 3.5 – Effect of Arrhenius Parameters on Temperature Profile

conditions results in a 20 degree change in the value of the hot spot. A further increase of only 5 degrees results in yet another 20 degree rise. These temperature profiles indicated that the operating conditions at an inlet temperature of 30 degrees were parametrically sensitive. Although these exact conditions were not used in the subsequent experimental work, they did serve as a basis for choosing the operating conditions which were used.

The preceding simulation results must be used with caution because all the simulations involved the use of the Arrhenius parameters determined by Mader. Figure 3.5 illustrates the effect of small changes in the activation energy on the temperature profile (the operating conditions chosen were those of the most sensitive profile in Figure 3.4). These large changes in the temperature profiles were of course to be expected as it was already known that the operating conditions were parametrically sensitive. However, this indicated that serious disagreement could occur between experimentally determined profiles and those evaluated from a mathematical model, simply because of a small error in the value of the activation energy used. This would make modeling the experimental data a very difficult task.

It was clear that the Arrhenius parameters had to be known with a greater deal of certainty. Mader's values were calculated using only four values of the rate constant (at different temperatures). The three values for the activation energy used in the simulations of Figure 3.5

were all well within the 95% confidence interval of Mader's value. Hence, Mader's values could not be used for modeling purposes. The parameters had to be determined more accurately. Therefore, the decision was made to design an experimental procedure that would more precisely determine the Arrhenius parameters for the sulfite reaction. The details of this procedure and the results obtained are discussed in the next section.

### 3.4 DETERMINATION OF KINETIC PARAMETERS

In order to determine the Arrhenius parameters of a particular reaction, the reaction rate constant must be determined at a minimum of two (but preferably more) different temperatures. This can be done in different ways, depending on the type of reactor used to acquire the data. In a batch reactor the concentration of one species is monitored as the reaction progresses (the other concentrations are determined from the reaction stoichiometry and initial conditions). From these data and the mathematical equation describing a batch reactor, the rate constant is determined. The process is repeated at another temperature and another rate constant is determined. With the rate constant determined at four or five different temperatures the Arrhenius equation is then used to determine the Arrhenius parameters for the reaction.

A continuously stirred tank reactor (CSTR) can also be used to determine Arrhenius parameters. With this reactor, the outlet stream



is analyzed for the concentration(s) of the reactants. The rate constant is then determined from the mathematical equation describing a CSTR. The rate constant is determined at four or five temperatures and the Arrhenius equation is used to evaluate the Arrhenius parameters.

For the sulfite reaction the methods outlined above were not applicable. There were two reasons for this: 1) there was no readily available method for continuously monitoring the concentration of either species and, 2) with the reaction being extremely exothermic it ~~would~~ have been nearly impossible to maintain the reaction mixture at a fixed temperature. Therefore, some other method had to be designed.

After some consideration it was decided that the concentration profile could be determined indirectly if the reaction conditions were adiabatic. In an adiabatic reaction, concentration would be directly related to temperature. A system for continuous temperature monitoring was readily available. Therefore, the concentration profile could be determined quite easily, albeit in an indirect manner. Of course, the fact that the reaction would not proceed isothermally meant that a different calculation procedure would have to be used in order to evaluate the Arrhenius parameters. This, however, was not a major problem.

In an adiabatic reactor, the heat generated by the reaction is used

entirely to heat up the reactor, reactants, and the products. Therefore, at any point in time, the temperature of the reaction system can be used to determine the concentration(s) of the reacting species (assuming the initial concentrations are known). In the case of the sulfite-peroxide reaction, an energy balance for a batch reactor yields:

$$\Delta H \cdot [C_A(t) - C_A(0)] \cdot V = [(mCp)_1 + (mCp)_2] \cdot [T(t) - T(0)] \quad (3.5)$$

where

$\Delta H$  - heat of reaction (J/mol)

$C_A(t)$ ,  $C_A(0)$  - concentration of limiting reactant, i.e., the sulfite, at time=t and time=0, respectively (mol/L)

$V$  - volume of reaction mixture (L)

$(mCp)_1$ ,  $(mCp)_2$  - thermal capacity of the reactor and product/reactant mixture, respectively (J/K)

$T(t)$ ,  $T(0)$  - temperature of the reacting system at time=t and time=0, respectively (K).

Thus, if the temperature at any time is known, the concentration of sulfite can be determined (assuming the initial concentration is known as well). From the reaction stoichiometry the concentration of the peroxide at each time can be determined as well. With the concentrations known, the rate law can then be used to determine the Arrhenius parameters. For the second order reaction between sulfite and peroxide the rate expression is

$$R_A = A \cdot \exp(-E_A/(R \cdot T)) \cdot C_A \cdot C_B \quad (3.6)$$

where

$R_A$  - rate of reaction (can be expressed as rate of disappearance of species A, i.e., the sulfite) (mol/(L·s))

A - pre-exponential factor (L/(mol·s))

$E_A$  - activation energy (J/mol)

R - universal gas constant (J/(mol·K))

T - temperature (K)

$C_A$ ,  $C_B$  - concentration of sulfite and peroxide, respectively (mol/L).

With the concentrations of the species known (from equation 3.5) at each time interval, values of  $R_A$  can be calculated ( $R_A$  is equal to  $-dC_A/dt$  and can be determined by numerical differentiation). With  $R_A$ , T,  $C_A$ , and  $C_B$  known at various times during the reaction, a plot of  $\ln(R_A/(C_A \cdot C_B))$  versus  $1/T$  can be constructed. This plot will be linear with a slope of  $-E_A/R$  and an intercept of  $\ln(A)$  if equation 3.6 adequately describes the reaction kinetics.

The data obtained from the adiabatic batch reactor, along with the Arrhenius parameters determined are discussed in section 3.4.2. In the following section the apparatus used to obtain the data is discussed, as well as the experimental procedure itself.

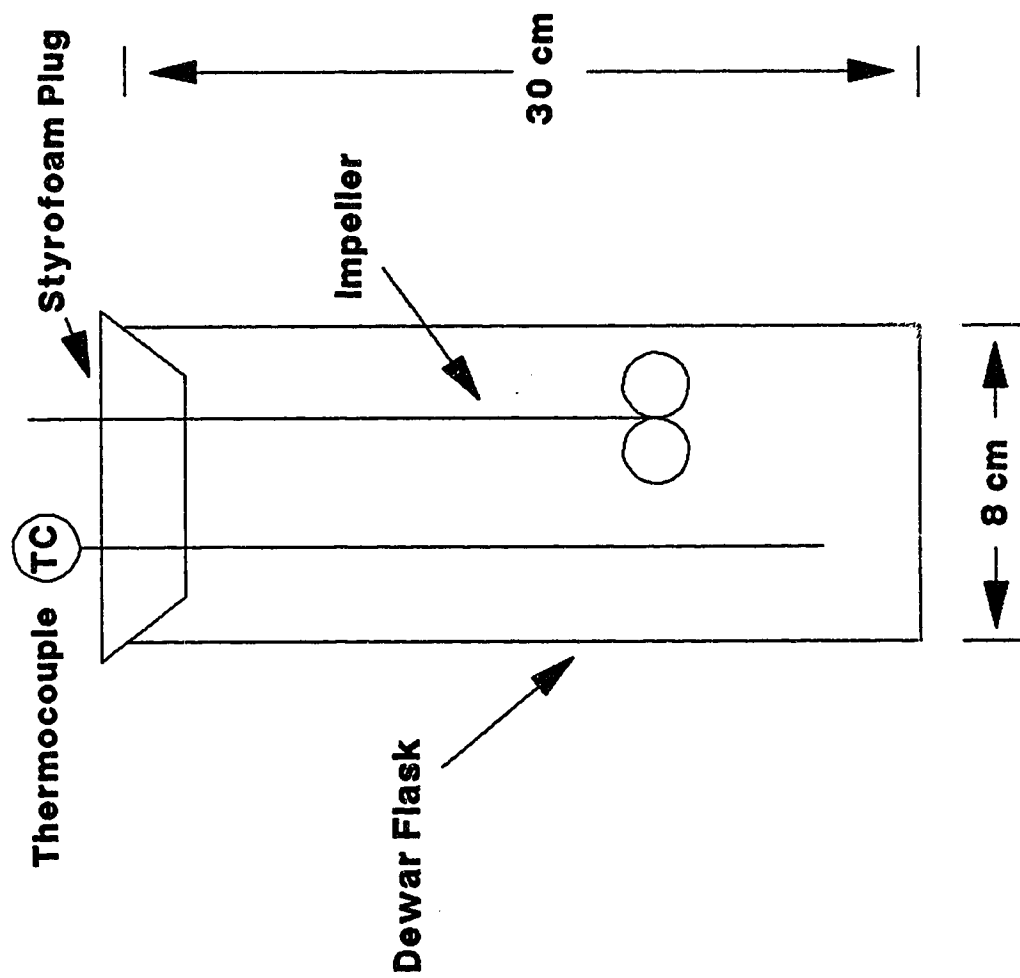


**Figure 3.6 Adiabatic Batch Reactor**

#### 3.4.1 ADIABATIC BATCH REACTOR SYSTEM

Figure 3.6 is a sketch of the system employed. It consisted of a 1 L dewar flask with a styrofoam plug inserted at the top. Two small holes were punched in the plug, large enough for a thermocouple and an impeller shaft, respectively. The impeller was connected to a small electric motor with a variable speed controller (Canlab Type R7R1) to produce an adequate stirring system. The thermocouple was used in conjunction with an OPTO 22 Input/Output process subsystem and an HP 1000 Series E computer. This allowed for continuous monitoring of temperature.

A preliminary study was undertaken to determine the thermal capacity of the reactor. The dewar flask was allowed to equilibrate with the ambient temperature. At the same time, a beaker filled with 500 ml of water was cooled to a sub-ambient temperature in an ice bath. Once the dewar temperature was determined to be at equilibrium, the cold water was added to the dewar. The flask was capped with the styrofoam plug and the entire system was mixed thoroughly. When the temperature of the system came to equilibrium, the plug was removed and the temperature recording ceased. The entire process was repeated with 500 ml of water at above ambient temperature. With the data obtained, it was determined that the heat capacity of the reactor was 202 J/K (see Appendix A for details).

The next set of experiments involved actual reactions between the

sulfite and the peroxide. Three different experiments were carried out, each using the same procedure. Initially, the dewar was filled with 475 - 480 ml of a buffered sodium sulfite solution. Di-potassium hydrogen orthophosphate ( $K_2HPO_4$ ), sodium phosphate tribasic ( $Na_3PO_4 \cdot 12H_2O$ ), sodium hydroxide (NaOH) and hydrochloric acid (HCl) were used to obtain a buffered solution of pH 10.2  $\pm$  0.2. The solution was sufficiently buffered so as to prevent a change of more than one pH unit during the course of the reaction. The concentrations of sulfite were chosen so that the sulfite would be the limiting reactant and the adiabatic temperature rise would be 35-45°C. The dewar and its contents, along with a beaker full of 25 - 30 ml of 35 wt %  $H_2O_2$ , were placed in an ice bath and cooled to approximately 15°C. The exact concentration of the peroxide was determined by iodometry using 0.1 N sodium thiosulfate as the titrant. The amount of peroxide used was sufficient to produce a relatively quick, but not instantaneous, reaction. With both reactants sufficiently cooled, the plug was quickly removed, the peroxide added to the dewar, the plug replaced and the stirring system turned on. While this was occurring the temperature of the contents of the dewar was being monitored (at one second intervals). Temperature measurements continued until the reaction was complete.

#### 3.4.2 ADIABATIC BATCH REACTOR RESULTS

The results obtained for each of the three experiments are illustrated in Figures 3.7, 3.8 and 3.9. A cursory analysis of the figures

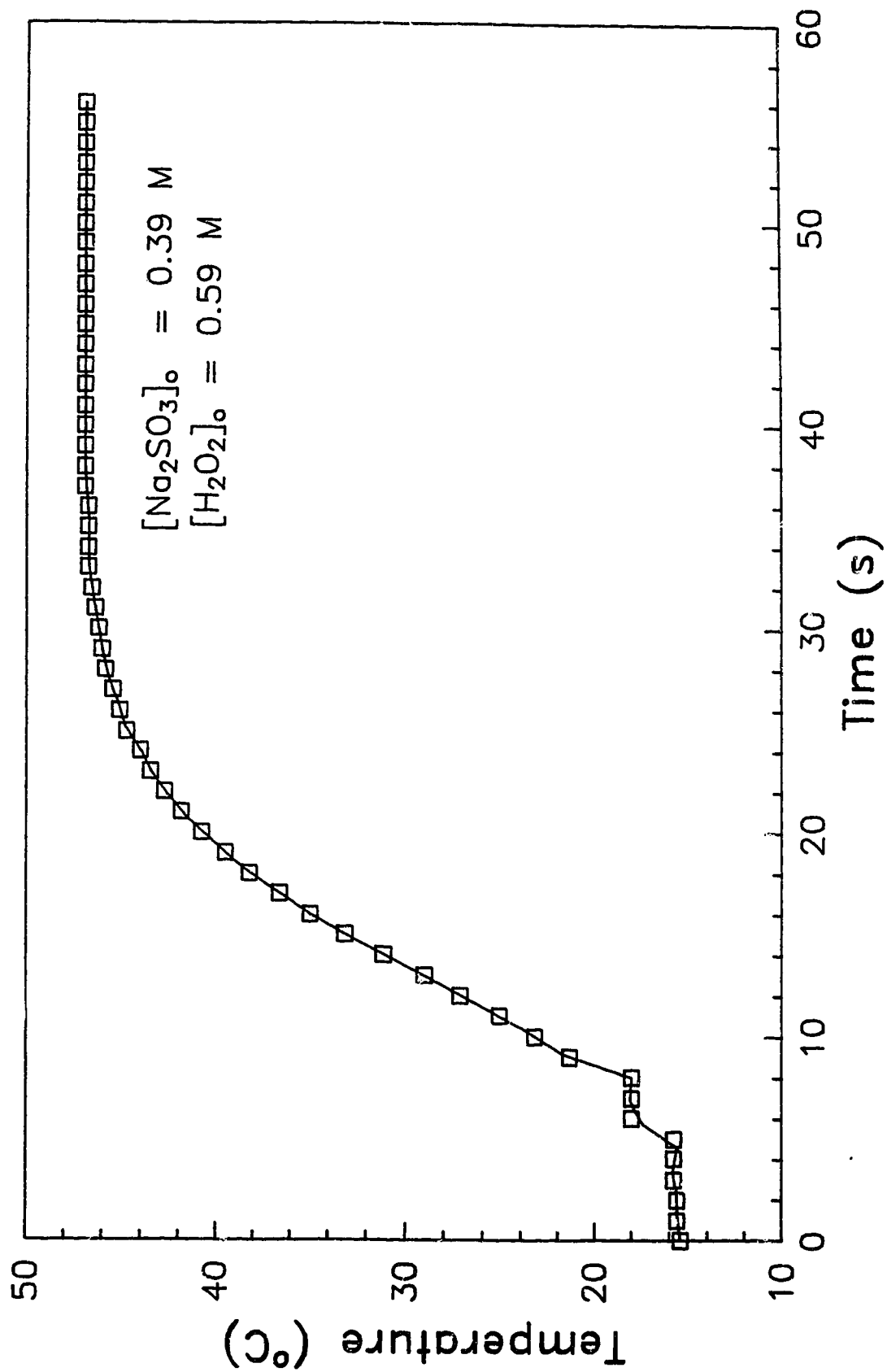


Figure 3.7 Adiabatic Batch Reactor Data

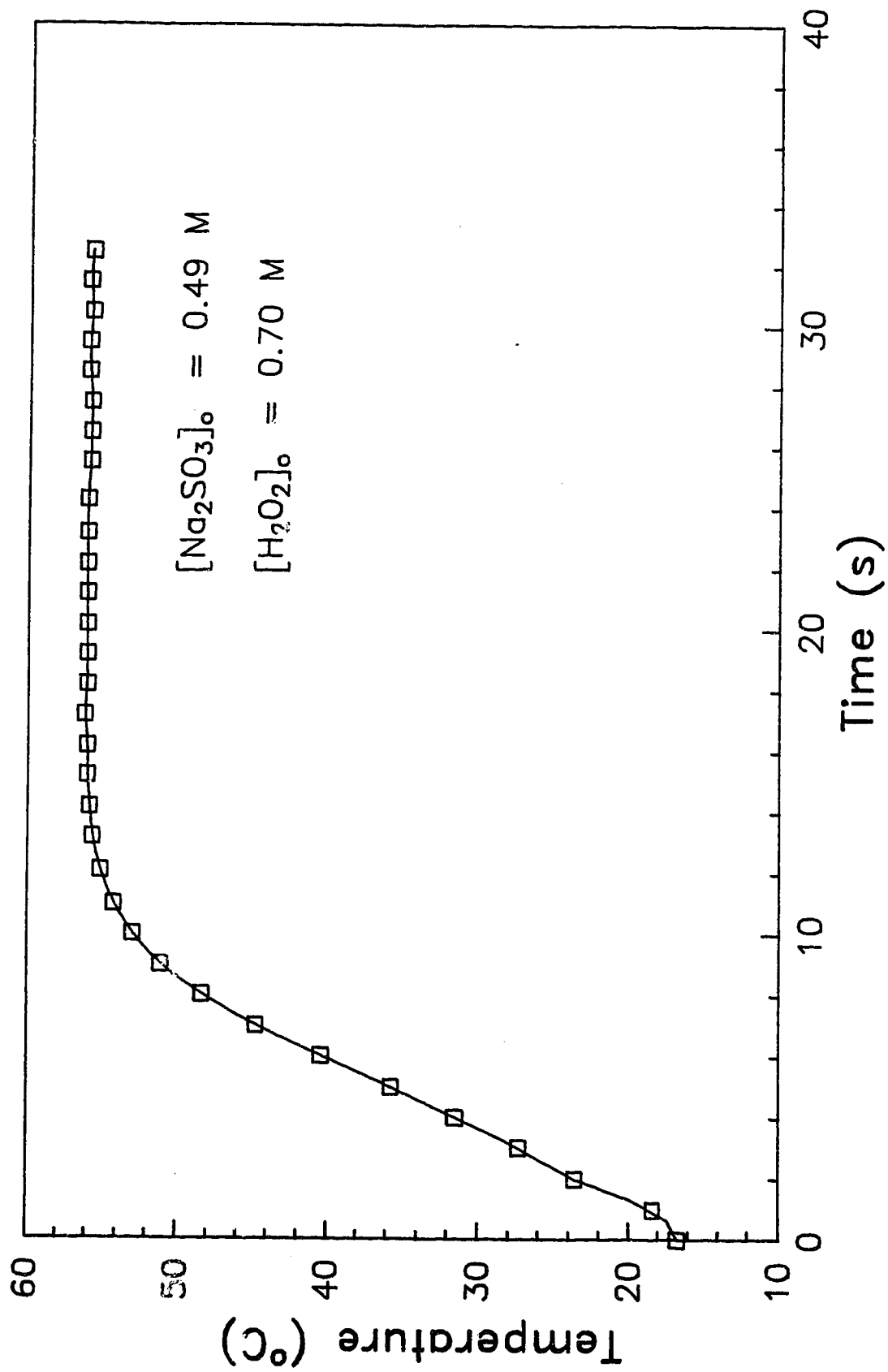


Figure 3.8 — Adiabatic Batch Reactor Data



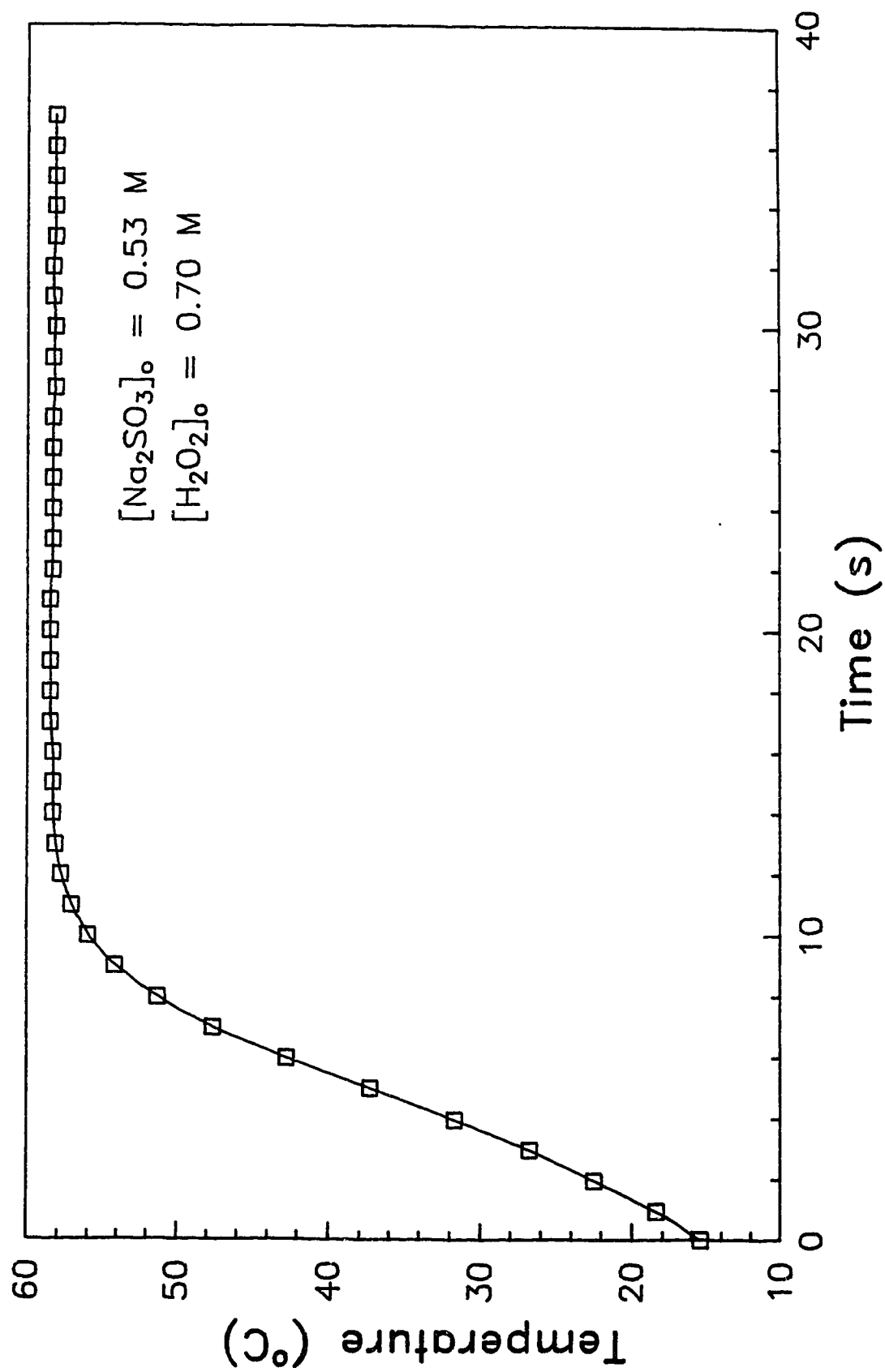


Figure 3.9 Adiabatic Batch Reactor Data

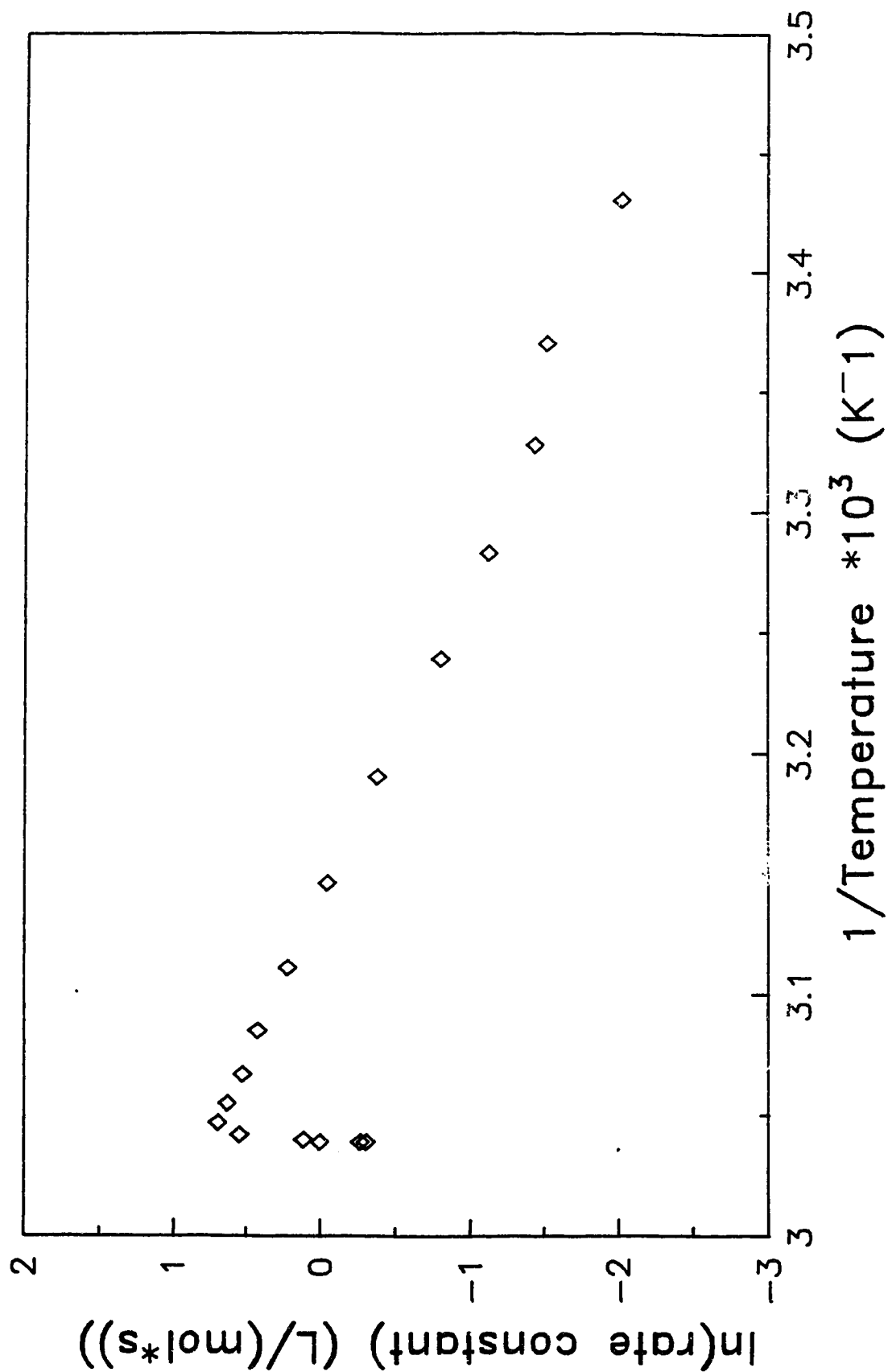


Figure 3.10 Typical Arrhenius Plot with Adiabatic Batch Reactor Data

indicates a sigmoidal shape for the temperature profile in each case. This is what would be expected for an adiabatic reaction. Also, the final temperature, once reached, remained stable for quite some time (relative to the length of time required for the reaction). This indicated that the reactor was essentially adiabatic as the rate of heat lost to the surroundings was low relative to the rate of heat generation inside the reactor. In addition, the temperature rise in each case was within 1% of the theoretical adiabatic temperature rise.

A plot of  $\ln(R_A/(C_A \cdot C_B))$  versus  $1/T$  for one set of experimental data is shown in Figure 3.10. Except at the ends, it is linear. This confirms the validity of using a second order rate law to describe the system. In order to determine the values of the Arrhenius parameters, data from all three experiments were used simultaneously in a linear regression (see Figure A.2 in Appendix A) of  $\ln(R_A/(C_A \cdot C_B))$  versus  $(1/T)$ . The results are shown in Table 3.1, along with the 95% confidence intervals in each case. The details of the calculations performed can be found in Appendix A.

TABLE 3.1 ARRHENIUS PARAMETERS FOR $\text{Na}_2\text{SO}_3 + \text{H}_2\text{O}_2$			
Batch Data Pre-Exponential Factor		Batch Data Activation Energy	
$3.56 \times 10^{10}$ (L/(mol·s))		64 268 (J/mol)	
95% C. I.	$1.00 - 12.48 \times 10^{10}$	95% C. I.	61 006 - 67 530
Pre-Exponential Factor (Mader)		Activation Energy (Mader)	
$3.08 \times 10^{10}$ (L/(mol·s))		63 820 (J/mol)	
95% C. I.	$1.29 - 7.33 \times 10^{10}$	95% C. I.	61 175 - 65 921

#### 4.0 EXPERIMENTAL TUBULAR REACTOR SYSTEM

A description of the system used in the experimental study is given in this section and shown schematically in Figure 4.1. A detailed sketch of the reactor is provided in Figure 4.2.

The apparatus consisted of three main sections: the reactant storage tanks, the feed lines along with the preheater/cooler and, the tubular reactor.

The reactant storage tanks were cylindrical in shape with a capacity of approximately 70 liters each. They were constructed of 304 stainless steel and fitted with sight glasses for measuring the level in each tank. Each tank was fitted with a 3-way valve at the bottom so that the feed line could be by-passed when the tank was being cleaned, as well as a 3-way valve on top of the tank that could be used either to pressurize or purge the tank. As a safety precaution, each vessel was also fitted with a pressure relief valve. The tanks were designed to operate at a pressure of 790 kPa. Nitrogen ( $N_2$ ) was used both to pressurize and purge the storage tanks.

At the bottom of each tank a reactant feed line was attached. This feed line consisted of 0.635 cm O.D. stainless steel tubing which ran from the tank outlet, through a rotameter and on to the precoolers/heater. Matheson rotameters (model numbers 7642-T605 and 7632-T604) were used. The sulfite solution was a 1.1 M phosphate

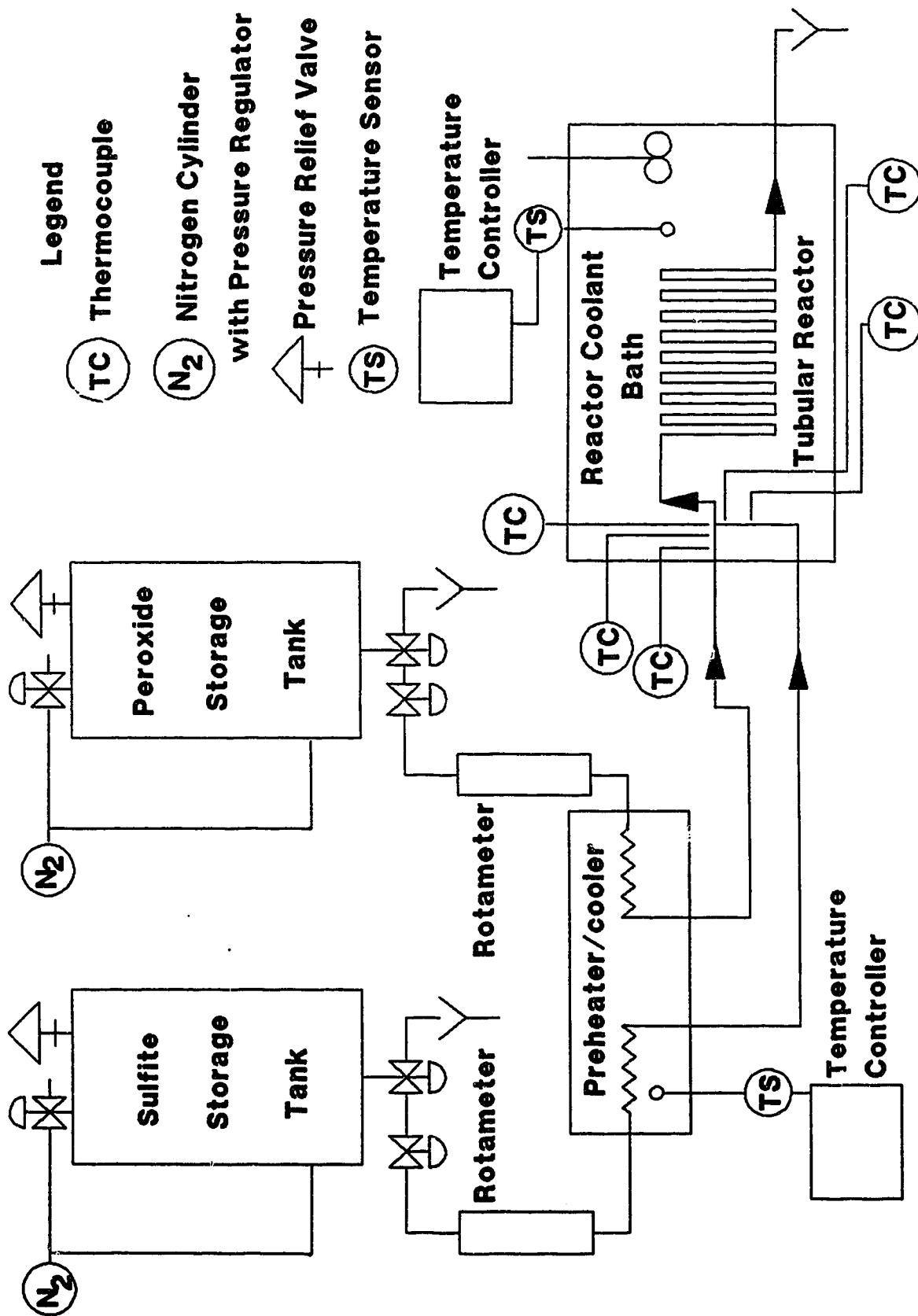


Figure 4.1 Experimental Apparatus Schematic

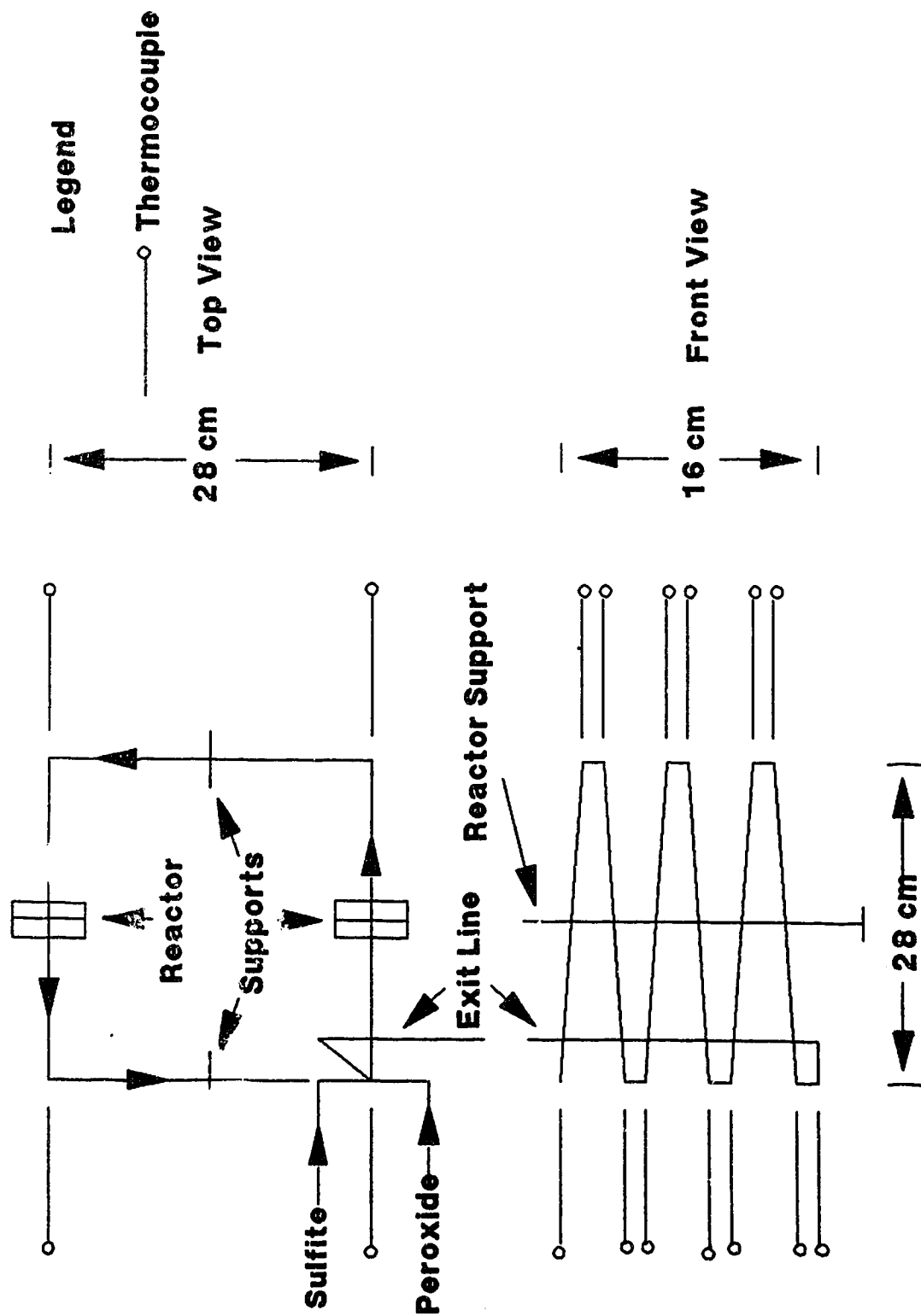


Figure 4.2 Top and Front Views of Tubular Reactor

buffered mixture. The buffering agents were the same as those used for the adiabatic batch reactor (see section 3.4.1). The peroxide solution was 35 wt% (approximately 11.7 M)  $\text{H}_2\text{O}_2$ . Its exact concentration was determined by the iodometric method outlined in section 3.4.1.

The preheater/cooler was a small (approximately 15 L) water bath with a 2.5 kW refrigeration unit attached. The bath was also equipped with a 1 kW heating element (thus the bath could either be a preheater or a precooler). A temperature controller was attached to the side of the bath. This controller consisted of a bi-metallic coiled temperature sensor connected to a solid-state relay. The relay controlled the bath temperature by appropriately turning on or off the heating and refrigeration units. Inside the bath the feed lines were attached (individually) to tightly wound tubing coils of approximately 150 cm in length which were used to allow the feed stream temperatures to approach the bath temperature. The coils were attached to small segments of 0.318 cm O.D. tubing which in turn were connected to the main reactor. Check valves were installed on both feed lines to prevent fluid backup into the storage tanks.

The main reactor section was immersed in a water bath (approximately 30 L capacity). This bath was also equipped with a 2.5 kW refrigeration unit and a 1 kW heating element. The temperature of the water was controlled by the same type of system used for the preheater/cooler bath. The stirring system used for the adiabatic



batch reactor was used to mix the bath.

The reactor itself consisted of twelve sections of 29 cm long 0.318 cm O.D. stainless steel tubing. The sections were attached with Swagelok™ union tees, the third branch of each tee being fitted with a thermocouple (type J). (This was the initial set-up of the reactor. For some of the later experiments the first two sections were cut in half and two extra thermocouples were inserted.) At the front of the reactor the feed lines were joined with a Swagelok™ union cross, the extra branch being used for temperature measurement. Two thermocouples were also inserted into each feed line at distances of 20 and 5 cm from the reactor entrance. The function of these thermocouples was to obtain an accurate measure of the average reactor inlet temperature. An exit line was attached to the end of the reactor.

The OPTO 22 input/output process system and the HP 1000 computer previously mentioned were used for the temperature monitoring.

#### 4.1 EXPERIMENTAL PROCEDURE

The procedure followed for a sample set of experiments is described in this section. In this set of experiments the bath temperature was maintained constant and the inlet temperature was varied.

After the sulfite storage tank was rinsed thoroughly with distilled water, a 40-45 L batch of 1.1 M sodium sulfite solution was poured

into the tank. The pH was adjusted so that its value was in the range of 10.0 to 10.4. The solution was sufficiently buffered so as to ensure that the pH of the solution at the end of the reaction was never less than 9.0. This was extremely important as the value of the reaction rate constant was known to change outside the pH range of 9.0 to 10.4.

The amount of peroxide used for any one experiment was extremely small, relative to the amount of sulfite. Therefore, once the peroxide storage tank was filled with 40 L of peroxide, it usually sufficed for 6 - 10 sulfite batches.

Once the sulfite tank was filled it was quickly covered so as to minimize the exposure of the solution to air (and thus prevent premature oxidation). The tank was then purged with nitrogen for 5-10 minutes to ensure that any remaining oxygen ( $O_2$ ) was removed. With the purging complete, the tank was then pressurized to 790 kPa. The peroxide tank, which was de-pressurized for safety reasons during the preparation of the new sulfite solution, was then also pressurized and the storage tanks were ready for the experiments to begin.

The preheater/cooler and the reactor bath were then set at the desired temperatures. For this example the bath temperature was set at 24°C ( $\pm 0.5^\circ\text{C}$ ) and the precoolers were set at approximately 2-3°C. (The temperature of the pre-heater/cooler was never specifically monitored.

Rather, the inlet temperature of each stream was monitored and then the temperature of the preheater/cooler was adjusted accordingly.) This pre-cooler temperature resulted in an average inlet temperature of approximately 11 °C. The stirrer speed was then adjusted to setting #6 (on a scale from 0-10). This speed ensured that the bath would be sufficiently mixed and hence, isothermal.

With all the temperatures set, the computer program for the data acquisition was started. The temperatures at each tee (13 in all) along with the inlet temperatures and bath temperature were monitored at 30 second intervals. The reactant feed lines were then opened. The rotameters were set so as to have an overall flow rate of 380 ml/min - 305 ml/min for the sulfite and 75 ml/min for the peroxide (prior to performing any experiments the rotameters were calibrated; the resulting calibration curves can be found in Appendix B). The resulting temperature profile in the reactor was carefully monitored, along with the inlet and bath temperatures. When the system was deemed to be at steady state the reactant feed lines were closed and the data acquisition stopped. (The system was deemed to be at steady state when all the temperatures did not vary by more than 0.5°C over a span of five minutes.)

With one experiment completed, the pre-cooler temperature was raised so as to have an average inlet temperature of approximately 18°C. When the inlet temperature stabilized, the reactant feed lines were once

again opened. The data acquisition was begun and the steady state temperature profile was determined. The same procedure was followed for inlet temperatures of 24, 30, 34, 41, 45, and 47°C.

The procedure outlined above was used for other experiments involving a fixed bath temperature and variable inlet temperatures. In addition to these, a set of experiments where the inlet concentration of sulfite was varied was also performed. In these instances less concentrated batches of sulfite were prepared (0.975 M, 0.85 M, 0.725 M and 0.6 M) and the experiments were carried out at 3 different conditions.

Finally, a set of experiments were carried out using the impeller speed as a variable. For these experiments the stirrer speed was set at positions 0, 3 and 10 (0 here simply refers to the lowest speed available and not to the absence of any mixing).

A list of all the experiments performed is given in Table 4.1. In all cases, the flow rate was 380 ml/min and the concentration of hydrogen peroxide entering the reactor was 2.31 M. The results obtained can be found in Appendix C.

#### 4.2 EXPERIMENTAL HEAT TRANSFER EVALUATION

It has been mentioned in section 3.3 that the value of the heat transfer coefficient inside the bath was unknown. This coefficient

TABLE 4.1 EXPERIMENTAL CONDITIONS							
Bath Temperature (+/- 0.5 C)	Inlet Temperature (+/- 1.0 C)			* [Na <sub>2</sub> SO <sub>3</sub> ] <sub>o</sub> (M)	Stirrer Speed		
19.0	10.99	18.29	24.56	0.88	6		
	30.59	33.96	40.75				
	45.70	47.71					
24.0	10.99	18.29	24.56	0.88	6		
	30.59	33.96	40.75				
	45.70	47.71					
29.0	11.08	17.4		0.88	6		
	24.25	29.96					
34.0	10.99	18.29	24.56	0.88	6		
	30.59	33.96					
	40.75	45.70					
44.0	10.99	18.29	24.56	0.88	6		
	30.59	33.96	40.75				
49.0	12.33	18.19		0.88	6		
	25.35	30.59					
24.0	48.4			0.78 0.68 0.58 0.48	6		
34.0	46.0			0.78 0.68 0.58 0.48			
44.0	39.08			0.78 0.68 0.58 0.48	6		
24.0	19.0			0.88			
34.0	46.0			0.88	0	3	10
24.0	34.0			0.88	0	3	10

\* NOTE - This refers to the sulfite concentration entering the reactor

could not be determined using standard heat transfer correlations. Rather, it had to be calculated with data taken from the experimental equipment. For this reason, a few extra experiments were performed.

These experiments consisted of the sodium sulfite flowing by itself through the reactor. The preheater/cooler and reactor bath were set at different temperatures so as to obtain either a steady-state "heating" profile, or, a steady-state "cooling" profile. In all cases, the stirrer speed was at setting #6. The list of experiments performed is given in Table 4.2. The results obtained can be found in Appendix C.

TABLE 4.2 HEAT TRANSFER EXPERIMENTS		
Flow (ml/min)	Inlet Temperature ( $^{\circ}\text{C}$ )	Bath Temperature ( $^{\circ}\text{C}$ )
305	28.24	50.56
305	25.28	44.52
305	18.20	2.90

## 5.0 EXPERIMENTAL TUBULAR REACTOR - CHARACTERIZATION OF HEAT TRANSFER

Although the value of the heat transfer coefficient inside the reactor could be determined from a standard correlation, no such correlation existed for the bath side coefficient. Thus, the heat transfer coefficient inside the bath had to be determined from experimental data. This process involved using the data in order to characterize the heat transfer in the system. Two mathematical models were used in this regard.

### 5.1 HEAT TRANSFER COEFFICIENT DETERMINATION

The ODPH model introduced earlier (equations 3.3 and 3.4) in section 3.3 can be simplified to the following form when no reaction takes place

$$\frac{dT}{dz} = - \frac{U \cdot \pi \cdot D \cdot (T - T_c)}{Q \cdot C_p \cdot \rho} \quad (5.1)$$

$$\frac{dC_A}{dz} = 0 \quad (\text{i.e., } C_A(z) = C_{A0}) \quad (5.2)$$

Equation 5.1 can be solved analytically, yielding an expression for T in terms of z with F,  $C_p$ ,  $\rho$ , D,  $T_c$  and U as the system parameters. If F,  $C_p$ ,  $\rho$ , D,  $T_c$  are known then temperature profiles can be determined with U as the only parameter.

The ODPH model, however, is not the only homogeneous model that can be

used to describe the behavior of a tubular reactor. If, in the ODPH model, the assumptions of negligible radial and axial heat and mass dispersion are relaxed, then a two dimensional model results. The equations describing this model (henceforth referred to as the two dimensional pseudo homogeneous model, or TDPH) are:

$$\frac{\partial^2 T}{\partial z^2} + \frac{\partial^2 T}{\partial r^2} + \frac{1}{r} \cdot \frac{\partial T}{\partial r} - \frac{u \cdot \rho \cdot C_p}{k_f} \cdot \frac{\partial T}{\partial z} = \frac{\Delta H \cdot R_A}{k_f} \quad (5.3)$$

$$\frac{\partial^2 C_A}{\partial z^2} + \frac{\partial^2 C_A}{\partial r^2} + \frac{1}{r} \cdot \frac{\partial C_A}{\partial r} - \frac{u}{D_e} \cdot \frac{\partial C_A}{\partial z} = \frac{R_A}{D_e} \quad (5.4)$$

where

$k_f$  = thermal conductivity of fluid (W/(m·K))

$D_e$  = effective diffusivity of species A (m<sup>2</sup>/s)

$R_A$  = reaction rate with respect to species A as defined in equation 3.3

The solution of these non-linear, coupled, partial differential equations is more difficult than that of the ODPH model. However, the equations can be simplified. The effective diffusivity,  $D_e$ , can usually be assumed to be quite small in value. When this assumption is made, the first three terms of equation 5.4 can be set to zero. If the conditions are such that no reaction is occurring, then  $C_A(z) = C_{A0}$  and the right hand side of (5.3) becomes 0. Thus, the temperature profile is described by:



$$\frac{\partial^2 T}{\partial z^2} + \frac{\partial^2 T}{\partial r^2} + \frac{1}{r} \cdot \frac{\partial T}{\partial r} - \frac{u \cdot \rho \cdot C_p}{k_f} \frac{\partial T}{\partial z} = 0 \quad (5.5)$$

The boundary conditions most commonly used are:

$$\left. \frac{\partial T}{\partial r} \right|_{r=0} = 0 \quad (5.5a)$$

$$-k_f \cdot \pi \cdot D_1 \cdot \left. \frac{\partial T}{\partial r} \right|_{r=D_1/2} = U_o \cdot \pi \cdot D_o \cdot (T - T_c) \Big|_{r=D_1/2} \quad (5.5b)$$

$$\left. \frac{\partial T}{\partial z} \right|_{z=L} = 0 \quad (5.5c)$$

$$u \cdot \rho \cdot C_p \cdot (T_o - T) \Big|_{z=0} = -k_f \cdot \left. \frac{\partial T}{\partial z} \right|_{z=0} \quad (5.5d)$$

Equation 5.5, along with the boundary conditions, can be solved numerically using standard finite difference methods. If the physical parameters of the system are specified then the resulting solution becomes a function of the overall heat transfer coefficient ( $U_o$ ) only.

The data obtained from the heat transfer experiments were compared with the numerical solutions of both models (ODPH and TDPH). In each case, an attempt was made to determine the value of the overall heat transfer coefficient that best correlated the data with the model. The results obtained for one set of data are illustrated in Figures 5.1, 5.2 and 5.3.

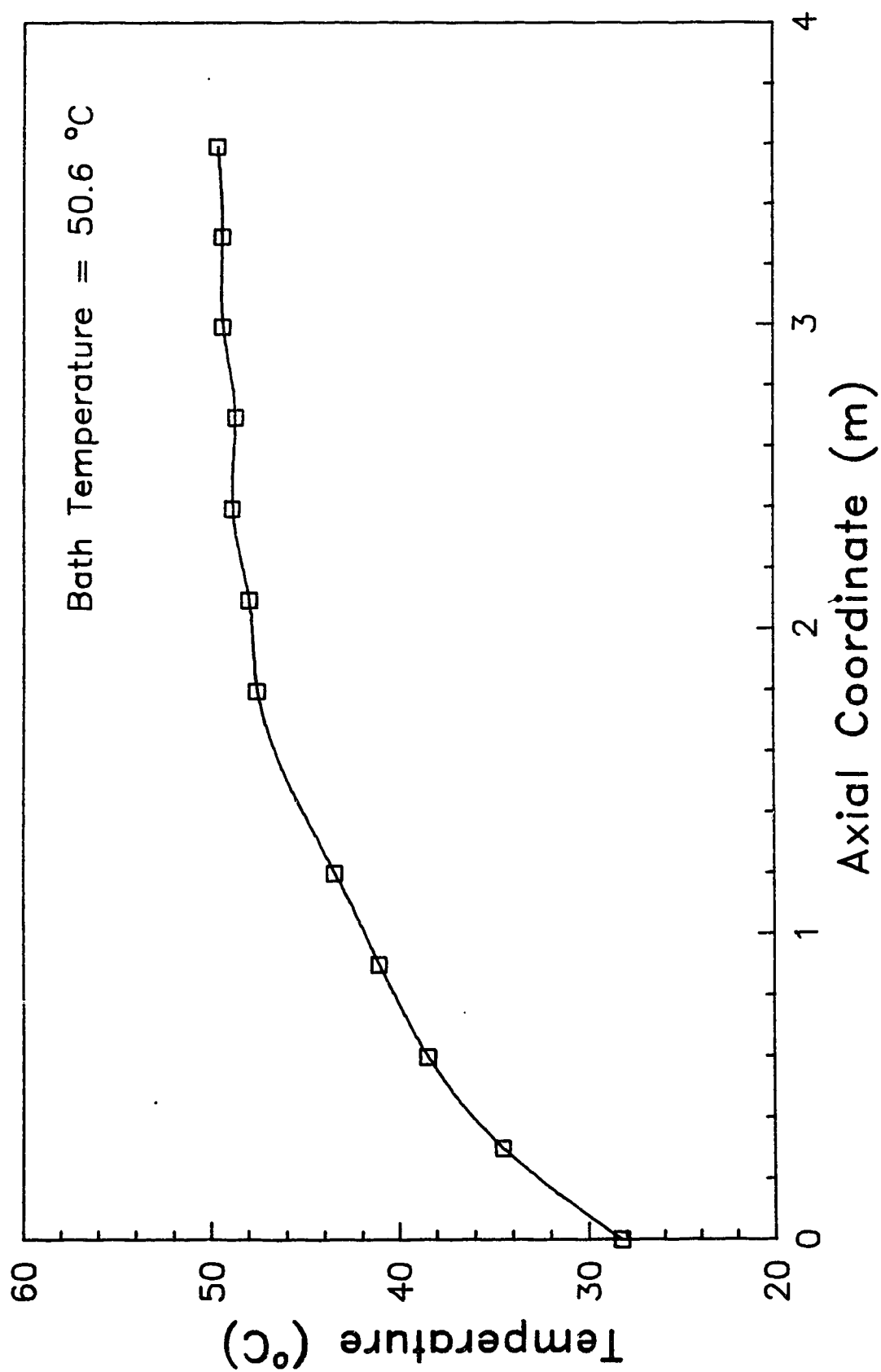


Figure 5.1 Experimental Heat Transfer Data  
Data from Table C.1

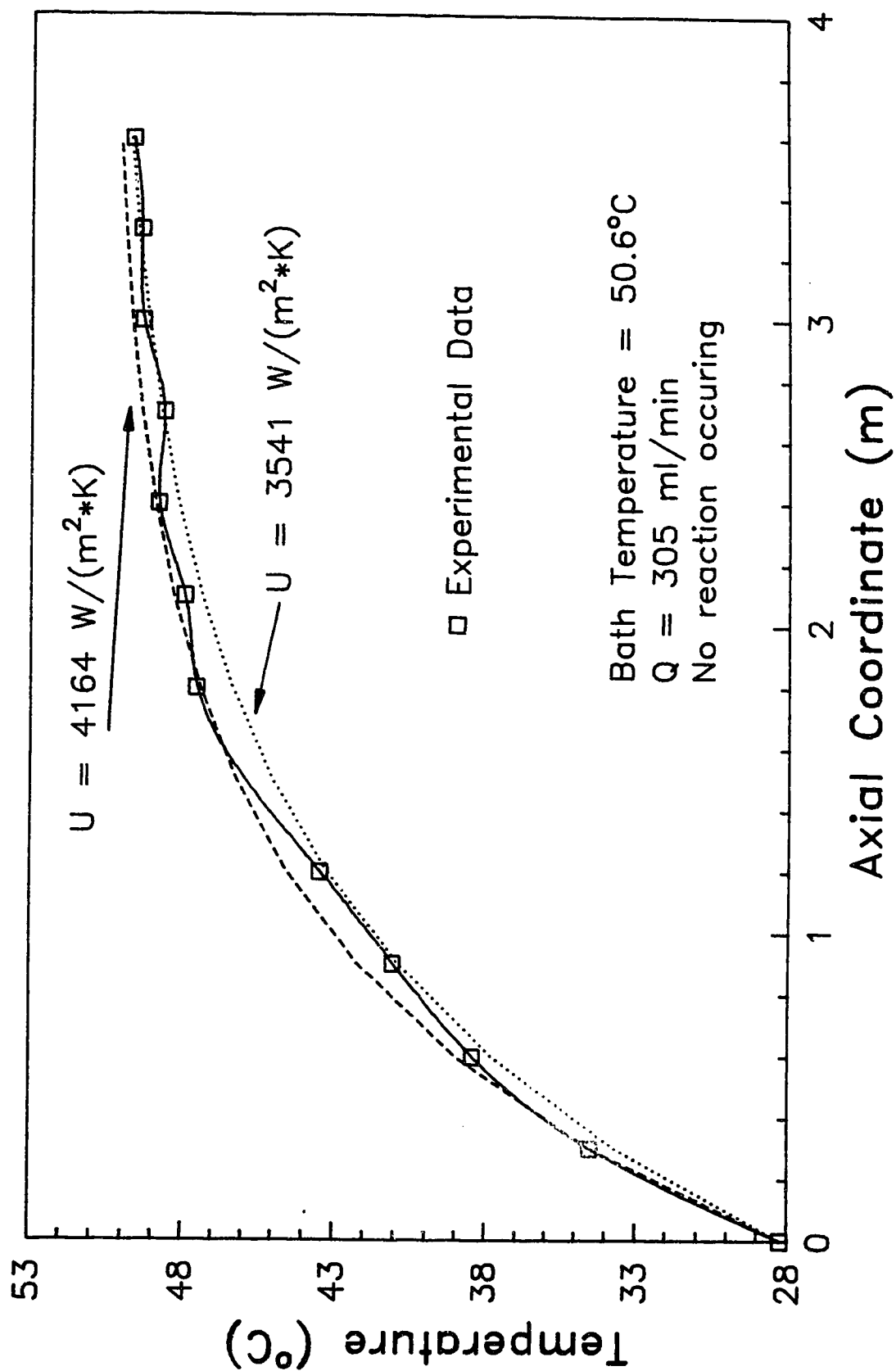


Figure 5.2 Comparison of Heat Transfer Data with ODPH Model

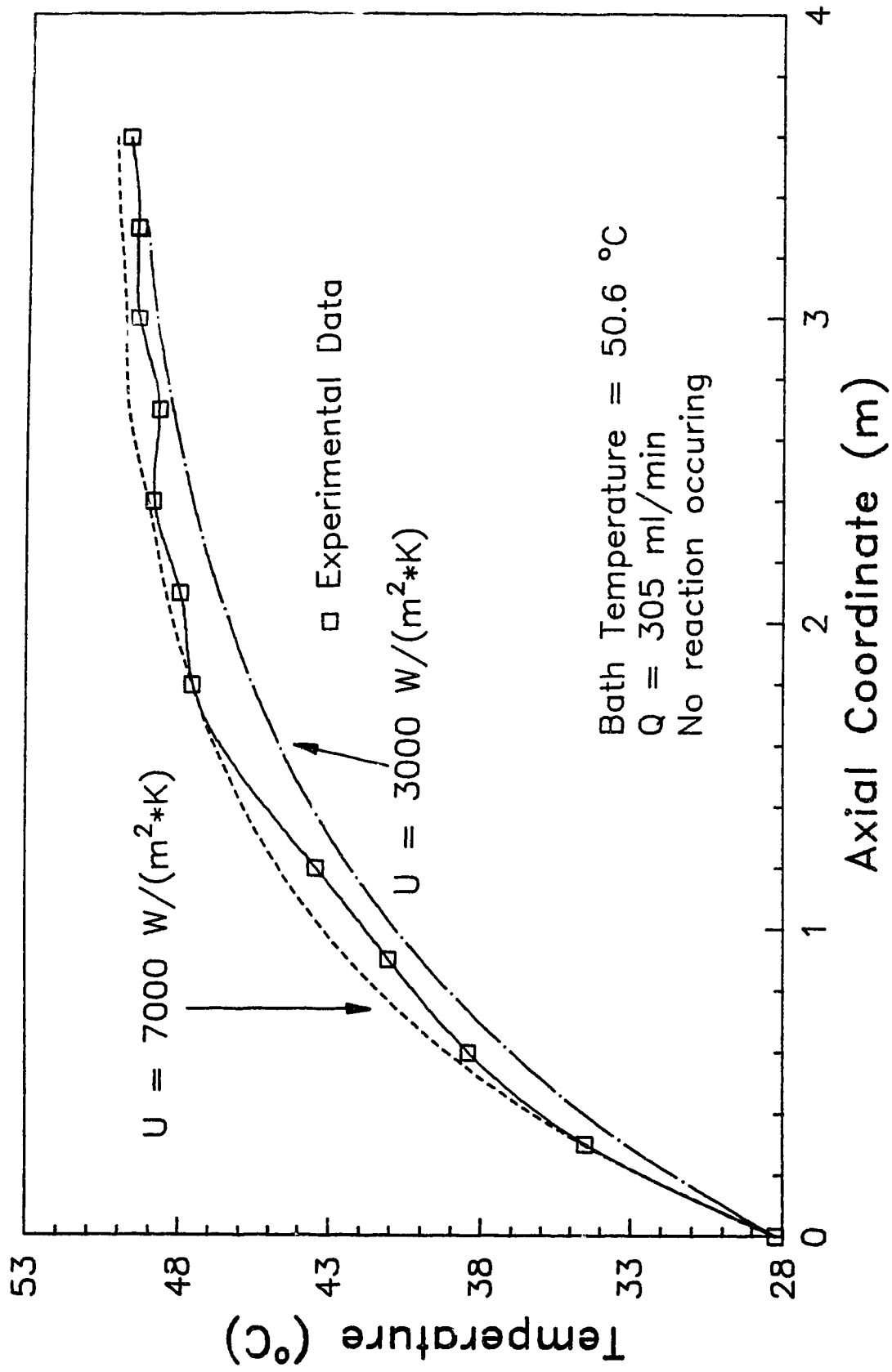


Figure 5.3 Comparison of Heat Transfer Data with TDPH Model

It is important to note here that, for both models, the effect of the change of tubing diameter and heat transfer area at the tees was taken into account (see Appendix D for a detailed explanation as to how this was done). In addition, the axial temperatures reported for the TDPH model are the radially averaged temperatures for those axial positions.

In addition, it should be noted that the evaluation of the overall heat transfer coefficient under non-reacting conditions is entirely permissible. Unlike a heterogeneous catalytic reactor where the heat transfer coefficient differs under reacting and non-reacting conditions, the heat transfer in a homogeneous reactor can be safely evaluated under non-reacting conditions.

It can be seen from both figures that, for each model, a value for the overall heat transfer coefficient exists that can adequately describe the data. This indicates that both models can be used to describe the experimental system when it used for heating/cooling purposes. The values of  $U$  that best describe the data are listed in Table 5.1. The value chosen in each case was that which minimized the sum of the square of the temperature differences between the profiles.

TABLE 5.1		
Overall Heat Transfer Coefficients (U) (W/(m <sup>2</sup> ·K))		
Heat Transfer Experiment	ODPH Model	TPH Model
1	3 823	5 000
2	4 005	6 000
3	2 920	2 500

NOTE : The ODPH values are based on inside area ( $U_i$ ) and are weighted averages due to the change in value of U at the tubing tees. The TDPH values are based on the outside area ( $U_o$ ).

Overall heat transfer coefficients are not necessarily constant along the entire length of the reactor. Entrance effects may result in the heat transfer coefficient at the inlet being significantly different than the coefficient inside the main section of the reactor. However, for this particular system, a variation of less than 5% in the heat transfer coefficient can be expected within 2-3 cm of the reactor inlet. This can be seen from examination of the entrance effect correlation illustrated by Holman (1981).

A closer examination of the results of the TDPH model indicated that the temperature of the fluid at the wall was essentially equal to the coolant temperature throughout the length of the reactor. This suggests that boundary condition 5.5b could be replaced by a simpler condition:

$$T = T_c \text{ at } r = D_i/2 \quad (5.5e)$$

In addition, it was noted that the radial temperature profile was essentially uniform from  $r=0$  to  $r=2/3 \cdot D_1/2$ . (This was also noted when the TDPH model was used with a reaction occurring as described in Chapter 7.) Thus from these last two observations, it can be said that a one dimensional model is an acceptable description of the heat transfer.

For the ODPH model the value of the overall heat transfer coefficient can be expressed as the inverse sum of a series of heat transfer resistances:

$$\frac{1}{U_1} = \frac{1}{h_1} + \frac{\Delta t}{k_t} \cdot \frac{D_1}{D_{lm}} + \frac{D_1}{D_o} \cdot \frac{1}{h_o} \quad (5.6)$$

(if  $U$  is based on the inside tubing area, or)

$$\frac{1}{U_o} = \frac{D_o}{D_1} \cdot \frac{1}{h_1} + \frac{\Delta t}{k_t} \cdot \frac{D_o}{D_{lm}} + \frac{1}{h_o} \quad (5.7)$$

(if  $U$  is based on the outer heat transfer area)

where

$h_o$  - outside heat transfer coefficient ( $W/(m^2 \cdot K)$ )

$h_1$  - inside heat transfer coefficient ( $W/(m^2 \cdot K)$ )

$k_t$  - thermal conductivity of tubing ( $W/(m \cdot K)$ )

$\Delta t$  - wall thickness of tubing (m)

$D_{lm}$  - log mean diameter  $= (D_o - D_1) / \ln(D_o / D_1)$

Therefore,  $U$  can be calculated from the inner and outer heat transfer coefficients (assuming the physical parameters are known). Conversely, the value for one of the heat transfer coefficients ( $h_o$  or  $h_i$ ) can be determined if the values for  $U$  and the other heat transfer coefficient are known. For the experimental tubular reactor both  $h_i$  (determined from a heat transfer correlation) and  $U$  (evaluated from the model/data correlations mentioned previously) were known. Thus, a value for  $h_o$ , which in this case was equivalent to the heat transfer coefficient in the bath, could be determined using equation 5.6 (or 5.7). The values of  $h_o$  obtained by this method are given in Table 5.2.

TABLE 5.2	
Bath Side Heat Transfer Coefficients Determined From ODPH Model	
Heat Transfer Experiment	Heat Transfer Coefficient ( $W/(m^2 \cdot K)$ )
1	4 800
2	5 600
3	2 700
Average Value	4 367

For the TDPH model, the relationship between  $U$  and the individual heat transfer coefficients differs from that of the ODPH model. Since the TDPH model does not assume that the entire heat transfer resistance exists at the wall, equations 5.6 and 5.7 are not strictly valid. Rather, a term that accounts for the heat transfer resistance within



the fluid itself must be included. Barkeley (1959) suggested the following:

$$\frac{1}{U_1} = \frac{1}{h_1} + \frac{\Delta t}{k_t} \cdot \frac{D_1}{D_{lm}} + \frac{D_1}{D_o} \cdot \frac{1}{h_o} + \frac{1}{8} \cdot \frac{D_1}{k_f} \quad (5.8)$$

For  $U_o$  the equation becomes:

$$\frac{1}{U_o} = \frac{D_o}{D_1} \cdot \frac{1}{h_1} + \frac{\Delta t}{k_t} \cdot \frac{D_o}{D_{lm}} + \frac{1}{h_o} + \frac{1}{8} \cdot \frac{D_1}{k_f} \quad (5.9)$$

Similar to the ODPH model, a value for  $h_o$  can be determined from equation 5.8 (or 5.9).

Attempts to calculate a value for  $h_o$  using equation 5.9 and the results from Table 5.1 proved unsuccessful however. This was due to the rather large value of the  $D_1/(8 \cdot k_f)$  term in the equation. This term was larger in value than any of the  $1/U_o$  values, thus requiring negative values of  $h_o$  in order for the equality to be satisfied. Negative values for  $h_o$  did not make any sense.

It was possible that equation 5.9 was inappropriate, or, that the values used for the physical parameters of the system were incorrect (i.e., the values used for parameters such as density, or thermal conductivity, were those of water at 0°C). These approximations were necessary as there were no values available for the actual solutions used. It is known that the effective value of the thermal conductivity is affected by the flow conditions during turbulent flow. Larger

effective values of  $k_f$  in equation 5.9 would result in physically reasonable values of  $h_o$ .

The only conclusion that could be drawn from the heat transfer experiments was this: either the ODPH or the TDPH model could be used to describe the data, with the ODPH model being an appropriate choice given the lack of significant profiles either radially, or axially along the wall.

## 6.0 EXPERIMENTAL TUBULAR REACTOR - RESULTS AND DISCUSSION

The data obtained for the parametric sensitivity experiments are examined here. The data will be presented in four sections. Three of the sections are characterized by the operating parameter which was varied during that set of experiments. A fourth section presents some transient experimental data. A complete list of the data can be found in Appendix C.

### 6.1 EXPERIMENTAL TUBULAR REACTOR - TRANSIENT DATA

As mentioned in section 4.1, the system was assumed to be at steady-state when the temperature measurements did not change by more than  $0.5^{\circ}\text{C}$  over a span of 10 sampling intervals (5 minutes). This "definition", at it were, was based on initial observations made of the reactor. These observations of the transient behavior of the reactor indicated that steady-state was reached well within 1 minute of the start of the experiment. This can be seen in Figure 6.1.

Figure 6.1 illustrates the change in the temperature profile as the peroxide solution is added to the sulfite (which is already flowing through the reactor). It should be noted from this point on that, for any experimental data presented in graphical form, a cubic spline has been fitted through the data so as to obtain a smooth curve. The initial temperature profile (at  $t = 0$ ) is the steady-state profile of the sulfite being cooled as it flows through the reactor. It can be seen that the reactor reaches steady-state well within 1 minute. This

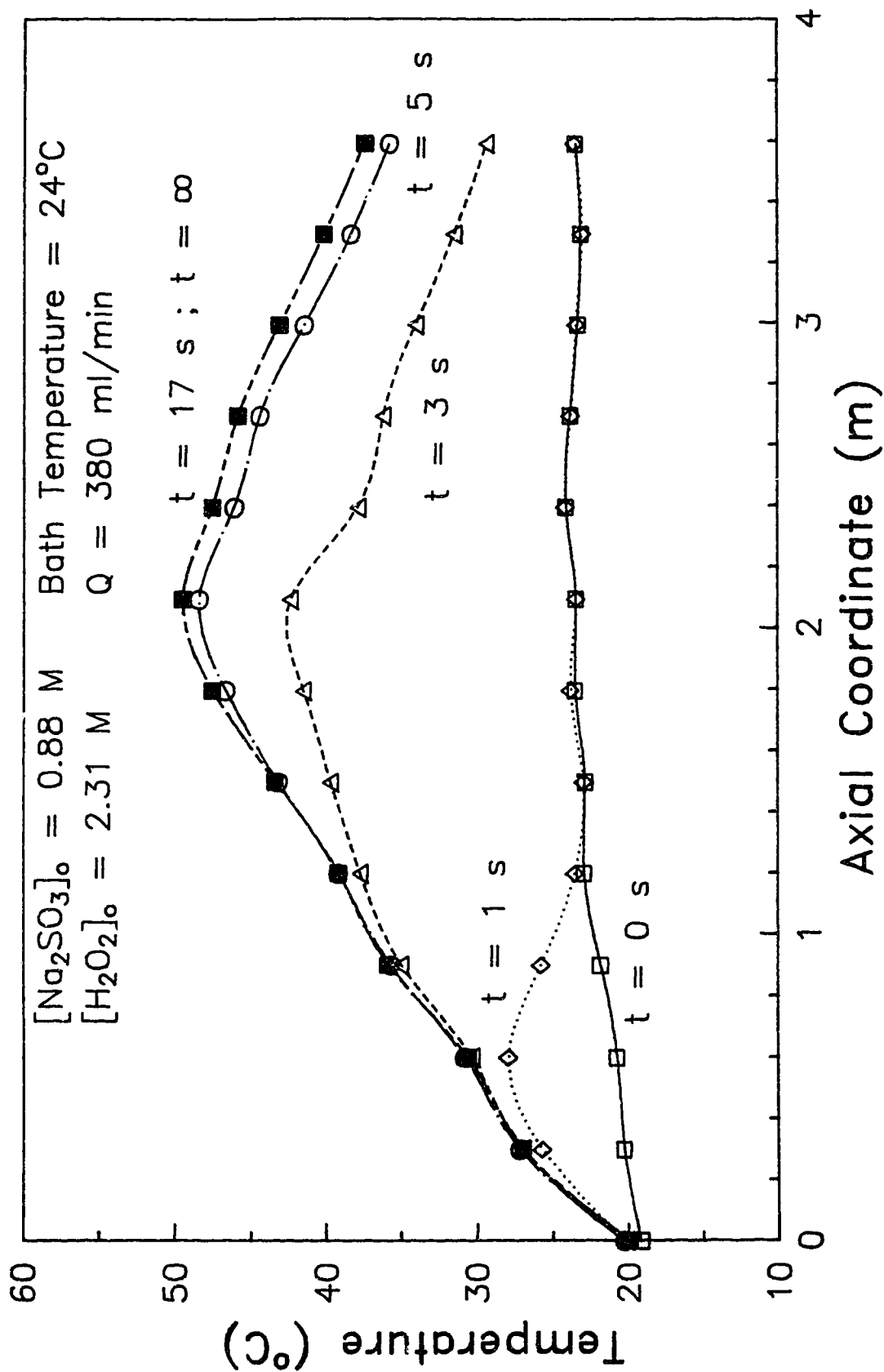


Figure 6.1 Tubular Reactor – Transient Experimental Data  
Data from Tables C.61A – C.61N

figure is representative of all the experiments and hence, shows the validity of using 10 sampling intervals as a basis for steady-state profile evaluation.

## 6.2 EXPERIMENTAL TUBULAR REACTOR - VARIATION OF INLET TEMPERATURE

Figure 6.2 is the steady-state profile illustrated in Figure 6.1. This profile, along with the other temperature profiles for a fixed bath temperature of  $24^{\circ}\text{C}$  are illustrated in Figure 6.3.

The data obtained for the other 5 bath temperatures are illustrated in Figures 6.4, 6.5, 6.6, 6.7 and 6.8 (a list of the bath temperatures and the inlet temperatures used for each set of profiles can be found in Table 4.1). Figure 6.4 will now be examined in more detail so as to discuss some of the features that are common to all six figures.

The temperature profile in Figure 6.4 corresponding to an inlet temperature of  $11^{\circ}\text{C}$  is shown by itself in Figure 6.9. With the maximum temperature located at the reactor outlet, the figure resembles that of a heating curve for a tube and shell heat exchanger (with constant shell-side temperature). The fact that the final temperature is higher than the bath temperature indicates that a finite, albeit small, amount of reaction took place.

The temperature profiles for inlet temperatures of  $11^{\circ}\text{C}$ ,  $19^{\circ}\text{C}$ ,  $25^{\circ}\text{C}$  and  $30^{\circ}\text{C}$  (again for a bath temperature of  $19^{\circ}\text{C}$ ) are repeated in Figure

6.10. It can be seen from this figure that, as the inlet temperature increases, the hot-spot moves from the reactor exit to somewhere in the middle of the reactor. This indicates that, as the inlet temperature is raised, the reaction rate, and hence the rate of heat generation, becomes a significant factor. The temperature profile thus begins to assume its characteristic shape (i.e., a bell shaped curve with a maximum located somewhere in the middle).

This last point can be illustrated by considering the two competing factors that contribute to the reactor behavior (and thus the temperature profile). These two factors are heat generation from the reaction and heat removal/addition to/from the bath by convection. (These factors are illustrated mathematically in equation 3.3, which is the energy balance for the ODPH Model. The two terms on the right hand side represent, respectively, the rate of heat generation by reaction and the rate of heat removal/addition to/from the bath by convection.) When the inlet temperature is low the convection term is much larger than the heat generation term (due to the low rate of reaction) and the reactor behaves as a tube and shell exchanger with constant shell side temperature. Under these conditions, the reactor is said to be heat transfer controlled. As the inlet temperature is increased, the rate of heat generation becomes significant and both factors contribute to the temperature change in the reactor. Under these conditions, the reactor can be said to be both heat transfer and reaction controlled.

It is in this instance (i.e., both heat transfer controlled and reaction controlled) that the characteristic hot-spot is observed. The occurrence of the hot-spot can be explained as follows. Since the rate of heat generation increases exponentially with temperature, whereas the heat removal rate only increases linearly, the temperature of the fluid in the reactor begins to rise. A point is eventually reached somewhere in the reactor where the reactants are sufficiently consumed so that the energy removal becomes larger than the energy generation and the temperature then begins to decrease.

It can be seen from Figure 6.4 that the effect of inlet temperature on the hot spot temperature is initially quite small. For the first twenty degree rise in inlet temperature, the hot-spot temperature does not change by more than 15 degrees. However, when the inlet temperature is increased from 34 to 41°C, the hot-spot temperature changes dramatically, increasing in value by about 20 degrees. Further increases of five degrees (or less) in the inlet temperature produce the same result.

The dramatic increase in the hot-spot temperature can again be explained by examination of the processes occurring in the reactor. If the inlet temperature is sufficiently high, then the energy generation rate term is initially much larger than the convection rate and the reactor behaves almost adiabatically. Thus the initial temperature increase will appear to be adiabatic. Eventually, as the temperature

increases and the amount of reactant decreases, the rate of heat loss by convection becomes significant and the temperature profile begins to take on its characteristic shape. However, by this point, the hot-spot temperature will be quite large, approaching the value of the maximum adiabatic temperature for the reaction conditions. This set of conditions corresponds to a reactor which is said to be reaction controlled.

The existence of parametrically sensitive operating conditions is illustrated in Figure 6.4. At or about an inlet temperature of 30 degrees, the hot-spot temperature becomes parametrically sensitive to the value of the inlet temperature. This change in conditions, from insensitive to sensitive, was the expected result. From this set of profiles, the sensitive operating conditions can be separated from the insensitive ones and the experimentally observed onset of parametric sensitivity can be compared with that predicted from various sensitivity criteria. By necessity this would have to involve an arbitrary definition of what constituted a set of experimental parametrically sensitive operating conditions. The discussion of this point will be reserved for section 8.1.

An interesting feature of this set of data is illustrated in Figure 6.11. This figure shows that a slight discrepancy exists between the inlet temperature and the temperature measured at thermocouple #1. In all cases, the inlet temperature is lower than the value of the



temperature measured at thermocouple #1. Based on the assumption that the only process occurring at the reactor inlet is the mixing of the two fluid streams, there should not be a temperature difference. However, since the temperature difference is obviously there, then the assumption is likely wrong. A few possible explanations for what was actually occurring were examined.

It is possible that the observed temperature difference was due to the heating/cooling of the fluids in the feed lines by the bath (by necessity, the last portions of the feed lines had to be immersed in the bath). However, if this were so, then the inlet temperature should have been higher than the temperature at thermocouple #1 for the case of an inlet temperature greater than the bath temperature. This was not observed in any case.

Another possible explanation is that the fluids were being mixed in a region that extended outside of the tubing union. This could be possible if one fluid reached the mixing point at a higher pressure than the fluid. In this case, the higher pressure fluid would push the other back up into the inlet line. The end result of this would be the creation of a "mixing zone", as it were, around the first thermocouple. Since the fluids would react upon mixing, the temperature at the thermocouple could be greater than that of inlet temperature. This explanation was plausible as the two inlet streams, although starting at the same pressure, traveled different lengths of

tubing at different flow rates and thus, did not necessarily arrive at the mixing point at the same pressure.

The temperature profile in Figure 6.6 corresponding to an inlet temperature of 35°C illustrates a peculiarity of some of the data. This peculiarity is a "kink", as it were, in the initial part of the profile (thermocouples 1, 1A, 2, 2A and 3). The profile is almost as if the temperature measured at thermocouple 1A were too high. Strangely, this only appeared for the later experiments where extra thermocouples (thermocouples 1A and 2A - see appendix C for exact locations) were inserted into front portion of the reactor. Since there is no theoretical explanation for this, the only conclusion that can be drawn is that thermocouple 1A was physically "damaged", in some sense, when it was placed in the reactor and this caused it to malfunction (i.e., perhaps the thermocouple was improperly positioned and, instead of measuring the fluid temperature, it was actually measuring the wall temperature, or a combination of the two).

### 6.3 EXPERIMENTAL TUBULAR REACTOR - VARIATION OF SULFITE CONCENTRATION

The effect of changing the inlet sulfite concentration was studied at three different operating conditions (characterized by the inlet and the bath temperatures). All other parameter values were maintained constant as the temperature profiles were determined for sulfite concentrations of 0.78, 0.68, 0.58 and 0.48 M. A list of the conditions studied can be found in Table 4.1.

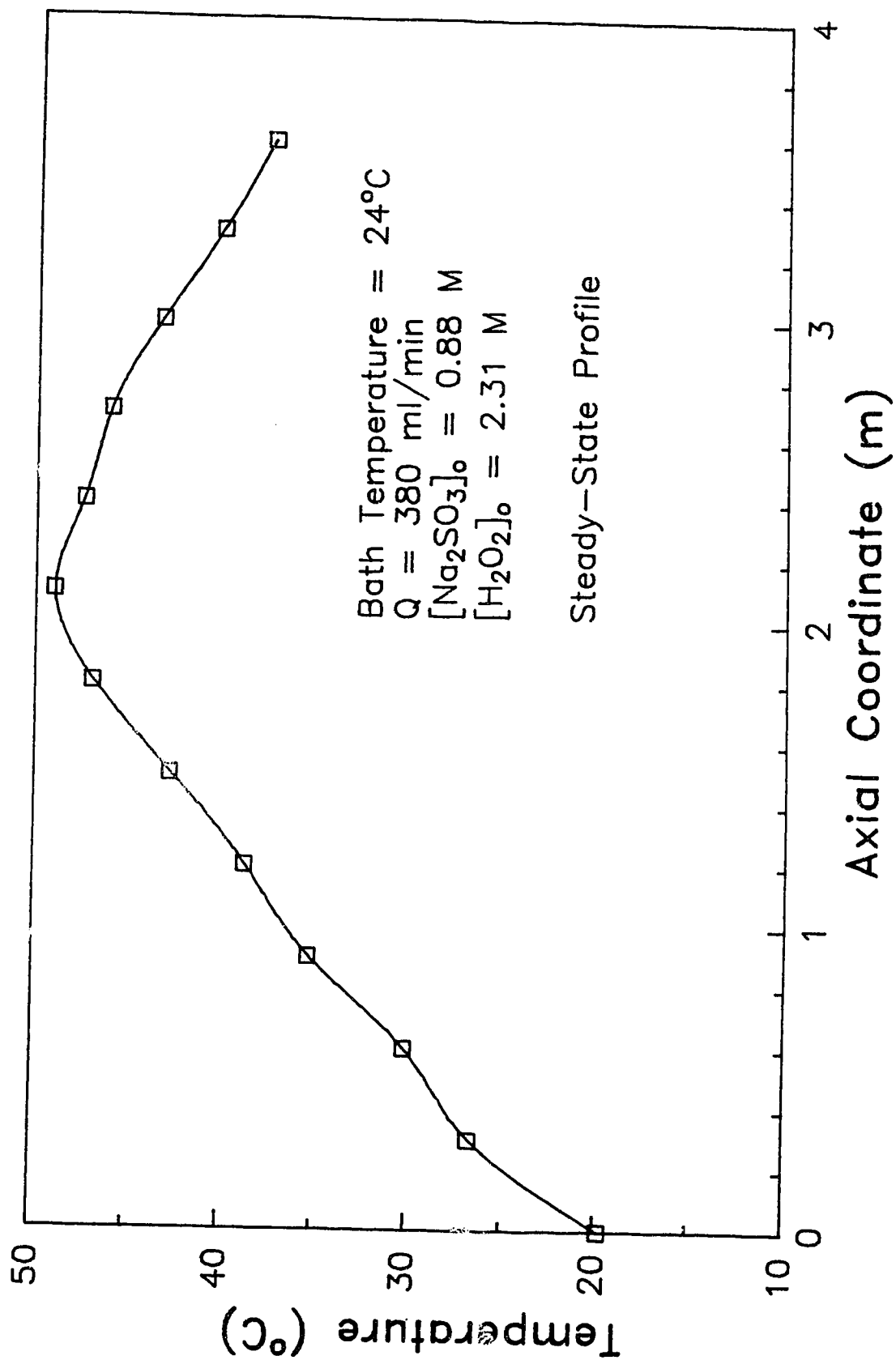


Figure 6.2 Tubular Reactor – Experimental Data

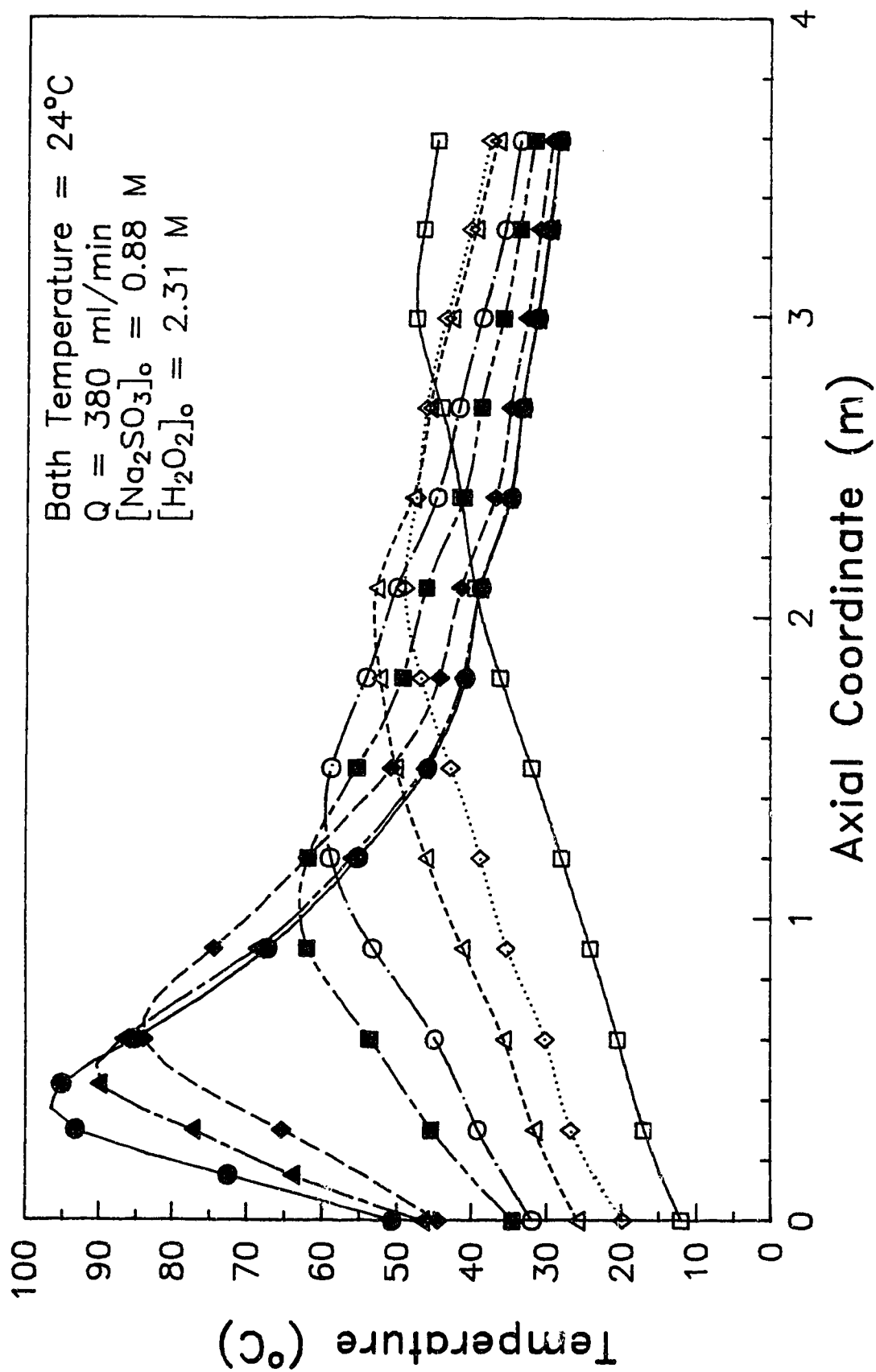


Figure 6.3 Experimental Data  
 Data from Tables C.4 – C.11

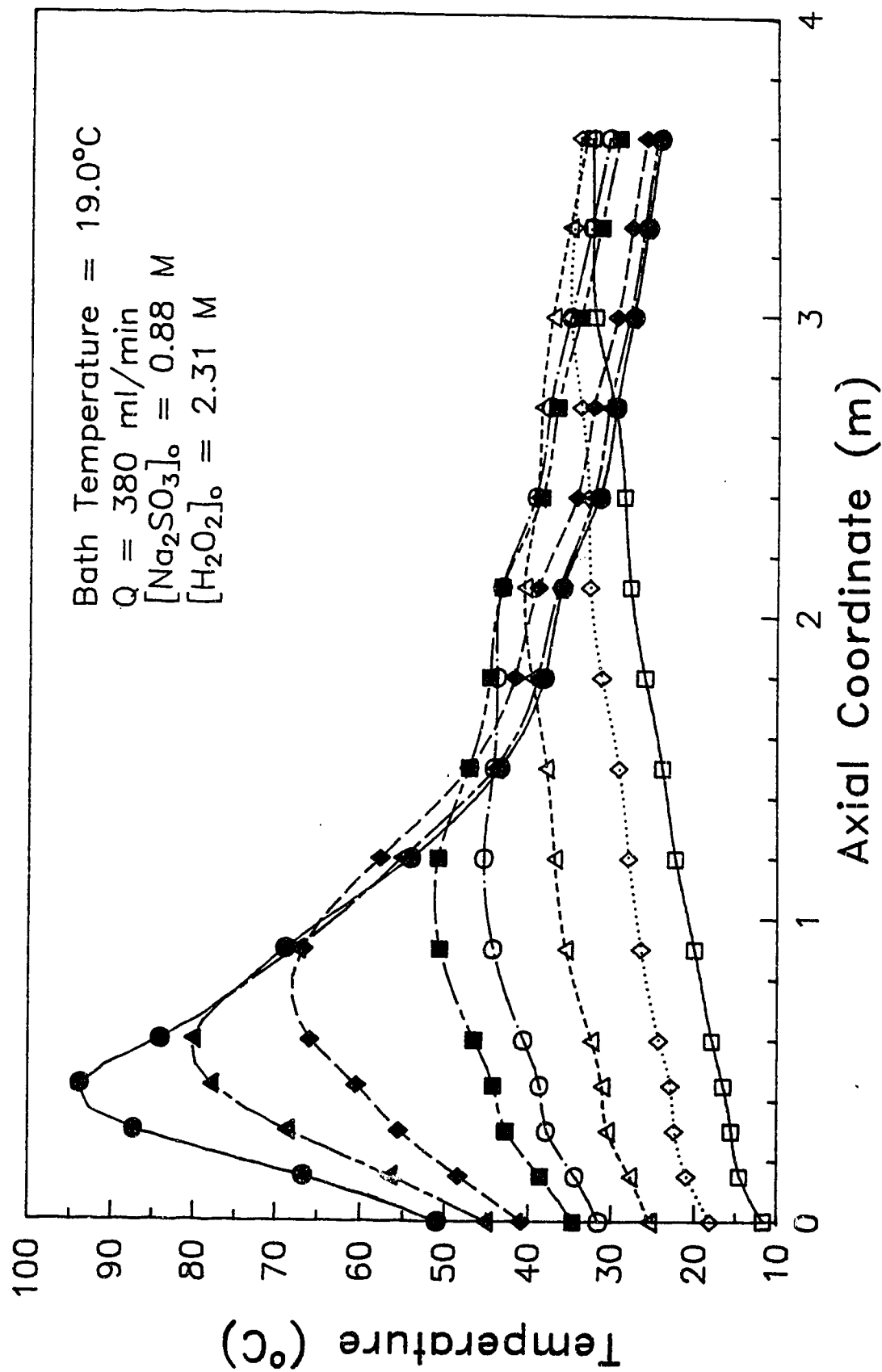


Figure 6.4 Experimental Data  
 Data from Tables C.29 – C.36



National Library  
of Canada

Bibliothèque nationale  
du Canada

Canadian Theses Service

Service des thèses canadiennes

Ottawa, Canada  
K1A 0N4

## NOTICE

The quality of this microform is heavily dependent upon the quality of the original thesis submitted for microfilming. Every effort has been made to ensure the highest quality of reproduction possible.

If pages are missing, contact the university which granted the degree.

Some pages may have indistinct print especially if the original pages were typed with a poor typewriter ribbon or if the university sent us an inferior photocopy.

Reproduction in full or in part of this microform is governed by the Canadian Copyright Act, R.S.C. 1970, c. C-30, and subsequent amendments.

## AVIS

La qualité de cette microforme dépend grandement de la qualité de la thèse soumise au microfilmage. Nous avons tout fait pour assurer une qualité supérieure de reproduction.

S'il manque des pages, veuillez communiquer avec l'université qui a conféré le grade.

La qualité d'impression de certaines pages peut laisser à désirer, surtout si les pages originales ont été dactylographiées à l'aide d'un ruban usé ou si l'université nous a fait parvenir une photocopie de qualité inférieure.

La reproduction, même partielle, de cette microforme est soumise à la Loi canadienne sur le droit d'auteur, SRC 1970, c. C-30, et ses amendements subséquents.

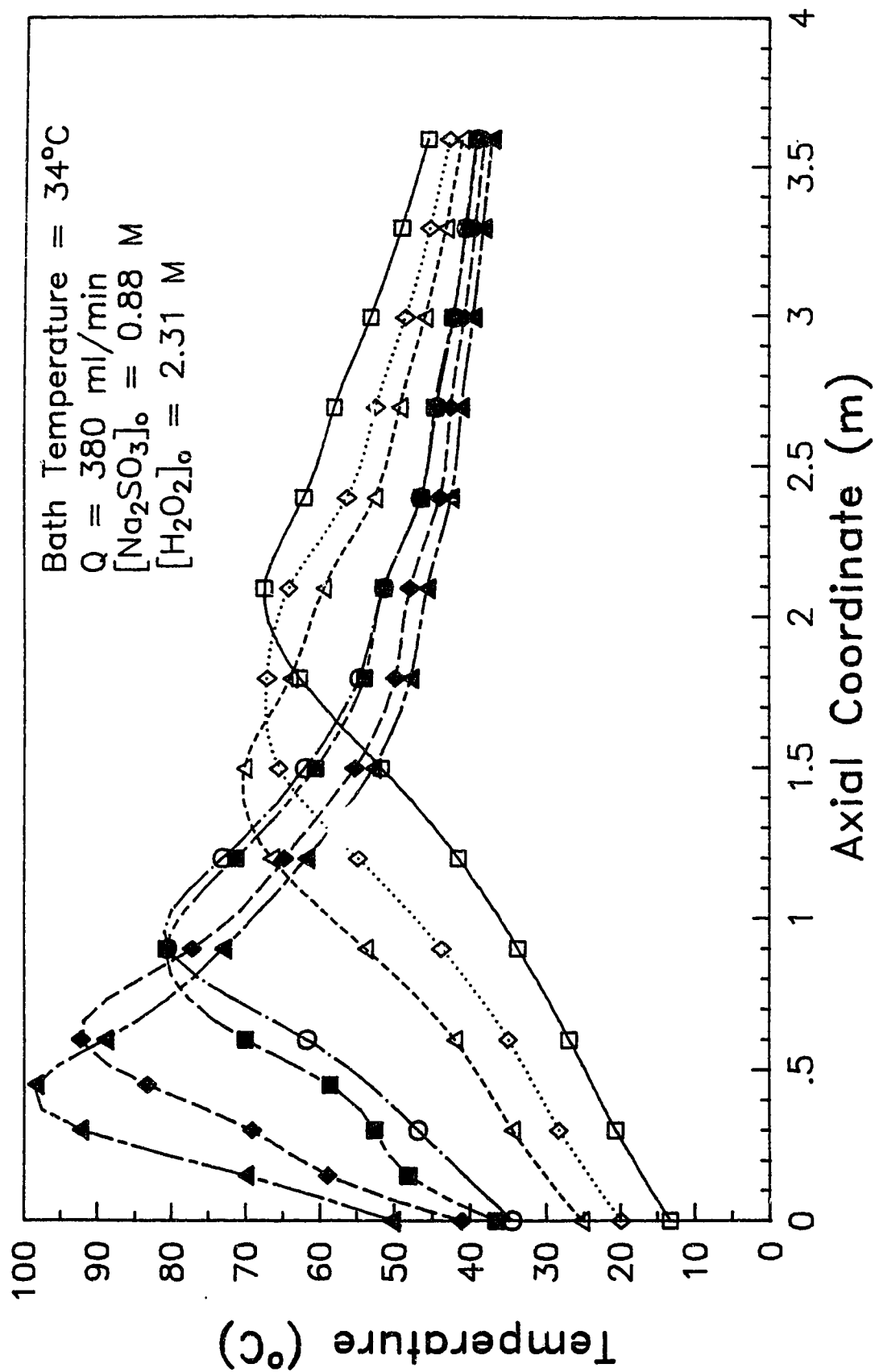


Figure 6.5 Experimental Data  
 Data from Tables C.12 – C.18

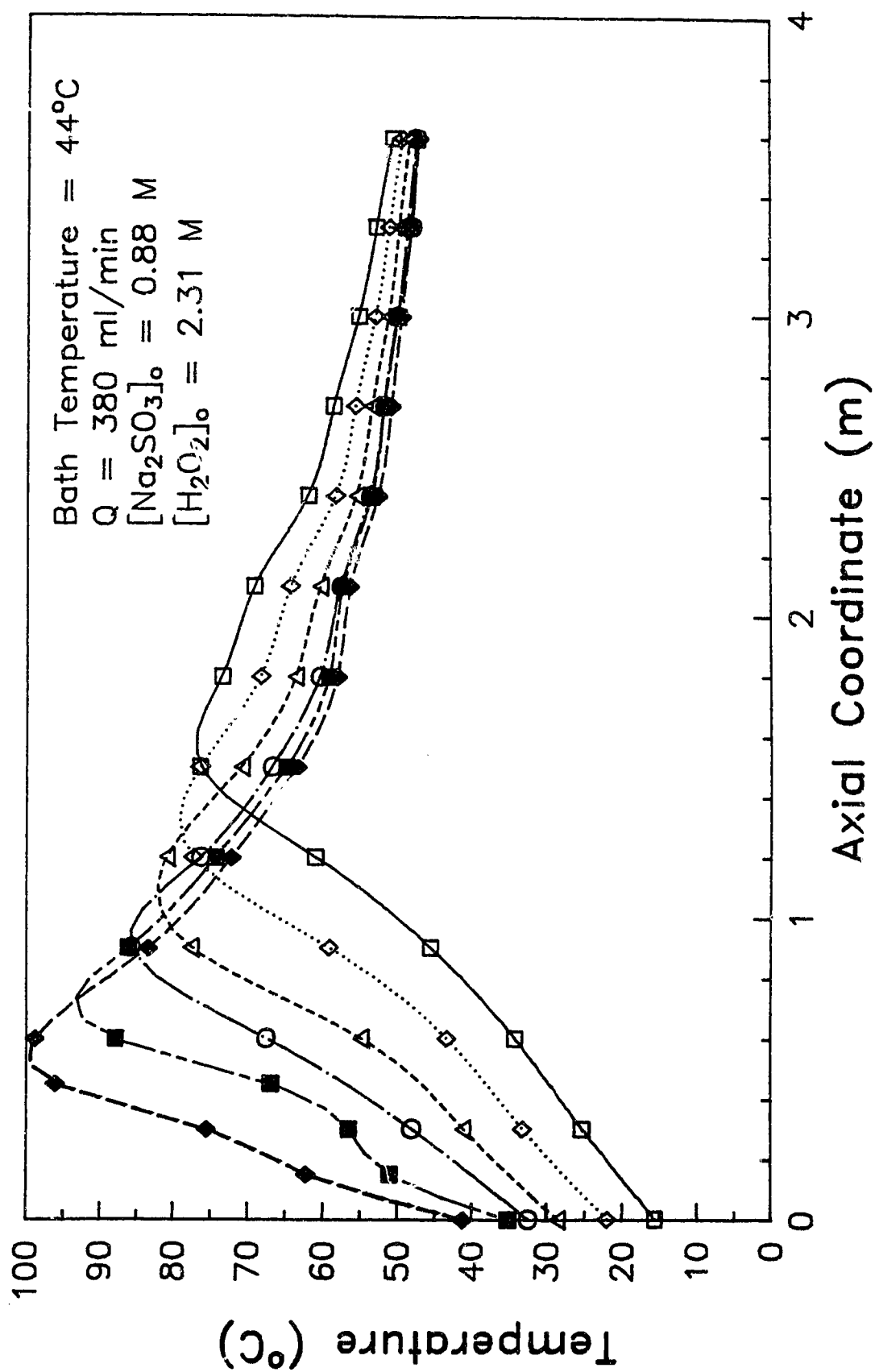


Figure 6.6 Experimental Data  
 Data from Tables C.19 – C.24



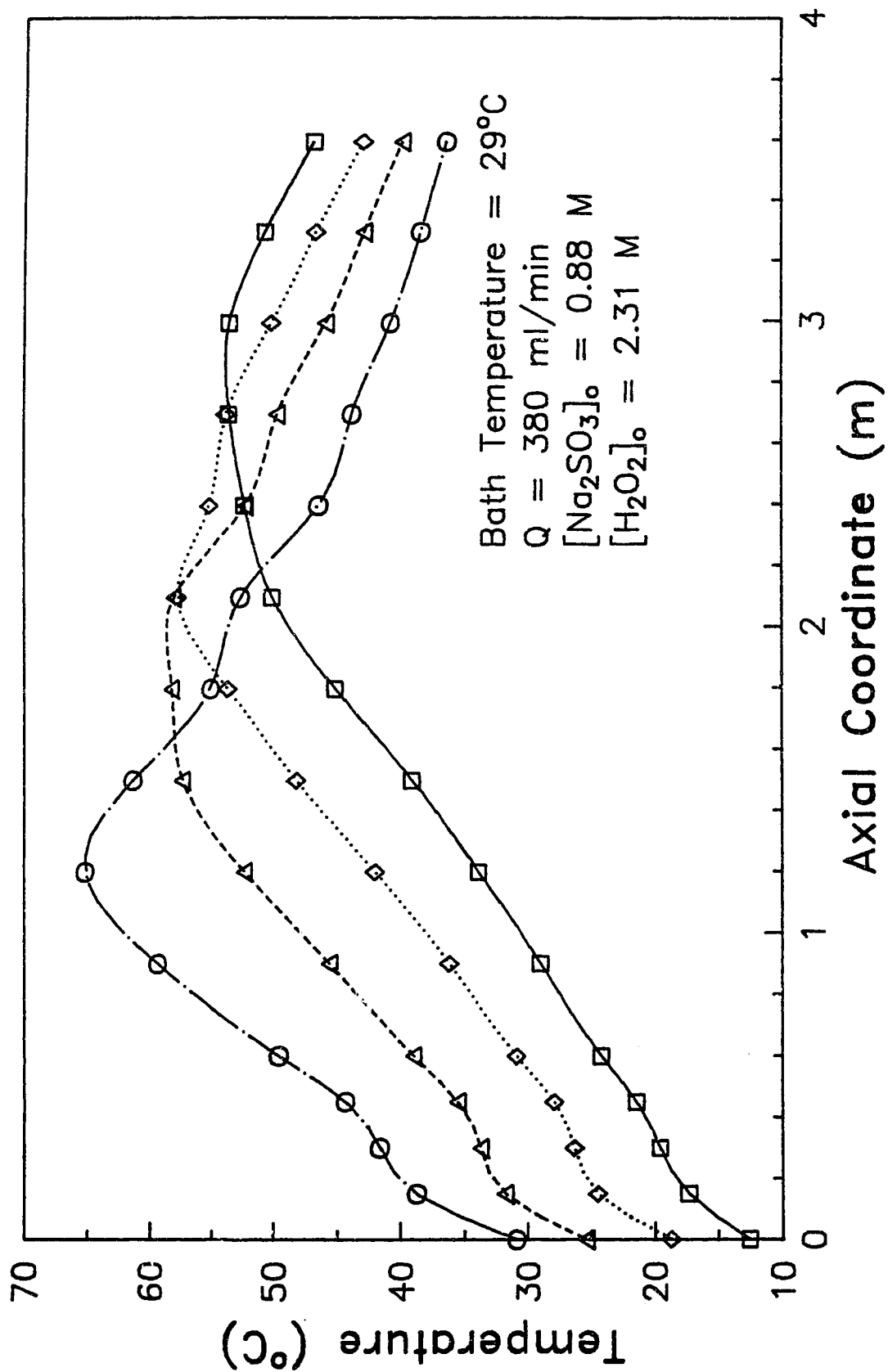


Figure 6.7 Experimental Data  
Data from Tables C.25 - C.28

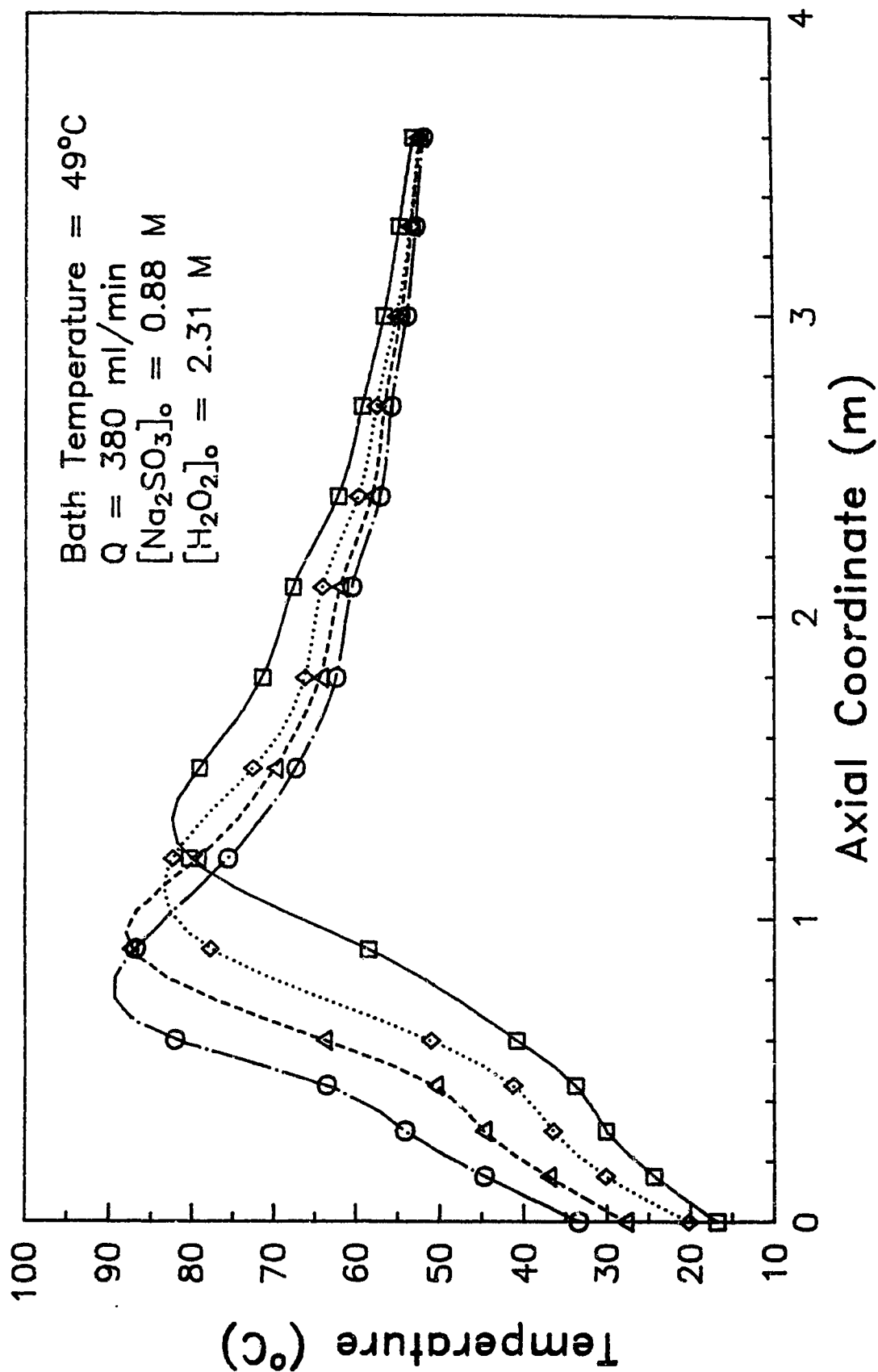


Figure 6.8 Experimental Data  
 Data from Tables C.37 - C.40

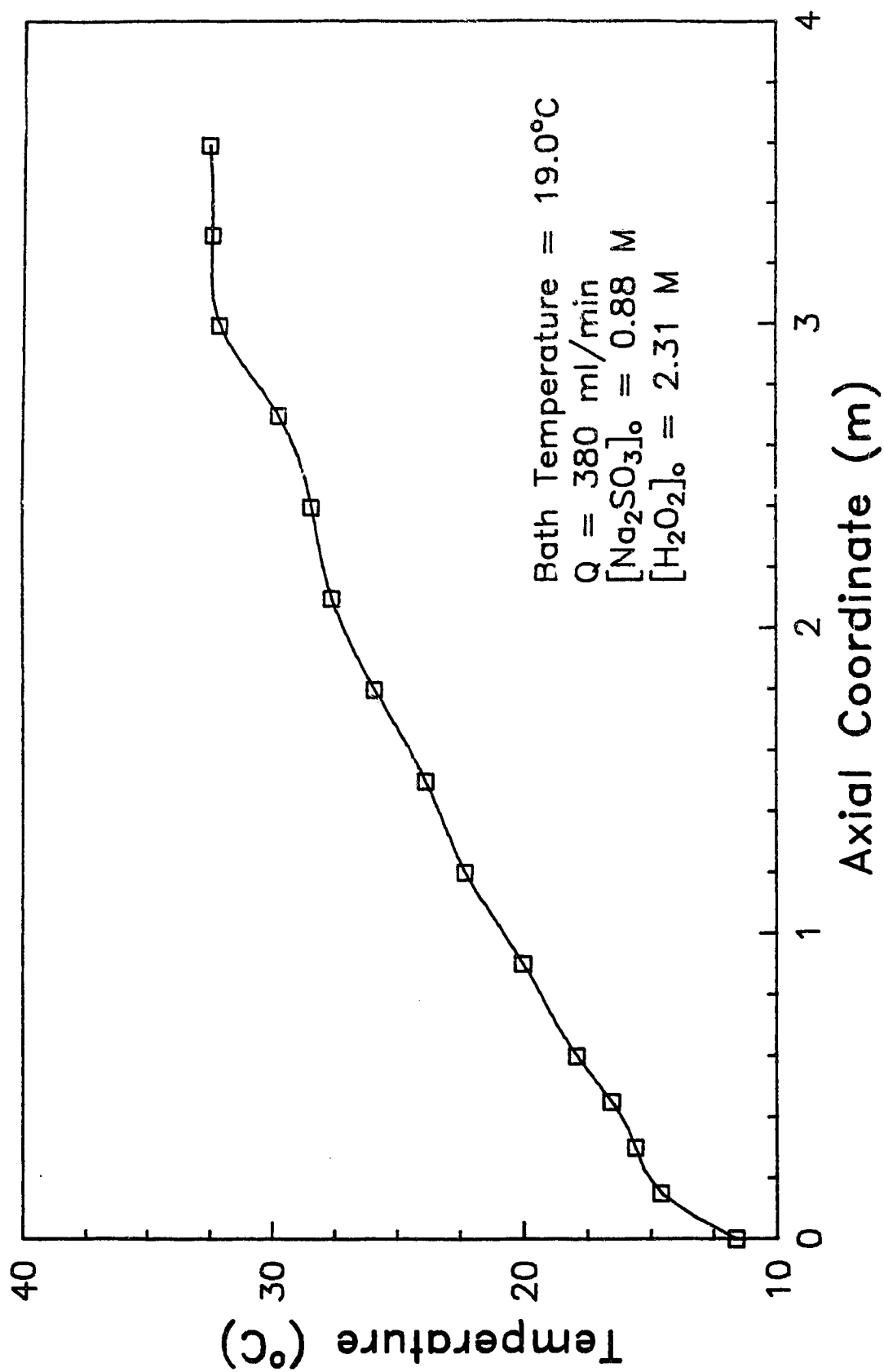


Figure 6.9 Experimental Data

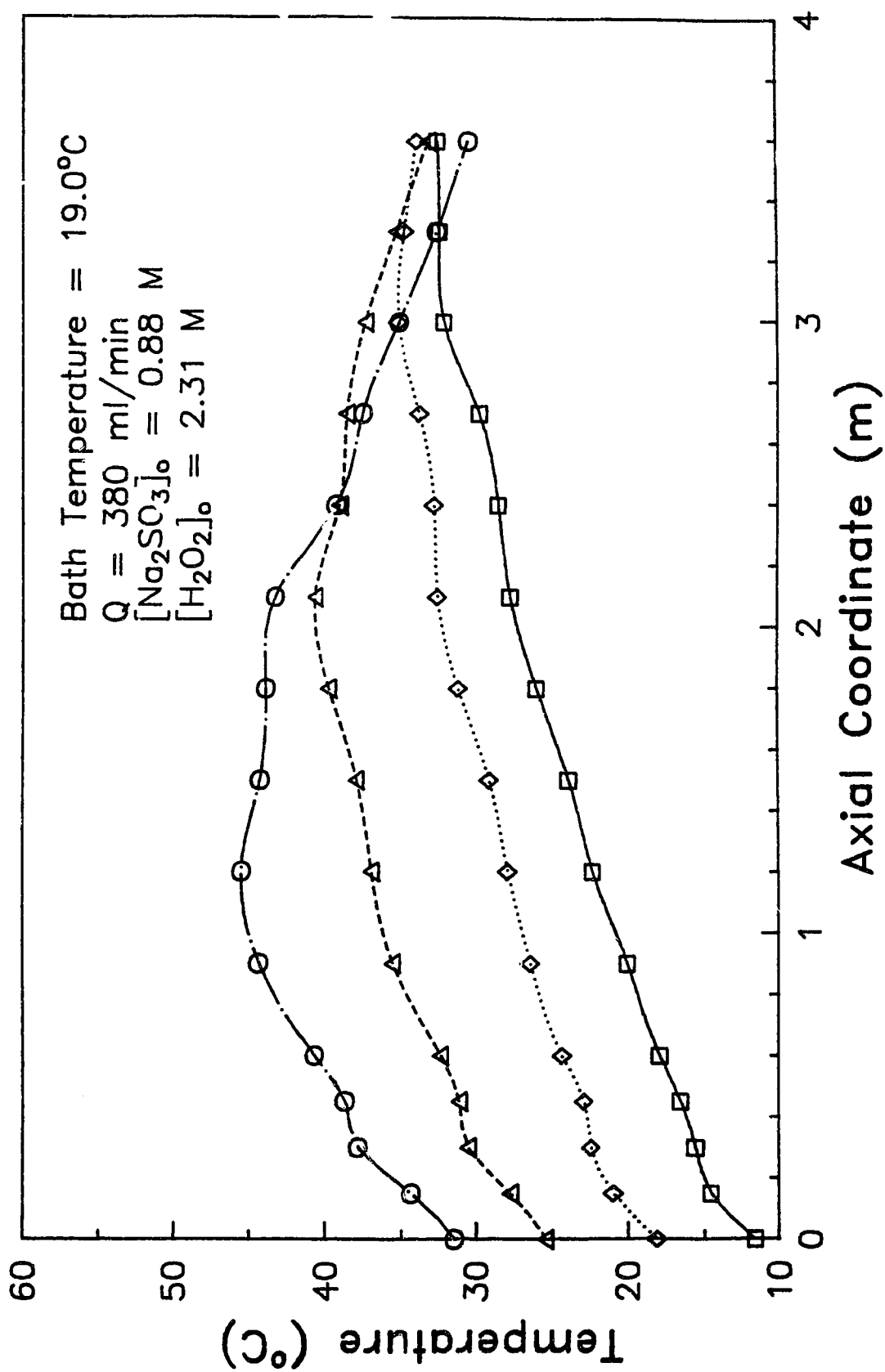
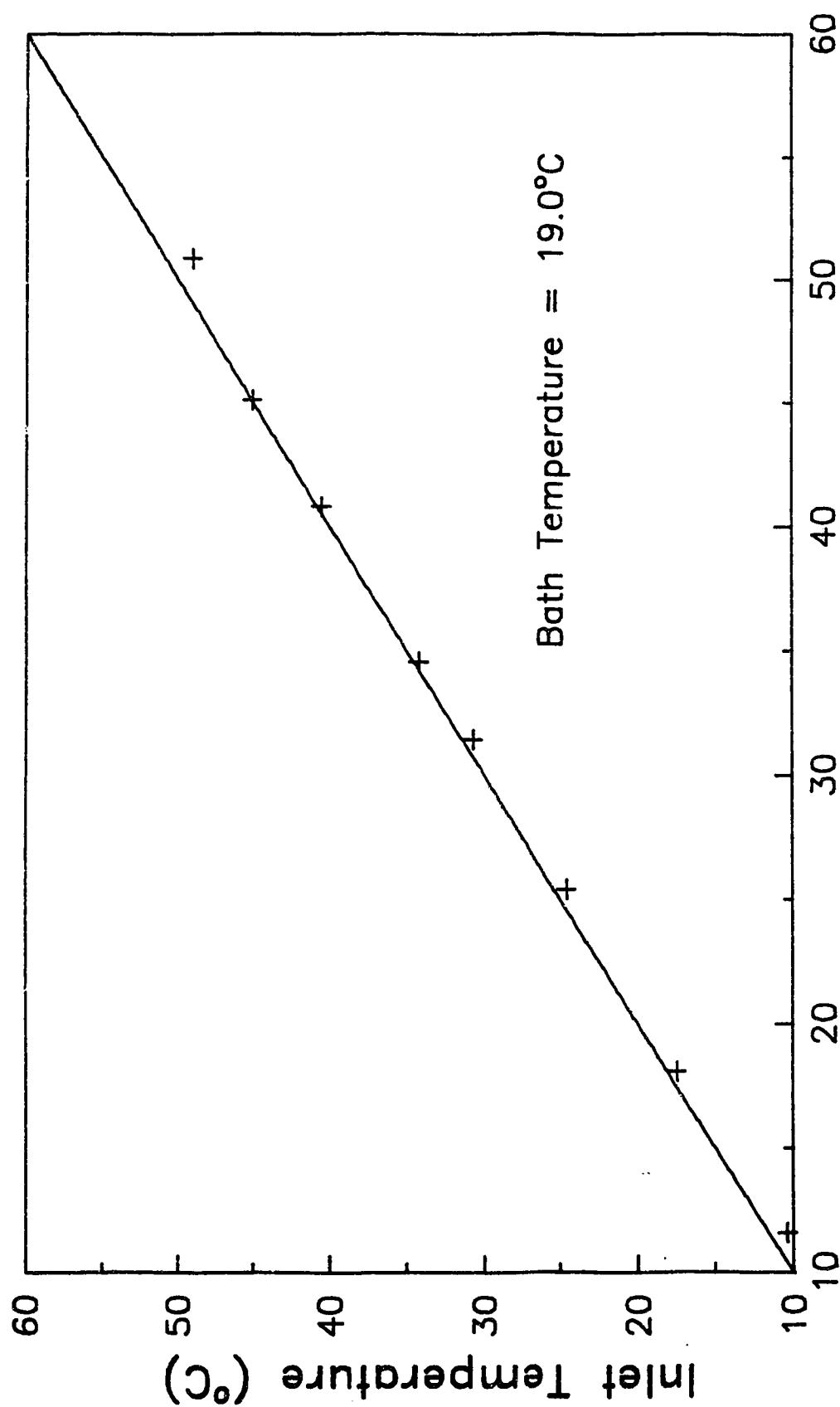


Figure 6.10 Experimental Data



Temperature at Thermocouple #1 (°C)

Figure 6.11 Temperature Readings at Reactor Inlet

The effect of changing the sulfite concentration for one set of operating conditions is shown in Figure 6.12. It should be noted here that the temperature profile corresponding to a concentration of 0.88 M is the same as that illustrated in Figure 6.3. Parametrically sensitive operating conditions can be seen once again. The initial change in the sulfite concentration produces a relatively small (considering the 0.1 M increase of one of the reactants) change in the value of the hot-spot (less than  $10^{\circ}\text{C}$ ). Progressive increases of 0.1 M result in temperature increases of greater than  $10^{\circ}\text{C}$ .

It is interesting to note that, the final increase in sulfite concentration results in a much less severe change in the hot-spot than the previous increase. This seems puzzling at first, but it can again be explained by considering the competing heat generation and removal processes.

As the inlet sulfite concentration is increased, the initial heat generation rate increases exponentially. Eventually, this becomes so much larger than the rate of heat removal term that the reactor behaves almost adiabatically. As noted earlier, this results in a hot-spot temperature which is close to the value of the maximum adiabatic temperature for the reaction. Thus, successive increases in the inlet concentration do not have as large an effect as previous increases on the hot-spot temperature because the hot-spot temperature becomes "fixed", as it were, by the reaction conditions of inlet

temperature and inlet concentration. In fact, if the inlet concentration is increased enough, the initial section of the reactor actually becomes adiabatic and the hot-spot temperature then only changes linearly with the value of the inlet concentration. This is what is occurring in Figure 6.12 as the inlet concentration reaches 0.88 M.

It can be seen from Figure 6.12 that the temperature profiles for 0.78 M, 0.68 M, and 0.58 M all lie within the envelope defined by the temperature profiles for 0.88 M and 0.48 M. In fact, all five profiles appear to merge into one at about two meters into the reactor. These features are due to the fact that all five profiles have the same inlet and bath temperatures. Thus, they must have the same initial and (assuming the reactor were long enough) final temperatures. Since the hot-spot temperature varies directly with the value of the inlet concentration, no curve can have a hot-spot greater than the one following it. The reason why the curves all merge into one is, by that point in the reactor, all the reaction has taken place and the parameter value that differentiated the curves (i.e., the sulfite concentration) is now equal to zero in all five cases. Thus, all the temperature profiles merge into the same cooling curve.

The temperature profiles for the other two sets of operating conditions can be seen in Figures 6.13 and 6.14. These profiles have the same characteristics that have been discussed so far this section.

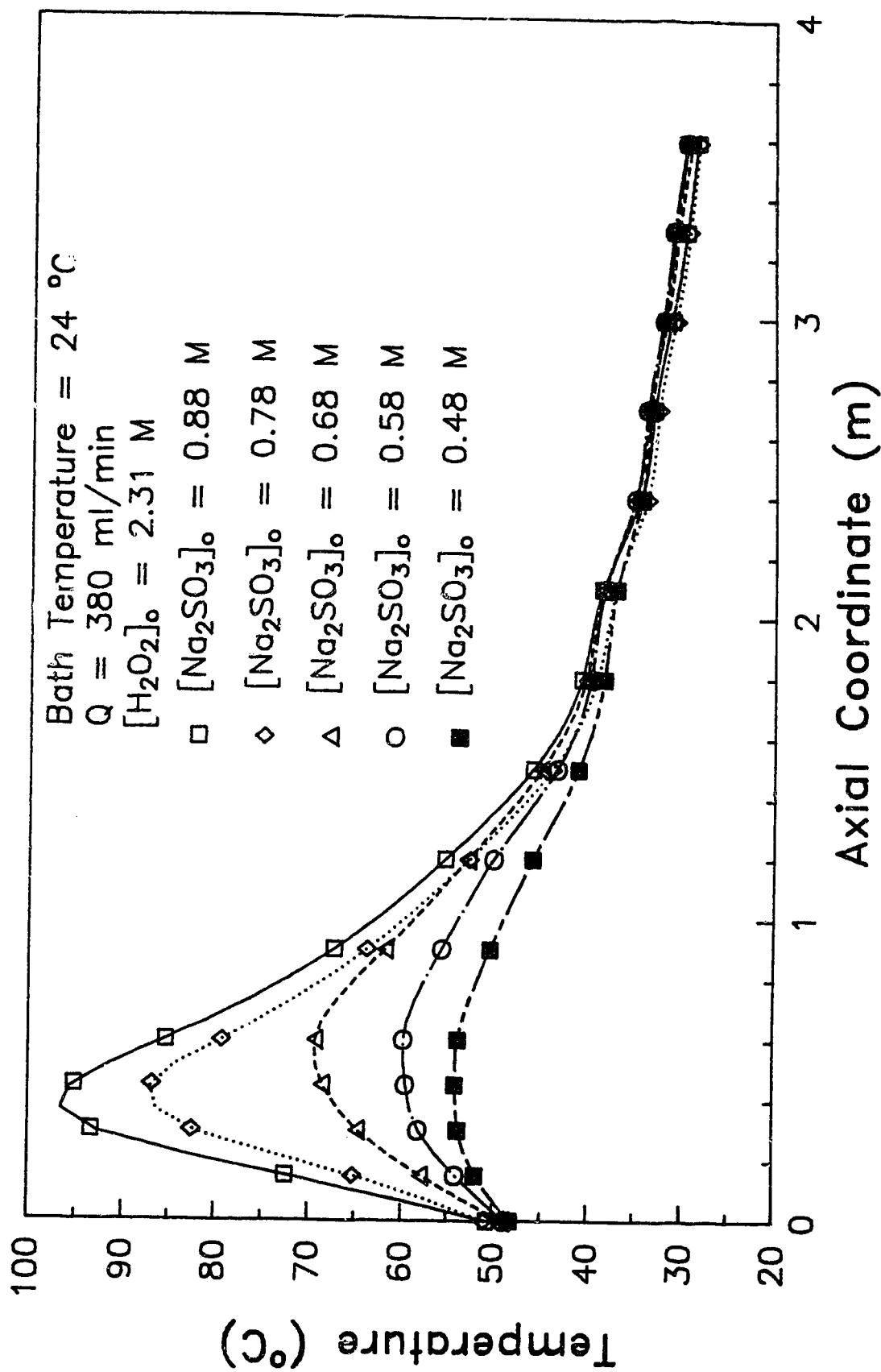


Figure 6.12 Experimental Data  
 Data from Tables C.41 C.44 C.47 C.50



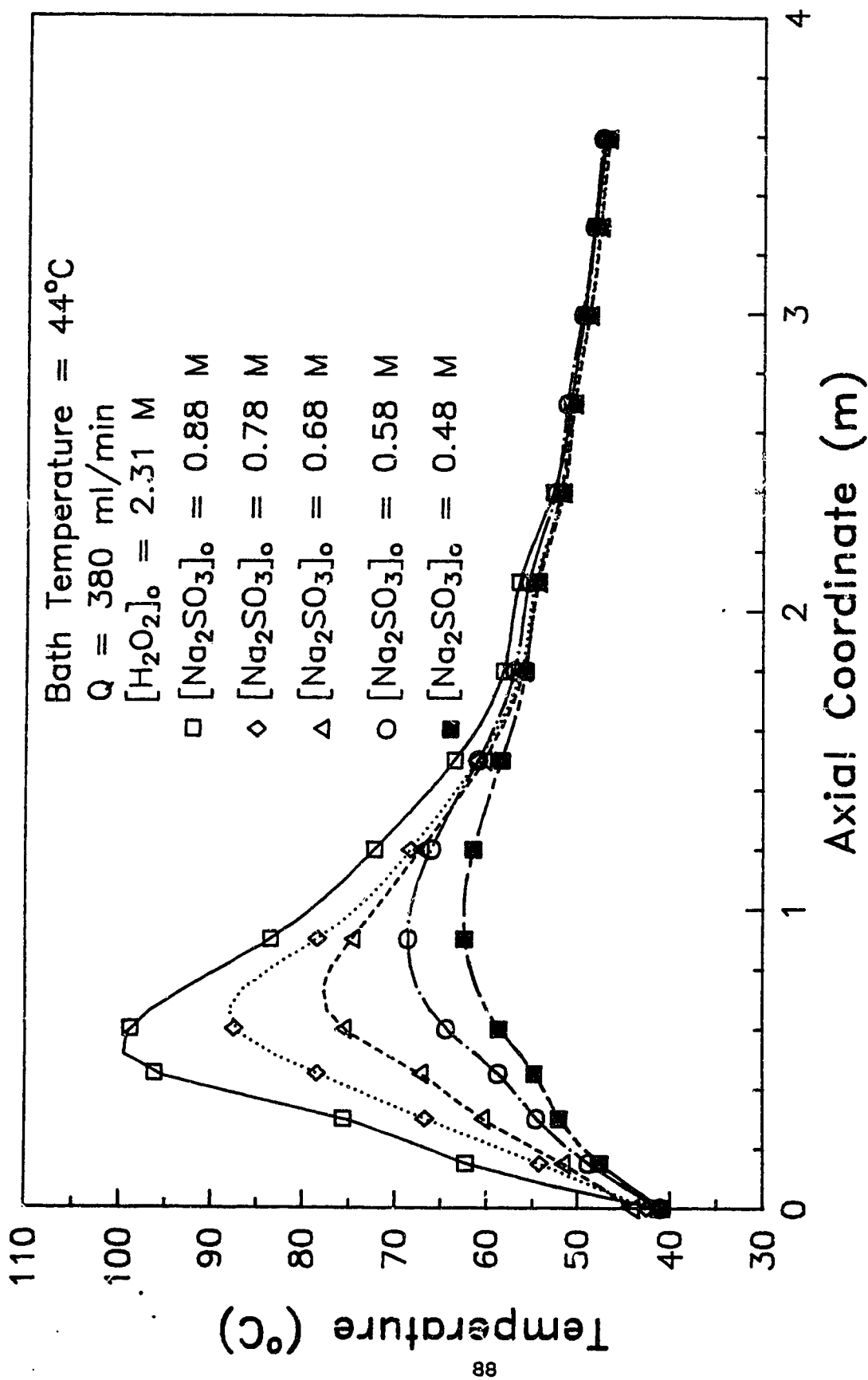


Figure 6.13 Experimental Data  
Data from Tables C.43 C.46 C.49 C.52

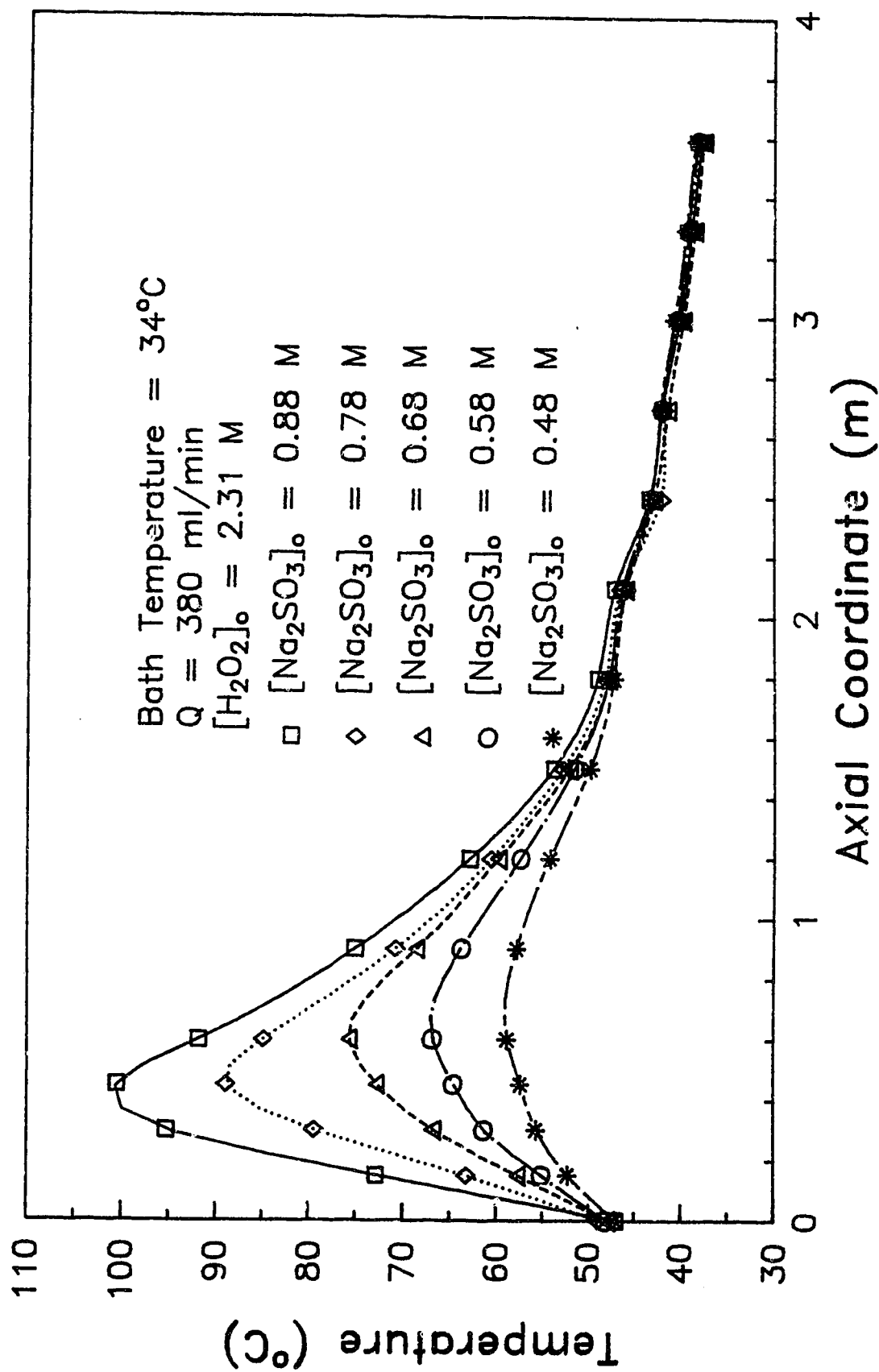


Figure 6.14 Experimental Data  
 Data from Tables C.42 C.45 C.48 C.51

To conclude this section, the following points can be made. Parametrically sensitive operating conditions were observed for the cases involving variable inlet sulfite concentration. The observed characteristics of the temperature profiles were as expected for the conditions studied.

#### 6.4 EXPERIMENTAL TUBULAR REACTOR

##### VARIATION OF OVERALL HEAT TRANSFER COEFFICIENT

The final set of data obtained involved the variation of the bath side heat transfer coefficient (and, hence, the overall heat transfer coefficient). Three different conditions were chosen for the study. These conditions, which are noted in Table 4.1, were chosen because they each were characteristic of a different regime of reactor operation. The first set (Bath = 24°C, Inlet = 19°C) was representative of the heat transfer controlled reactor regime; the second (Bath = 24°C, Inlet = 34°C) represented the normal case with both reaction and heat transfer controlling while the third set (Bath = 34°C, Inlet = 45°C) was representative of the reaction controlled reactor regime.

It should be noted here there were no experiments carried out to determine the value of the overall heat transfer coefficient for stirrer speeds 0, 3 and 10 (similar to the evaluation of the heat transfer coefficient for stirrer speed #6 as discussed in section 5.0). The only quantitative information available is that stirrer

speed #10 corresponded to a higher rate of mixing, and hence a larger heat transfer coefficient, than stirrer speed #6 which in turn corresponded to a higher mixing rate than speed #3, etc. Thus, the discussion here will be largely a qualitative one.

Figure 6.15 illustrates the effect of changing the bath side heat transfer coefficient for the heat transfer controlled conditions. It should be noted that the profile corresponding to a stirrer speed of 6 is the same as that shown in Figure 6.3 for an inlet temperature of  $19^{\circ}\text{C}$ . As the heat transfer coefficient is lowered, the hot-spot increases with a large jump being noted as the stirrer speed is decreased from 3 to 0. Whether the operating conditions at stirrer speed #3 can strictly be considered parametrically sensitive is not clear. This is because there is no way of knowing the magnitude of the change in the value of the overall heat transfer coefficient. However, on a qualitative basis, parametric sensitivity is certainly evident (i.e., a large change in the value of the hot-spot is seen).

It is worth noting that the temperature profile essentially retains its "heating curve" shape as the heat transfer coefficient is varied. This is to be expected as the inlet temperature is low enough for the profile to be heat transfer controlled (i.e., rate of heat generation much less than rate of heat exchange to the surrounding). Lowering the value of the heat transfer coefficient will result in a change in the temperature profile, but this change will have little effect on

either the hot-spot, or, the basic shape of the curve (i.e., it will still be heat transfer controlled). However, if the heat transfer coefficient is lowered enough, then the rate of heat generation may become important and the hot-spot become more pronounced. This may be what occurred as the stirrer speed was reduced to the 0 setting.

For case of both heat transfer and reaction control of the reactor, the effect of changing the heat transfer coefficient is shown in Figure 6.16. Parametric sensitivity is again evident on a qualitative level. In fact, the change in the value of the hot-spot as the stirrer speed setting is reduced from #6 to #0 is greater here than in the previous case.

The effect of changing the heat transfer coefficient for the last case is illustrated in Figure 6.17. Here, the change in the heat transfer coefficient has almost no effect on the temperature profiles. This is not unexpected as the conditions were such that the reactor was reaction controlled (i.e., the initial temperature rise was essentially adiabatic). Therefore, the effect of a heat transfer coefficient change should have been negligible.

A study of the Figures 6.15, 6.16 and 6.17 together provides an excellent insight into the phenomenon of parametric sensitivity. On a physical level, parametric sensitivity occurs when the reactor is both reaction and heat transfer controlled. Specifically, it occurs when

the conditions are such that a small change in the value of one of the parameters throws off the "balance" between the reaction rate and the heat transfer rate, resulting in a reaction rate (and hence, a heat generation rate) that is much greater than the heat transfer rate. The temperature balance, as it were, is then disturbed and the hot-spot temperature begins to increase dramatically.

Therefore, given the three different reactor regimes, it would be expected that the condition most likely to be parametrically sensitive would be that where the reactor was both heat transfer and reaction rate controlled. The operating conditions where the reactor was either reaction rate controlled or heat transfer controlled, would be relatively insensitive. Of course, in this case, since the heat transfer coefficient was being lowered, the heat transfer controlled condition would eventually become sensitive as well (if the heat transfer coefficient were lowered enough). However, the expected change in the hot-spot temperature would likely be less than for the case of heat transfer and reaction rate control.

An examination of Figures 6.15, 6.16 and 6.17 together shows that this is exactly what happened as the heat transfer coefficient was lowered (from setting #6 to setting #0). Measuring the relative sensitivity by the change in the value of the hot-spot temperature, regime #2 (Bath = 24°C, Inlet = 34°C) was most sensitive ( $\Delta T = 20^\circ\text{C}$ ) followed by regime #1 (Bath = 24°C, Inlet = 19°C) with  $\Delta T = 10^\circ\text{C}$  and then regime #3 (Bath

= 34°C, Inlet = 45°C) with  $\Delta T \approx 7^\circ\text{C}$ .

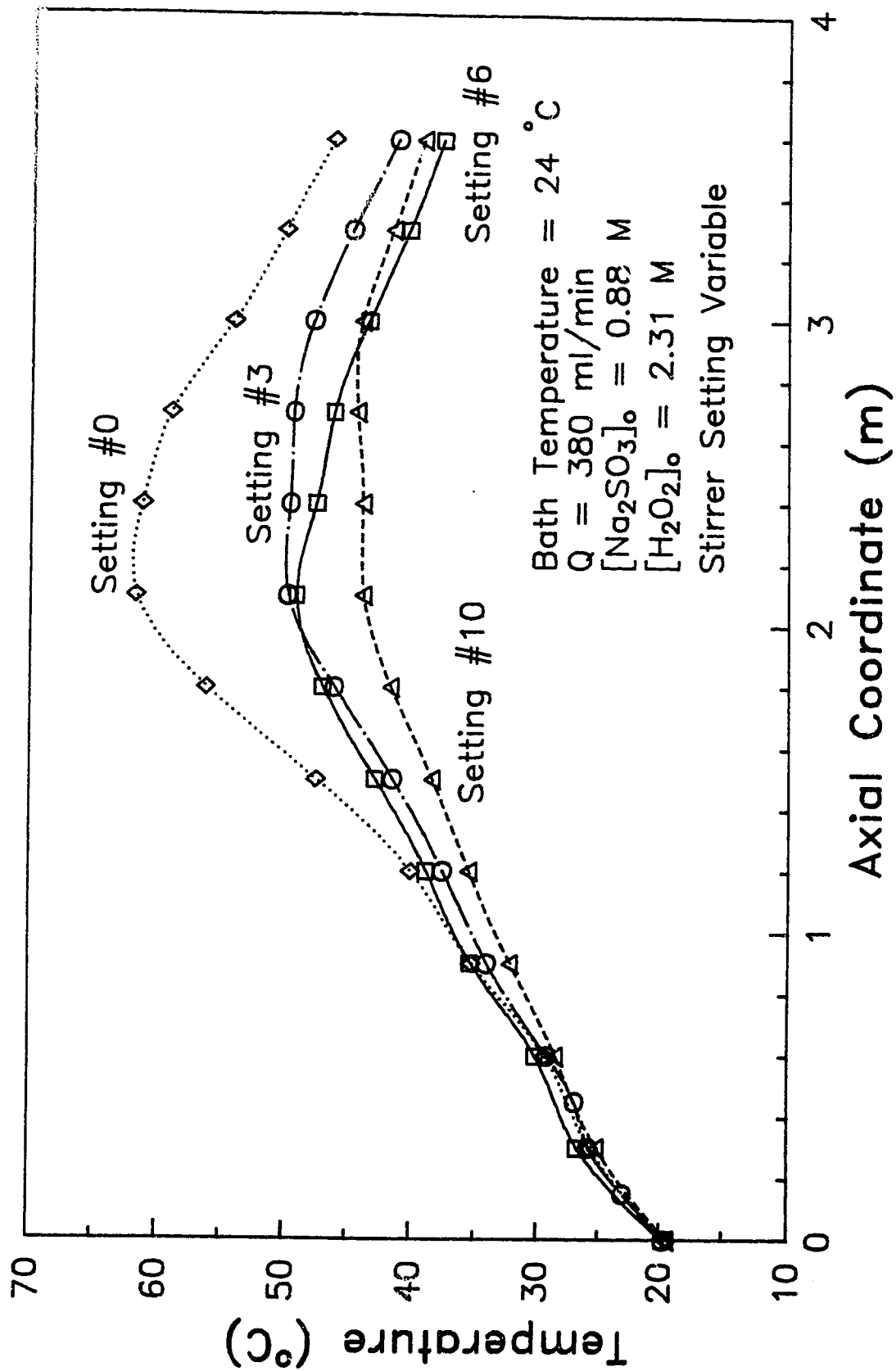


Figure 6.15 Experimental Data  
 Data from Tables C.53 – C.55



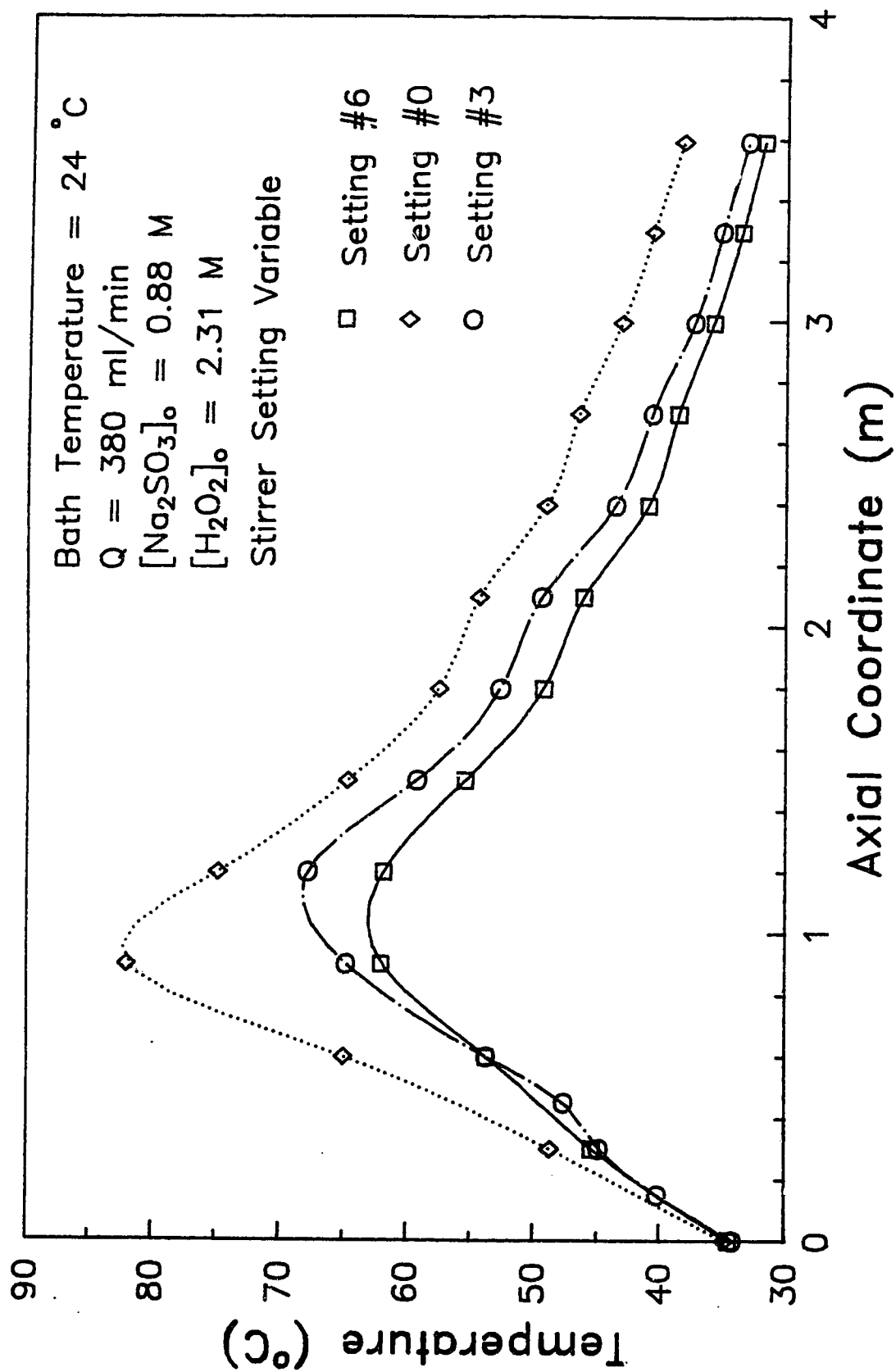


Figure 6.16 Experimental Data  
 Data from Tables C.56 – C.58

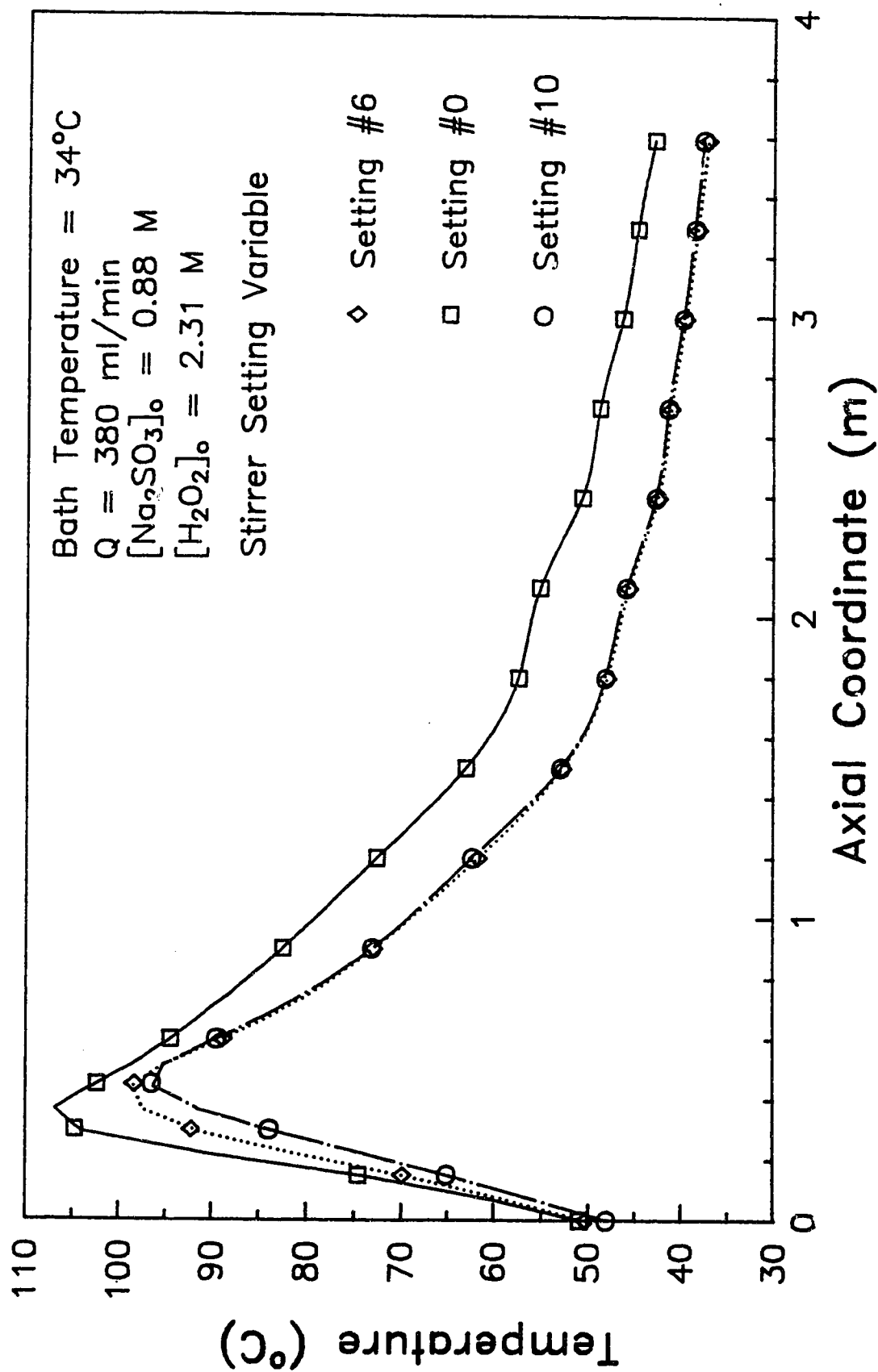


Figure 6.17 Experimental Data  
Data from Tables C.59 – C.60

## 7.0 COMPARISON OF EXPERIMENTAL DATA WITH REACTOR MODELS

A comparison of the experimental data with the ODPH and TDPH reactor models is presented here. The computer programs used to generate the data for the models are discussed in Appendix E.

Before beginning the comparison it is necessary to remember the observed temperature differences (inlet vs. thermocouple #1) at the reactor inlet which were discussed in section 6.2. The observed temperature difference at the reactor inlet in no way affects the validity of the experimental data. It does, however, create a problem when the data is compared with the ODPH and TDPH reactor models. The problem is this: which temperature can be considered as the true "inlet" temperature? If the mixing zone postulated actually does exist, then the temperature recorded at thermocouple #1 is not a valid "inlet" temperature. On the other hand, the apparent inlet temperature measured cannot be assumed to be correct either as the exact location of the reactor "inlet" is not known.

The solution arrived at for this problem is as follows. When comparing the experimental data with the models, the measured inlet temperature will be assumed to be correct. The temperature recorded at the first thermocouple will be illustrated as the first temperature measured inside the reactor. This temperature measurement will be located at the position it would be found if the reactor behaved adiabatically from the inlet temperature up until that point. In other words, it was

assumed that a finite amount of reaction was taking place somewhere between the inlet temperature measurement points and the first thermocouple and that it was this reaction that was creating the observed temperature difference. The assumption that this little "reaction zone" was adiabatic was made in order to be able to determine the "equivalent length" of reactor that would be required to obtain the observed temperature increase. Given the relative size of the temperature discrepancy ( $3-4^{\circ}\text{C}$ ) to the actual temperature rise during the course of the reaction, this assumption of a small adiabatic section was not unreasonable. Again, it must be pointed out that this manipulation in no way affected the validity of the data. It was only necessary to do this in order to be able to compare adequately the data with the models.

The comparison of one temperature profile with the profile predicted by the ODPH model is given in Figure 7.1. Figure 7.2 is a comparison with the TDPH model. In both cases, the model prediction is in qualitative agreement with what was actually observed. Both models tended to underestimate the temperature rise. However, the basic "heat exchanger" shape was predicted in both cases.

The model comparisons for a different experimental profile (one with a more dramatic temperature rise) are illustrated in Figures 7.3 and 7.4. Although the basic shape of the experimental curve is predicted by the models, both models over estimate the observed hot-spot. In

addition, there is disagreement (in both cases) at the inlet of the reactor. This may be due to the problem with the inlet temperature discussed previously.

The location of the hot-spot, as predicted by the TDPH model, appears to be different than that of the experimental data. The ODPH model hot-spot is at the same location as the experimental hot-spot. Also, the cooling portion of the TDPH profile is more "sluggish" than that of the ODPH profile. That is to say, the fluid appears to cool faster in the ODPH model.

This last point may be attributable to the overall heat transfer coefficients used for the simulation. For the ODPH model, the previously determined value of the bath side heat transfer coefficient ( $h_o = 4367 \text{ W/(m}^2 \cdot \text{K)}$ ) was used to calculate the overall heat transfer coefficient. The average value of  $U$  ( $\approx 4500 \text{ W/(m}^2 \cdot \text{K)}$ ) determined from the overall heat transfer coefficients (Table 5.1) was used in the TDPH model simulation. This value, however, was not strictly correct for this situation as the parametric sensitivity experiments were performed at a flow rate of 380 ml/min while the heat transfer experiments were carried out with a flow rate of 305 ml/min. Since the contribution to the overall heat transfer coefficient by internal convection would be increased at a higher flow rate, the value of  $U$  used in the simulation underestimated the actual value of the heat transfer coefficient. Given that the flow rates were not that

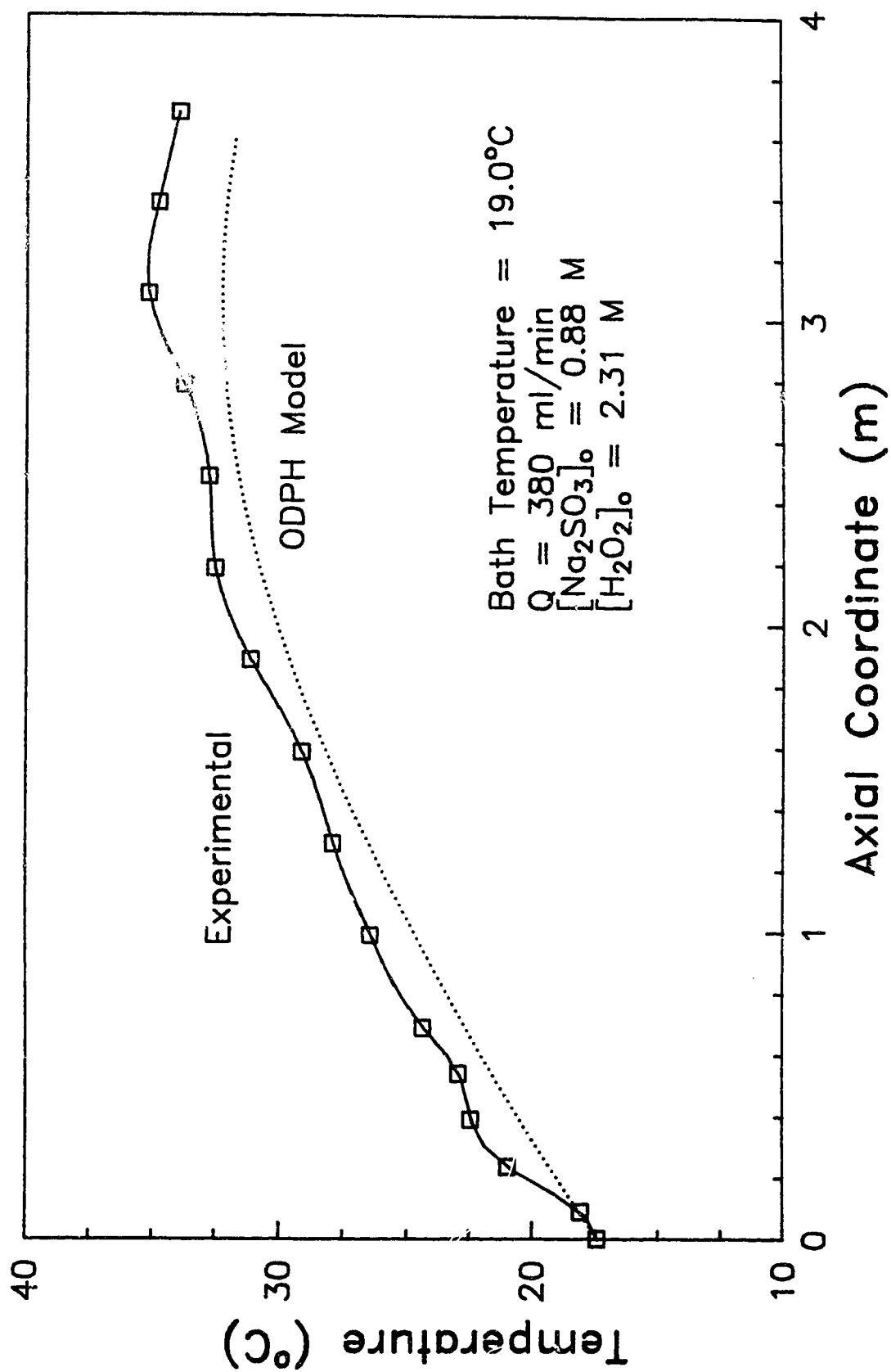


Figure 7.1 Experimental Data Comparison with ODPH Model

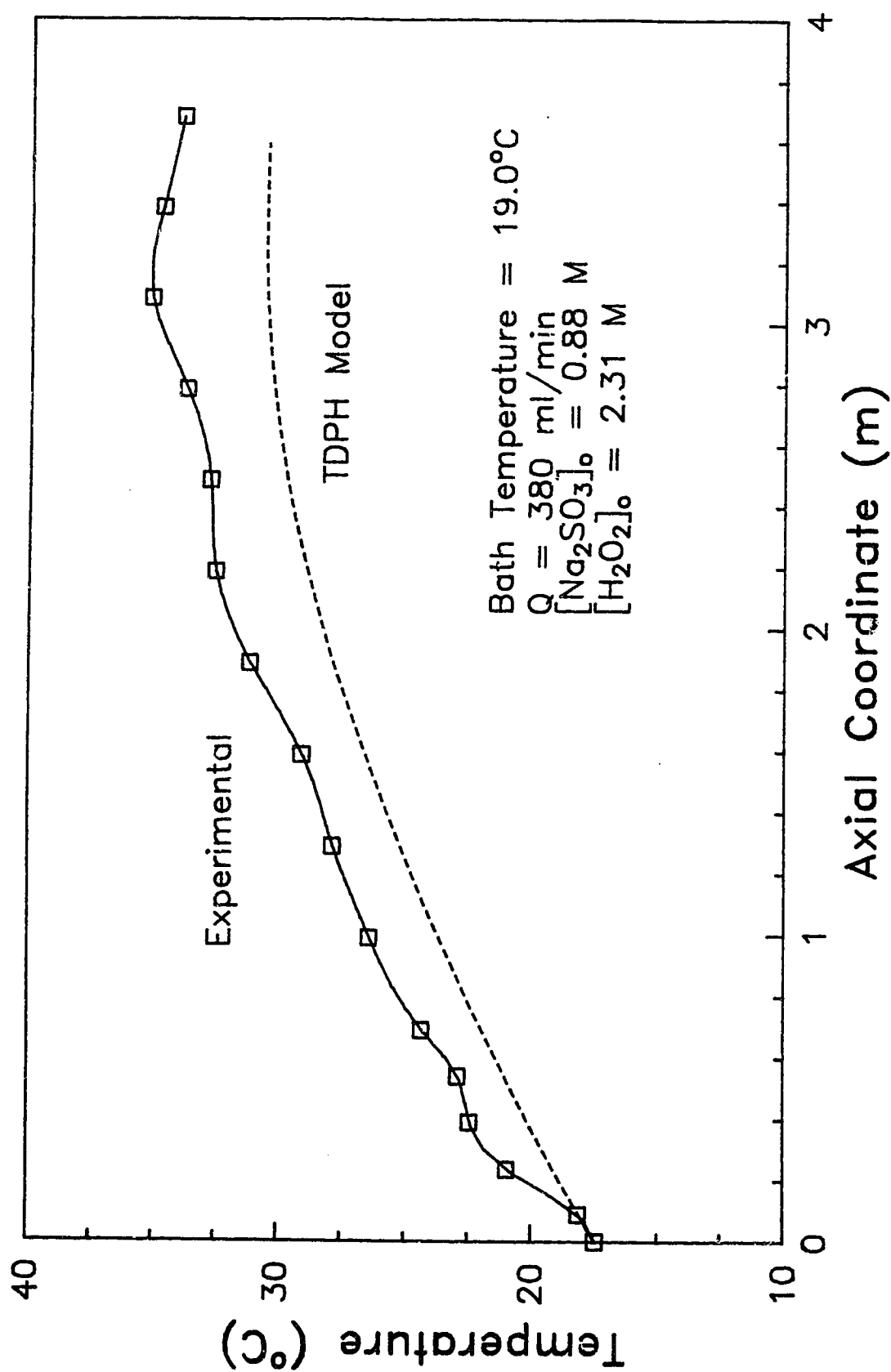


Figure 7.2 Experimental Data Comparison with TDPH Model

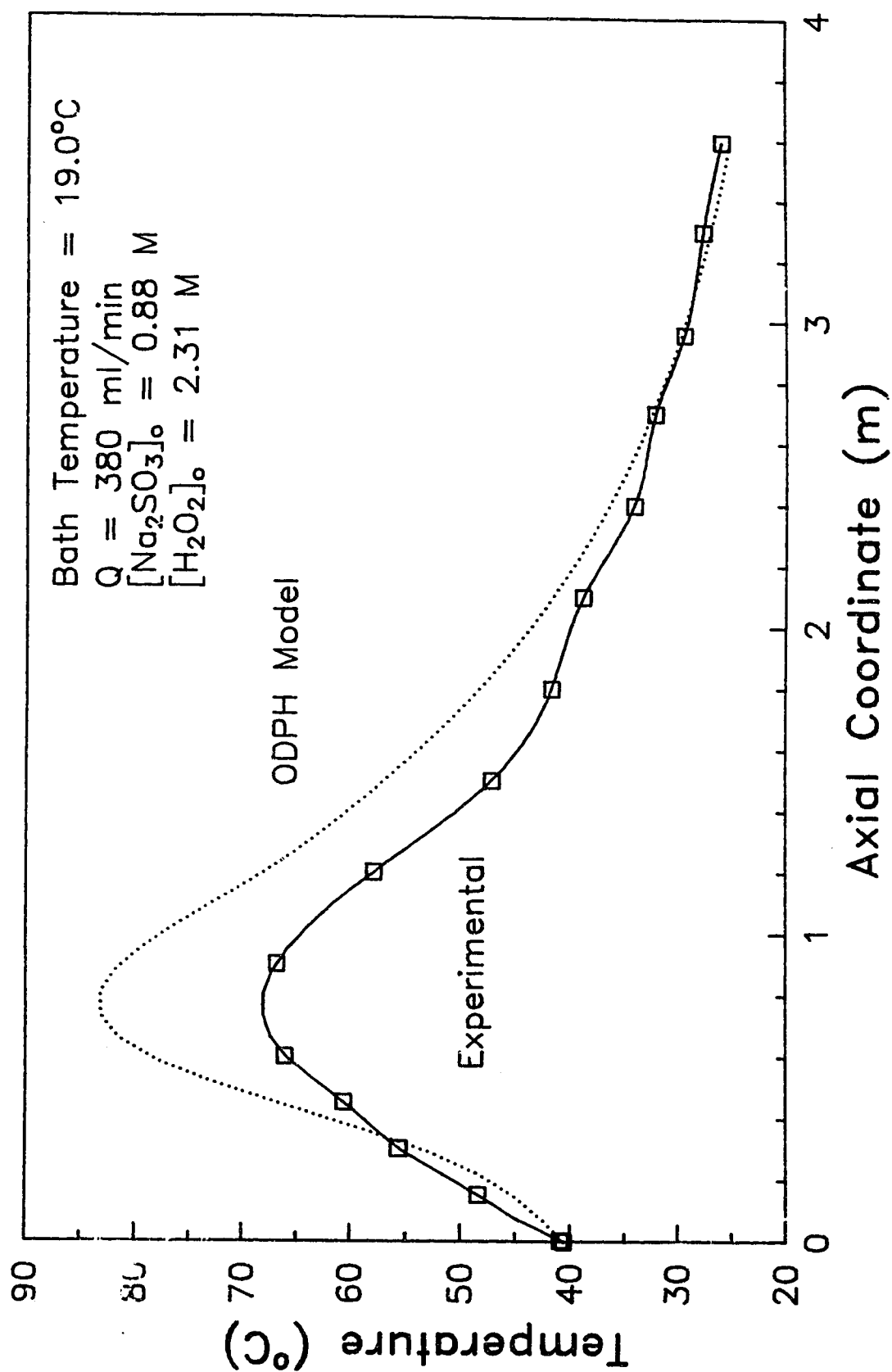


Figure 7.3 Experimental Data Comparison with ODPH Model



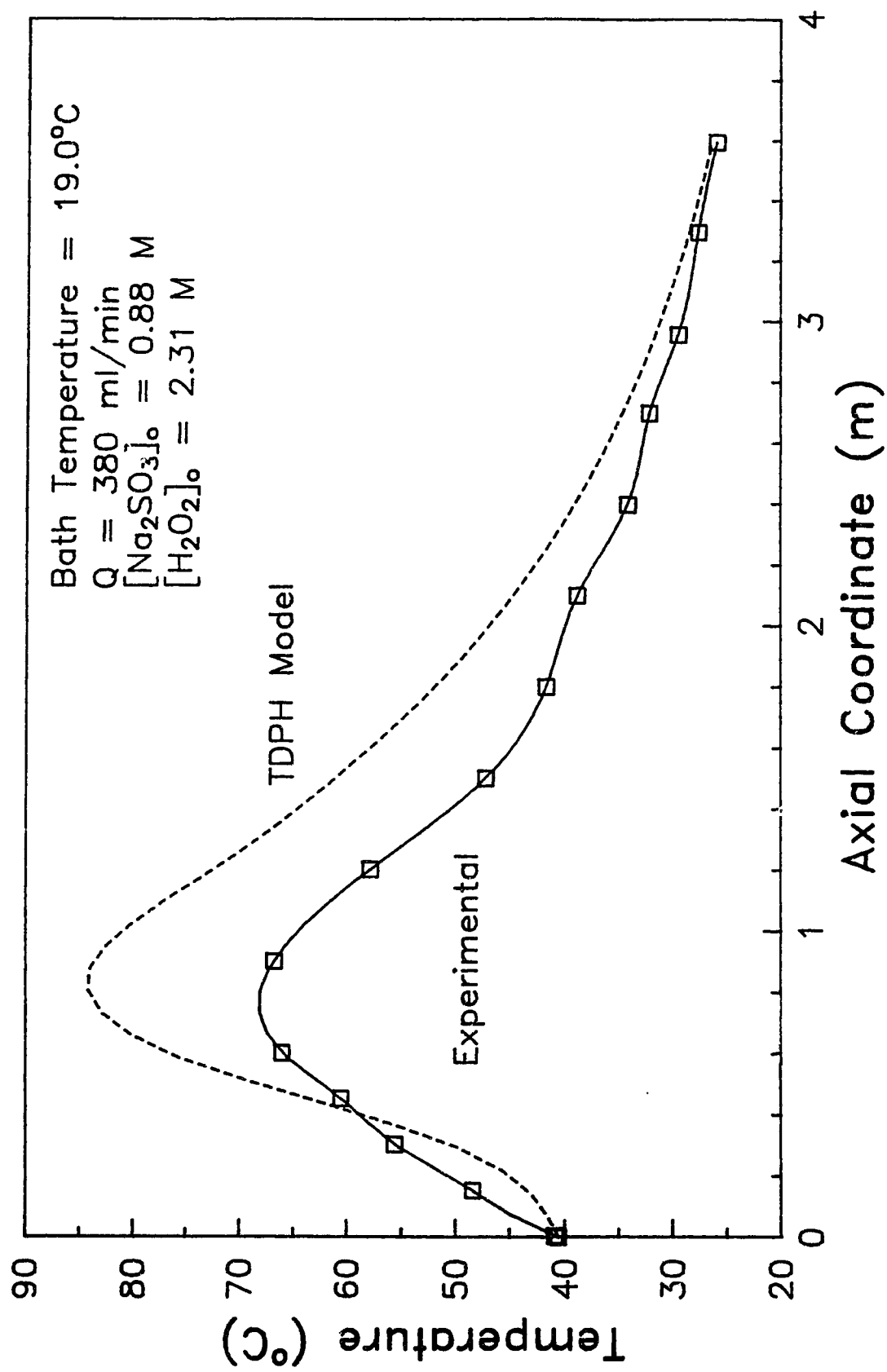


Figure 7.4 Experimental Data Comparison with TDPH Model

different and that internal convection was but one of the contributing factors to the overall heat transfer coefficient, this underestimation may not have been too severe. However, it is important to note that this may be the cause of the "sluggish" behavior of the TDPH model.

Figures 7.5 through 7.16 are more comparisons of the experimental data with the two models. These particular profiles were chosen so as to represent the entire range of operating conditions. The following trends are evident from these, and the preceding figures.

In all cases, the ODPH and TDPH models predict the general shape of the experimental curve quite well. With the exception of the operating conditions that could be classified as heat transfer controlled (i.e., low inlet temperature), the models both tend to over predict the value of the hot-spot. In addition, the TDPH model tends to locate the hot-spot further into the reactor than the ODPH model. The ODPH model tends to predict accurately the location of the hot-spot.

Since these deviations were systematic, an attempt was made to determine if these deviations could be attributable to errors in the values of the parameters used in the simulations. This attempt was made for one experimental profile and the results obtained are shown in Figures 7.17, 7.18 and 7.19.

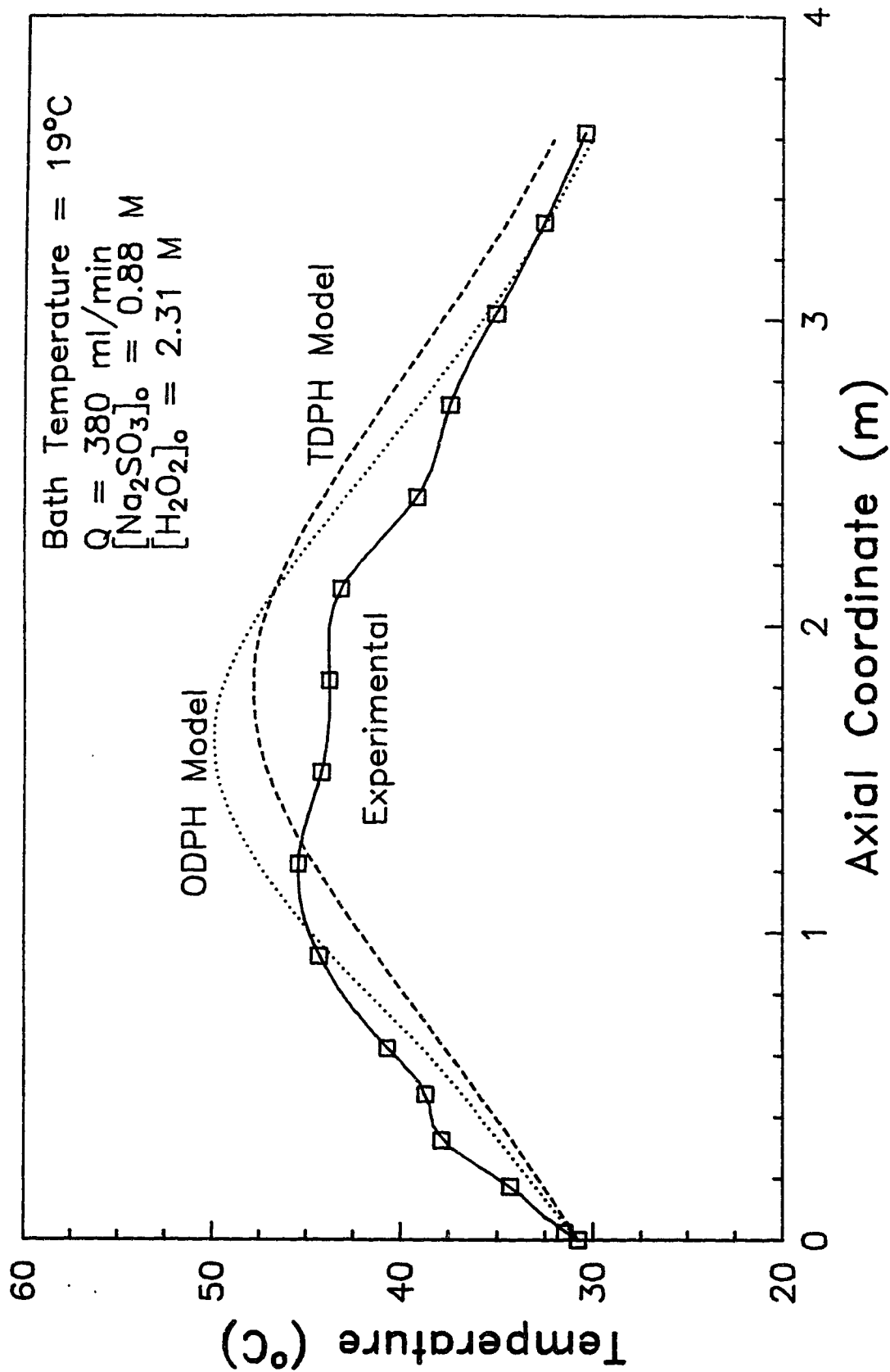


Figure 7.5 Experimental Data Comparison with ODPH and TDPH Models

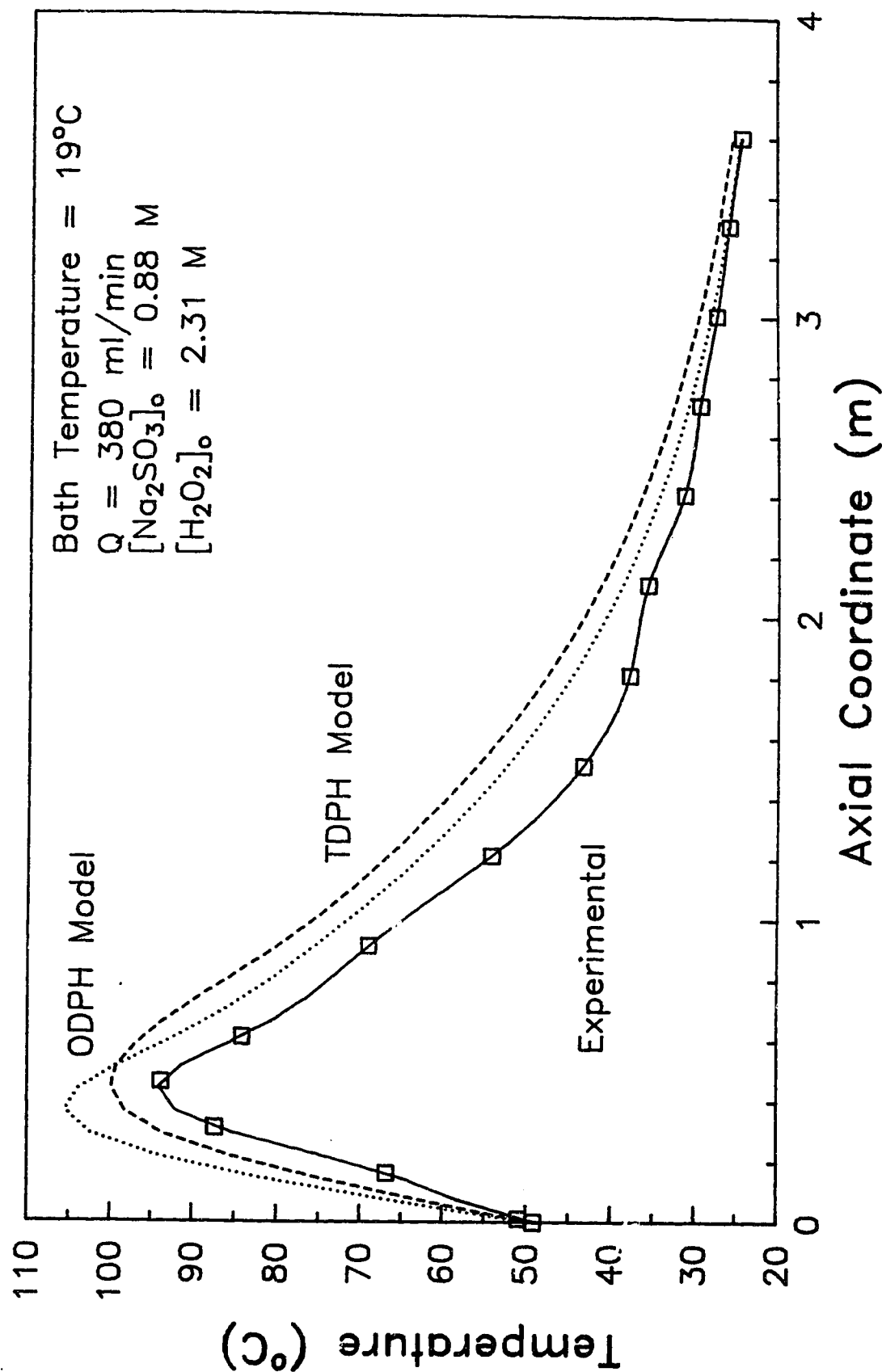


Figure 7.6 Experimental Data Comparison with ODPH and TDPH Models

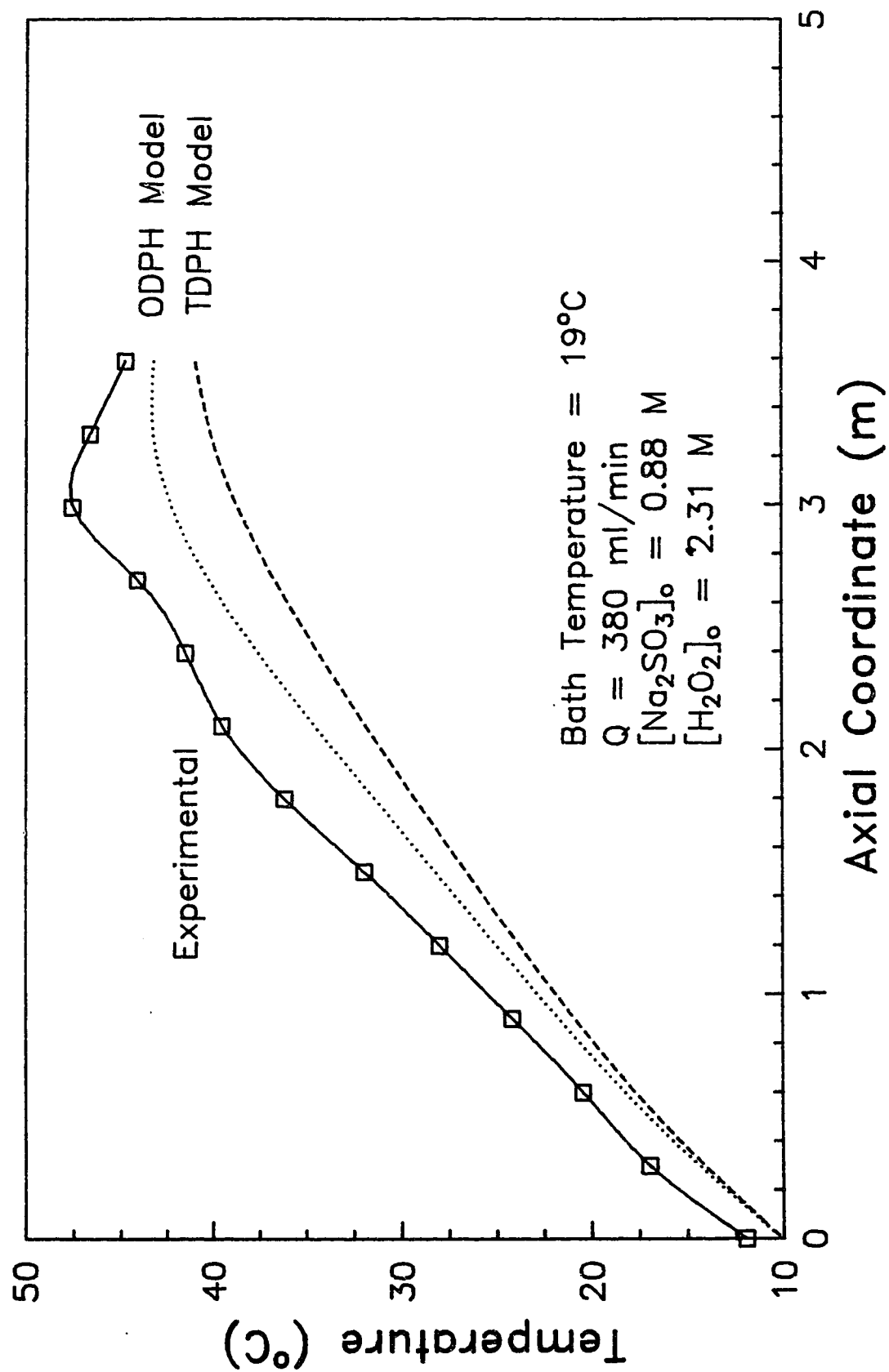


Figure 7.7 Experimental Data Comparison with ODPH and TDPH Models

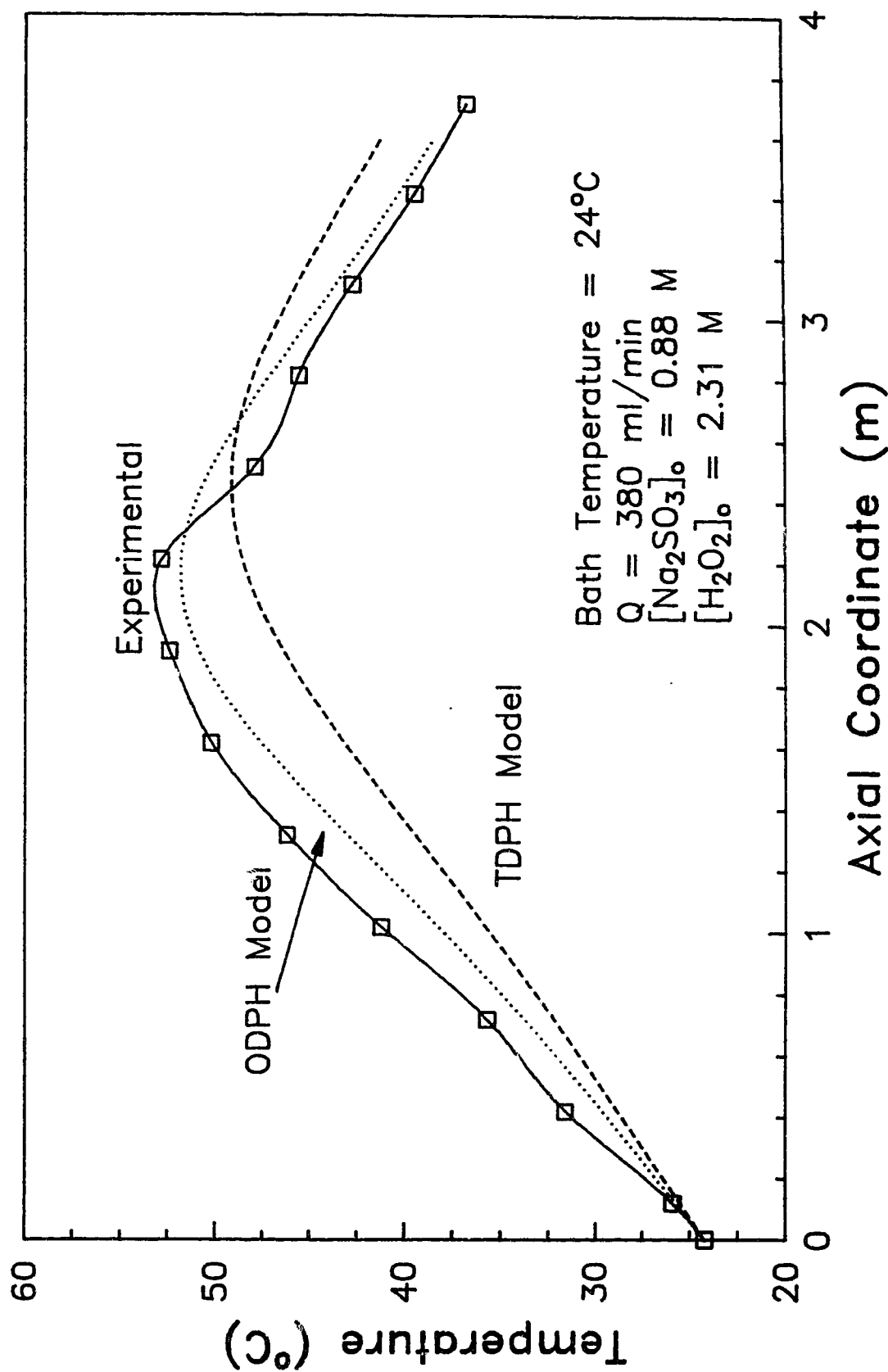


Figure 7.8 Experimental Data Comparison with ODPH and TDPH Models

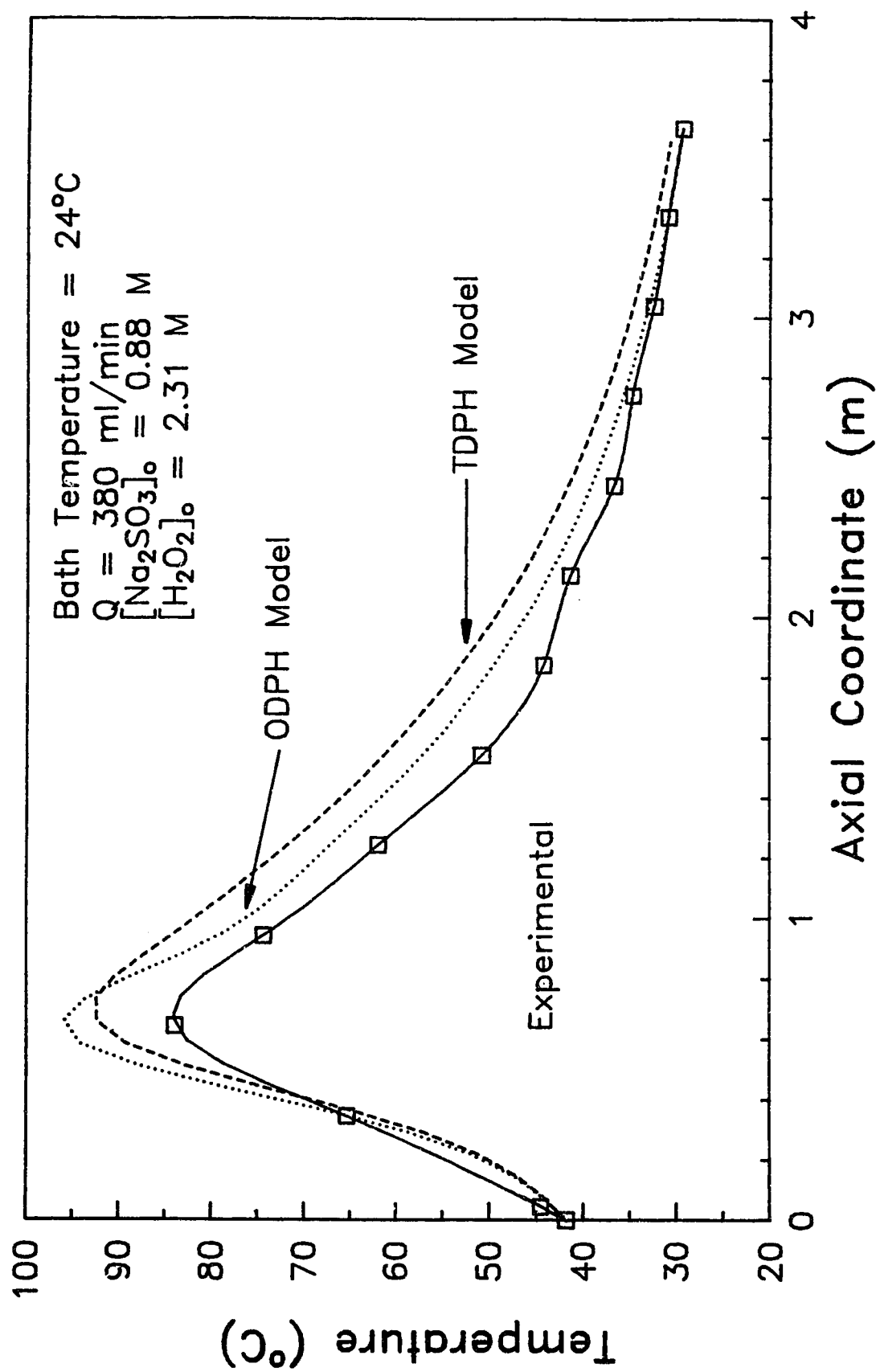


Figure 7.9 Experimental Data Comparison with ODPH and TDPH Models

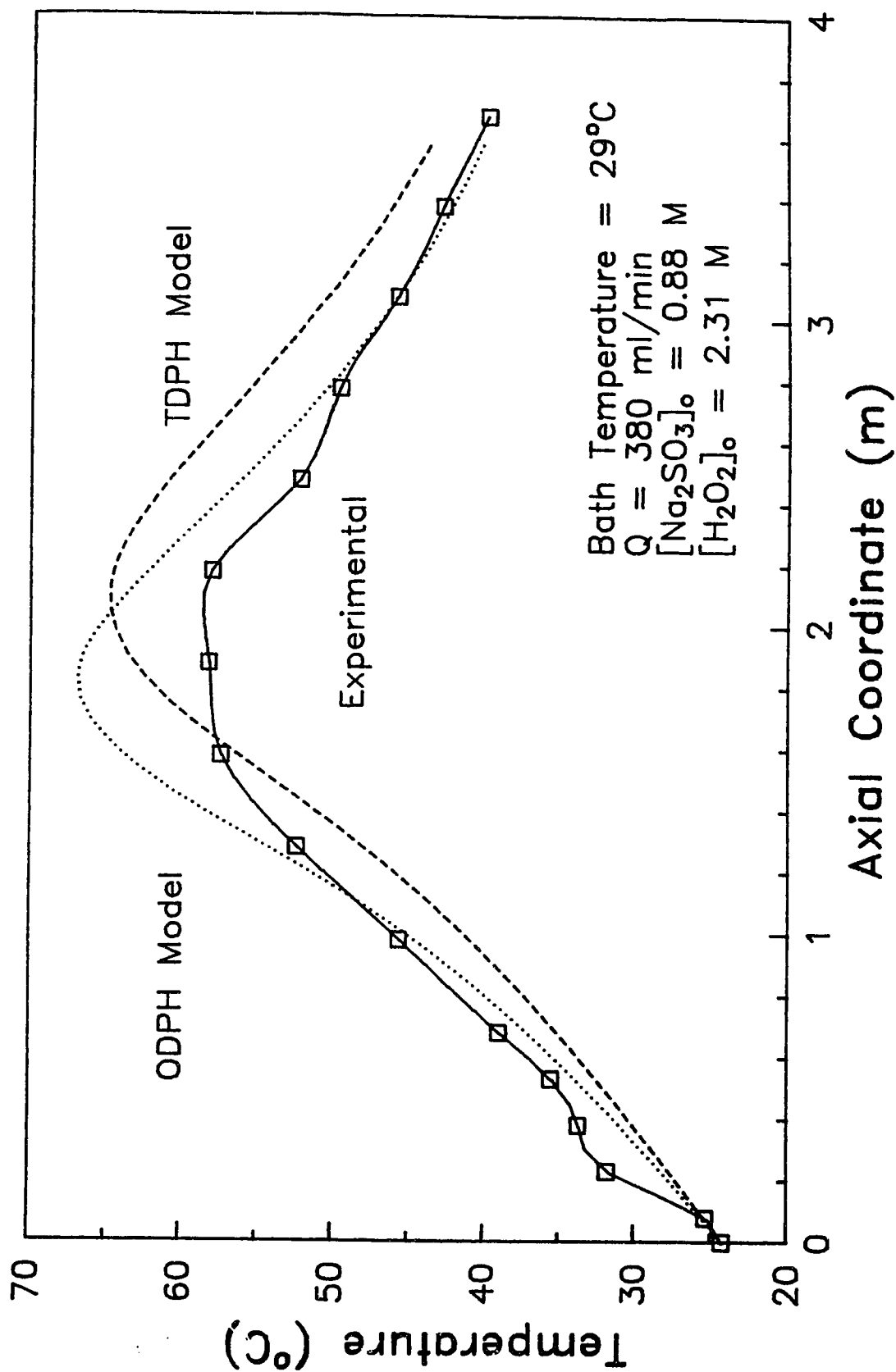


Figure 7.10 Experimental Data Comparison with ODPH and TDPH Models



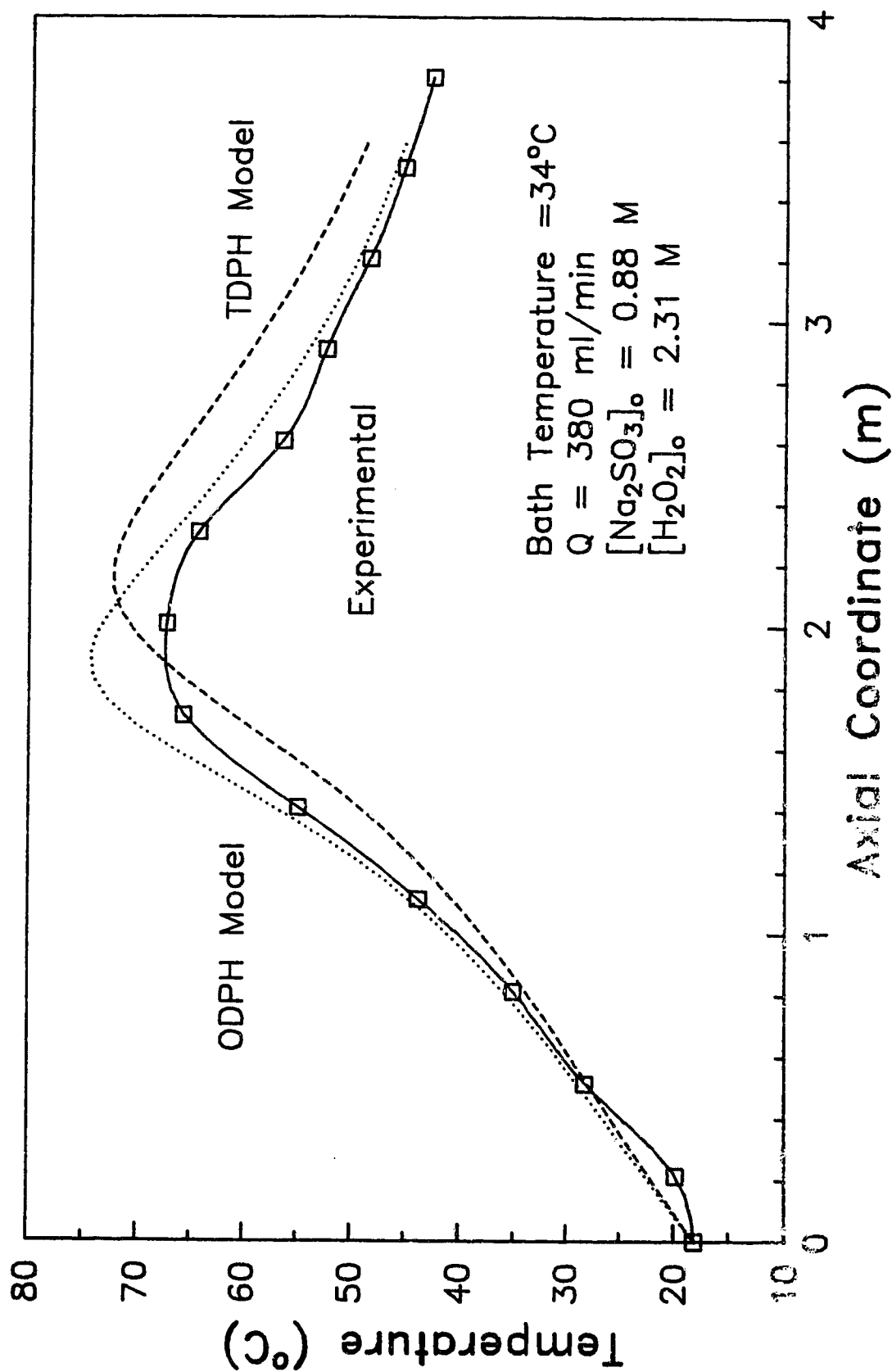


Figure 7.11 Experimental Data Comparison with ODPH and TDPH Models

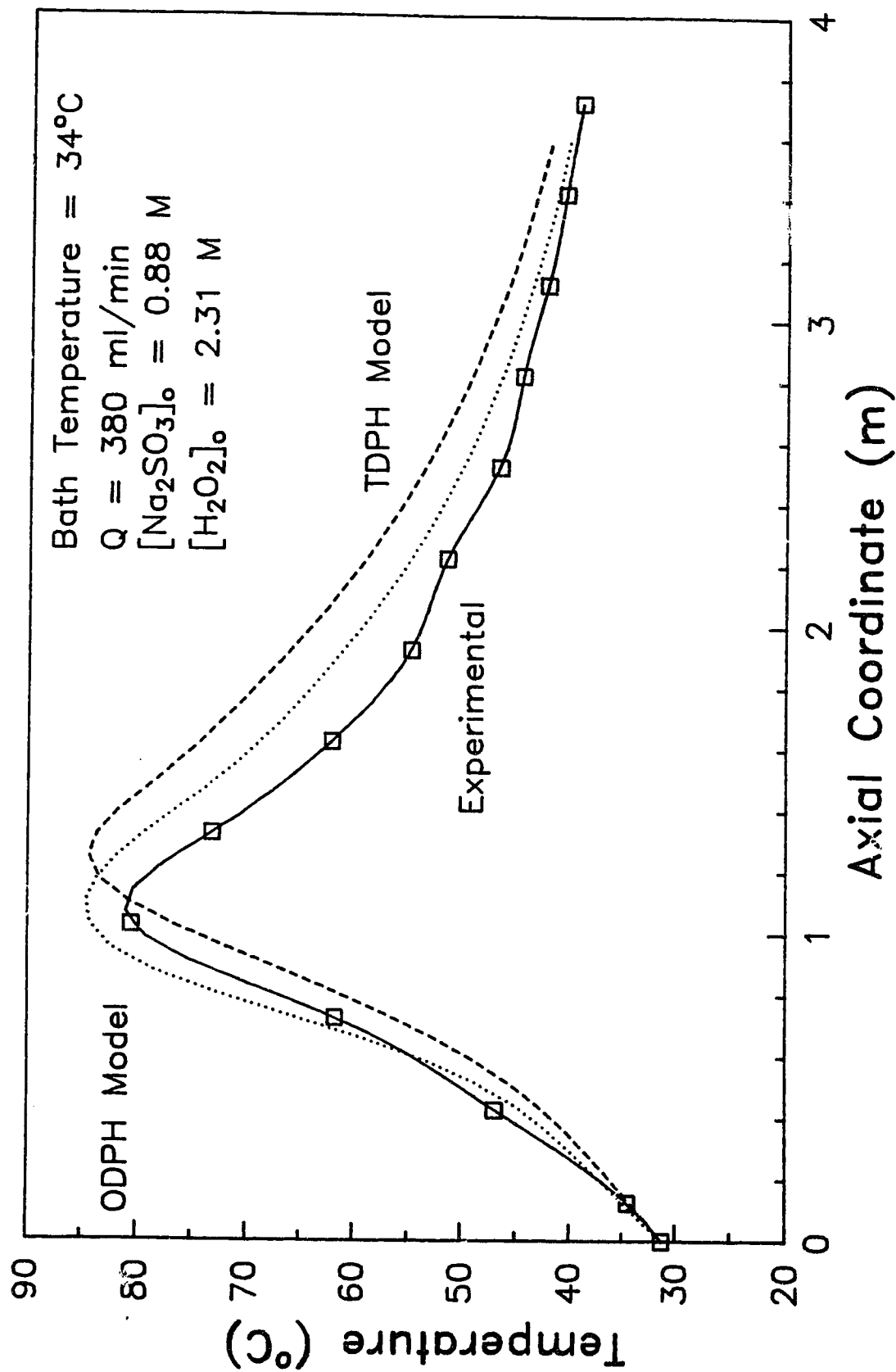


Figure 7.12 Experimental Data Comparison with ODPH and TDPH Models

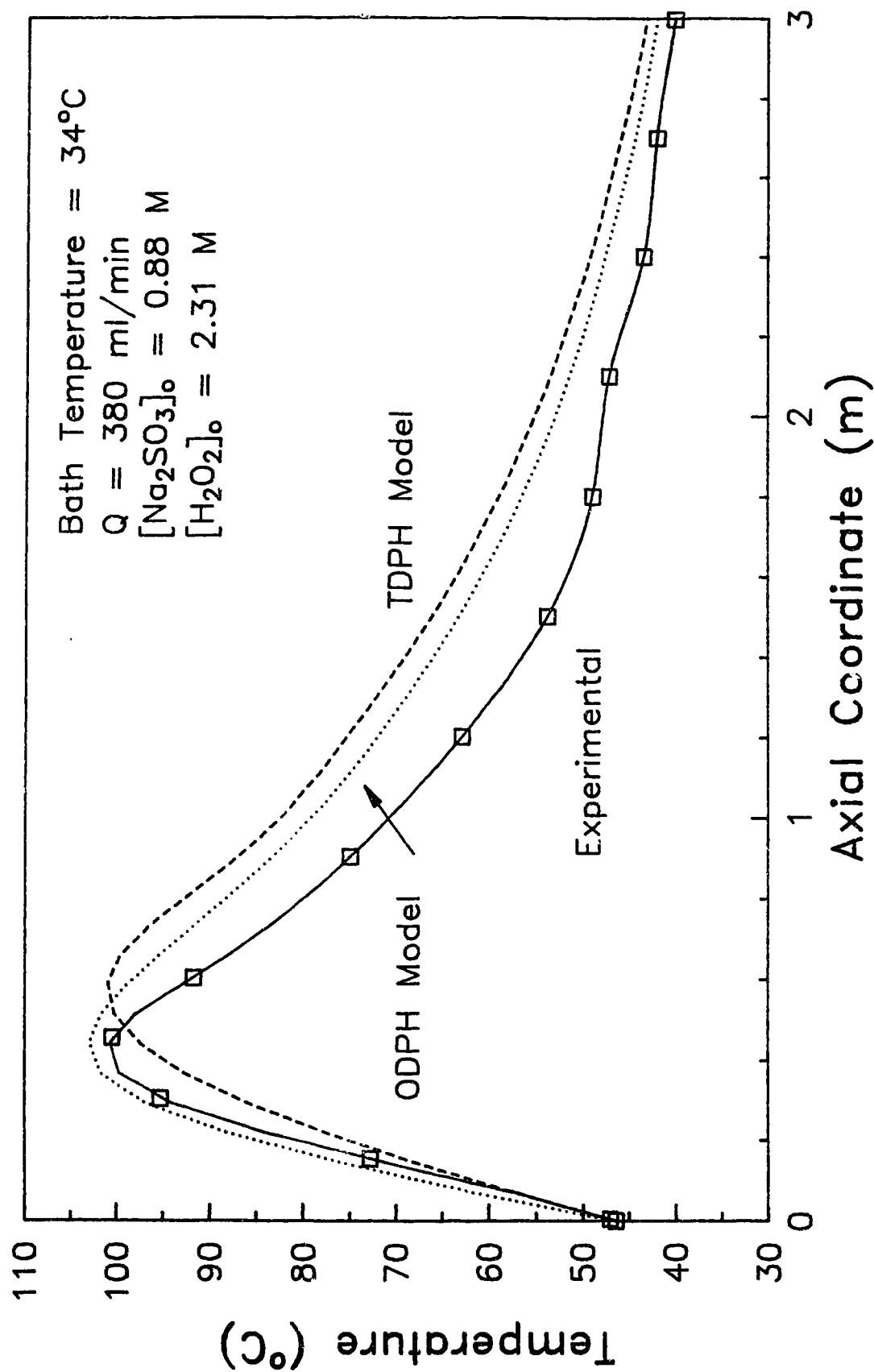


Figure 7.13 Experimental Data Comparison with ODPH and TDPH Models

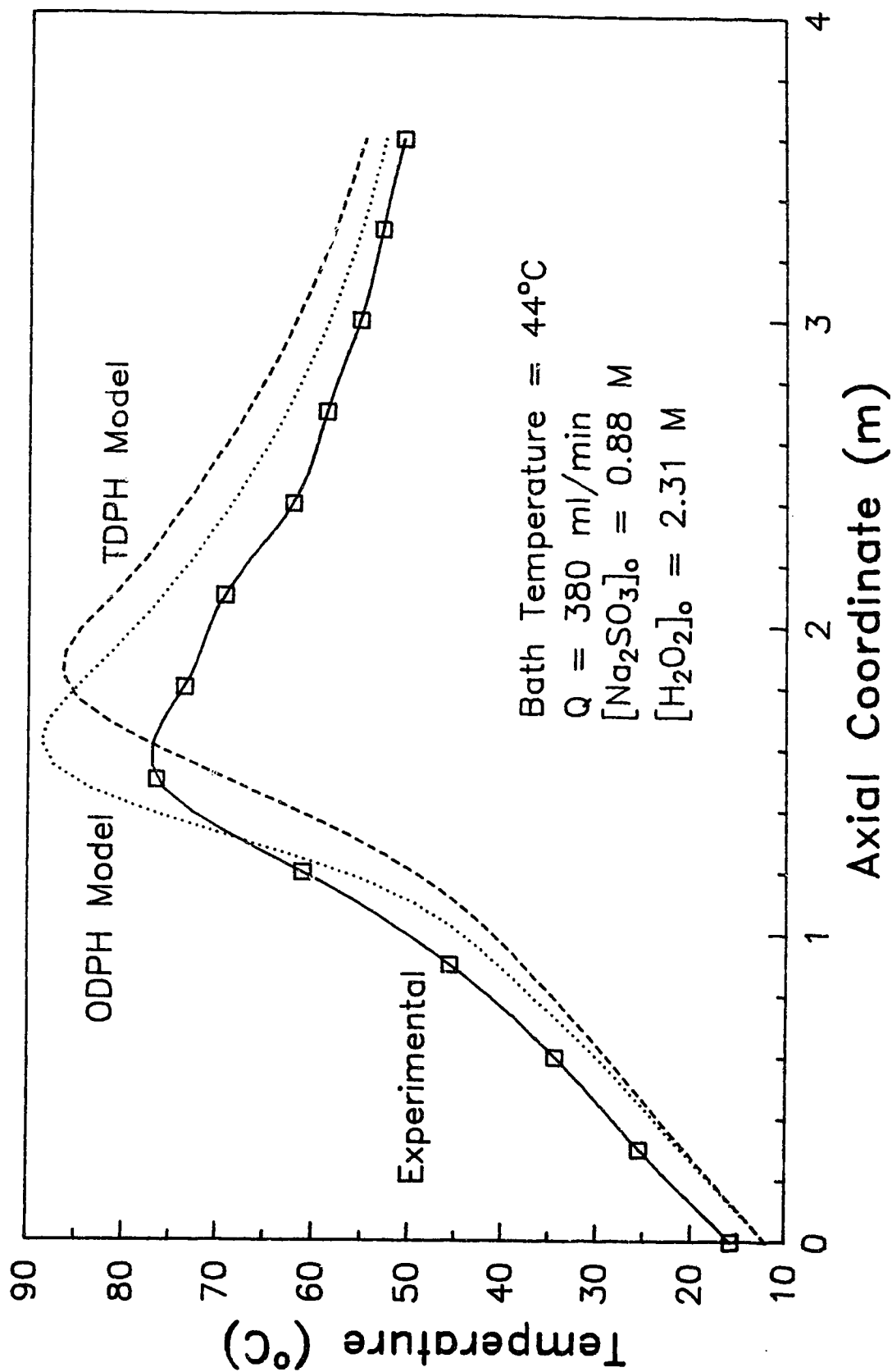


Figure 7.14 Experimental Data Comparison with ODPH and TDPH Models

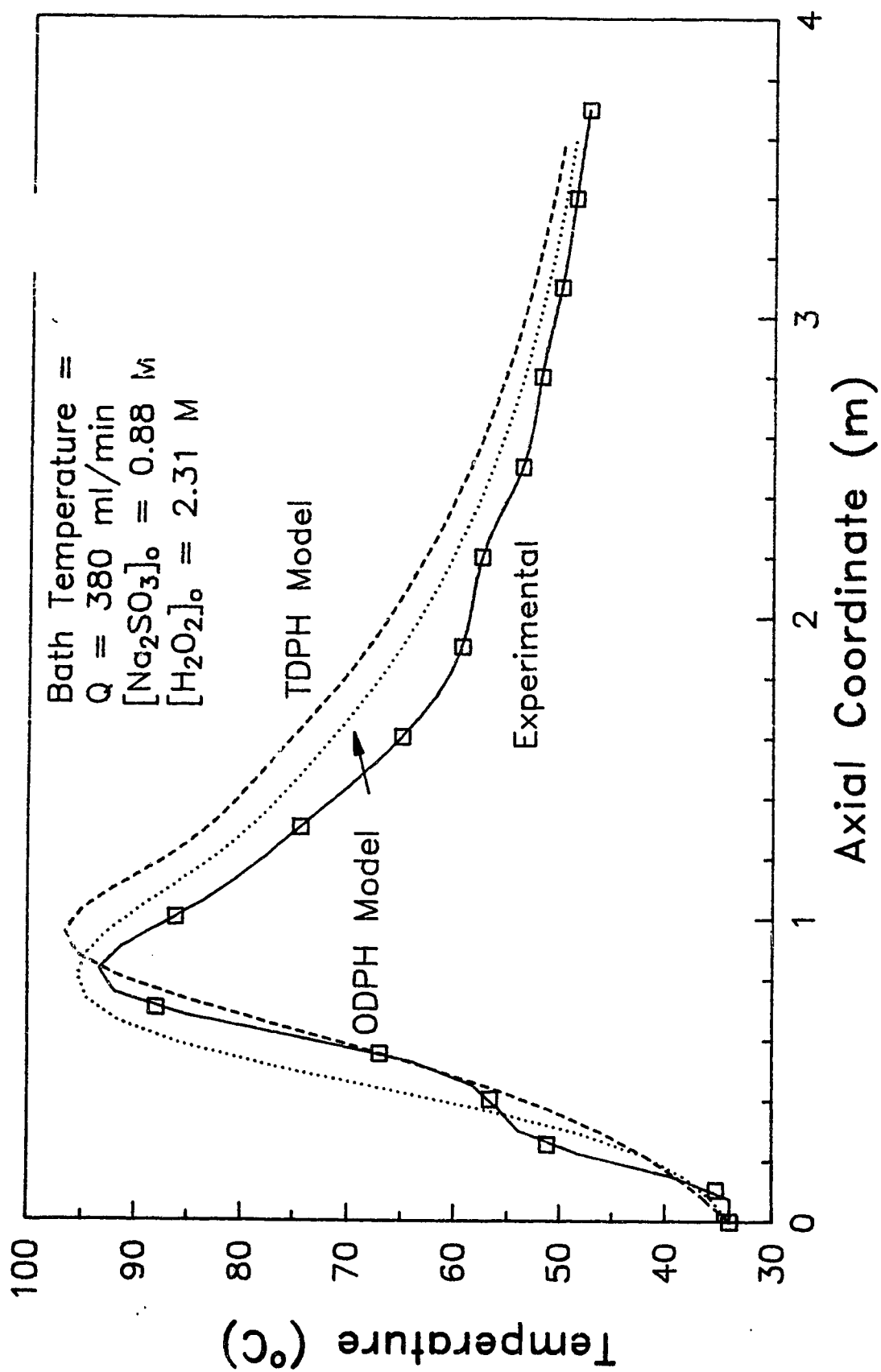


Figure 7.15 Experimental Data Comparison with ODPH and TDPH Models

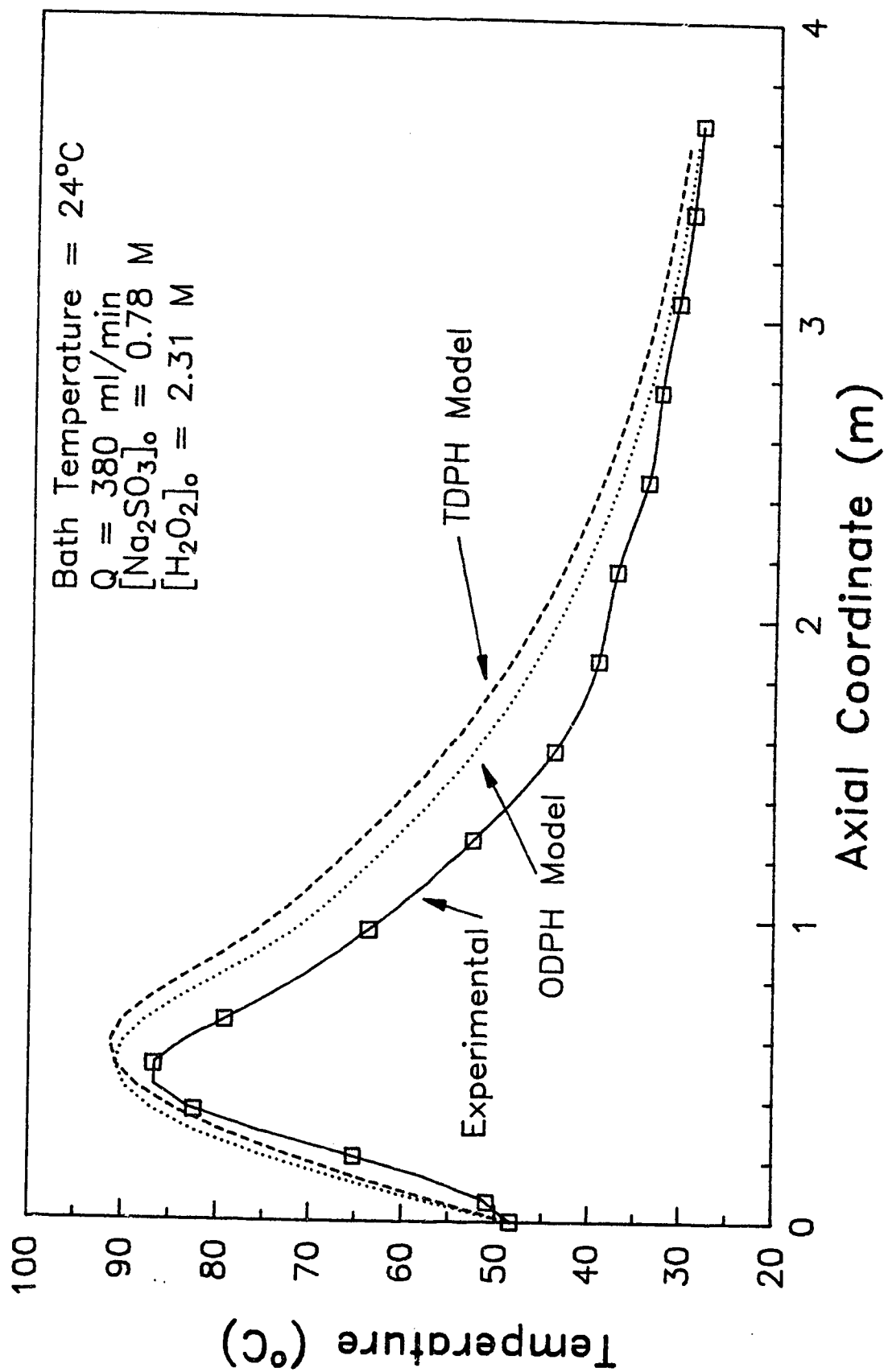


Figure 7.16 Experimental Data Comparison with ODPH and TDPH Models

Figure 7.17 illustrates the effect on the ODPH simulation if the initial concentration of sulfite is changed by 5%. This value was chosen because it was assumed that this was the likely error bar on the sulfite concentration. This figure shows that the difference between the curves cannot be attributed to an error in the concentration measurement. Figure 7.18 illustrates that a 10% change in the value of the overall heat transfer coefficient is insufficient to obtain agreement.

Figure 7.19 illustrates the changes in the ODPH model as the Arrhenius parameters are varied. It is clear that, much closer agreement between the model and the experimental data is possible by adjusting the value of the Arrhenius parameters. This was not surprising as it had been shown previously (section 3.3) that the temperature profile was extremely sensitive to the values of the Arrhenius parameters. What is important here is that the values of the Arrhenius parameters used in Figure 7.19 (and that appear to describe the experimental data fairly well), are well within the 95% confidence intervals for the values determined from the adiabatic batch reactor (section 3.4.2). Thus, the observed difference between the ODPH model and the experimental may be due to effect of the Arrhenius parameters. Similar results can be seen with the TDPH model in Figure 7.20.

In addition to the parameter values being in error, the possibility of the actual model being inappropriate must be considered. It has

already been noted that, both the ODPH and TDPH models are based on the assumption of plug flow. It has also been noted that the Reynolds number inside the reactor is approximately 5,000. This indicates that the flow is in the transition region, not being quite yet turbulent. Thus, the radial velocity profile in the reactor is probably not uniform (i.e., plug flow). Therefore, the model may fall short of describing the data for this reason alone. Further simulations of equations 5.3 and 5.4, with an appropriate form of the velocity profile (i.e.,  $u=\phi(r)$ ) taken into consideration, would determine whether this was the case.

A final possible reason for the observed difference between the data and the models must be considered. It is possible that, in the tubular reactor, as the temperature increased, some of the reacting mixture vaporized. This would have the effect of keeping the hot-spot temperature lower than it would otherwise be in the absence of vaporization. This possibility was not taken into consideration in the model and thus, if it did occur in the experimental reactor, the model would tend to over predict (relative to the experimental data) the temperatures in and around the location of the hot-spot.



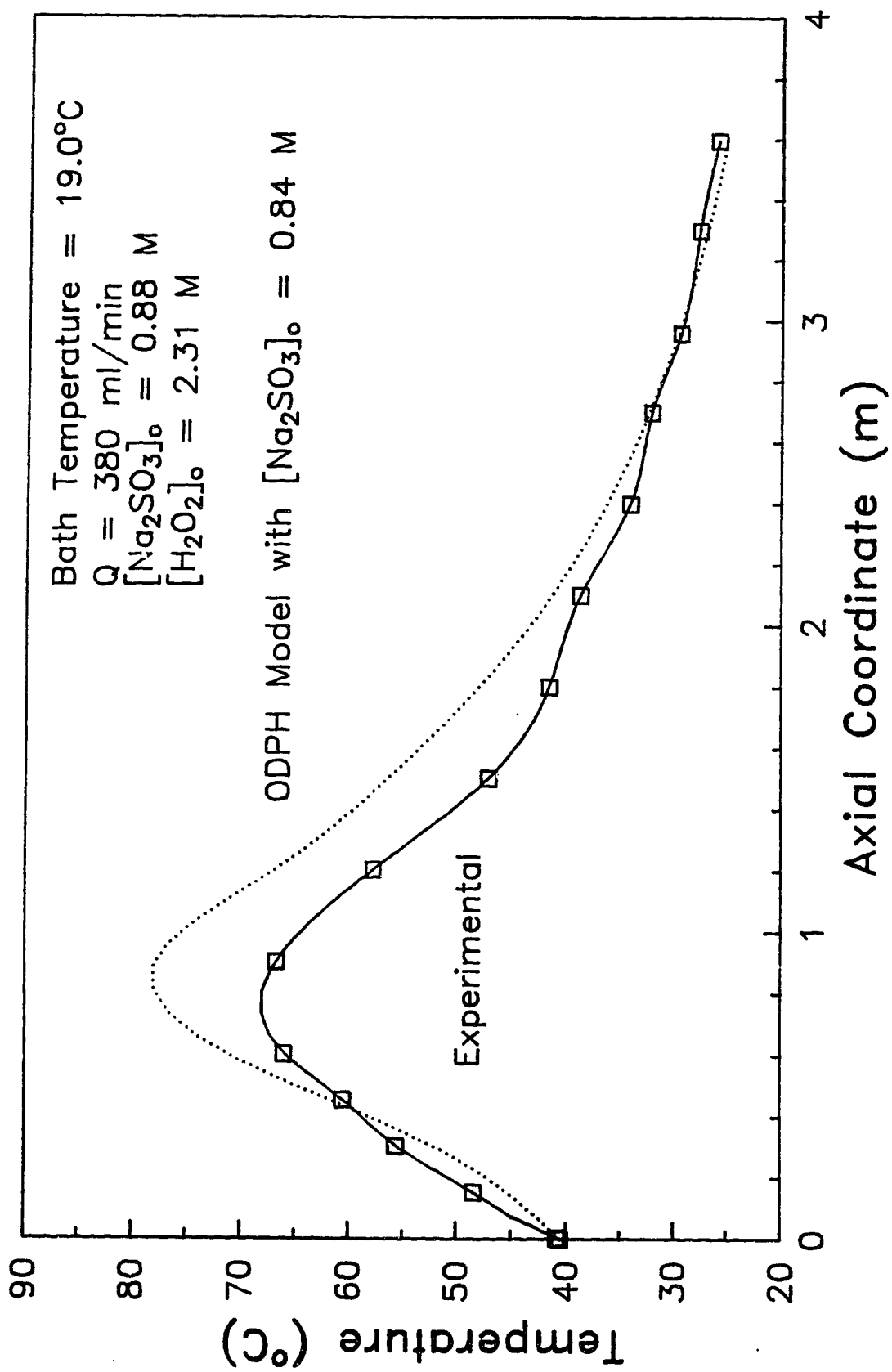


Figure 7.17 Experimental Data Comparison with ODPH Model

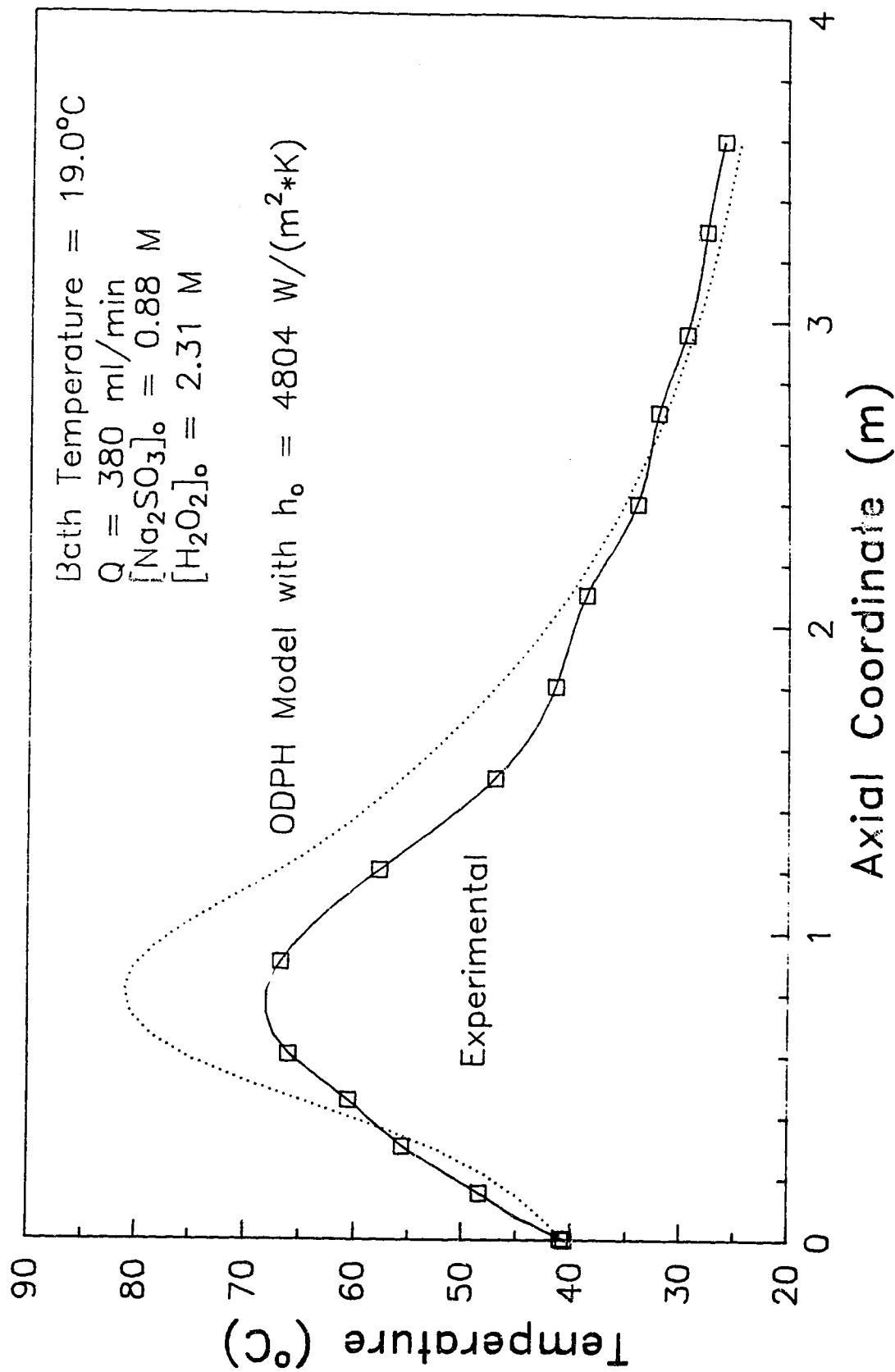


Figure 7.18 Experimental Data Comparison With ODPH Model

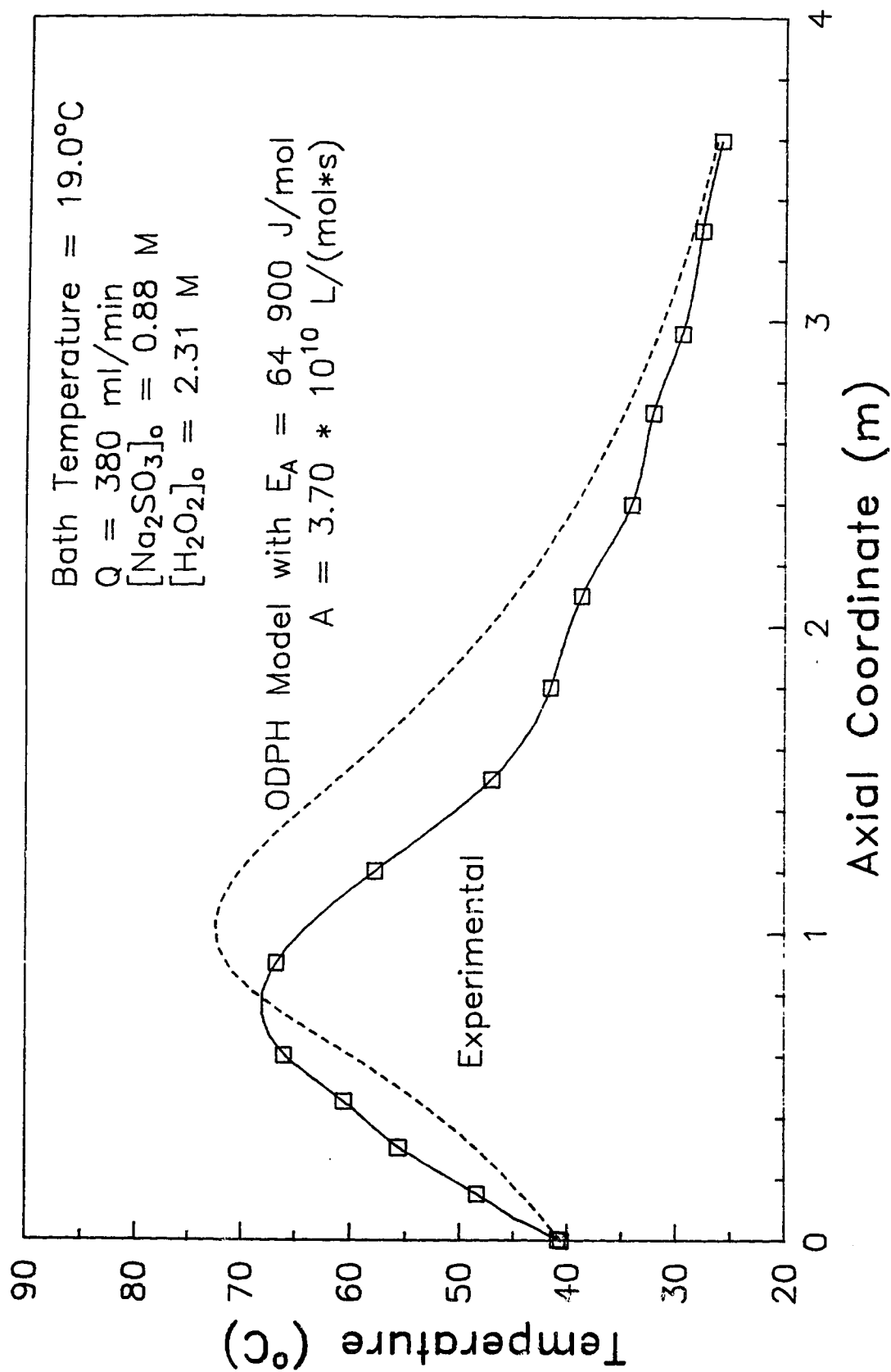


Figure 7.19 Experimental Data Comparison with ODPH Model

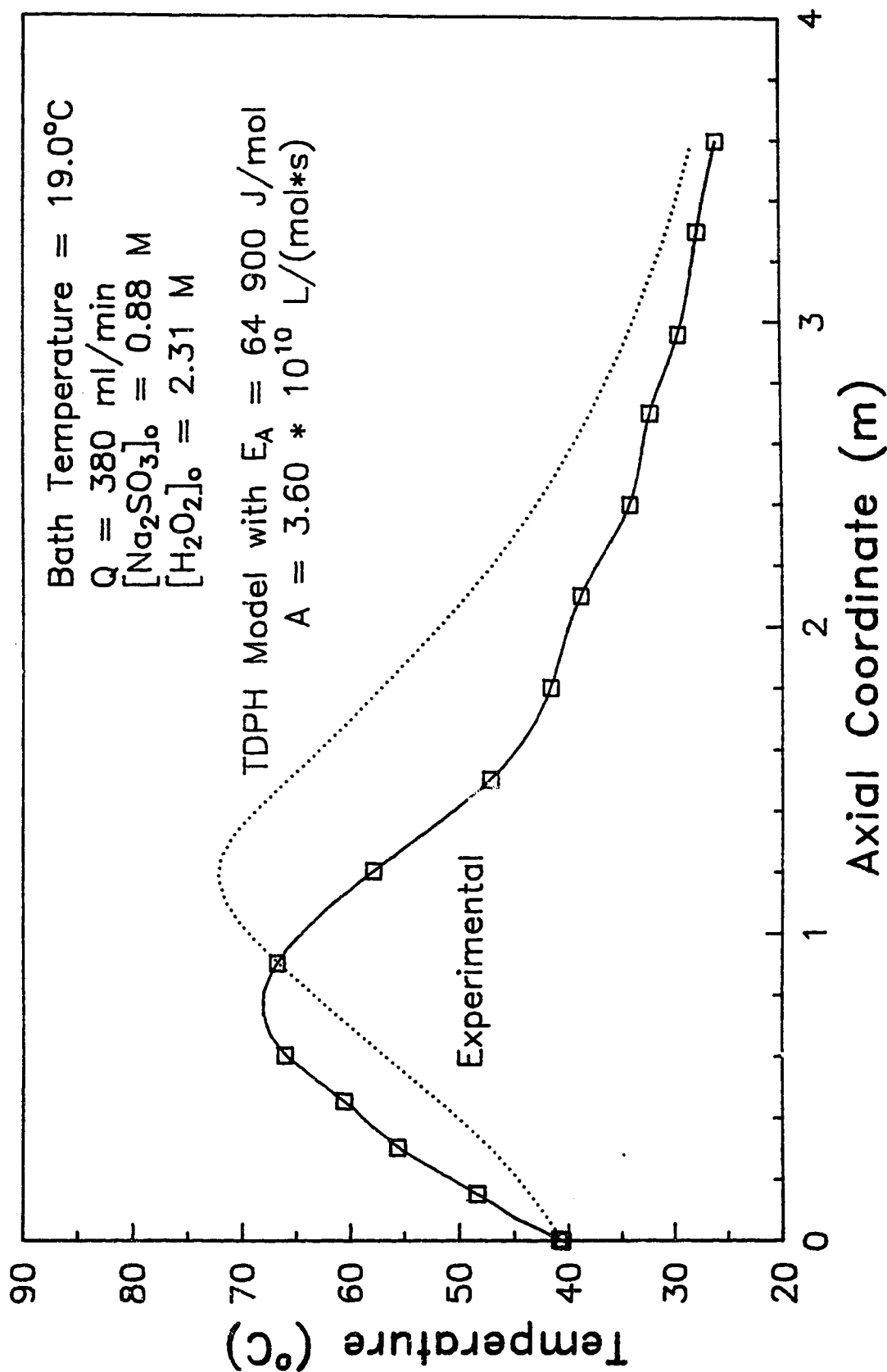


Figure 7.20 Experimental Data Comparison with TDPH Model

## 7.1 COMPARISON OF EXPERIMENTAL DATA WITH REACTOR MODELS

### DETERMINATION OF MOST APPROPRIATE PARAMETER FIT

Since both the ODPH and TDPH models described the experimental profiles fairly well, either model can be considered appropriate for describing the experimental plug flow reactor. However, because the ODPH model tends to predict the location of hot-spot quite accurately and because there is some degree of uncertainty in the value of the overall heat transfer coefficient for the TDPH model for a flow rate of 380 ml/min, the ODPH model is the one that will be considered as the best model to describe the experimental data.

Although the ODPH model does describe the data reasonably well, it still falls short of predicting the value of the hot-spot in most cases. It has been noted previously that the Arrhenius parameters have a very large effect on the shape the temperature profile. In addition, it has already been suggested that the difference between the ODPH model and the experimental data may be attributable to small errors in the value of the Arrhenius parameters used in the simulation. Therefore, an attempt was made to "fine tune" the Arrhenius parameters so as to obtain the parameters that provide the best agreement with the experimental data. This attempt to determine these "best-fit" parameters was made so that these values could be used in the evaluation of parametric sensitivity criteria. In this way, the criteria could be fairly evaluated.

In order to do this, 3 experimental temperature profiles were chosen. These profiles, which are illustrated in Figure 7.21, represent the 3 different reactor operating regimes (as discussed in chapter 6). Using these profiles, an attempt was made to find a set of Arrhenius parameters ( $A, E_A$ ) that could simultaneously describe all three profiles.

From Figure 7.21 it can be seen that the parameter values of  $2.90 \cdot 10^{10}$  L/(mol·s) for the pre-exponential factor and 64,000 J/mol for the activation energy are able to describe all three data sets. The error in the hot-spot prediction is less than 5°C in all cases. Figure 7.22 indicates how well these parameter values describe the batch reactor data. It can be seen from this figure that using these Arrhenius parameters for modeling purposes is certainly reasonable given the batch reactor data available. In addition, from Table 3.1 it can be seen that these parameter values lie within the experimentally determined confidence intervals. (It can also be shown that these parameters are statistically acceptable, given the adiabatic batch reactor data. This is shown at the end of Appendix E.)

Figures 7.23 - 7.25 illustrate how well the ODPH model with these new "fine-tuned" parameters describes the experimental data. Although only some of the experimental data are used, trends are evident. For the steep temperature profiles (i.e., mostly adiabatic), the model still over predicts the hot-spot temperature. For the profiles which

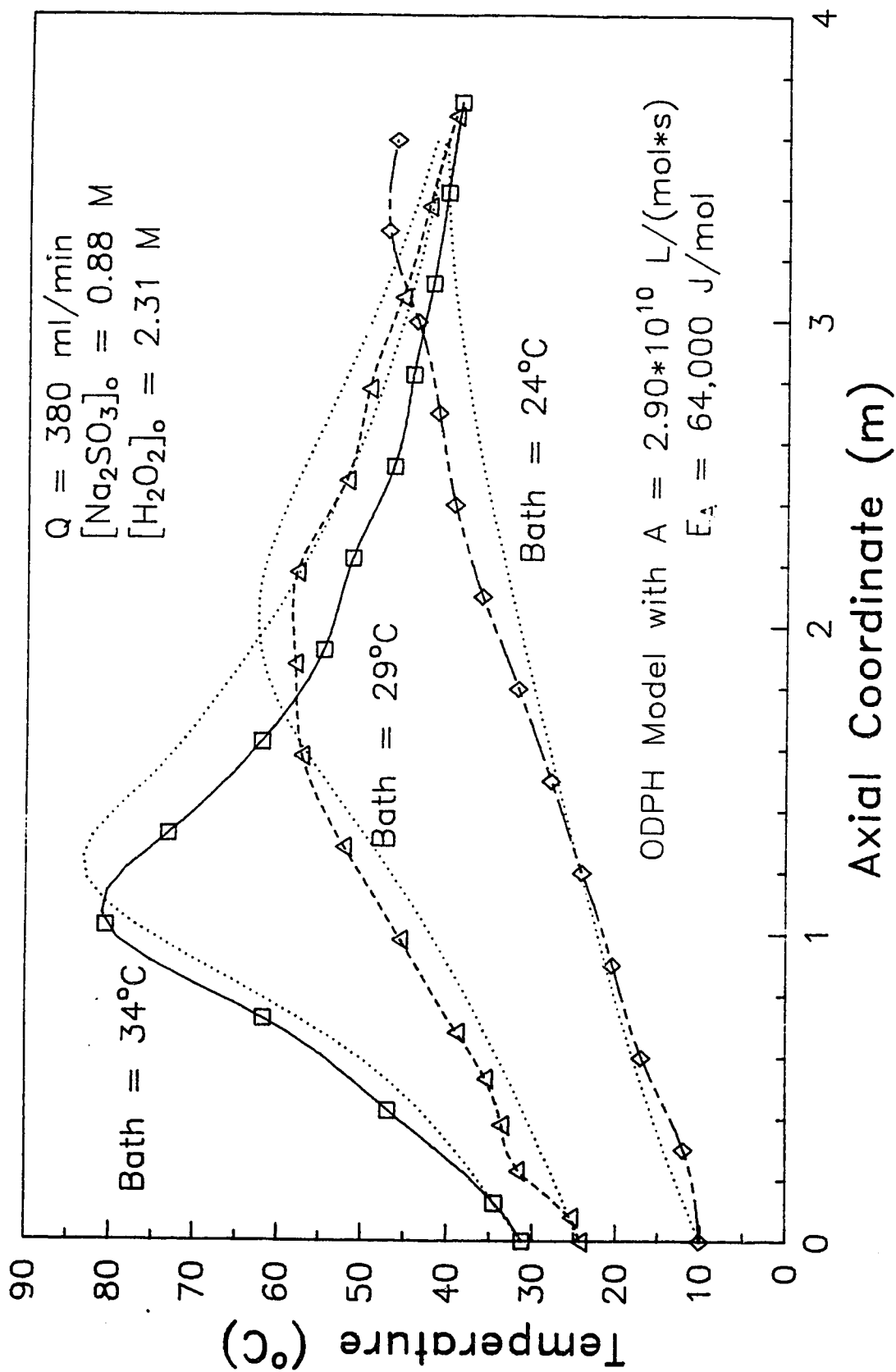


Figure 7.21 Determination of Optimal Arrhenius Parameters

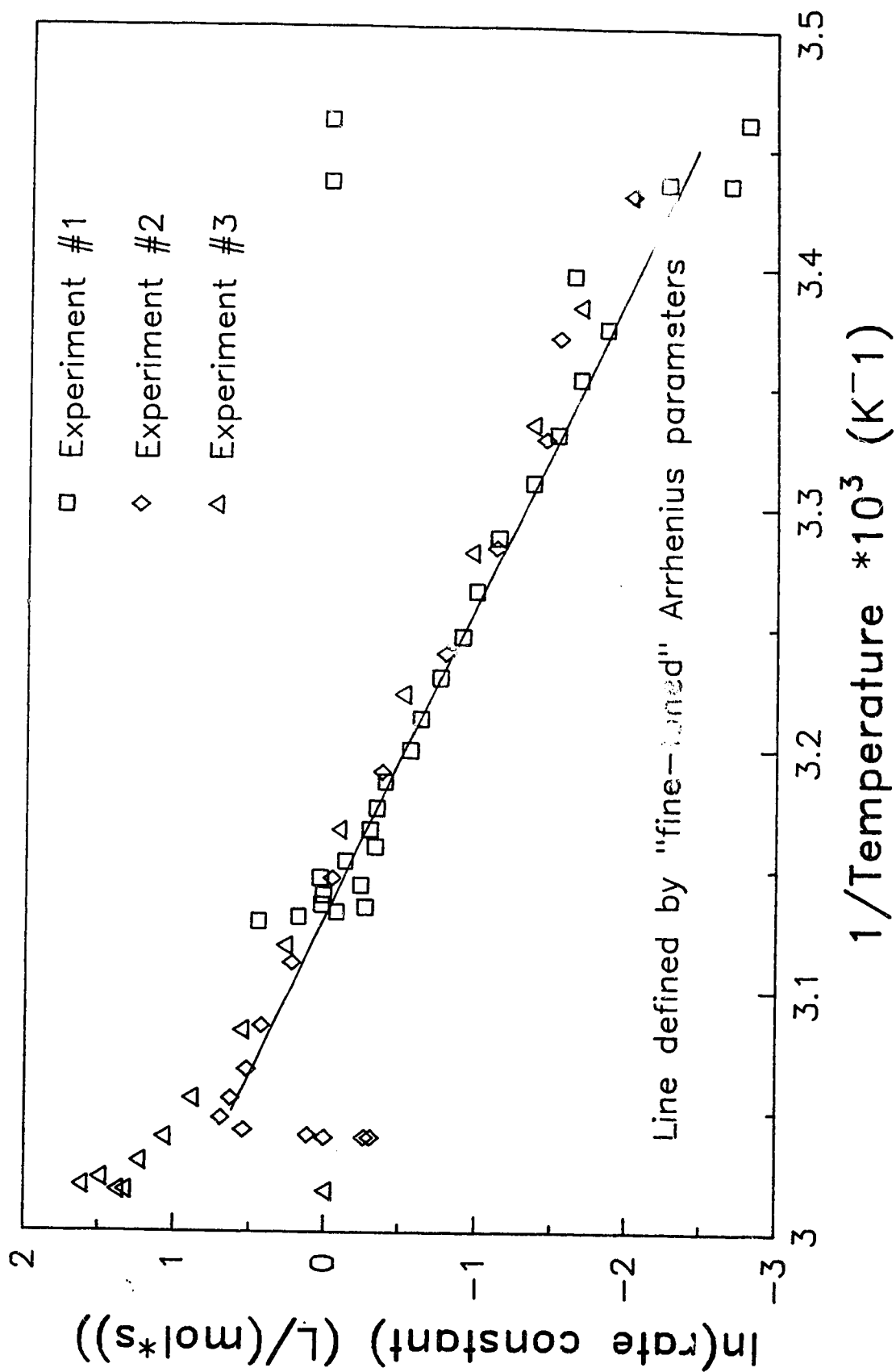


Figure 7.22 Arrhenius Plot using all Adiabatic Batch Reactor Data



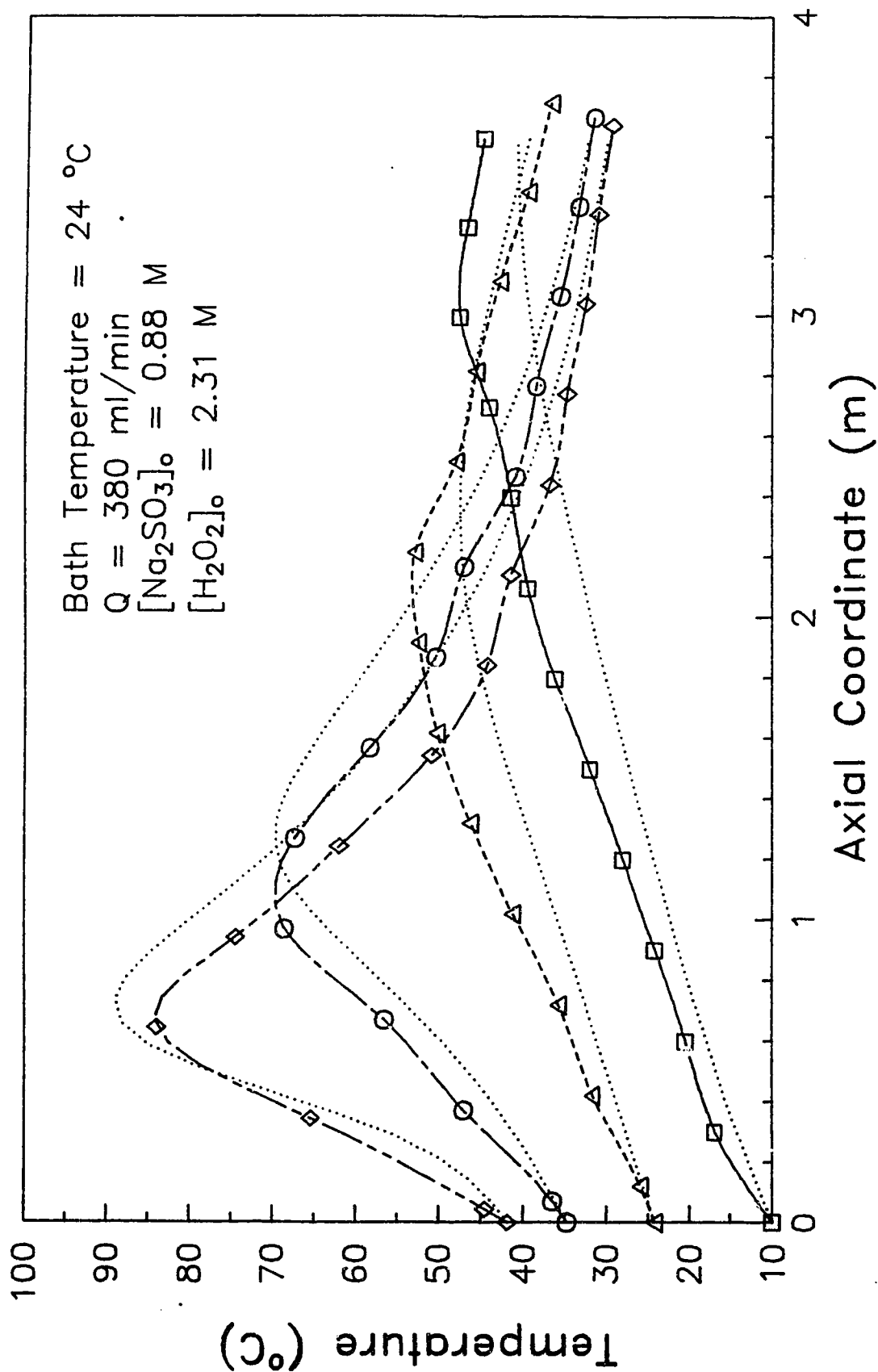


Figure 7.23 Experimental Data Comparison with ODPH Model Using Optimal Arrhenius Parameters

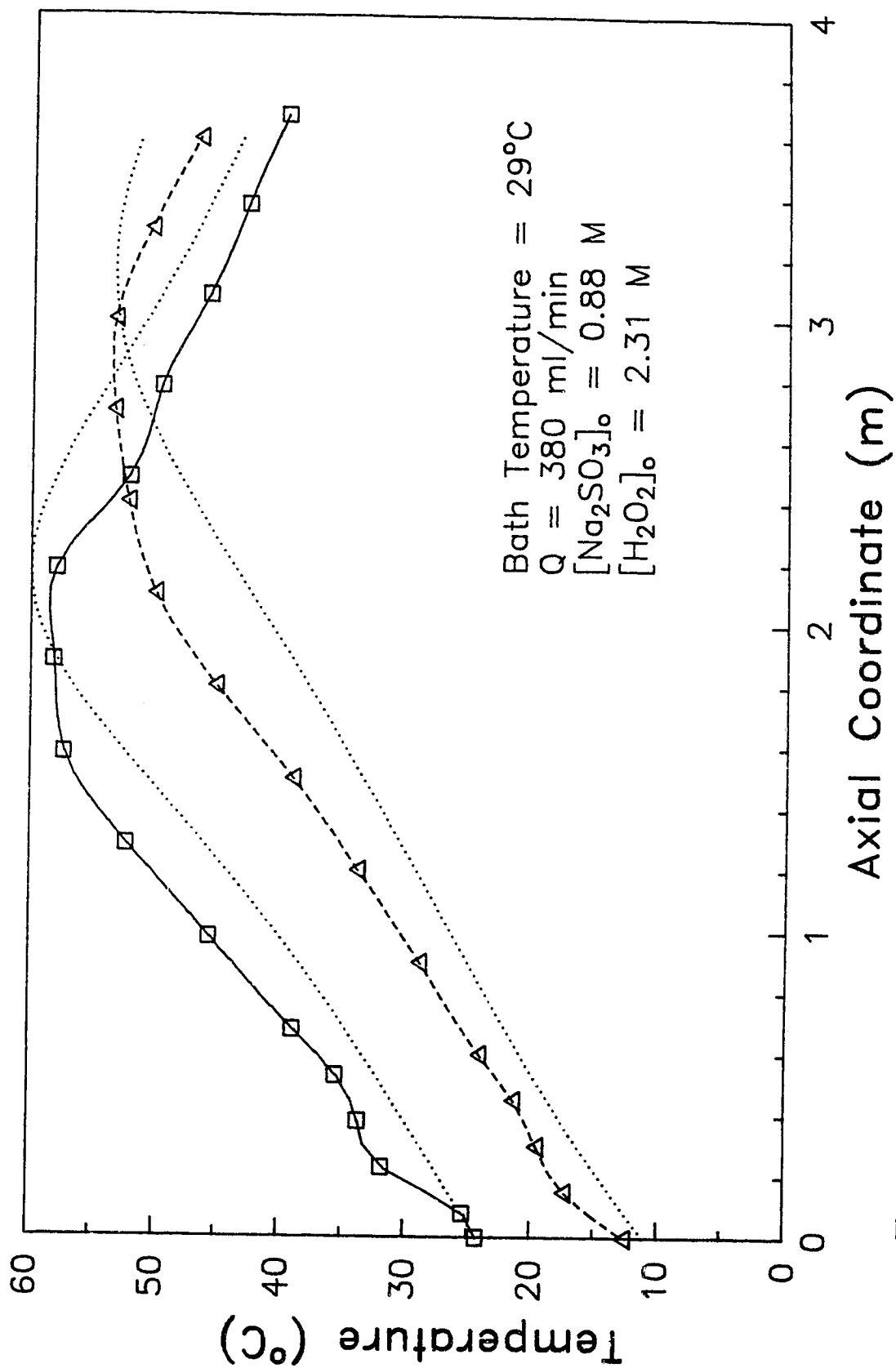


Figure 7.24 Experimental Data Comparison with ODPH Model Using Optimal Arrhenius Parameters

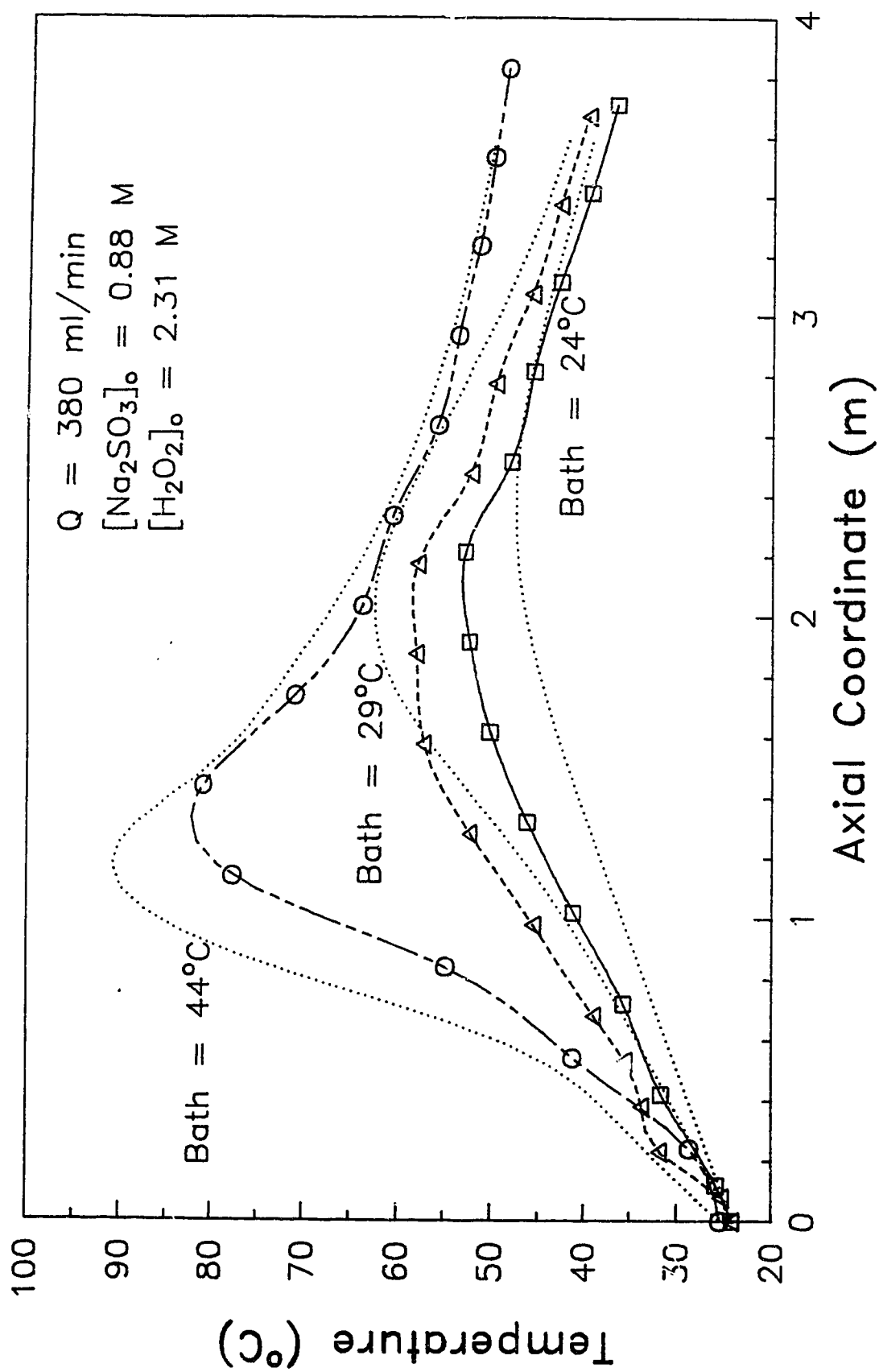


Figure 7.25 Experimental Data Comparison with ODPH Model Using Optimal Arrhenius Parameters

correspond to low inlet temperatures (i.e., mostly heat transfer controlled) the model under predicts the hot-spot temperature. This last point suggests that any further fine-tuning should perhaps involve the overall heat transfer coefficient. For the remaining profiles (i.e., those which are both heat transfer and reaction controlled), the hot-spot temperature is predicted rather accurately with only a slight misplacement of its location in some cases. This is an improvement over the previous model (i.e., with the original Arrhenius parameters) in which the hot-spot was consistently over predicted.

The fact that the ODPH model with the "fine-tuned" Arrhenius parameters appears to be able to predict better the hot-spot temperature in the operating regime where heat transfer and reaction kinetics are both controlling is not surprising. This is because the other two operating regimes are hardly affected by the Arrhenius parameters. For the heat transfer controlled region the overall heat transfer coefficient has the biggest influence on the hot-spot temperature whereas for the reaction controlled regime the profile is almost adiabatic so the hot-spot temperature is essentially determined by the inlet concentrations. Thus, "fine-tuning" the parameters will only really affect the temperature profiles which are controlled by both heat transfer and reaction kinetics.

This attempt to obtain agreement by "fine tuning" the parameters suggests an interesting new way of determining Arrhenius parameters. As noted previously, the determination of Arrhenius parameters for this reaction (and others like it) can be difficult. (Even Mader, who used a traditional batch reactor method, was forced to use extremely dilute solutions in order to maintain isothermal conditions.) However, if parametrically sensitive experimental data are available, then the data can be compared with an appropriate reactor model, with the Arrhenius parameters adjusted until a good fit is obtained. This method of course presupposes that an appropriate model exists and that the physical parameters of the reactor (including the heat transfer coefficient) are known. The advantage of this method is that, because the temperature profiles are extremely sensitive to the values of the Arrhenius parameters, there will only be a very narrow band of parameter values that will be able to match the data. Thus, the Arrhenius parameters can be determined very accurately. (It should be emphasized that the presupposition of the existence of an appropriate model and knowledge of the other (i.e., not the Arrhenius parameters) parameter values should not be taken lightly. If the model is inappropriate, or the parameter values are inaccurate, then the Arrhenius parameters that result in the best agreement with the data will not be the true Arrhenius parameters.)

In conclusion then, it has been shown that both the ODPH and the TDPH models with the experimentally determined (section 3.4.2 and 5.1)

Arrhenius parameters and heat transfer coefficient predict the reactor behavior reasonably well. The models predict the shape of the temperature profiles very well but tend to overestimate the value of the hot-spot by 10-15°C. The TDPH model tends to predict that the location of the hot-spot will be further into the reactor than that observed experimentally. "Fine-tuning" of the Arrhenius parameters for the ODPH model results in much better agreement at the hot-spot with temperature differences of around 5°C in most cases. For the operating regime where both heat transfer and reaction kinetics are controlling, the use of the "fine-tuned" parameters results in almost exact agreement at the hot-spot. This tuning also results in a slight misplacement of the hot-spot (similar to that of the TDPH model) in some cases. Nonetheless, it appears that the ODPH model with the Arrhenius parameters tuned is the model that best describes the experimental tubular reactor. In addition, as described in Chapter 5, the lack of significant temperature profiles radially, or axially along the wall indicates that the use of the TDPH model is not warranted.

## 8.0 EXPERIMENTAL TUBULAR REACTOR

### EVALUATION OF PARAMETRIC SENSITIVITY

This section examines the experimental data with the aim of extracting the parametrically sensitive operating conditions. These conditions will be used in chapter 9 to evaluate some of the existing sensitivity criteria.

Because the inlet temperatures chosen for each of the fixed bath temperature experiments were the same, it is possible to plot the data with the bath temperature as the variable parameter. This can be seen in Figures 8.1- 8.6. These figures are simply the data from figures 6.3-6.8 replotted with the inlet temperature fixed and the bath temperature variable.

Parametric sensitivity is once again evident. Looking at Figure 8.1 as an example, increasing the bath temperature from  $29^{\circ}\text{C}$  to  $34^{\circ}\text{C}$  results in an increase in the hot-spot temperature of approximately  $15^{\circ}\text{C}$ . Similar observations can be made for the other figures. It should be noted here that, the parametrically sensitive profiles are not as "sharply" (i.e., characterized by a steep rise and fall around the hot-spot) defined as those for the case of fixed bath temperatures. The reason for this is that, as the bath temperature is increased, the hot-spot increases but so does the temperature of the output stream (because it cannot be cooled to any lower than the bath temperature). Thus, the profiles are much smoother than those of the fixed bath

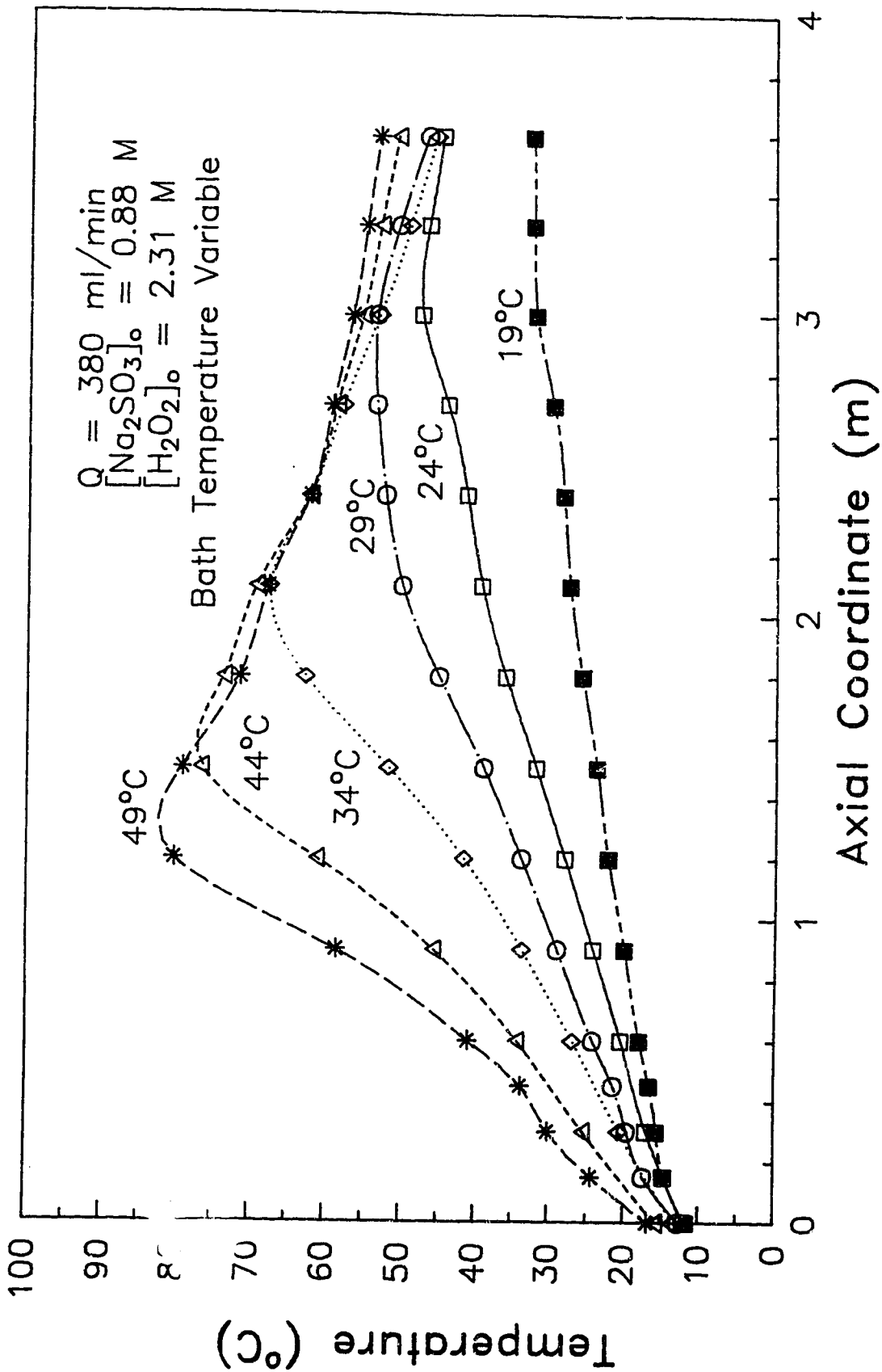


Figure 8.1 Experimental Data  
 Data from Tables C.4 C.12 C.19 C.28 C.29 C.37



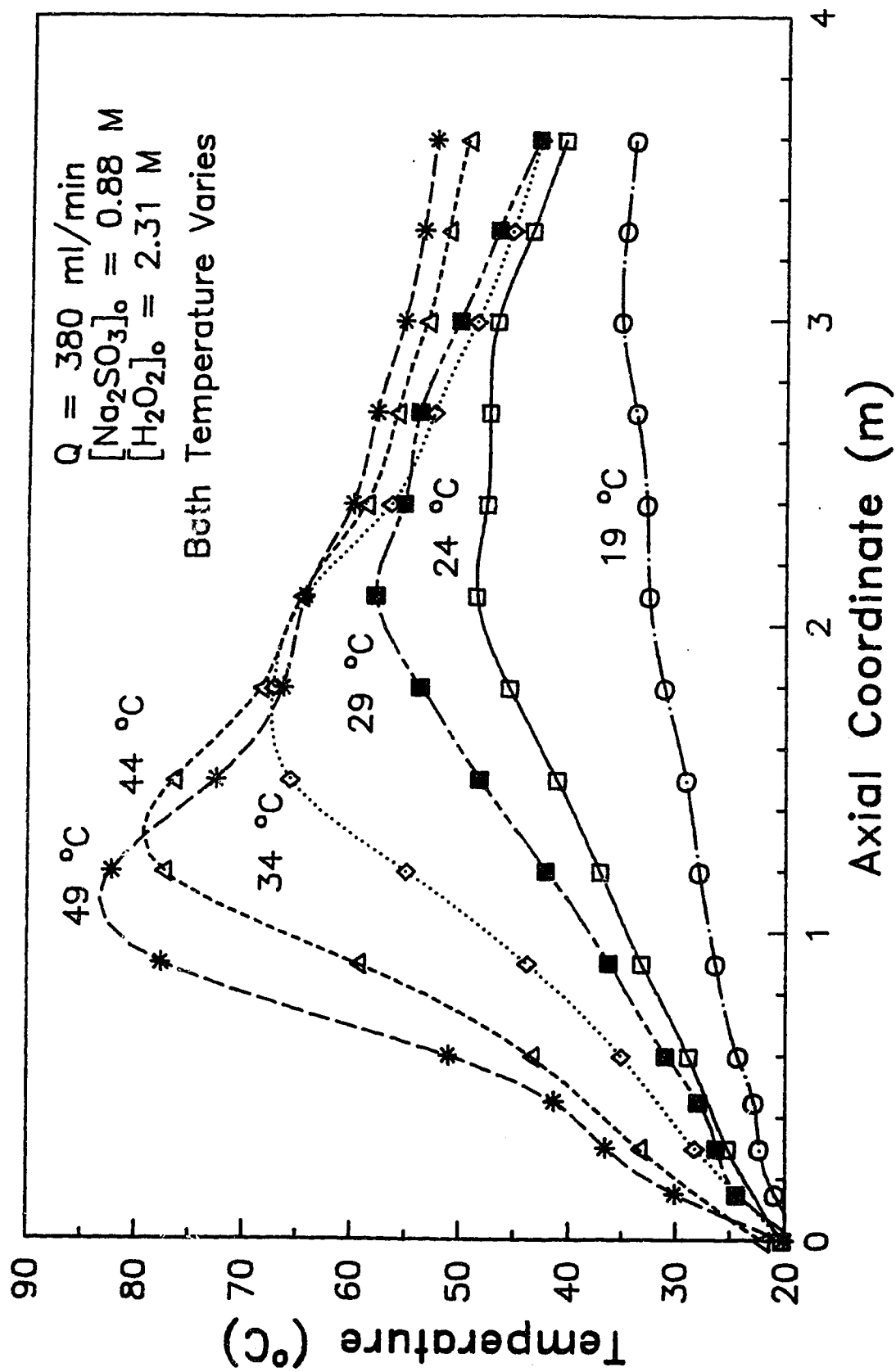


Figure 8.2 Experimental Data  
Data from Tables C.5 C.13 C.20 C.25 C.30 C.38

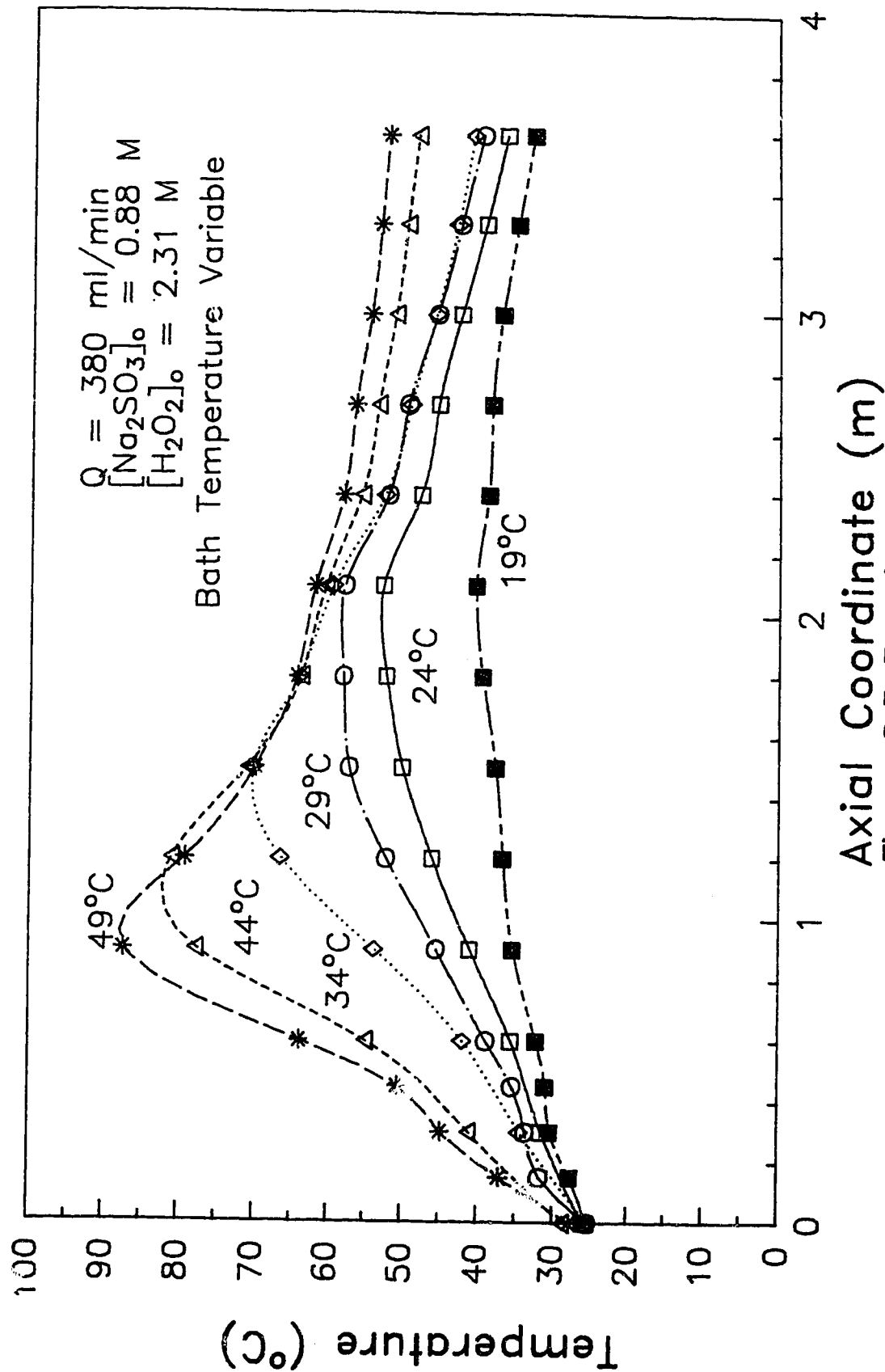


Figure 8.3 Experimental Data

Data from Tables C.6 C.14 C.21 C.26 C.31 C.39

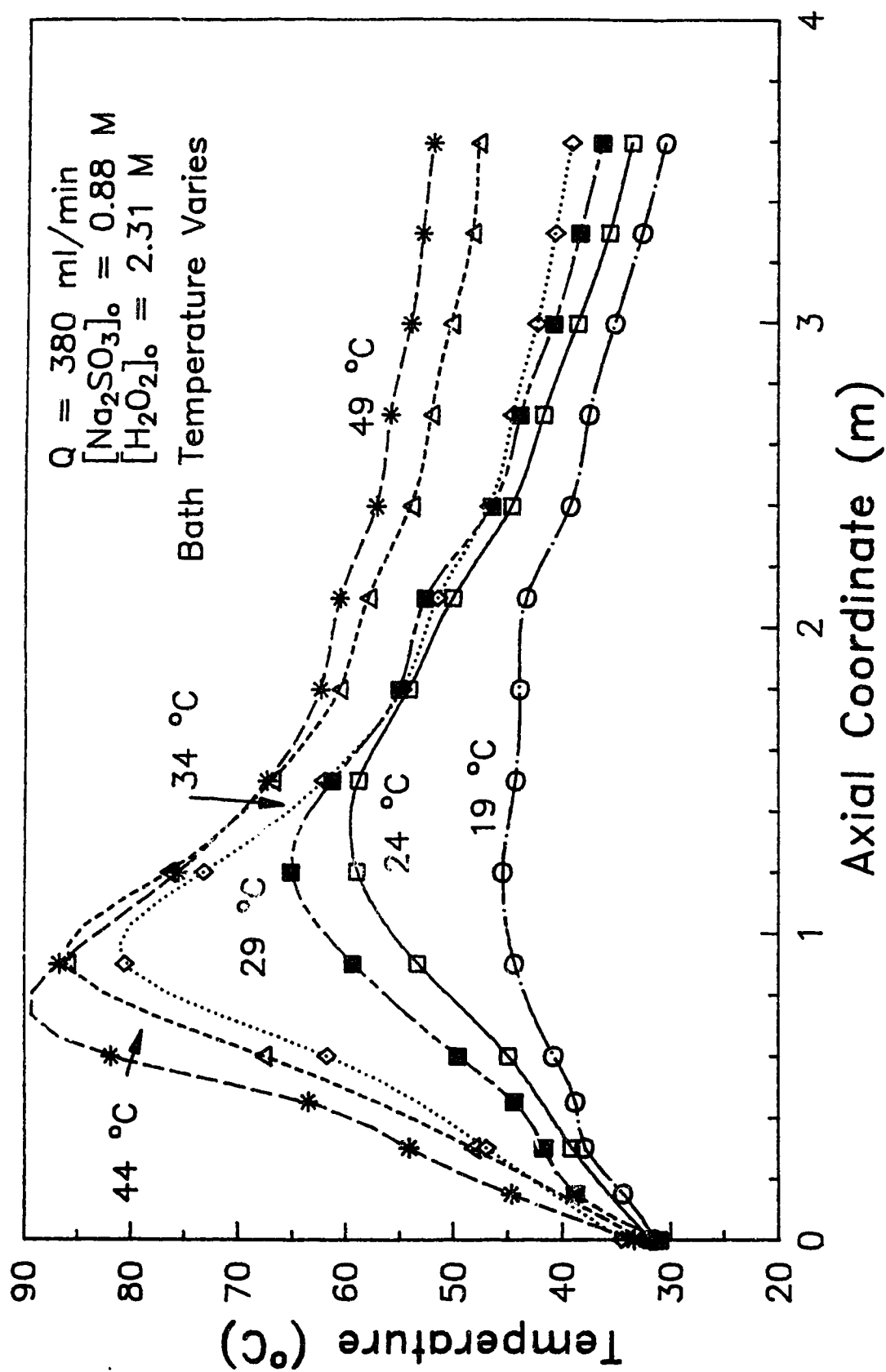


Figure 8.4 Experimental Data  
 Data from Tables C.7 C.15 C.22 C.27 C.32 C.40

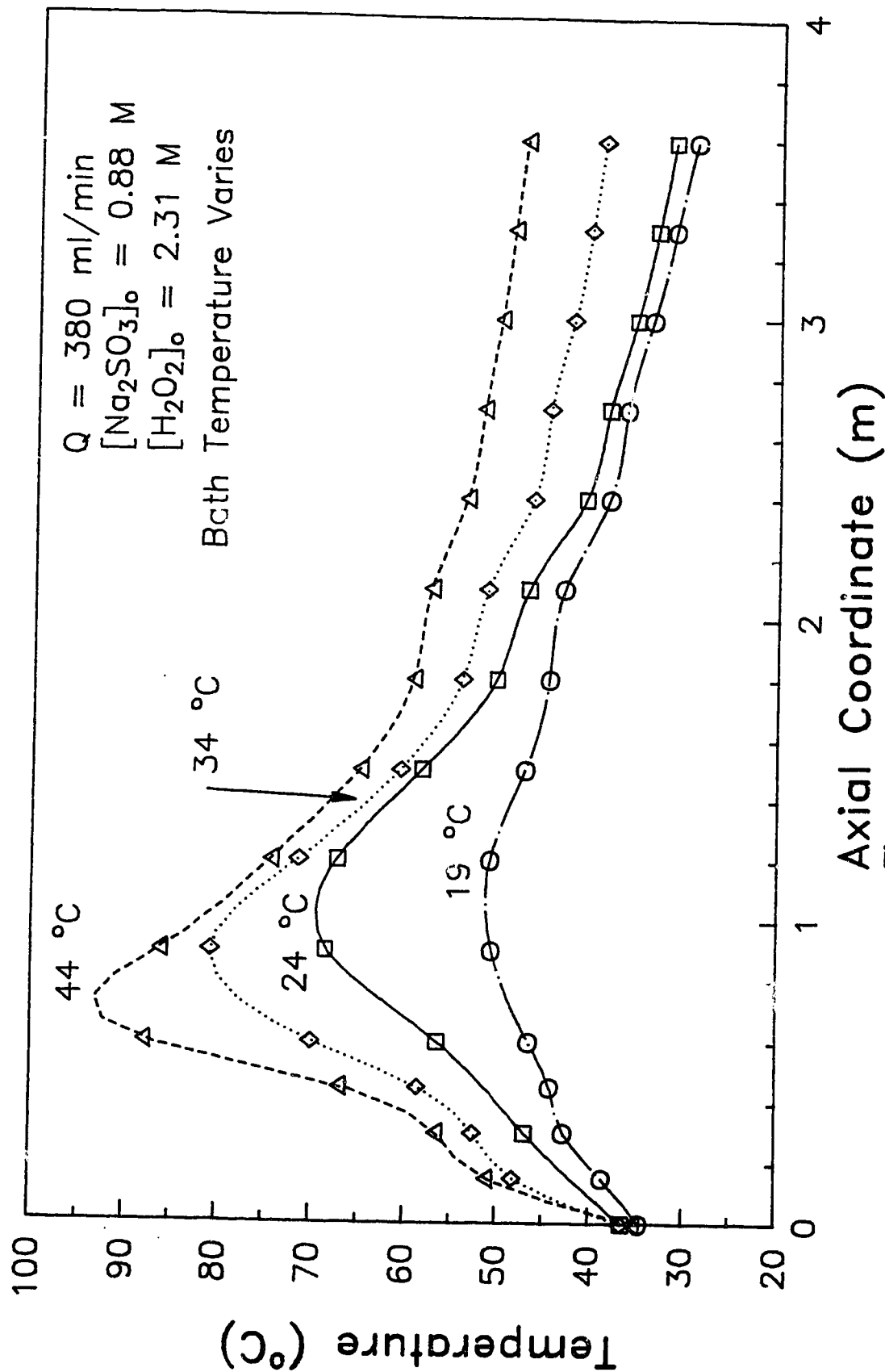


Figure 8.5 Experimental Data

Data from Tables C.8 C.16 C.23 C.33

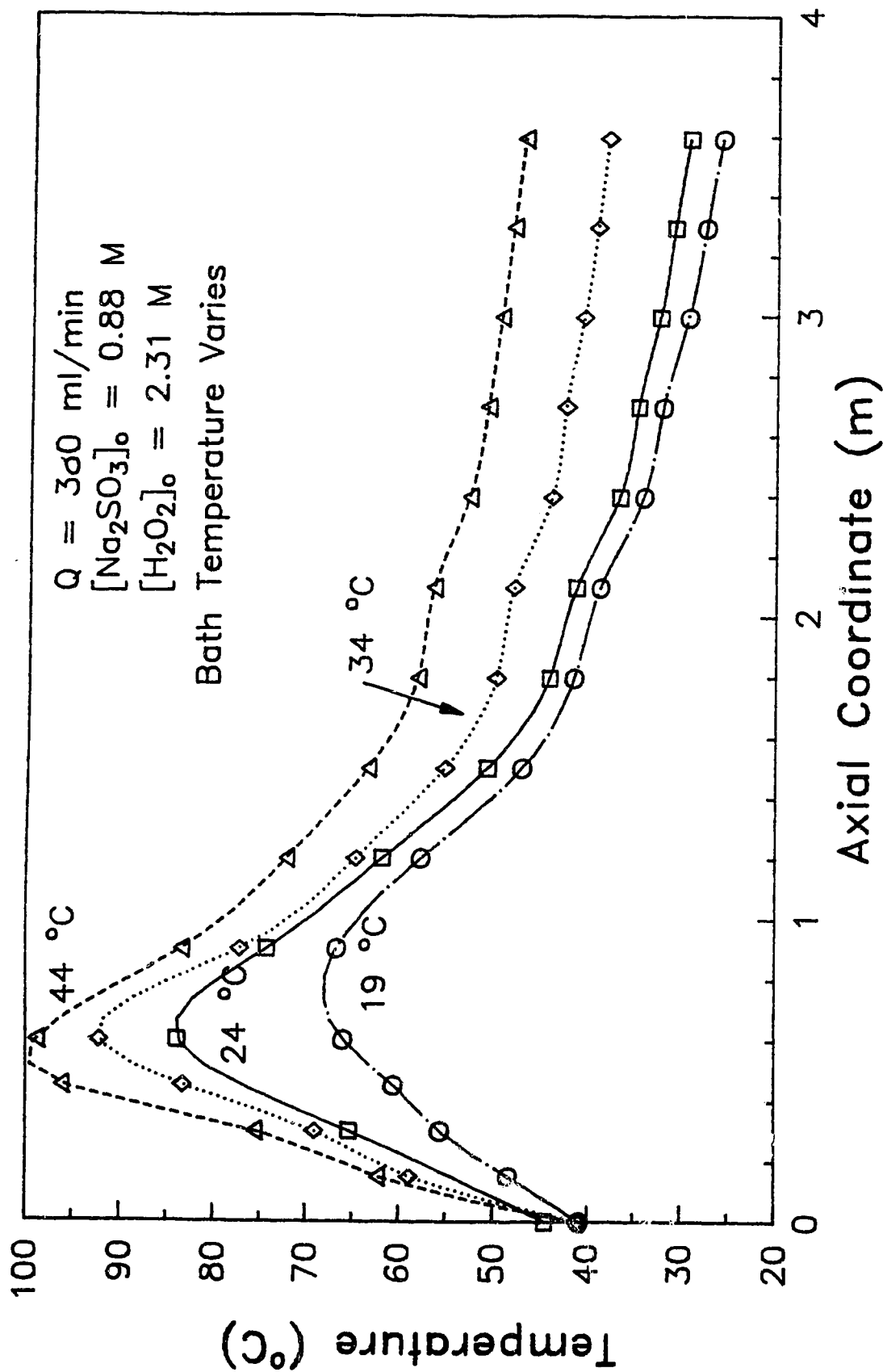


Figure 8.6 Experimental Data  
 Data from Tables C.9 C.17 C.24 C.34

temperature experiments. For the fixed bath temperature profiles, the increased hot-spot also resulted in a much steeper cooling section as the bath temperature was constant throughout.

### 8.1 PARAMETRIC SENSITIVITY - EXTRACTION OF CRITICAL CONDITIONS

Before sensitive conditions can be extracted from the data, a working definition of parametric sensitivity must be formulated. In this case, two different conditions were employed. One condition was applied for the case of variable inlet or bath temperature, the other was used for variable inlet sulfite concentration.

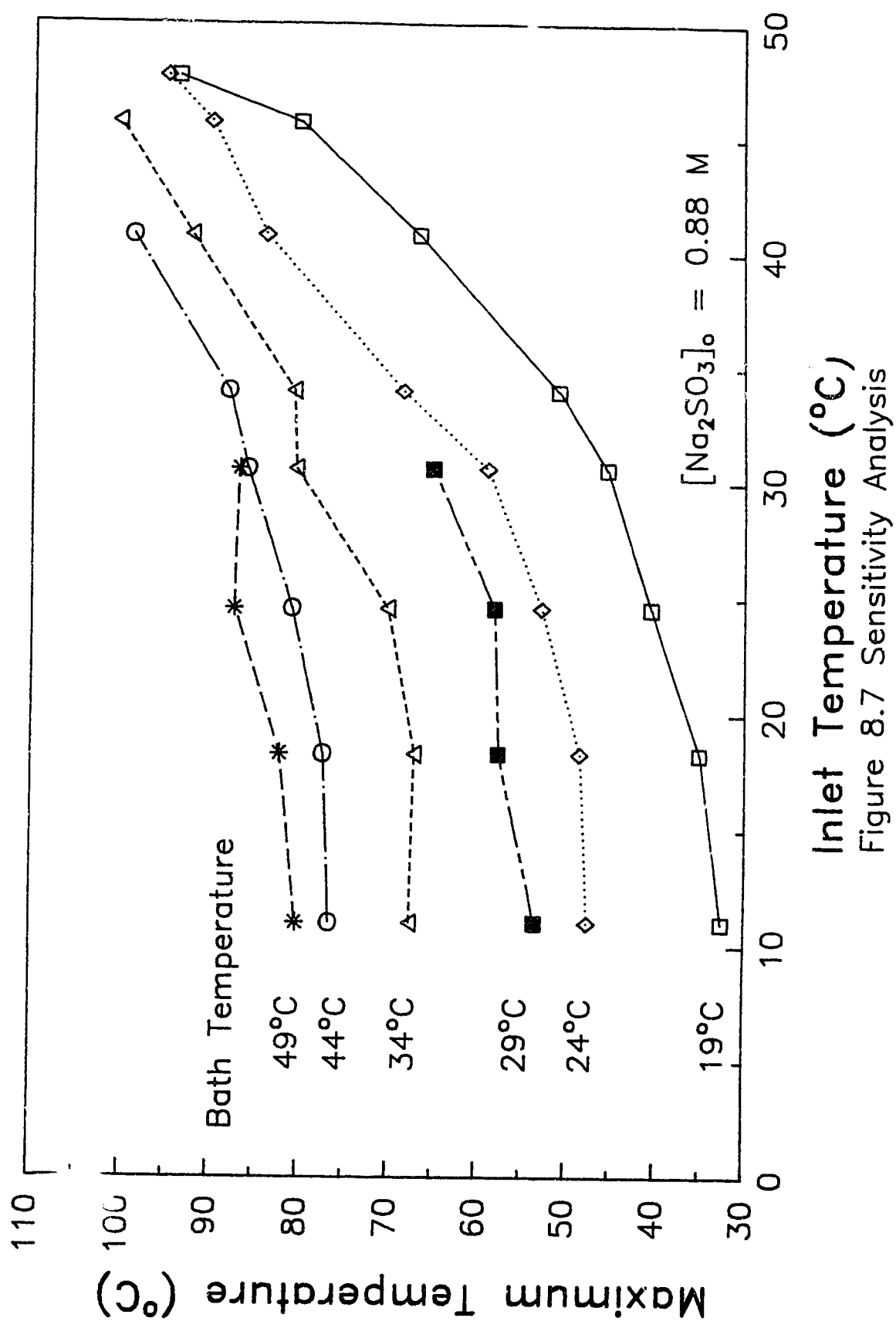
An increase of  $1^{\circ}\text{C}$  in the inlet temperature resulting in greater than a  $1^{\circ}\text{C}$  increase in the hot-spot temperature was defined as parametric sensitivity for the case of variable inlet temperature. The exact inlet temperature where this occurs can be determined from a plot of the hot-spot temperature versus inlet temperature. When the slope of this curve equals unity (i.e.,  $dT_m/dT_i = 1$ ), the conditions are sensitive. A similar condition was set out for the case of variable bath temperature (i.e., a  $1^{\circ}\text{C}$  increase in the bath temperature resulting in greater than a  $1^{\circ}\text{C}$  increase in the hot-spot temperature).

For the case of variable inlet concentration, a different condition was used. Parametric sensitivity was said to occur when a 1 molar increase in the concentration resulted in a hot-spot temperature increase greater than the adiabatic temperature rise for a 1 molar

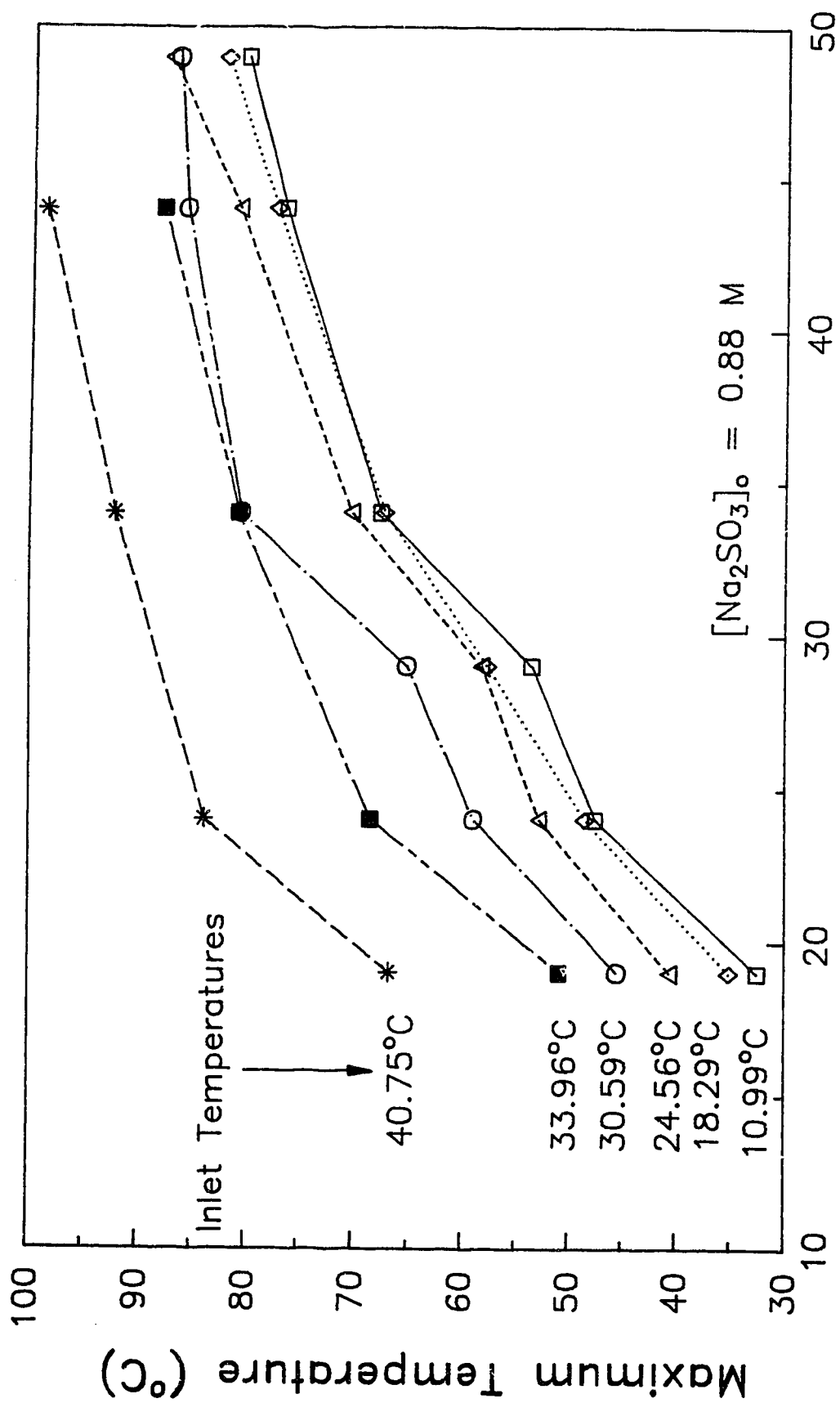
(limiting reactant) solution. For the sulfite reaction, the adiabatic temperature rise was  $89^{\circ}\text{C}/(\text{mole limiting reactant})$ . Thus, a plot of hot-spot temperature versus inlet concentration can be constructed with the critical condition being  $dT_m/dC_{Ao} = 89^{\circ}\text{C}/(\text{mol/L})$ .

It should be noted that these conditions are both based on the assumption that, parametrically sensitive operating conditions are those which result in a hot-spot change equal, or greater, to that which would be expected under adiabatic conditions. In the case of a variable inlet temperature, under adiabatic conditions a  $1^{\circ}\text{C}$  increase in inlet temperature results in a  $1^{\circ}\text{C}$  rise in the hot-spot temperature. Thus a hot-spot increase of greater than  $1^{\circ}\text{C}$  per  $1^{\circ}\text{C}$  change in inlet temperature is considered sensitive. For variable inlet concentration, a 1 molar change by definition results in a hot-spot change equal to the adiabatic temperature rise. Thus an increase in the hot-spot greater than the adiabatic amount is considered sensitive.

The application of these methods can be seen in Figures 8.7 through 8.9. In Figures 8.7 and 8.9 the curves follow the same basic shape. The slope is initially close to zero. The curve increases sigmoidally in the middle section and eventually decreases with the slope approaching a value of 1. This is the expected result and can be explained as follows.







Bath Temperature (°C)

Figure 8.8 Sensitivity Analysis

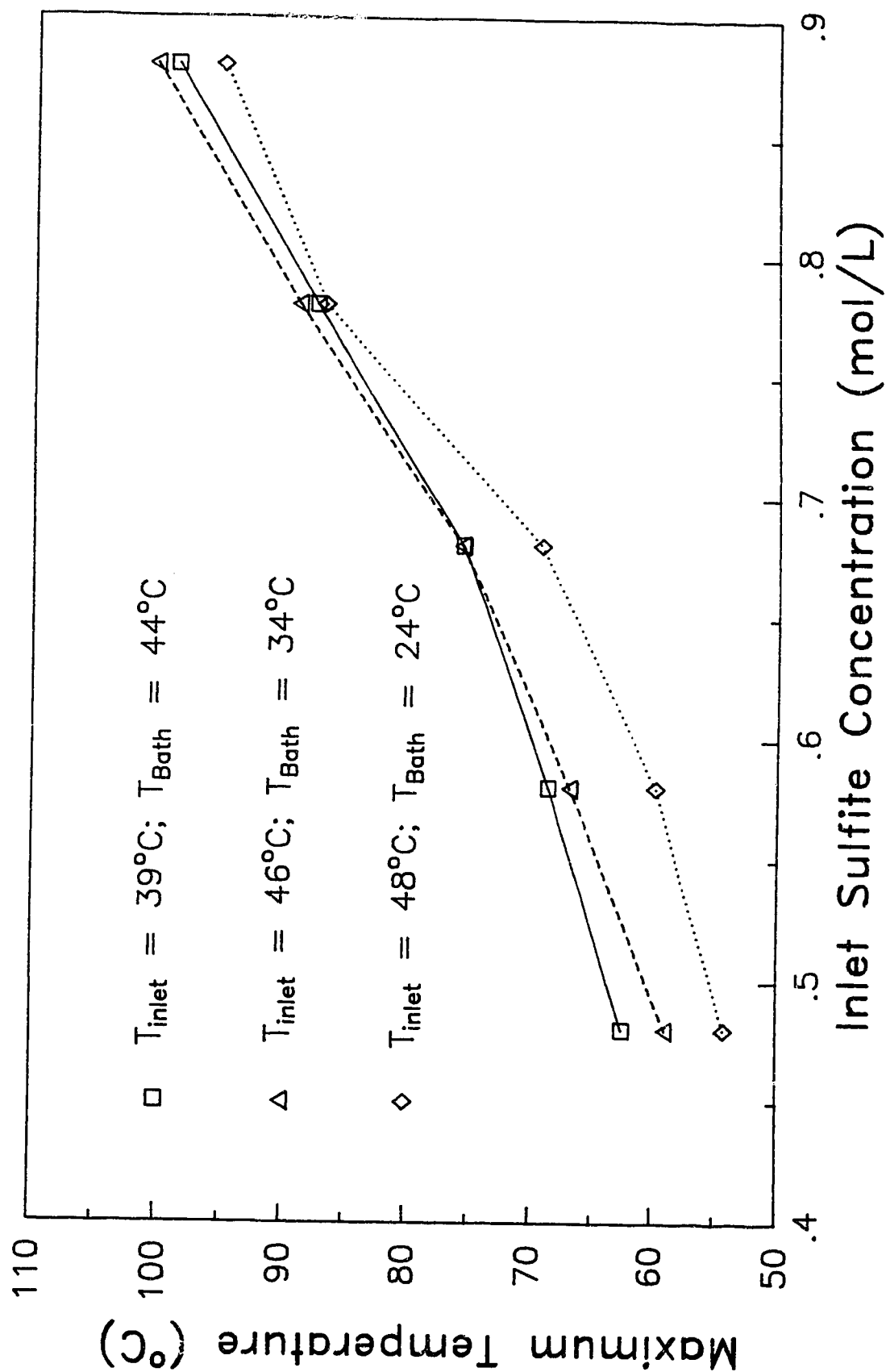


Figure 8.9 Sensitivity Analysis

Taking the case of a fixed bath temperature as an example, an initial increase in the inlet temperature has virtually no effect on the hot-spot. As the inlet temperature is increased and the conditions become more sensitive, the hot-spot begins to rise. Eventually the inlet temperature reaches a point where the reactor begins to behave adiabatically. At this point, the hot-spot temperature will change in direct proportion to the inlet temperature (i.e., a 1:1 ratio). Thus a plot of  $T_m$  versus  $T_i$  will initially have a slope of 0. At the end it will have a slope of 1. In the middle it will increase sigmoidally, the slope changing in value from 0, to a value much greater than 1, and then eventually back to 1.

The curves in figure 8.8 behave in a different manner. Initially, the slope is quite large. As the bath temperature is increased, the slope approaches zero. This is due to the fact that, as the bath temperature is increased, the temperature profile becomes adiabatic. Under adiabatic conditions, the bath temperature has no effect on the hot-spot temperature. Thus, the slope should approach zero. It is also interesting to note that, for low bath temperatures (i.e., heat transfer control of the reactor) the hot-spot temperature will increase in direct proportion to the bath temperature. Therefore, the hot-spot versus bath temperature curve is, in a sense, the opposite of the hot-spot versus inlet temperature curve because it has an initial slope of 1 and a final slope of 0.

With this considered, it now seems that the condition chosen to define sensitivity for the fixed inlet, variable bath temperature data is not a good one. This is because the slope of the maximum temperature versus bath temperature curve will only be equal to one at the very low end of the scale (i.e., heat transfer controlling), or at the high end of the scale when the conditions are approaching adiabatic. Thus, any critical conditions chosen in this way will be extremely unconservative (i.e., they will not be the conditions indicating the start of parametric sensitivity but rather, they will be conditions where parametric sensitivity already exists). On the other hand, the argument can be made that the sensitivity conditions extracted from the variable inlet temperature (or concentration) data are rather conservative. Conceivably then, the combination of the two will map out a fairly realistic region of parametric sensitivity.

For each curve in Figures 8.7, 8.8 and 8.9, a third order polynomial was fitted through the data (see Appendix F) and, from this, the critical values of the inlet temperature, bath temperature and inlet concentration were found. The results are summarized in Table 8.1.

TABLE 8.1 - PARAMETRICALLY SENSITIVE CONDITIONS (EXPERIMENTAL)		
Inlet Temperature ( $^{\circ}\text{C}$ )	Bath Temperature ( $^{\circ}\text{C}$ )	$[\text{Na}_2\text{SO}_3]_0$ (mol/L)
28.19	19.0	0.88
24.81	24.0	0.88
30.64	29.0	0.88
26.20	34.0	0.88
31.42	44.0	0.88
48.0	24.0	0.576
46.0	34.0	0.587
39.0	44.0	0.667
10.99	41.21	0.88
18.29	41.57	0.88
24.56	45.7	0.88
30.59	38.48	0.88
33.96	35.3	0.88
40.75	33.81	0.88

NOTE: In all cases the flowrate is 380 ml/min and the stirrer speed #6

Figures 3.10 and 8.11 illustrate the data in Table 8.1 in the form of a two dimensional plot with the third parameter (from the table) fixed. These diagrams can be considered as sensitivity plots as they mark out the regions of sensitivity and insensitivity. In each case, the region of sensitivity lies above and to the right of the data.

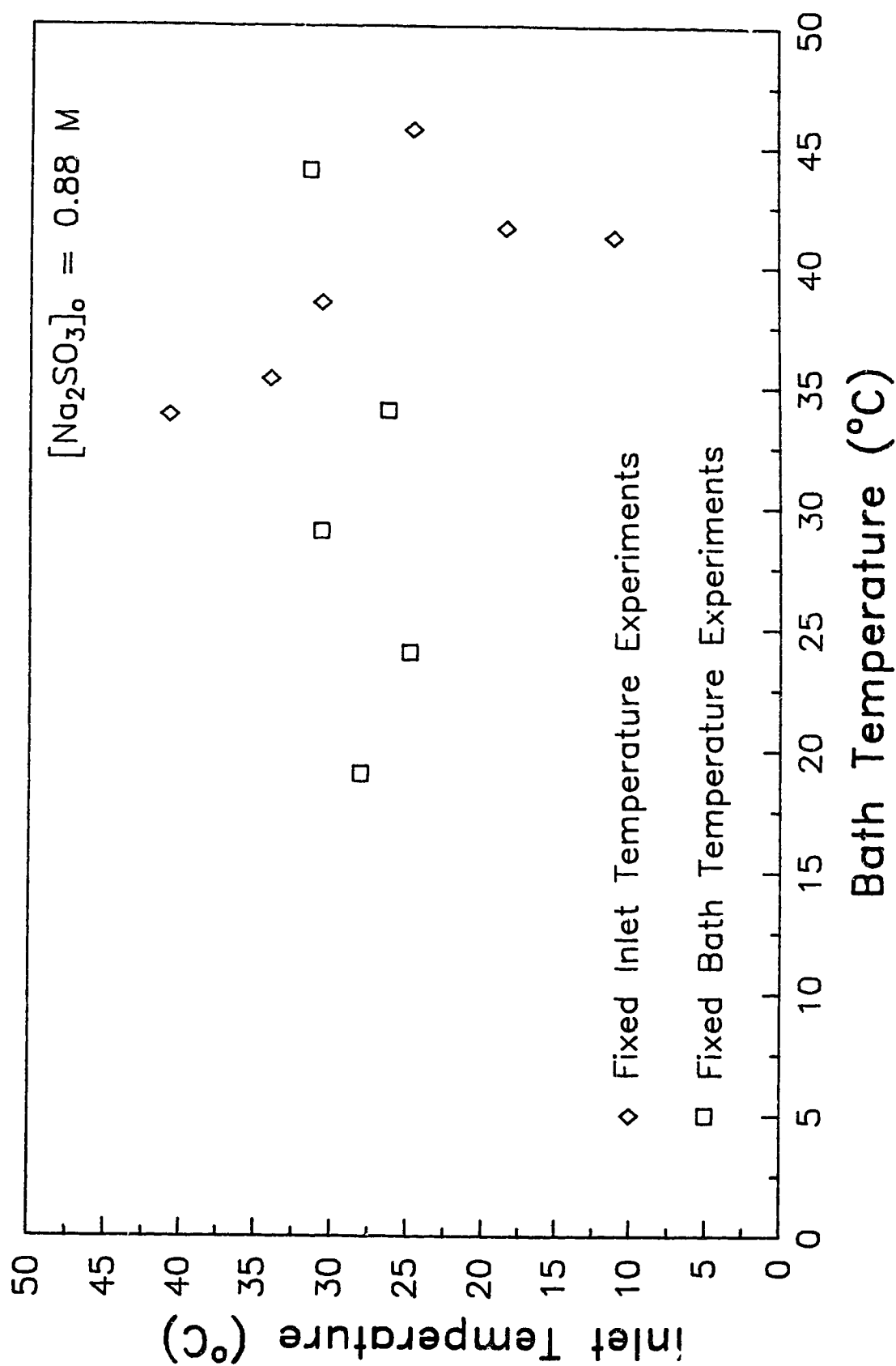


Figure 8.10 Experimentally Determined Critical Points

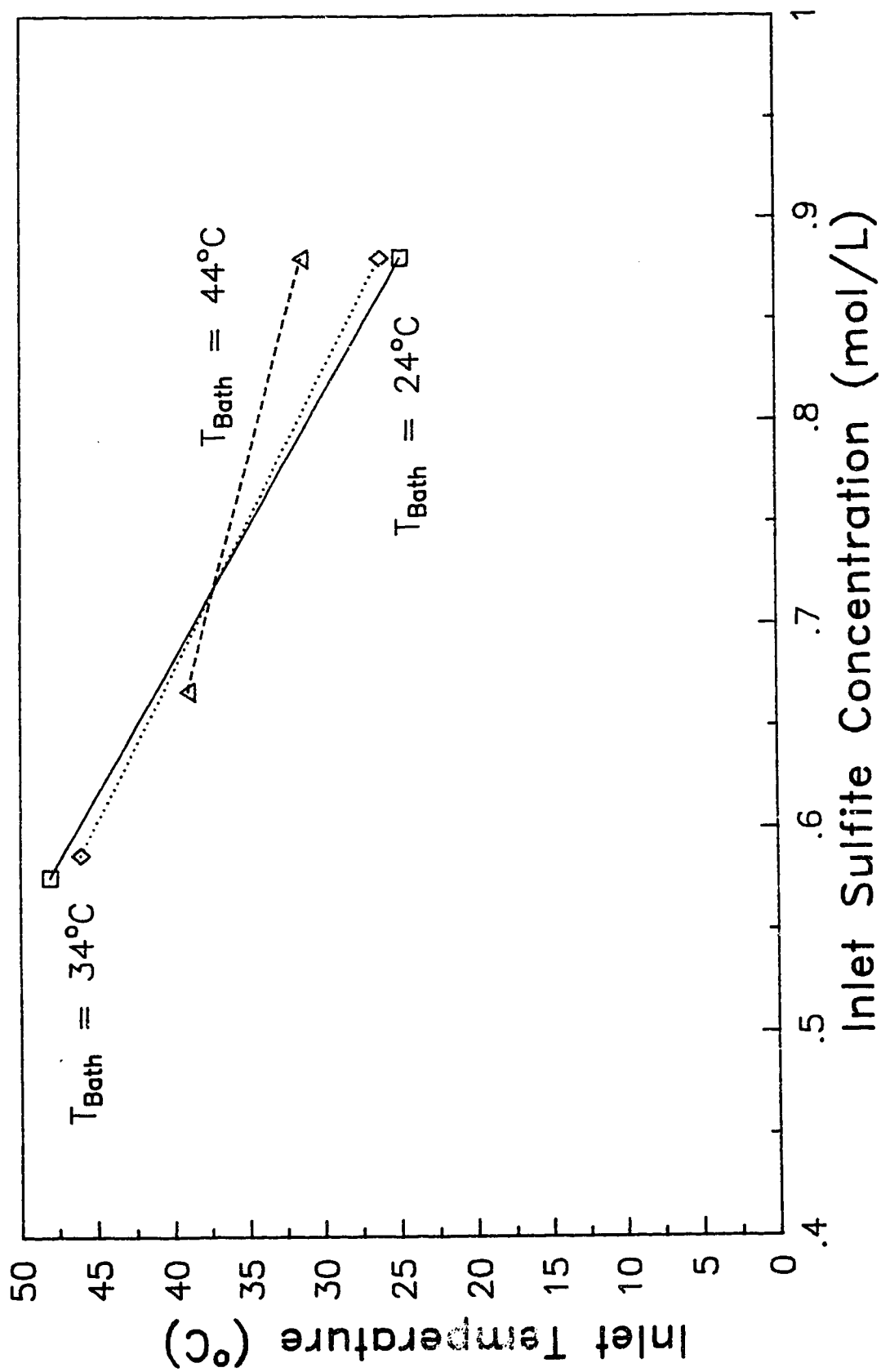


Figure 8.11 Experimentally Determined Critical Points

From Figure 8.10 it can be seen that the sensitive conditions are fairly scattered. The data extracted from the fixed bath temperatures seem to indicate the sensitivity begins at an inlet temperature of 26-27°C, regardless of the bath temperature. The data for the fixed inlet temperatures generally follows the more logical trend of having inlet and bath temperature in inverse relation (i.e., a higher bath temperature requires a lower inlet temperature for sensitivity). The data in Figure 8.11, although being only two points per curve, also follows this trend (in this case a larger concentration requires a lower inlet temperature).

It has been noted previously that the two sets of data in Figure 8.10, if examined together, may provide a more realistic picture of the actual sensitivity region. For this reason a linear regression was performed simultaneously on all of the data. The results can be seen in Figure 8.12. Although it does not provide a good fit through the data, the line does mark out roughly the division between sensitive and insensitive regions. The line indicates an inverse relationship between inlet and bath temperature, which is intuitively correct. The linear correlation, however, cannot be considered as a definitive demarcation of the regions of sensitivity and insensitivity. It is clear that more experiments are needed so as to obtain more data points for this diagram (as well as for Figure 8.11). These experiments should involve the evaluation of the bath side heat transfer coefficient for the other 3 stirrer speeds (see section 6.3)



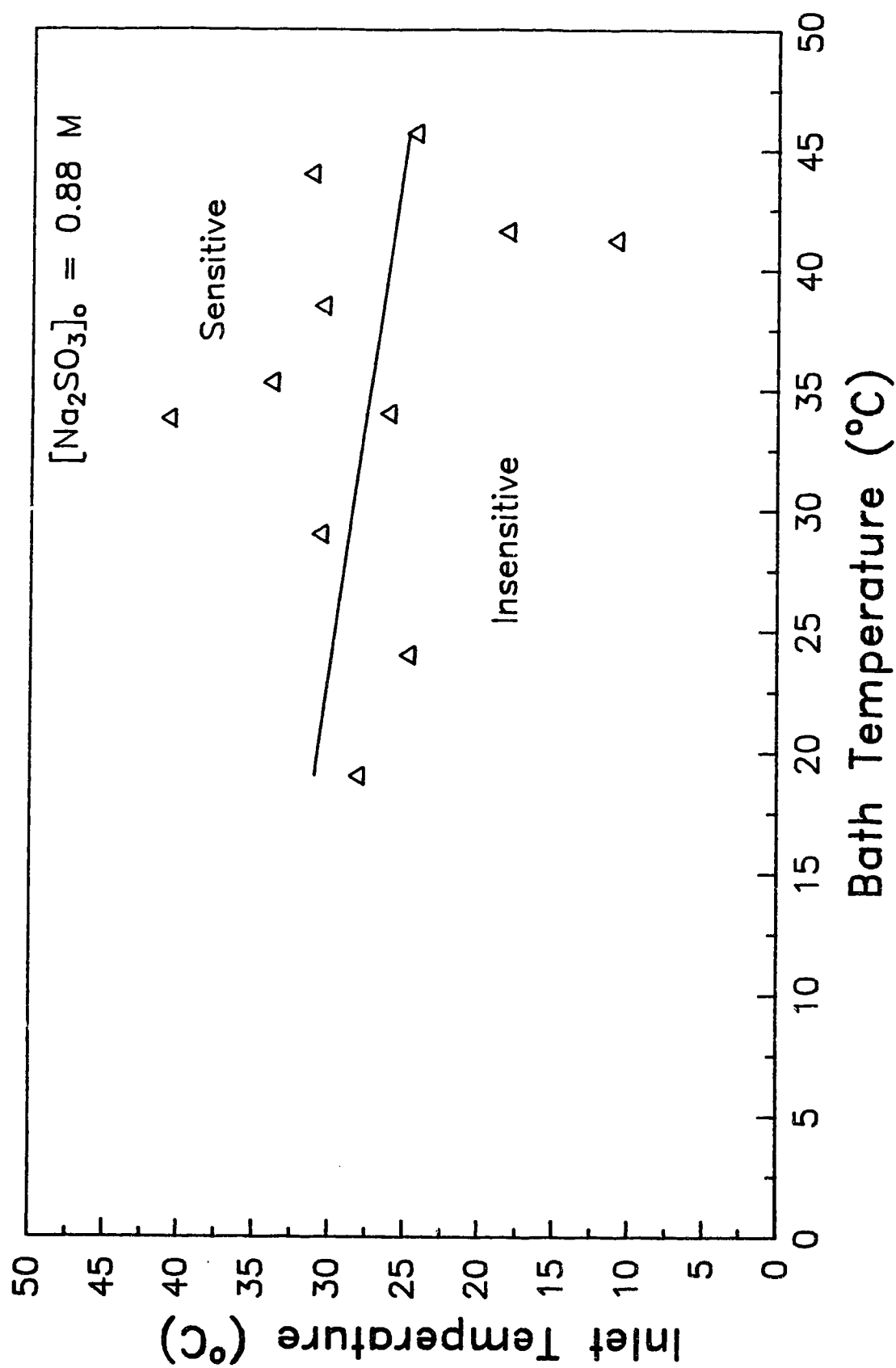


Figure 8.12 Sensitivity Plot for Fixed Inlet Concentration

so that a sensitivity plot can also be constructed for the overall heat transfer coefficient.

It is appropriate here to suggest an alternate working definition of parametric sensitivity. From Figures 8.7 through 8.9 and from the discussion concerning such figures, it can be noted that in all cases, the slope of the curve goes through a maximum. In other words, there is an inflection point present. The value of the variable parameter (i.e., the bath temperature or inlet temperature or adjusted concentration) at that inflection point should be used as the critical parameter value (i.e., marking the onset of sensitivity). In this way, the prediction of the onset of sensitivity will be based on a characteristic which is shared by all three types of profiles and occurs in roughly the same location on each profile. It is interesting to note that, the value of the slope of the hot-spot versus operating parameter curve at any position corresponds directly to the value of the sensitivity coefficient as defined by Morbidelli and Varma (1986b). Thus, defining parametric sensitivity as the point where the slope (and thus the value of the sensitivity coefficient) reaches a maximum also corresponds to the criterion for parametric sensitivity postulated by Morbidelli and Varma (1986b).

## 9.0 PARAMETRIC SENSITIVITY - EVALUATION OF EXISTING CRITERIA

In this chapter the previously obtained critical conditions will be used to evaluate some of the existing criteria for parametric sensitivity. The parameter values that will be used in these calculations are those that were found to provide the best fit of the ODPH model with the experimental data. These, along with the physical parameters of the system, are summarized in Table 9.1.

TABLE 9.1 PARAMETER VALUES FOR EXPERIMENTAL TUBULAR REACTOR	
$Q = 380 \text{ ml/min}$	$h_o \text{ (bath side)} = 4\,367 \text{ W/(m}^2\cdot\text{K)}$
$[H_2O_2]_o = 2.31 \text{ M}$	$U_1 \text{ (avg)} = 4\,115 \text{ W/(m}^2\cdot\text{K)}$
$D_1 \text{ (avg)} = 1.78 \cdot 10^{-3} \text{ m}$	$E_A = 64\,000 \text{ J/mol}$
$\rho = 1\,000 \text{ kg/m}^3$	$\Lambda = 2.90 \cdot 10^{10} \text{ L/(mol}\cdot\text{s)}$
$C_p = 4\,180 \text{ J/(kg}\cdot\text{K)}$	$\Delta H = 372\,230 \text{ J/mol}$

The evaluation of the criteria and the discussion of the results follows in the next 5 sections. The details of the specific calculations can be found in Appendix F.

### 9.1 EVALUATION OF THE CRITERION OF BARKELEW

Barkelew (1959) developed a criterion for parametric sensitivity based on the results of over 700 computer simulations. The results were illustrated in the form of sensitivity diagrams. On a given diagram (essentially a plot of the dimensionless overall heat transfer coefficient versus the dimensionless heat of reaction parameter) the

regions of sensitivity and insensitivity were mapped out as a function of dimensionless inlet temperature and reaction order. Because the only diagrams that were usable for the particular kinetics studied were those for the case of equal inlet and bath temperatures, the criteria could only be checked for those experiments where this was the case (namely,  $T_o = T_{\text{bath}} = 19, 24, 29, 34$  and  $44^{\circ}\text{C}$ ). A summary of the results obtained is illustrated in Table 9.2.

TABLE 9.2 SUMMARY OF BARKELEW CRITERION		
Inlet Conditions $T_{\text{inlet}} = T_{\text{bath}}$	Prediction from Barkelew	Observed (from Figure 8.12)
$T = 19^{\circ}\text{C}$ $[\text{Na}_2\text{SO}_3]_o = 0.88 \text{ M}$	Insensitive	Insensitive
$T = 24^{\circ}\text{C}$ $[\text{Na}_2\text{SO}_3]_o = 0.88 \text{ M}$	Sensitive	Insensitive
$T = 29^{\circ}\text{C}$ $[\text{Na}_2\text{SO}_3]_o = 0.88 \text{ M}$	Sensitive	Sensitive
$T = 34^{\circ}\text{C}$ $[\text{Na}_2\text{SO}_3]_o = 0.88 \text{ M}$	Sensitive	Sensitive
$T = 44^{\circ}\text{C}$ $[\text{Na}_2\text{SO}_3]_o = 0.88 \text{ M}$	Sensitive	Sensitive

It can be seen from the table that Barkelew's criteria predicts the reactor behavior four times out of five. For an inlet temperature of  $24^{\circ}\text{C}$ , the criteria is conservative, predicting sensitivity where none was evident from the experiments.

Butt (1960) replotted Barkelew's stability curves for zeroth, first and second order reactions in which the bath and inlet temperatures are equal. Two stability curves, for first order reactions in which

the bath and inlet temperatures are not equal, were also illustrated. The latter two curves were used to study some of the experimental conditions for which the bath and inlet temperatures were not equal. These stability curves were of course only valid for first order reactions.

TABLE 9.3 SUMMARY OF BARKELEW CRITERION WITH $T_c \neq T_o$				
Inlet (°C)	Bath (°C)	$[Na_2SO_3]_o$ (M)	Prediction	Observed Figure 8.12
24.56	19.0	0.88	Insensitive	Insensitive
30.59	19.0	0.88	Sensitive	Sensitive
18.29	24.0	0.88	Sensitive	Insensitive
30.59	24.0	0.88	Sensitive	Sensitive
33.96	24.0	0.88	Sensitive	Sensitive
24.25	29.0	0.88	Sensitive	Insensitive
30.59	34.0	0.88	Sensitive	Sensitive
40.75	34.0	0.88	Sensitive	Sensitive
45.70	34.0	0.88	Sensitive	Sensitive
40.75	44.0	0.88	Sensitive	Sensitive
46.0	34.0	0.58	Sensitive	Insensitive
46.0	34.0	0.68	Sensitive	Sensitive
39.0	46.0	0.58	Sensitive	Insensitive
39.0	46.0	0.68	Sensitive	Sensitive

For this reason, the peroxide concentration was assumed to be constant throughout the reaction (i.e., pseudo-first-order kinetics). For calculation purposes, the concentration was assumed to be equal in value to the geometric mean of its initial (i.e., 2.31 M) and final (assuming reaction went to completion) values. The details of the calculations can be found in Appendix F. The results obtained are illustrated in Table 9.3.

From Table 9.3 it can be seen that the prediction of reactor behavior is accurate in most cases. Again, where there is an error in prediction, it is a conservative one.

## 9.2 EVALUATION OF THE CRITERION OF VAN WELSENAERE AND FROMENT

Two criteria for parametric sensitivity were developed by Van Welsenaere and Froment (1970). The second criterion, which states that parametric sensitivity occurs when there is an inflection point before the hot-spot in the axial temperature profile, has become one of the most commonly used criterion for parametric sensitivity. Using this criterion, Van Welsenaere and Froment developed a method for determining the maximum allowable inlet concentration (i.e., maximum concentration that will still yield insensitive reactor behavior) for a given set of operating conditions. This method, however, was only applicable to pseudo-first-order reactions and conditions where the inlet and coolant temperatures were equal.

The method outlined by Van Welsenaere and Froment was used to determine the maximum allowable inlet sulfite concentration for the operating conditions where  $T_o = T_c$ . These results are summarized in Table 9.4. It should be noted that the geometric mean of the initial and final (based on the assumption of the reaction going to completion) peroxide concentration was used for calculation purposes (see Appendix F). This was necessary as the method was only applicable to pseudo-first-order reactions.

The results in Table 9.4 are similar to those obtained using the criteria of Barkelew in that sensitivity is predicted at an inlet temperature of  $24^{\circ}\text{C}$  where none was evident experimentally. The criterion predicted the observed reactor behavior in the other four instances.

TABLE 9.4 SUMMARY OF VAN WELSENAERE AND FROMENT CRITERION			
Inlet Conditions $T_o = T_c$	Critical $C_{Ao}$ Calculated	Prediction for $C_A = 0.88 \text{ M}$	Observed From Fig 8.12
$T = 19^{\circ}\text{C}$	0.93 M	Insensitive	Insensitive
$T = 24^{\circ}\text{C}$	0.71 M	Sensitive	Insensitive
$T = 29^{\circ}\text{C}$	0.56 M	Sensitive	Sensitive
$T = 34^{\circ}\text{C}$	0.45 M	Sensitive	Sensitive
$T = 44^{\circ}\text{C}$	0.34 M	Sensitive	Sensitive

Although the specific method outlined by Van Welsenaere and Froment is only applicable for pseudo-first-order kinetics and operating conditions where the bath and inlet temperatures are equal, the criterion for sensitivity can be applied to any kinetics and any set of inlet/bath temperatures (see Appendix F). With this criterion it is possible to determine the critical hot-spot temperature (leading to runaway). Once the critical hot-spot temperature is known, it is then possible to estimate the critical inlet concentration. In order to obtain such an estimate, it is assumed that the initial portion of the temperature profile (up to the hot-spot) is adiabatic. With this assumption it is then quite easy to determine the critical inlet temperature. Of course, the use of this assumption will produce conservative (i.e., low) estimates for the critical inlet concentration.

The results obtained using the Van Welsenaere and Froment criterion, as applied to all of the experimental operating conditions, is illustrated in Table 9.5. Once again, the estimates of sensitivity are extremely conservative. This is of course expected, given the adiabatic trajectory assumption outlined previously. Nonetheless, the criterion predicts that all the operating conditions should be sensitive when in fact, many of them are not. In a sense, these predictions provide no practical information about parametric sensitivity.



**TABLE 9.5 SUMMARY OF RESULTS USING VAN WELSENAERE AND FROMENT  
CRITERION AS APPLIED TO ALL EXPERIMENTAL OPERATING CONDITIONS**

Inlet (°C)	Bath (°C)	Critical $C_{Ao}$ (M)	Prediction for $C_A=0.88$ M	Observed From Fig 8.12
10.99	19.0	0.72	Sensitive	Insensitive
18.29	19.0	0.61	Sensitive	Insensitive
24.56	19.0	0.53	Sensitive	Insensitive
30.59	19.0	0.45	Sensitive	Sensitive
33.96	19.0	0.40	Sensitive	Sensitive
40.75	19.0	0.31	Sensitive	Sensitive
45.70	19.0	0.25	Sensitive	Sensitive
47.71	19.0	0.22	Sensitive	Sensitive
10.99	24.0	0.62	Sensitive	Insensitive
18.29	24.0	0.53	Sensitive	Insensitive
24.56	24.0	0.45	Sensitive	Insensitive
30.59	24.0	0.37	Sensitive	Sensitive
33.96	24.0	0.33	Sensitive	Sensitive
40.75	24.0	0.24	Sensitive	Sensitive
45.70	24.0	0.18	Sensitive	Sensitive
47.71	24.0	0.15	Sensitive	Sensitive
11.08	29.0	0.57	Sensitive	Insensitive
17.4	29.0	0.5	Sensitive	Insensitive
24.25	29.0	0.41	Sensitive	Insensitive

TABLE 9.5 SUMMARY OF RESULTS USING VAN WELSENARE AND FROMENT CRITERION (CONTINUED)				
Inlet (°C)	Bath (°C)	Critical $C_{Ao}$ (M)	Prediction for $C_A=0.88$ M	Observed From Fig 8.12
29.96	29.0	0.35	Sensitive	Sensitive
10.99	34.0	0.57	Sensitive	Insensitive
18.29	34.0	0.48	Sensitive	Insensitive
24.56	34.0	0.41	Sensitive	Insensitive
30.59	34.0	0.34	Sensitive	Sensitive
33.96	34.0	0.29	Sensitive	Sensitive
40.75	34.0	0.21	Sensitive	Sensitive
45.70	34.0	0.15	Sensitive	Sensitive
10.99	44.0	0.62	Sensitive	Insensitive
18.29	44.0	0.53	Sensitive	Insensitive
24.56	44.0	0.46	Sensitive	Insensitive
30.59	44.0	0.39	Sensitive	Sensitive
33.96	44.0	0.35	Sensitive	Sensitive
40.75	44.0	0.27	Sensitive	Sensitive
12.33	49.0	0.64	Sensitive	Insensitive
18.19	49.0	0.57	Sensitive	Insensitive
25.35	49.0	0.49	Sensitive	Sensitive
30.59	49.0	0.43	Sensitive	Sensitive
48.4	24.0	0.14	Sensitive	Sensitive

TABLE 9.5 SUMMARY OF RESULTS USING VAN WELSENAERE AND FROMENT CRITERION (CONTINUED)				
Inlet (°C)	Bath (°C)	Critical $C_{Ao}$ (M)	Prediction for $C_A=0.88$ M	Observed From Fig 8.12
46.0	34.0	0.15	Sensitive	Sensitive
39.08	44.0	0.29	Sensitive	Sensitive

### 9.3 EVALUATION OF THE CRITERION OF OROSKAR AND STERN

Oroskar and Stern (1979), utilizing the method of isoclines introduced by Chambré (1956), also developed a sensitivity diagram. The parameter groupings were similar to those used by Barkelew (i.e., dimensionless overall heat transfer coefficient versus the dimensionless heat of reaction parameter). The diagram, however, was only applicable to first order reactions with the inlet and coolant temperatures equal. Thus, once again, comparisons could only be made with a selected number of experimental conditions. The results obtained are illustrated in Table 9.6. It should be noted that, an average value for the peroxide concentration was necessary for calculation purposes (i.e., in order to simulate pseudo-first-order reaction kinetics).

TABLE 9.6 SUMMARY OF OROSKAR AND STERN CRITERION		
Inlet Conditions $T_{\text{inlet}} = T_{\text{bath}}$	Prediction	Observed (from Figure 8.12)
$T = 19^{\circ}\text{C}$ $[\text{Na}_2\text{SO}_3]_0 = 0.88 \text{ M}$	Insensitive	Insensitive
$T = 24^{\circ}\text{C}$ $[\text{Na}_2\text{SO}_3]_0 = 0.88 \text{ M}$	Insensitive	Insensitive
$T = 29^{\circ}\text{C}$ $[\text{Na}_2\text{SO}_3]_0 = 0.88 \text{ M}$	Sensitive	Sensitive
$T = 34^{\circ}\text{C}$ $[\text{Na}_2\text{SO}_3]_0 = 0.88 \text{ M}$	Sensitive	Sensitive
$T = 44^{\circ}\text{C}$ $[\text{Na}_2\text{SO}_3]_0 = 0.88 \text{ M}$	Sensitive	Sensitive

It can be seen from the table that the reactor behavior was correctly predicted in all five cases.

#### 9.4 EVALUATION OF THE CRITERION OF MORBIDELLI AND VARMA

Morbideilli and Varma (1982), utilizing the criterion of an inflection point before the hot-spot (see Van Welsenaere and Froment), obtained sensitivity diagrams for various inlet temperatures, reaction orders, and activation energies. The parameter groupings for these diagrams were identical to those developed by Oroskar and Stern (1979).

These diagrams were used to evaluate some of the experimental conditions. It was again necessary to restrict the evaluations to those conditions where inlet and bath temperatures were equal. In addition, it should be noted that some interpolation was required as sensitivity diagrams were not available for the exact experimental values of  $\gamma$  (dimensionless activation energy) and  $n$  (reaction order).

A summary of the results is given in Table 9.7.

TABLE 9.7 SUMMARY OF MORBIDELLI AND VARMA CRITERION		
Inlet Conditions $T_{\text{inlet}} = T_{\text{bath}}$	Prediction	Observed (from Figure 8.12)
$T = 19^{\circ}\text{C}$ $[\text{Na}_2\text{SO}_3]_0 = 0.88 \text{ M}$	Sensitive	Insensitive
$T = 24^{\circ}\text{C}$ $[\text{Na}_2\text{SO}_3]_0 = 0.88 \text{ M}$	Sensitive	Insensitive
$T = 29^{\circ}\text{C}$ $[\text{Na}_2\text{SO}_3]_0 = 0.88 \text{ M}$	Sensitive	Sensitive
$T = 34^{\circ}\text{C}$ $[\text{Na}_2\text{SO}_3]_0 = 0.88 \text{ M}$	Sensitive	Sensitive
$T = 44^{\circ}\text{C}$ $[\text{Na}_2\text{SO}_3]_0 = 0.88 \text{ M}$	Sensitive	Sensitive

It appears from Table 9.7 that the predictions of Morbidelli and Varma are even more conservative than those of Barkelew or Van Welsenaere and Froment (see Figures 9.2 and 9.4). In every case, even for the lowest bath temperature, sensitive behavior is predicted.

#### 9.5 EVALUATION OF THE CRITERION OF AKELLA AND LEE

Akella and Lee (1983) developed a method of analyzing parametric sensitivity in a reactor where the coolant flows counter-currently to the reactants (i.e., as in a tube and shell heat exchanger). This method, referred to as a "phase-plane" analysis, involves the construction of a diagram of inlet reactor temperature vs inlet coolant temperature where the regions of insensitivity and sensitivity are separated according to specified criteria. Although the method is designed for counter-current operation, it can also be used to analyze a reactor with an isothermal coolant. The method was applied to the

experimental tubular reactor system for an inlet sulfite concentration of 0.88 M. The results are illustrated in Figure 9.1.

From Figure 9.1 it is clear that the "safe operating" (i.e., non-sensitive) region predicted by Akella and Lee is extremely conservative. The lateral "ignition" line is located at  $T = 287\text{ K}$  ( $14^{\circ}\text{C}$ ) which predicts that, any coolant temperature greater than this will result in sensitive reactor behavior. Experimentally, non-sensitive behavior was observed for many conditions with the coolant temperature above this value (see Fig 8.12). In fact, the entire range of experimental operating conditions ( $T_o = 10 - 48^{\circ}\text{C}$ ,  $T_c = 19 - 44^{\circ}\text{C}$ ) is located in the "ignition" (i.e., sensitive) region of the diagram. The experimental results clearly indicated that not all of these conditions were parametrically sensitive.

#### 9.6 CRITERION SELECTION

An analysis of the five criteria presented so far indicates that, for most operating conditions, the criteria predict that the reactor will behave sensitively. Experimentally, this was not the case as there were many operating conditions that were observed to be insensitive. Thus the criteria are often in error, although when they do err in predicting reactor behavior, they do so conservatively (i.e., predicting sensitivity where non-sensitive behavior was observed experimentally). This is certainly the desired way to err, if indeed an error is to be made. However, judging from the results illustrated in

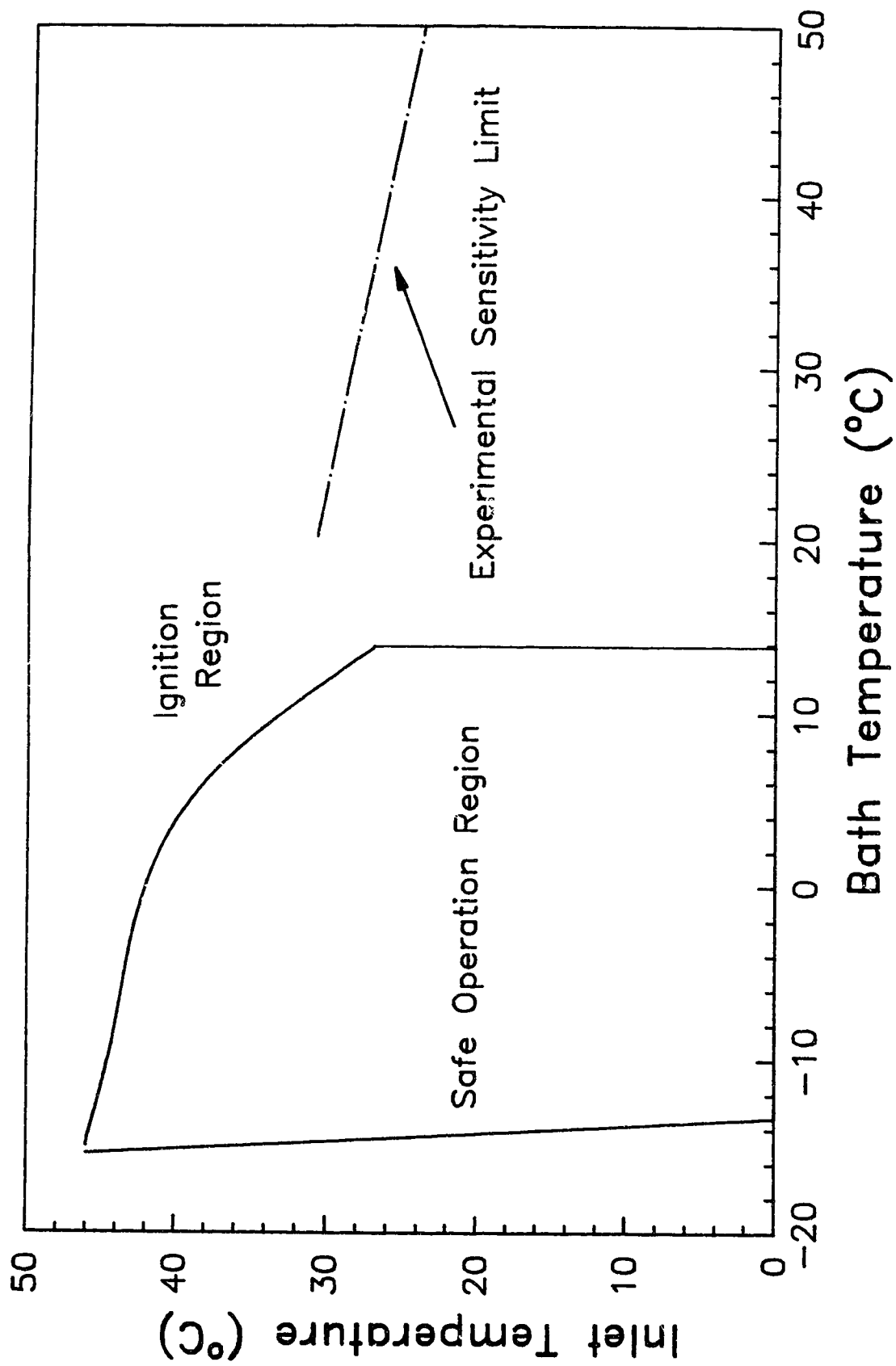


Figure 9.1 Phase Plane Analysis for Sulfite Reaction

the preceding tables and figures in this chapter, it can be said that the existing parametric sensitivity are too conservative. This is undesirable as criteria that are too conservative are not of much practical use. In addition, they can cause a needless over design of the system. This is illustrated by Figure 9.1. If this diagram were consulted initially to determine, for example, the required inlet temperature to ensure insensitivity, it would result in an unnecessary amount of refrigeration being designed for the system.

The fact that the five criteria tend to make similar predictions in some cases is not surprising, considering that the parameter groupings for the sensitivity diagrams of Barkelew, Oroskar and Stern, and Morbidelli and Varma are essentially the same. In all of these three cases, the heat of reaction parameter, commonly referred to as " $\alpha$ ", is the same ( $\alpha = \Delta H \cdot C_{A0} \cdot E_A / (C_p \cdot \rho \cdot R \cdot T_c^2)$ ). The heat transfer parameter, usually defined by the symbol  $\beta$ , is a little bit different in each case (see Appendix F) but this is only because of the way the kinetic expression is defined. In addition, the criterion of Van Welsenaere and Froment regarding the inflection point before hot-spot, is used by Morbidelli and Varma to determine the regions of parametric sensitivity. The criterion used by Akella and Lee to define the upper ignition line is also based on the existence of a positive second derivative somewhere before the hot-spot.



It would therefore appear that there is little to choose from among the first four criteria (the last criterion, that of Akella and Lee, is of course completely different than the first four). It is suggested here, however, that the sensitivity diagrams designed by Barkelew are the ones that should be consulted for any sensitivity analysis. This is due to the fact that they encompass a wide range of kinetics (unlike the others); they are relatively simple to use and they provide reasonable sensitivity predictions (i.e., not much better or worse than any other criteria). Although the basis for these diagrams is undeniably empirical, the fact that the parameter groupings are almost exactly the same as those determined by much more rigorous methods, validates their usage.

The "phase-plane" method of Akella and Lee would certainly be even more appropriate to use than the sensitivity diagrams, if it were (apparently) not so conservative. The advantage of this method lies in the fact that once the "phase-plane" is constructed, no further calculations are required to determine the suitability of a given set of operating conditions. For the sensitivity diagrams, the parameter groupings must be re-evaluated for each successive set of operating conditions to be checked.

### CONCLUSIONS

- 1) The oxidation of sodium sulfite ( $\text{Na}_2\text{SO}_3$ ) by hydrogen peroxide ( $\text{H}_2\text{O}_2$ ), in a 0.175 cm diameter tubular reactor with isothermal coolant, for a flow rate of 380 ml/min and inlet and coolant temperatures in the range of 10 to 50°C, displays parametric sensitivity of the hot-spot temperature with respect to changes in the value of the inlet temperature, the coolant temperature, the inlet sulfite concentration and the overall heat transfer coefficient.
- 2) The parametric sensitivity criteria of Barkelew (1959), Van Welsenaere and Froment (1970), Oroskar and Stern (1979), Morbidelli and Varma (1982) and Akella and Lee (1983) are all generally quite conservative in nature. The most useful criterion, due to its wide range of applicability, is that of Barkelew (1959).
- 3) For the experimental plug flow reactor used to investigate the sulfite reaction, both the standard ODPH (One Dimensional Pseudo Homogeneous) and the TDPH (Two Dimensional Pseudo Homogeneous) tubular reactor models can be used to describe the axial temperature profiles. Both models, however, tend to overestimate the value of the hot-spot by 10 to 15°C. A small adjustment of the value of the Arrhenius parameters in the ODPH model results in good agreement between the experimental hot-spot temperatures and the model predictions.
- 4) An adiabatic batch reactor can be used to obtain reasonably good

estimates of the Arrhenius parameters for a given reaction. Using this method for the oxidation of sodium sulfite by hydrogen peroxide, the activation energy is found to be 64,268 J/mol with the pre-exponential factor being  $3.56 \cdot 10^{10}$  (L/(mol·s)).

## REFERENCES

- Adler, J. and J.W. Enig, "The Critical Conditions in Thermal Explosion Theory with Reactant Consumption", *Comb. Flame.* 8, 97 - 103 (1964).
- Agnew, J.B. and O.E. Potter, "The Design of Stable Packed Tubular Reactors for Highly Exothermic Reactions", *Trans. Instn. Chem. Engrs.* 44, 216 - 223 (1966).
- Akella, L.M. and Hong H. Lee, "A Design Approach Based on Phase Plane Analysis: Countercurrent Reactor/Heat Exchanger with Parametric Sensitivity", *AIChE J* 29, 87 - 94 (1983).
- Barkelew, C.H. "Stability of Adiabatic Reactors", *ACS Symp. Ser.* 237, 337 - 359 (1984).
- Barkelew, C.H. "Stability of Chemical Reactors", *Chem. Engng. Prog. Symp. Ser.* 55(25), 37 - 46 (1959).
- Bauman, E., Varma, A., Lorusso, J., Dente M. and M. Morbidelli, "Parametric Sensitivity in Tubular Reactors with Co-Current External Cooling", *Chem. Engng. Sci.* 45, 1301 - 1307 (1990).
- Bauman, E., and A. Varma, "Parametric Sensitivity and Runaway in Catalytic Reactors: Experiments and Theory Using Carbon Monoxide Oxidation as an Example", *Chem. Engng. Sci.* 45, 2133 - 2141 (1990).
- Bilous, O. and Neal R. Amundson, "Chemical Reactor Stability and Sensitivity II - Effect of Parameters on Sensitivity of Empty Tubular Reactors", *AIChE J* 2, 117 - 126 (1956).
- Butt, J.B., *Reactor Kinetics and Reactor Design*, Prentice-Hall, New Jersey, (1980).
- Chambré, Paul "On the Characteristics of a Non-Isothermal Chemical Reactor", *Chem. Engng. Sci.* 5, 209 - 216 (1956).

- Chemburkar, R.M., Morbidelli, M. and A. Varma, "Parametric Sensitivity of a CSTR", *Chem. Engng. Sci.* **41**, 1647 - 1654 (1986).
- Deans, H.A., and L. Lapidus, "A Computational Model For Predicting and Correlating the Behavior of Fixed-Bed Reactors: I Derivation of Model for Nonreactive Systems", *AIChE J* **6**, 656 - 663 (1960).
- Dente, M. and A. Collina, "La determinazione delle condizioni di stabilità del regime dei reattori chimici", *La Chimica E L'Industria* **46**, 915 - 928 (1964a).
- Dente, M. and A. Collina, "Applicazione del metodo delle perturbazioni allo studio della stabilità del regime dei reattori chimici a flusso longitudinale", *La Chimica E L'Industria* **46**, 1445 - 1449 (1964b).
- Dente, M., Cappelli, A., Buzzi Ferraris, G. and A. Collina, "La sensitività del regime dei reattori chimici a flusso longitudinale Nota I - Influenza del parametro di Arrhenius  $E/RT$  sui limiti di sensitività", *Quad. Dell'Ingng. Chim. Ital.* **2**, 5 - 9 (1966a)
- Emig, G., Hoffman, H., Hoffman, U. and U. Fland, "Experimental Studies On Runaway of Catalytic Fixed-Bed Reactors (Vinyl Acetate Synthesis)", *Chem. Engng. Sci.* **35**, 249 - 257 (1980).
- Gray, P. and P.R. Lee, "Thermal Explosions and the Effect of Reactant Consumption on Critical Conditions", *Comb. Flame.* **9**, 201 - 203 (1965).
- Gray, B.F., "Critical Behaviour in Chemically Reacting Systems - III An Analytical Criterion for Insensitivity", *Comb. Flame.* **24**, 43-52 (1975).
- Henning, G.P. and G. Perez, "Parametric Sensitivity in Fixed-Bed Catalytic Reactors", *Chem. Engng. Sci.* **41**, 83 - 88 (1986).
- Herskowitz, M. and P.S. Hagan, "Accurate One-Dimensional Fixed-Bed Reactor Model Based on Asymptotic Analysis", *AIChE J* **34**, 1367 - 1372 (1988a).

- Hoffman, M.R. and J.O. Edwards, "Kinetics of the Oxidation of Sulfite by Hydrogen Peroxide in Acidic Solution", *J. Phys. Chem.* 79, 2096 - 2098 (1975).
- Holman, J.P., *Heat Transfer, 5th Edition*, McGraw-Hill, (1981)
- Hosten, L.H. and G.F. Froment, "Parametric Sensitivity in Co-Currently Cooled Tubular Reactors", *Chem. Engng. Sci.* 41, 1073 - 1080 (1986).
- Kheshgi, H.S., Hagan, P.S., Reyes, S.C. and J.C. Pirkle Jr., "Transients in Tubular Reactors: Comparison of One- and Two-Dimensional Models", *AIChE J* 34, 1373 - 1375 (1988b).
- Mader, P.M. "Kinetics of the Hydrogen Peroxide-Sulfite Reaction in Alkaline Solution", *J. Am. Chem. Soc.* 80, 2634 - 2639 (1958).
- McGreavy, C. and C.I. Adderly, "Generalized Criteria for Parametric Sensitivity and Temperature Runaway in Catalytic Reactors", *Chem. Engng. Sci.* 28, 577 - 584 (1973).
- McGreavy, C. and C.I. Adderly, "Parametric Sensitivity and Temperature Runaway in Heterogeneous Fixed Bed Reactors", *Adv. In Chemistry Ser.* 133, 519 - 531 (1974).
- Morbidelli, M. and A. Varma, "Parametric Sensitivity and Runaway in Tubular Reactors", *AIChE J* 28, 705 - 713 (1982).
- Morbidelli, M. and A. Varma, "On Parametric Sensitivity and Runaway Criteria of Pseudohomogeneous Tubular Reactors", *Chem. Engng. Sci.* 40, 2165 - 2168 (1985).
- Morbidelli, M. and A. Varma, "Parametric Sensitivity in Fixed-Bed Catalytic Reactors: The Role of Interparticle Transfer Resistances", *AIChE J* 32, 297 - 306 (1986a).
- Morbidelli, M. and A. Varma, "Parametric Sensitivity in Fixed-Bed Catalytic Reactors", *Chem. Engng. Sci.* 41, 1063 - 1071 (1986b).

- Morbidelli, M. and A. Varma, "Parametric Sensitivity in Fixed-Bed Reactors: Inter- and Intraparticle Resistance", *AIChE J* 33, 1949 - 1958 (1987a).
- Morbidelli, M. and A. Varma, "A Generalized Criterion For Parametric Sensitivity: Application to Thermal Explosion Theory", *Chem. Engng. Sci.* 43, 91 - 102 (1988).
- Morbidelli, M. and A. Varma, "A Generalized Criterion For Parametric Sensitivity: Application To A Pseudohomogeneous Tubular Reactor With Consecutive or Parallel Reactions", *Chem. Engng. Sci.* 44, 1675 - 1696 (1989).
- Oroskar, A. and S.A. Stern, "Stability of Chemical Reactors", *AIChE J* 25, 903 - 905 (1979).
- Penkett, S.A., Jones, B.M.R., Brice K.A., and A.E.J. Eggleton, "The Importance of Atmospheric Ozone and Hydrogen Peroxide in Oxidising Sulphur Dioxide in Cloud and Rainwater", *Atms. Envrn.* 13, 123 - 137 (1979).
- Perry R.H., Green, D.W., and J.O. Maloney, *Perry's Chemical Engineers' Handbook, 6th Edition*, McGraw-Hill, (1984).
- Rajadhyaksha, R.A. and K. Vasudeva, "Parametric Sensitivity in Fixed-Bed Reactors", *Chem. Engng. Sci.* 30, 1399 - 1408 (1975).
- Root, R.B. and R.A. Schmitz, "An Experimental Study of Steady State Multiplicity in a Loop Reactor", *AIChE J* 15, 670 - 679 (1969).
- Root, R.B. and R.A. Schmitz, "An Experimental Study of Unstable States in a Loop Reactor", *AIChE J* 16, 356 - 358 (1970).
- Soria Lopez, A., De Lasa, H.I. and J.A. Porras, "Parametric Sensitivity of a Fixed Bed Catalytic Reactor - Cooling Flow Influence", *Chem. Engng. Sci.* 36, 285 - 291 (1981).
- Tjahjadj, M., Gupta, S.K., Morbidelli M. and A. Varma, "Parametric Sensitivity in Tubular Polymerization Reactors", *Chem. Engng. Sci.* 42, 2385 - 2394 (1987).

- Van Welsenaere, R.J. and G.F. Froment "Parametric Sensitivity and Runaway in Fixed Bed Catalytic Reactors", *Chem. Engng. Sci.* 25, 1503 - 1516 (1970).
- Vejtasa, S. and R.A. Schmitz, "An Experimental Study of Steady State Multiplicity and Stability in an Adiabatic Stirred Reactor", *AIChE J* 16, 410 -419 (1970).
- Westerterp, K.R. and K.J. Ptasinski, "Safe Design of Cooled Tubular Reactors for Exothermic Multiple Reactions; Parallel Reactions - I", *Chem. Engng. Sci.* 39, 235 - 244 (1984a).
- Westerterp, K.R. and K.J. Ptasinski, "Safe Design of Cooled Tubular Reactors for Exothermic Multiple Reaction; Parallel Reactions - II", *Chem. Engng. Sci.* 39, 245 - 252 (1984b).
- Westerterp, K.R., Ptasinski, K.J. and R.R.M. Overtoom, "Safe Design of Cooled Tubular Reactors for Exothermic Multiple First Order Reactions", *ACS Symp. Ser.* 237, 323 - 335 (1984c).
- Westerterp, K.R., and R.R.M Overtoom, "Safe Design of Cooled Tubular Reactors for Exothermic Multiple Reactions. Consecutive Reactions", *Chem. Engng. Sci.* 40, 155 - 165 (1985).
- Wilson, K.B. "Tubular Reactors Part I - Calculation and Analysis of Longitudinal Temperature Gradients in Tubular Reactors", *Trans. Inst. Chem. Engs.* 24, 77 - 83 (1946).



## APPENDIX A

### Determination of Thermal Capacity of Dewar Flask

Table A.1 - Experimental Data I

---

Initial Temperature of Dewar Contents - 21.71 °C

Initial Water Temperature - 6.81 °C

Amount of water added to dewar - 500.0 ml

Final Temperature of Dewar & Water - 7.93 °C

#### Calculations:

Adiabatic Process, therefore -

Amount of heat lost by dewar = amount of heat gained by water

$$(mCp)_{\text{dewar}} \cdot (\Delta T)_{\text{dewar}} = V_T \cdot \rho_w \cdot Cp_w \cdot (\Delta T)_w \quad (A.1)$$

$$\text{thus, } (mCp)_{\text{dewar}} = 1.0 \cdot 0.5 \cdot 4180.0 \cdot (7.93 - 6.81) / (21.71 - 7.93)$$

$$(mCp)_{\text{dewar}} = 170 \text{ (J/K)}$$

Table A.2 - Experimental Data II

---

Initial Temperature of Dewar Contents - 20.50 °C  
Initial Water Temperature - 40.35 °C  
Amount of water added to dewar - 500.0 ml  
Final Temperature of Dewar and Water - 38.35 °C

#### Calculations

Using same procedure as above,

$$\begin{aligned} (mCp)_{\text{dewar}} &= 1.0 \cdot 0.5 \cdot (4180) \cdot (40.35 - 38.35) / (38.35 - 20.50) \\ &= 234 \text{ (J/K)} \end{aligned}$$

AVERAGE VALUE FOR THERMAL CAPACITY OF DEWAR IS 202 (J/K)

It should be noted that the precision of the thermocouple used to measure the temperature of the reactor and its contents is approximately  $\pm 0.2^{\circ}\text{C}$ . This may explain the observed difference in the values obtained for the thermal capacity (from experiments 1 and 2). For example, if the final temperature of the dewar and water for experiment #2 is actually  $38.55^{\circ}\text{C}$  (i.e.,  $0.2^{\circ}\text{C}$  greater than the initially measured value), then the value obtained for the thermal capacity becomes 210 J/K. Similarly, if the true final temperature of experiment #1 was  $8.13^{\circ}\text{C}$  (again,  $0.2^{\circ}\text{C}$  difference), then the thermal capacity would be calculated as 200 J/K.

TABLE A.3 EXPERIMENTAL BATCH REACTOR DATA				
Experiment #1	$[\text{Na}_2\text{SO}_3]_0 = 0.39 \text{ M}$		$[\text{H}_2\text{O}_2]_0 = 0.59 \text{ M}$	
Time (s)	Temperature (°C)	$[\text{Na}_2\text{SO}_3] \text{ (M)}$ from eq 3.5	$[\text{H}_2\text{O}_2] \text{ (M)}$ from eq 3.5	$-dT/dt \text{ (°C/s)}$ *numerically
0.00	15.38	0.39	0.59	-
0.99	15.57	0.388	0.588	0.096
2.00	15.57	0.388	0.588	0.091
2.99	15.75	0.385	0.585	0.091
4.04	15.75	0.385	0.585	0.0
5.00	15.75	0.385	0.585	1.109
6.01	17.99	0.358	0.558	1.109
6.99	17.99	0.358	0.558	0.0
8.02	17.99	0.358	0.558	1.692
9.01	21.34	0.317	0.517	2.634
10.00	23.21	0.294	0.494	1.865
11.01	25.07	0.271	0.471	1.956
12.00	27.12	0.245	0.445	1.956
13.01	28.98	0.223	0.423	1.970
14.02	31.10	0.196	0.396	2.044
15.02	33.09	0.172	0.372	1.933
15.99	34.91	0.15	0.35	1.723
17.02	36.54	0.13	0.33	1.624
18.00	38.17	0.109	0.309	1.460
19.01	39.44	0.094	0.294	1.270
20.00	40.71	0.078	0.278	1.181
21.01	41.80	0.065	0.265	0.985
22.02	42.70	0.054	0.254	0.818
23.00	43.43	0.045	0.245	0.635
24.03	43.97	0.038	0.238	0.642
24.99	44.70	0.029	0.229	0.558
26.00	45.06	0.025	0.225	0.353
27.03	45.42	0.02	0.22	0.365
28.00	45.79	0.016	0.216	0.281
29.00	45.97	0.013	0.213	0.177
30.03	46.15	0.011	0.211	0.178
31.02	46.33	0.009	0.209	0.183
32.00	46.51	0.007	0.207	0.178
33.05	46.69	0.005	0.205	0.09
34.00	46.69	0.005	0.205	0.0
35.03	46.69	0.005	0.205	0.0
36.03	46.69	0.005	0.205	0.091
37.00	46.87	0.002	0.202	0.091

TABLE A.3 (Continued)				
Experiment #1	[Na <sub>2</sub> SO <sub>3</sub> ] = 0.39 M		[H <sub>2</sub> O <sub>2</sub> ] = 0.59 M	
Time (s)	Temperature (°C)	[Na <sub>2</sub> SO <sub>3</sub> ] (M) from eq 3.5	[H <sub>2</sub> O <sub>2</sub> ] (M) from eq 3.5	-dT/dt (°C/s) *numerically
38.00	46.87	0.002	0.202	0.0
39.03	46.87	0.002	0.202	0.0
40.04	46.87	0.002	0.202	0.0
41.00	46.87	0.002	0.202	0.0
42.05	46.87	0.002	0.202	0.0
43.00	46.87	0.002	0.202	0.0
44.03	46.87	0.002	0.202	0.0
45.02	46.87	0.002	0.202	0.0
45.99	46.87	0.002	0.202	0.0
47.00	46.87	0.002	0.202	0.0
47.99	46.87	0.002	0.202	0.0
49.07	46.87	0.002	0.202	0.0
50.02	46.87	0.002	0.202	0.0
51.01	46.87	0.002	0.202	0.0
52.02	46.87	0.002	0.202	0.0
53.01	46.87	0.002	0.202	0.0
54.00	46.87	0.002	0.202	0.0
55.11	46.87	0.002	0.202	0.0
56.00	46.87	0.002	0.202	0.0

$$* -dT/dt = (((T_{i+1} - T_i)/\Delta t) + ((T_i - t_{i-1})/\Delta t))/ 2.0$$

from eq 3.5, (with appropriate substitutions)  $dC_A/dt = -0.01231 \cdot dT/dt$

Observed Temperature Rise = 46.87 - 15.38 = 31.49 °C

$$\text{Adiabatic Temperature Rise} = \frac{\Delta H_{\text{rxn}} \cdot V_T \cdot [\text{Na}_2\text{SO}_3]_0}{[(mCp)_{\text{dewar}} + (\rho_w \cdot V_T \cdot Cp_w)]} \quad (\text{A.2})$$

For  $V_T = 500$  ml and  $\Delta H_{\text{rxn}} = 372\,230$  (J/mol), the expression becomes

$$\begin{aligned} \text{Adiabatic Temperature Rise} &= 81.2 \cdot [\text{Na}_2\text{SO}_3]_0 \\ &= 31.67 \text{ } ^\circ\text{C} \end{aligned}$$

Therefore, in this case, actual temperature rise = 99.4 % of the theoretical maximum.

TABLE A.4 EXPERIMENTAL BATCH REACTOR DATA				
Experiment #2	$[\text{Na}_2\text{SO}_3]_0 = 0.49 \text{ M}$		$[\text{H}_2\text{O}_2]_0 = 0.70 \text{ M}$	
Time (s)	Temperature (°C)	$[\text{Na}_2\text{SO}_3] \text{ (M)}$ from eq 3.5	$[\text{H}_2\text{O}_2] \text{ (M)}$ from eq 3.5	$-dT/dt \text{ (°C/s)}$ *numerically
0.00	16.68	0.49	0.70	-
0.99	18.36	0.469	0.679	3.433
2.00	23.58	0.405	0.615	4.408
3.02	27.30	0.359	0.569	3.946
4.00	31.46	0.308	0.518	4.229
4.99	35.63	0.257	0.467	4.397
6.02	40.35	0.199	0.408	4.511
7.00	44.70	0.145	0.355	3.994
8.02	48.32	0.101	0.310	3.162
9.00	51.04	0.067	0.277	2.298
10.00	52.86	0.044	0.254	1.551
10.99	54.13	0.028	0.239	1.050
12.09	55.03	0.018	0.228	0.661
13.18	55.58	0.011	0.221	0.343
14.17	55.76	0.009	0.219	0.177
15.21	55.94	0.007	0.217	0.087
16.18	55.94	0.007	0.217	0.0
17.19	55.94	0.007	0.217	0.09
18.19	56.12	0.004	0.214	0.0
19.19	55.94	0.007	0.217	-0.091
20.17	55.94	0.007	0.217	0.0
21.19	55.94	0.007	0.217	0.0
22.17	55.94	0.007	0.217	0.0
23.18	55.94	0.007	0.217	0.0
24.27	55.94	0.007	0.217	0.0
25.53	55.94	0.007	0.217	-0.091
26.50	55.76	0.009	0.219	-0.091
27.49	55.76	0.009	0.219	0.0
28.51	55.76	0.009	0.219	0.09
29.49	55.94	0.007	0.217	0.091
30.48	55.94	0.007	0.217	-0.090
31.50	55.76	0.009	0.219	0.0
32.49	55.94	0.007	0.217	0.0
33.49	55.76	0.009	0.219	-

$$*dT/dt = (((T_{i+1}-T_i)/\Delta t) + ((T_i-T_{i-1})/\Delta t)) / 2.0$$

from eq 3.5, (with appropriate substitutions)  $dC_A/dt = -0.01231 \cdot dT/dt$

$$\text{Observed Temperature Rise} = 55.94 - 16.68 = 39.44 \text{ }^{\circ}\text{C}$$

$$\begin{aligned} \text{From eq A.2, adiabatic temperature rise} &= 81.2 \cdot [\text{Na}_2\text{SO}_3]_0 \\ &= 39.79 \text{ }^{\circ}\text{C} \end{aligned}$$

Therefore in this case, actual temperature rise = 99.1 % of the theoretical maximum.

TABLE A.5 EXPERIMENTAL BATCH REACTOR DATA				
Experiment #3		$[\text{Na}_2\text{SO}_3]_0 = 0.53 \text{ M}$	$[\text{H}_2\text{O}_2]_0 = 0.70 \text{ M}$	
Time (s)	Temperature (°C)	$[\text{Na}_2\text{SO}_3] \text{ (M)}$ from eq 3.5	$[\text{H}_2\text{O}_2] \text{ (M)}$ from eq 3.5	$-dT/dt \text{ (°C/s)}$ *numerically
0.00	15.38	0.53	0.7	-
1.96	18.36	0.493	0.663	3.602
3.96	22.46	0.443	0.613	4.195
5.96	27.75	0.390	0.560	4.615
7.95	31.64	0.330	0.500	5.172
9.99	37.26	0.260	0.430	5.449
11.98	42.70	0.194	0.364	5.222
13.97	47.60	0.133	0.303	4.309
15.96	51.23	0.089	0.259	3.255
17.98	54.13	0.053	0.223	2.336
19.97	55.94	0.031	0.201	1.467
21.96	57.03	0.018	0.188	0.907
23.97	57.75	0.008	0.178	0.545
25.95	58.12	0.004	0.174	0.276
27.98	58.30	0.002	0.172	0.087
29.99	58.30	0.002	0.172	0.0
31.98	58.30	0.002	0.172	0.092
33.96	58.48	0.0	0.17	0.091
35.97	58.48	0.0	0.17	0.0
37.96	58.48	0.0	0.17	0.0
39.97	58.48	0.0	0.17	0.0
41.97	58.48	0.0	0.17	-0.091
43.96	58.30	0.002	0.172	-0.091
45.96	58.30	0.002	0.172	0.0
47.97	58.30	0.002	0.172	0.0
49.98	58.30	0.002	0.172	0.0
51.96	58.30	0.002	0.172	0.0
53.97	58.30	0.002	0.172	0.09
55.96	58.30	0.002	0.172	0.0
57.95	58.12	0.004	0.174	0.0
59.95	58.30	0.002	0.172	0.0
61.97	58.12	0.004	0.174	0.0
63.98	58.30	0.002	0.172	-0.09
65.97	58.30	0.002	0.172	-0.091
67.96	58.12	0.004	0.174	0.00
69.98	58.12	0.004	0.174	0.00
71.97	58.12	0.004	0.174	0.00
73.97	58.12	0.004	0.174	0.00
75.97	58.12	0.004	0.174	0.00
77.00	58.12	0.004	0.174	-

$$*dT/dt = (((T_{i+1} - T_i)/\Delta t) + ((T_i - T_{i-1})/\Delta t)) / 2.0$$

from eq 3.5, (with appropriate substitutions)  $dC_A/dt = -0.01231 \cdot dT/dt$

$$\text{Observed temperature rise} = 58.48 - 15.38 = 43.10 \text{ }^{\circ}\text{C}$$

$$\begin{aligned} \text{From eq A.2 adiabatic temperature rise} &= 81.2 \cdot [\text{Na}_2\text{SO}_3]_0 \\ &= 43.04 \text{ }^{\circ}\text{C} \end{aligned}$$

Therefore in this case, actual temperature rise = 100 % of the theoretical maximum.



### DETERMINATION OF ARRHENIUS PARAMETERS FOR THE SULFITE REACTION

The adiabatic batch reactor energy balance is

$$\Delta H_{\text{rxn}} \cdot [C_A(t) - C_A(0)] \cdot V = [(mCp)_{\text{dewar}} + (\rho_w \cdot V \cdot Cp_w)] \cdot [T(t) - T(0)] \quad (3.5)$$

where  $C_A(t)$ ,  $C_A(0)$  are the concentrations of sulfite at any time,  $t$ , and initially at  $t = 0$  and  $T(t)$ ,  $T(0)$  are the temperatures at any time,  $t$ , and initially at  $t=0$ .

From this equation a plot of  $C_A$  versus  $t$  can be constructed. This is illustrated (using the data from experiment #3) in Figure A.1. Using this plot,  $-dC_A/dt$  can be determined numerically.

From the rate equation for the reaction

$$R_A = A \cdot \exp(-E_A/(R \cdot T)) \cdot C_A \cdot C_B \quad (3.6)$$

where  $R_A$  = rate of reaction =  $-dC_A/dt$

$C_B$  = concentration of peroxide (which can be determined from stoichiometry if  $C_{B0}$  and  $C_A$  values are known)

$$\text{then } \ln(R_A/(C_A \cdot C_B)) = \ln(A) - E_A/(R \cdot T) \quad (3.6a)$$

thus a plot of  $\ln(R_A/(C_A \cdot C_B))$  (or, more simply,  $\ln(k)$ ) versus  $1/T$  is linear with a slope of  $-E_A/T$  and an intercept of  $\ln(A)$ . This is illustrated in Figure 3.10 with the data of experiment #2. Figure A.2

is a similar plot using all the data. It can be seen from the tables that data points near the beginning and the end of the reaction should not be used. The reason for this is the fact that, due to the time lag in the thermocouple, the numerical derivatives of concentration were found to be close to zero at the beginning. At the end, they were also found to be close to zero because of the very low reaction rate at this point.

In order to determine the Arrhenius parameters for the sulfite reaction, a linear regression of  $\ln(k)$  versus  $1/T$  was carried out using data from all three experiments. The statistical package MINITAB was used to perform the necessary calculations. A listing of the program follows at the end of this Appendix.

Figure A.3 is a comparison of the data of experiment #2 with a computer simulation of the homogeneous, adiabatic batch reactor model.

The model equations are:

$$\frac{dC_A}{dt} = -R_A \quad (A.3)$$

$$\frac{dT}{dt} = \frac{\Delta H \cdot R_A}{C_p \cdot \rho} \quad (A.4)$$

$$\text{where } R_A = A \cdot \exp(-E_A/(R \cdot T)) \cdot C_A \cdot C_B \quad (3.6)$$

The Arrhenius parameter values determined from the adiabatic batch reactor data were used in the simulation. It can be seen that the model describes the data very well.

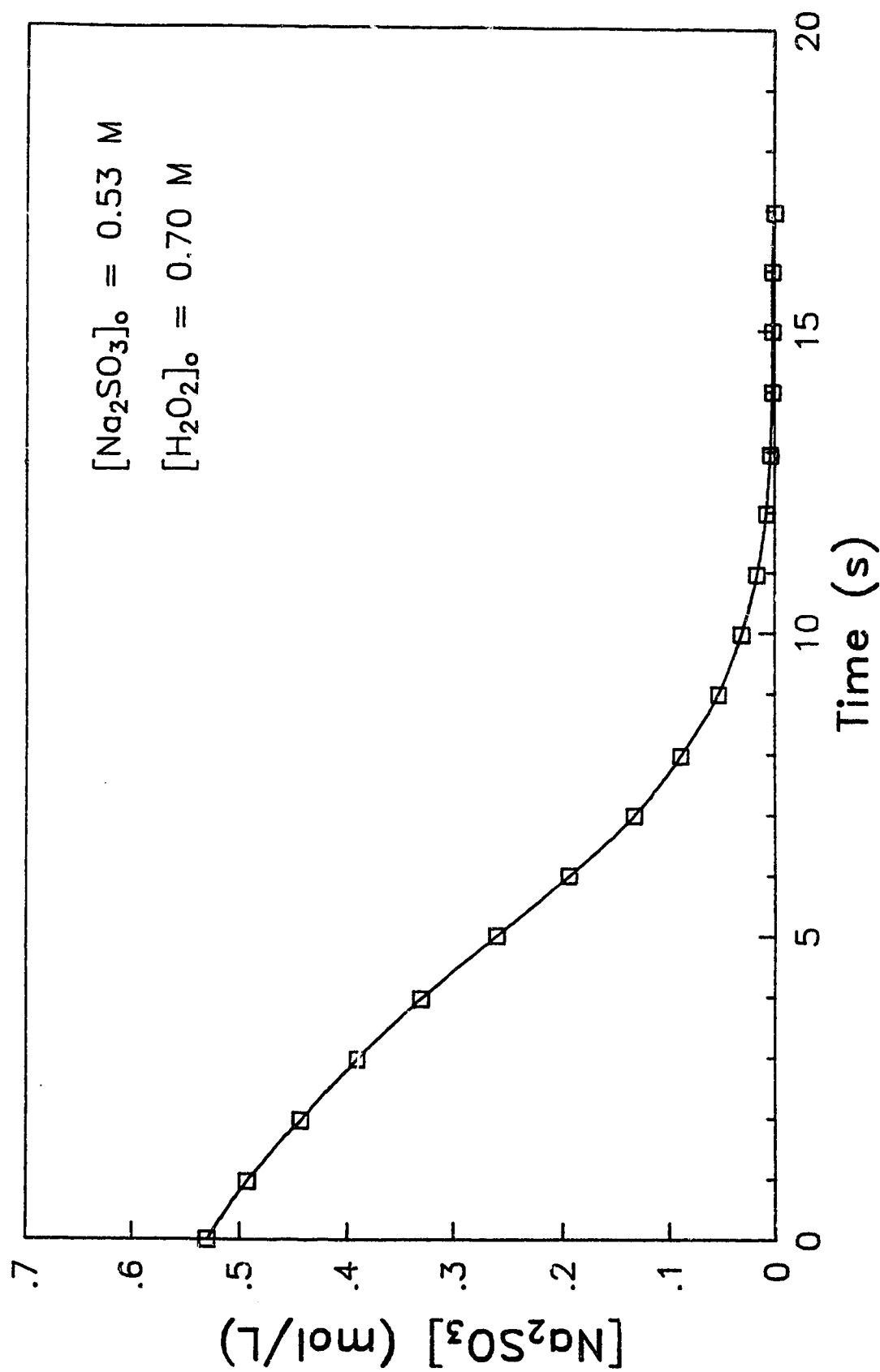


Figure A.1 Concentration Profile for Batch Reactor Experiment #3  
Data from Table A.5

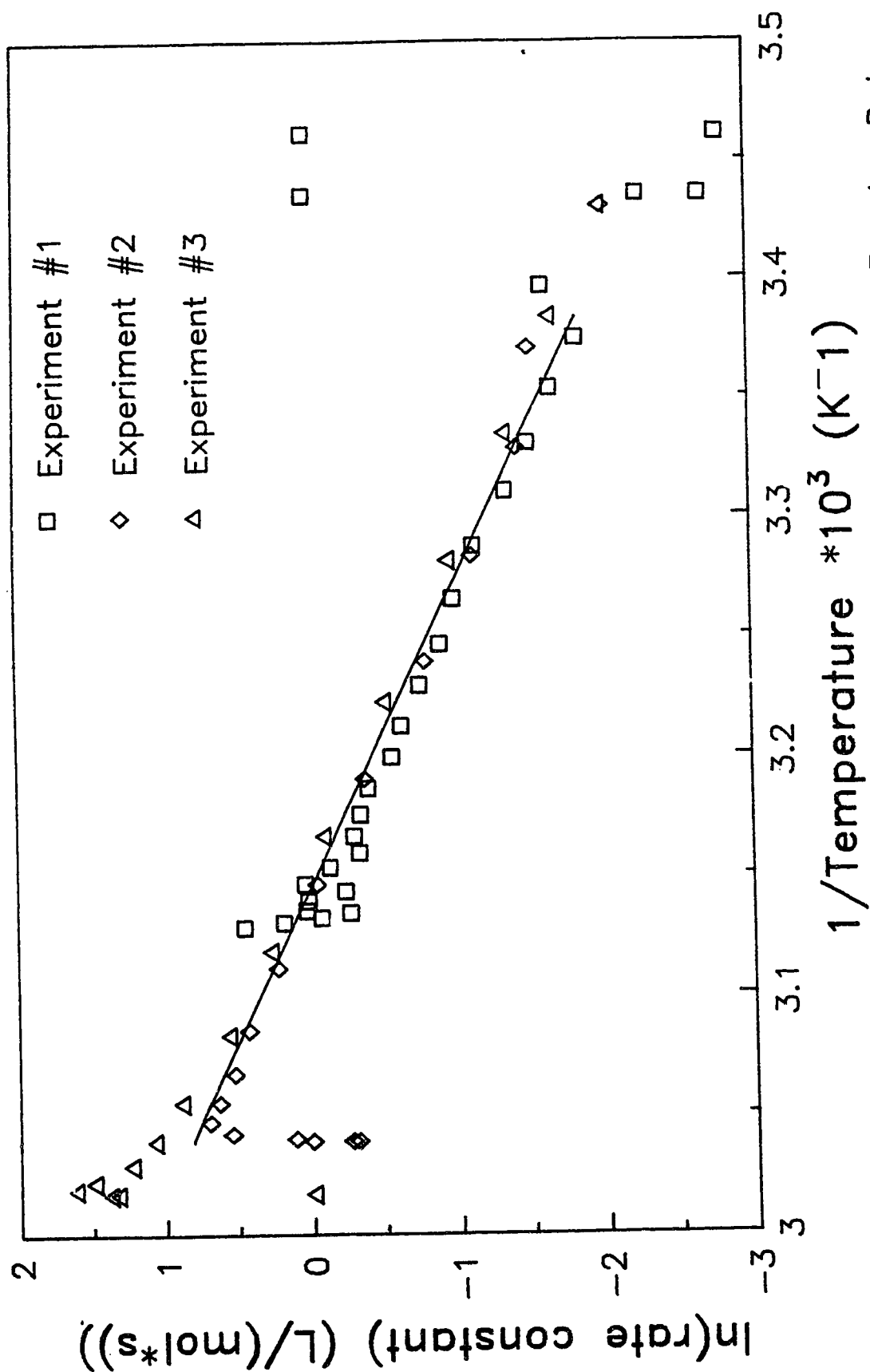


Figure A.2 Arrhenius Plot using all Adiabatic Batch Reactor Data

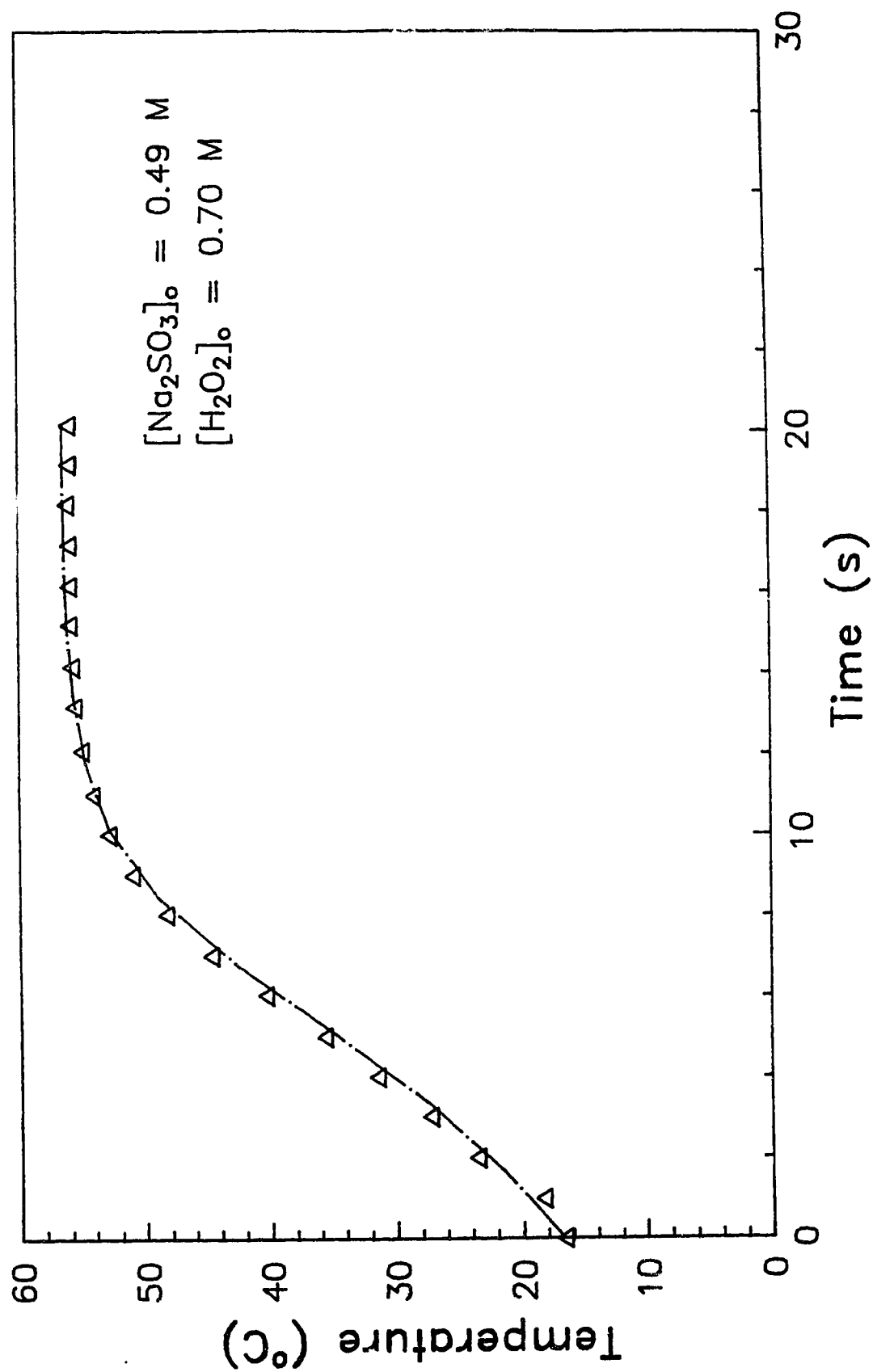


Figure A.3 Comparison of Adiabatic Batch Reactor Data with Adiabatic Batch Reactor Model

### ODPH Model Simulation Program

A computer program was implemented to solve the ODPH model equations (see equations 3.3 and 3.4). The equations were solved using a 4th order Runge-Kutta routine. A listing of the program follows.

```

C      PROGRAM SULFITE
C      SIMULATION OF ODPH TUBULAR REACTOR MODEL
C
C      DEFINE VARIABLES
C
      REAL K1,K2,K3,K4,L1,L2,L3,L4,TW,PI,CB,DH,HO,QR
      REAL CAO,CBO,T,CA,Q,D,PT,V,CP,RO,A,EA,R,MU,KF,KS,Z,DZ
      INTEGER I,J
      PI = 3.14159
      DZ = 0.01
C
C      SET PHYSICAL CONSTANTS
C
      CP = 4180
      RO = 1000
      MU = 0.001
      KF = 0.637
      R = 8.314
      KS = 16.27
      DH = 372230
      A = 3.08*10**7.0
      EA = 63 820
C
C      INPUT INTIAL CONDITIONS, FLOW, AND PIPE SIZE
C
      WRITE(6,*) 'INPUT INITIAL CONCENTRATIONS CAO & CBO'
      READ(5,*) CAO,CBO
      WRITE(6,300) CAO/1000.,CBO/1000.
300  FORMAT(1X,'CAO = ',F5.2,' CBO = ',F5.2)
      CA = CAO
      WRITE(6,*) 'INPUT FLOWRATE, INTERNAL DIAMETER AND PIPE THICKNESS'
      READ(5,*) Q,D,PT
      WRITE(6,*) Q*60000.
      WRITE(6,*) 'INPUT INITIAL TEMPERATURE'
      READ(5,*) T
      WRITE(6,*) 'INITIAL TEMPERATURE = ',T
      WRITE(6,*) 'INPUT BATH TEMPERATURE'
      READ(5,*) TW
      WRITE(6,*) 'BATH TEMPERATURE = ',TW
      WRITE(6,*) 'INPUT OUTSIDE HEAT TRANSFER COEFFICIENT'
      READ(5,*) QR
C
C      CALCULATE OVERALL HEAT TRANSFER COEFFICIENT
C
      U = HEAT(Q,RO,D,MU,CP,KF,KS,PT,QR)
      WRITE(6,*) 'U = ',U
C
C      PERFORM R-K 4TH ORDER INTEGRATION

```

```

C      WRITE(6,*) '    Z          T          C'
      Z = 0
      WRITE(6,100) Z,T-273,CA
      DO 10 I=1,340
      Z = REAL(I)/100.0
      CB = CBO - CAO +CA
      K1 = DZ*DTZ(T,CA,CB,D,A,EA,R,CP,RO,Q,TW,DH,U)
      L1 = DZ*DCZ(T,CA,CB,D,A,EA,R,CP,RO,Q,TW,DH)
      K2 = DZ*DTZ(T+K1/2.0,CA+L1/2.0,CB,D,A,EA,R,CP,RO,Q,TW,DH,U)
      L2 = DZ*DCZ(T+K1/2.0,CA+L1/2.0,CB,D,A,EA,R,CP,RO,Q,TW,DH)
      K3 = DZ*DTZ(T+K2/2.0,CA+L2/2.0,CB,D,A,EA,R,CP,RO,Q,TW,DH,U)
      L3 = DZ*DCZ(T+K2/2.0,CA+L2/2.0,CB,D,A,EA,R,CP,RO,Q,TW,DH)
      K4 = DZ*DTZ(T+K3,CA+L3,CB,D,A,EA,R,CP,RO,Q,TW,DH,U)
      L4 = DZ*DCZ(T+K3,CA+L3,CB,D,A,EA,R,CP,RO,Q,TW,DH)
      T = T + (K1+2.0*K2+2.0*K3+K4)/6.0
      CA = CA + (L1+2.0*L2+2.0*L3+L4)/6.0
      IF(REAL(I/14.0).EQ.(I/14)) THEN
      WRITE(6,100) Z,T-273,CA
      END IF
C      WRITE(6,100) Z,T-273,CA
100    FORMAT(3X,F5.2,2X,F15.2,2X,F15.2)
10     CONTINUE
      STOP
      END

C
C      FUNCTION TO CALCULATE THE OVERALL HEAT-TRANSFER COEFFICIENT
C
      FUNCTION HEAT(Q,RO,D,MU,CP,KF,KS,PT,QR)
      REAL HEAT,V,RE,PR,H,HO,PI,MU,KF,KS,DL,PC
      PI = 3.14159
      DL = 2*PT/LOG((D+2*PT)/D)
      V = Q/(PI*D*D/4.0)
      RE = V*RO*D/MU
      WRITE(6,*) 'RE # = ',RE
      PR = CP*MU/KF
      H = 0.116*(RE**(0.667)-125)*PR**(0.333)*KF/D
      WRITE(6,*) 'H = ',H
      PC = (KS*DL)/(PT*(D+2*PT))
      WRITE(6,*) 'PIPE CONTROL = ',PC
      HO=QR
      WRITE(6,*) 'HO = ',HO
      HEAT = 1.0/(((D+2.0*PT)/(D*H)) + 1.0/PC + 1.0/HO)
C      HEAT = HO
      RETURN
      END

C
C      FUNCTION DT/DZ

```



C

```
FUNCTION DTZ(T, CA, CB, D, A, EA, R, CP, RO, Q, TW, DH, U)
REAL PI
PI = 3.14159
DTZ = DH*CA*(CB)*PI*D*D*A*EXP(-1.0*EA/R/T)/(CP*RO*Q*4.0)
DTZ = DTZ - U*PI*(D+2.0*PT)*(T-TW)/(CP*RO*Q)
RETURN
END
```

C

C

C

```
FUNCTION DC/DZ
```

```
FUNCTION DCZ(T, CA, CB, D, A, EA, R, CP, RO, Q, TW, DH)
REAL PI
PI = 3.14159
DCZ = -1.0*PI*D*D*CA*(CB)*A*EXP(-1.0*EA/R/T)/(4.0*Q)
RETURN
END
```

NOTE  
 NOTE REGRESSION TO DETERMINE ARRHENIUS PARAMETERS FROM BATCH DATA  
 NOTE  
 NOTE  
 NOTE DEFINE  $mC_p/DH^*V$  FOR THE SYSTEM  
 NOTE  
 LET K1 = 0.01231  
 NOTE  
 NOTE READ IN BATCH DATA #1  
 NOTE  
 READ INTO C1 C2  

0.00	15.38
0.99	15.57
2.00	15.57
2.99	15.75
4.04	15.75
5.00	15.75
6.01	17.99
6.99	17.99
8.02	17.99
9.01	21.34
10.00	23.21
11.01	25.07
12.00	27.12
13.01	28.98
14.02	31.10
15.02	33.09
15.99	34.91
17.02	36.54
18.00	38.17
19.01	39.44
20.00	40.71
21.01	41.80
22.02	42.70
23.00	43.43
24.03	43.97
24.99	44.70
26.00	45.06
27.03	45.42
28.00	45.79
29.00	45.97
30.03	46.15
31.02	46.33
32.00	46.51
33.05	46.69

 NOTE  
 NOTE CALCULATE NUMERICALLY  $DCA/DT$  AT ALL POINTS  
 NOTE FIND  $LN(K)$  VS  $1/T$

```

NOTE
PICK ROWS 1 TO 32 OF C1 PUT INTO C11
PICK ROWS 1 TO 32 OF C2 PUT INTO C12
PICK ROWS 2 TO 33 OF C1 PUT INTO C13
PICK ROWS 2 TO 33 OF C2 PUT INTO C14
PICK ROWS 3 TO 34 OF C1 PUT INTO C15
PICK ROWS 3 TO 34 OF C2 PUT INTO C16
LET C32 = ((C14-C12)/(C13-C11)+(C16-C14)/(C15-C13))/2
PRINT C32
LET K32 = 15.38
LET C38 = LOG(K1*C32/((0.39-K1*(C14-K32))*(0.59-K1*(C14-K32))))
LET C39 = 1.0/(C14+273.15)
NOTE
NOTE READ IN BATCH DATA #2
NOTE
READ INTO C1 C2
0.00 16.68
0.99 18.36
2.00 23.58
3.02 27.30
4.00 31.46
4.99 35.63
6.02 40.35
7.00 44.70
8.02 48.32
9.00 51.04
10.00 52.86
10.99 54.13
12.09 55.03
13.18 55.58
14.17 55.76
15.21 55.94
16.18 55.94
17.19 55.94
18.19 56.12
NOTE
NOTE CALCULATE NUMERICALLY DCA/DT AT ALL POINTS
NOTE FIND LN(K) VS 1/T
NOTE
PICK ROWS 1 TO 17 OF C1 PUT INTO C11
PICK ROWS 1 TO 17 OF C2 PUT INTO C12
PICK ROWS 2 TO 18 OF C1 PUT INTO C13
PICK ROWS 2 TO 18 OF C2 PUT INTO C14
PICK ROWS 3 TO 19 OF C1 PUT INTO C15
PICK ROWS 3 TO 19 OF C2 PUT INTO C16
LET C42 = ((C14-C12)/(C13-C11)+(C16-C14)/(C15-C13))/2
PRINT C42
LET K42 = 16.68

```

```

LET C48 = LOG(K1*C42/((0.49-K1*(C14-K42))*(0.70-K1*(C14-K42))))
LET C49 = 1.0/(C14+273.15)
NOTE
NOTE READ IN BATCH DATA #3
NOTE
READ INTO C1 C2
0.00 15.38
0.96 18.36
1.96 22.46
2.96 26.75
3.95 31.64
4.99 37.26
5.98 42.70
6.97 47.60
7.96 51.23
8.98 54.13
9.97 55.94
10.96 57.03
11.97 57.75
12.95 58.12
13.98 58.30
14.99 58.30
15.98 58.30
16.96 58.48
NOTE
NOTE CALCULATE NUMERICALLY DCA/DT AT ALL POINTS
NOTE FIND LN(K) VS 1/T
NOTE
PICK ROWS 1 TO 16 OF C1 PUT INTO C11
PICK ROWS 1 TO 16 OF C2 PUT INTO C12
PICK ROWS 2 TO 17 OF C1 PUT INTO C13
PICK ROWS 2 TO 17 OF C2 PUT INTO C14
PICK ROWS 3 TO 18 OF C1 PUT INTO C15
PICK ROWS 3 TO 18 OF C2 PUT INTO C16
LET C52=((C14-C12)/(C13-C11)+(C16-C14)/(C15-C13))/2
PRINT C52
LET K52 = 15.38
LET C58=LOG(K1*C52/((0.53-K1*(C14-K52))*(0.70-K1*(C14-K52))))
LET C59 = 1.0/(C14+273.15)
NOTE
NOTE PRINT OUT LN(K) VS 1/T VALUES
NOTE
PRINT C38 C39 C48 C49 C58 C59
NOTE
NOTE PICK OUT SUITABLE DATA FOR REGRESSION AND PERFORM REGRESSION
NOTE
PICK ROWS 10 TO 25 OF C39 AND PUT INTO C70
PICK ROWS 2 TO 11 OF C49 AND PUT INTO C71

```

PICK ROWS 2 TO 10 OF C59 AND PUT INTO C72  
PICK ROWS 10 TO 25 OF C38 AND PUT INTO C73  
PICK ROWS 2 TO 11 OF C48 AND PUT INTO C74  
PICK ROWS 2 TO 10 OF C58 AND PUT INTO C75  
JOIN C70,C71,C72, PUT INTO C69  
JOIN C73,C74,C75, PUT INTO C68  
REGRESS Y IN C68 ON 1 PREDICTOR IN C69 &  
STORE ST. RESIDUALS IN C90 AND PRED. Y IN C91 AND COEF. IN C92  
NOTE  
NOTE PRINT OUT RESULTS  
NOTE  
PRINT C69 C68 C91 C90  
LET C39=C39\*1000  
LET C49=C49\*1000  
LET C59=C59\*1000  
PRINT C38 C39 C48 C49 C58 C59  
STOP

```

NOTE
NOTE  MINITAB PROGRAM TO FIND VALUES OF ARRHENIUS PARAMETERS
NOTE  USING MADER'S 1957 DATA
NOTE
READ INTO C1
  0.0196
  0.0829
  0.196
  0.464
READ INTO C2
  273.4
  288.0
  298.0
  308.0
NOTE
NOTE  FIND LN(K) AND 1/T VALUES AND PERFORM REGRESSION
NOTE
  LET C3 = LOG(C1)
  LET C4 = 1.0/C2
REGRESS C3 ON 1 PREDICTOR C4 & STORE ST.RESIDUALS IN C5 AND PRED Y IN C6
PRINT C3 C4 C6 C5
STOP

```

## APPENDIX B

Estimation of the maximum flow through a 0.175 cm internal diameter reactor -

Using Bernoulli's equation

$$\frac{\Delta P}{\rho} + \frac{u_f^2 - u_o^2}{2} + g \cdot \Delta z - W_f = 0 \quad (\text{B.1})$$

where  $\Delta P$  = pressure drop (Pa)

$\rho$  = fluid density ( $\text{kg/m}^3$ )

$u_f$  = fluid final velocity (m/s)

$u_o$  = fluid initial velocity (m/s)

$g$  = acceleration due to gravity ( $9.81 \text{ m/s}^2$ )

$W_f$  = work lost to friction (J/kg)

$$= 32 \cdot f \cdot L_e \cdot Q^2 / (\pi^2 \cdot D^5) \quad (\text{B.2})$$

$\Delta z$  = height change (m)

with  $f$  = Fanning friction factor =  $\phi$ (Reynolds number, tubing type)

$L_e$  = equivalent length of tubing (m)

$Q$  = flow rate ( $\text{m}^3/\text{s}$ )

$D$  = reactor diameter (m)

Assuming a reactor length of 3.5 m and using the properties of water for fluid density and viscosity,

$$\text{Re} = 4 \cdot Q \cdot \rho / (\pi \cdot D \cdot \mu) = 7.28 \cdot 10^8 \cdot Q$$

$$W_f = 6.91 \cdot 10^{14} \cdot f \cdot Q^2$$

If the pressure drop is 690 kPa and the change in height is assumed to be negligible then equation B.1 becomes

$$690 = W_f \quad (B.3)$$

Equation B.3 can be solved using the following algorithm.

- 1) Estimate flow rate
- 2) Determine the corresponding Reynolds number
- 3) Calculate  $f$  from an appropriate correlation
- 4) Determine  $W_f$  using  $f$  value found in 3
- 5) Check equation B.3 for equality
- 6) Repeat steps 1 through 5 if necessary

The maximum flow rate through this system was found to be approximately 470 ml/min. This however, was based on a 3.5 m long reactor with no consideration given to the effect of the tees and the thermocouples on the pressure drop. Thus, the flow rate determined is a rough estimate.

Sample Calculation:

Assume  $Q = 6.67 \cdot 10^{-6} \text{ m}^3/\text{s}$  (i.e., 400 ml/min)

Thus,  $Re = 4853$

$f = 0.017$  from Fanning friction factor correlation (figure can be found in Perry's *Chemical Engineers' Handbook*, 6th Edition)



and  $W_f = 523.17$

Equation B.3 is not satisfied so another iteration is required.

Assume  $Q = 8.33 \cdot 10^{-6} \text{ m}^3/\text{s}$  (i.e., 500 ml/min)

Thus,  $Re = 6064$

$f = 0.017$  from friction factor correlation

and  $W_f = 890$

Equation B.3 is not satisfied so another iteration is required.

Assume  $Q = 7.83 \cdot 10^{-6} \text{ m}^3/\text{s}$  (i.e., 470 ml/min)

Thus  $Re = 5700$

$f = 0.017$  from friction factor correlation

and  $W_f = 710$

Equation B.3 is thus satisfied to desired tolerance so,

Approximate maximum flow rate = 470 ml/min

Rotameter Tube Calibration			
Tube Number	Fluid	Scale Reading	Measured Flow (ml/min)
605	1.1 M	60	164, 160
	Buffered	70	192, 196
	Sodium	80	232, 238
	Sulfite	90	268, 272
		100	304, 304
		110	352, 350
604	35 wt %	30	30, 30
	Hydrogen	40	44, 44
	Peroxide	50	60, 64
		60	74, 76
		70	90, 90, 90

Linear Regression of Average Measured Flow as a function of scale  
Reading -

For the 605 tube

$$\text{Flow Rate (ml/min)} = 3.74 x - 65.5$$

where  $x$  = scale reading

For the 604 tube

$$\text{Flow Rate (ml/min)} = 1.51 x - 15.3$$

where  $x$  = scale reading

Figure B.1 illustrates the linearity of the data

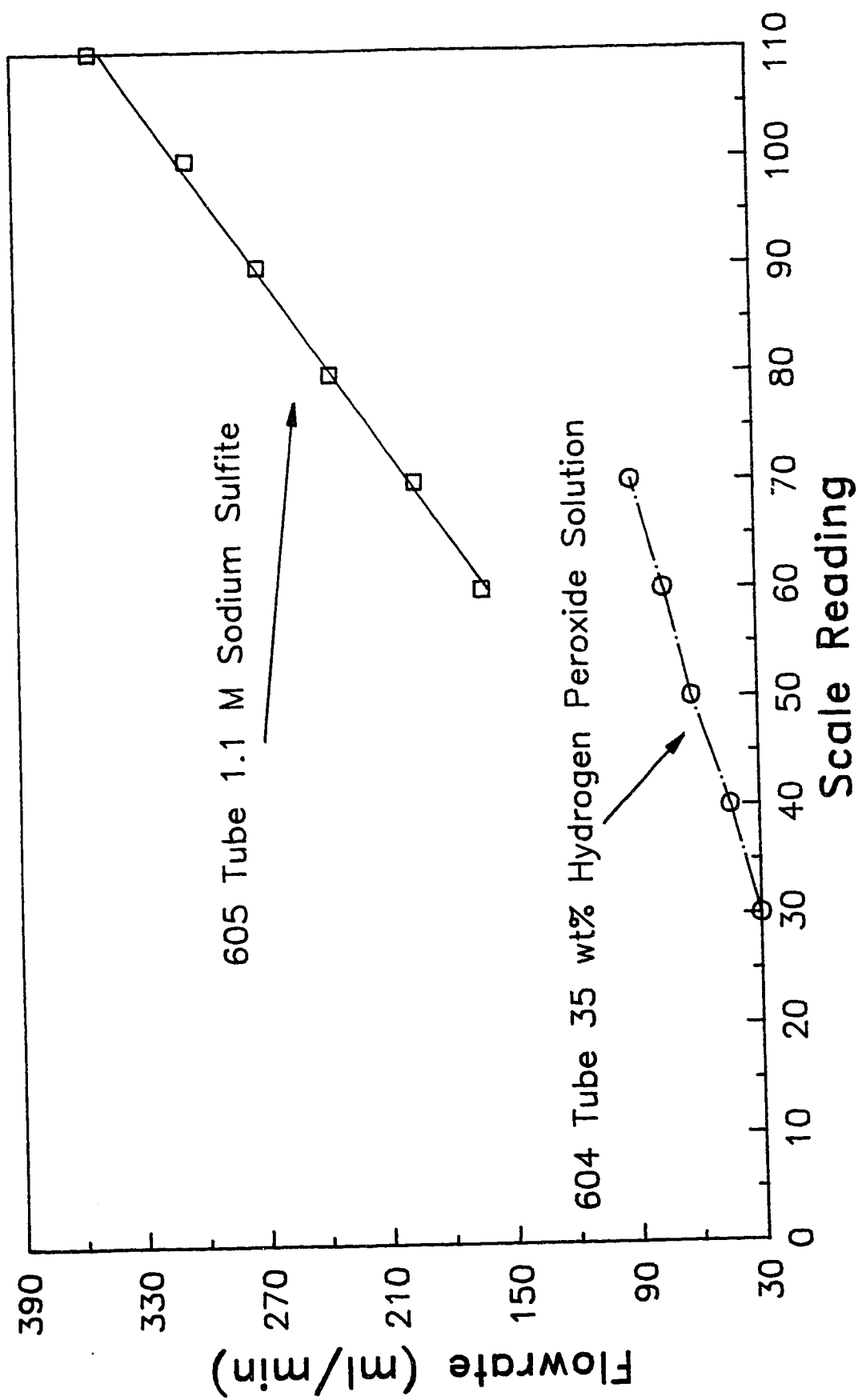


Figure B.1 – Rotameter Tube Calibration Curves

## APPENDIX C

### A) Heat Transfer Experiments

In all cases, the temperature reported is the average temperature recorded at that thermocouple over the last 5 minutes (i.e, 10 sampling intervals) of the particular experiment. The inlet temperature given is the volumetric average of the temperatures recorded 5 cm (in each stream) from the first thermocouple. The stirrer speed setting is #6.

TABLE C.1                      HEAT TRANSFER EXPERIMENT #1		
Flow = 305 ml/min $[\text{Na}_2\text{SO}_3]_0 = 1.1 \text{ M}$ $[\text{H}_2\text{O}_2]_0 = 0.00 \text{ M}$ Bath = 50.56°C		
Thermocouple Number	Position (m)	Temperature °C
Inlet	-	-
1	0.0	28.24
2	0.299	34.50
3	0.598	38.43
4	0.897	41.06
5	1.196	43.46
6	1.496	-
7	1.795	47.56
8	2.094	47.95
9	2.393	48.84
10	2.692	48.64
11	2.992	49.37
12	3.291	49.41
13	3.590	49.70

Data plotted in Figure 5.1

TABLE C.2                      HEAT TRANSFER EXPERIMENT #2		
Flow = 305 ml/min $[\text{Na}_2\text{SO}_3]_0 = 1.1 \text{ M}$ $[\text{H}_2\text{O}_2]_0 = 0.00 \text{ M}$ Bath = 44.52°C		
Thermocouple Number	Position (m)	Temperature °C
Inlet	-	-
1	0.0	25.28
2	0.299	30.83
3	0.598	34.63
4	0.897	36.89
5	1.196	39.18
6	1.496	-
7	1.795	41.85
8	2.094	42.28
9	2.393	43.06
10	2.692	43.38
11	2.992	43.54
12	3.291	43.75
13	3.590	43.99

TABLE C.3                      HEAT TRANSFER EXPERIMENT #3		
Flow = 305 ml/min $[\text{Na}_2\text{SO}_3]_0 = 1.1 \text{ M}$ $[\text{H}_2\text{O}_2]_0 = 0.00 \text{ M}$ Bath = $2.90^\circ\text{C}$		
Thermocouple Number	Position (m)	Temperature $^\circ\text{C}$
Inlet	-	-
1	0.0	18.20
2	0.299	14.63
3	0.598	12.17
4	0.897	10.02
5	1.196	8.67
6	1.496	-
7	1.795	6.49
8	2.094	6.19
9	2.393	5.50
10	2.692	5.39
11	2.992	4.90
12	3.291	4.46
13	3.590	4.20



## B) Parametric Sensitivity Experiments

In all cases, the temperature reported is the average temperature recorded at that thermocouple over the last 5 minutes (i.e, 10 sampling intervals) of the particular experiment. The inlet temperature given is the volumetric average of the temperatures recorded 5 cm (in each stream) from the first thermocouple. The stirrer speed setting is #6, unless otherwise noted.

TABLE C.4                      PARAMETRIC SENSITIVITY EXPERIMENT E1		
Flow = 380 ml/min $[\text{Na}_2\text{SO}_3]_0 = 0.88 \text{ M}$ $[\text{H}_2\text{O}_2]_0 = 2.31 \text{ M}$ Bath = 24.0°C		
Thermocouple Number	Position (m)	Temperature °C
Inlet	-	10.03
1	0.0	11.94
2	0.299	16.93
3	0.598	20.42
4	0.897	24.19
5	1.196	28.03
6	1.496	31.97
7	1.795	36.18
8	2.094	39.50
9	2.393	41.45
10	2.692	44.03
11	2.992	47.51
12	3.291	46.58
13	3.590	44.72

Data plotted in Figure 6.3

TABLE C.5		PARAMETRIC SENSITIVITY EXPERIMENT Q1
Flow = 380 ml/min $[\text{Na}_2\text{SO}_3]_0 = 0.88 \text{ M}$ $[\text{H}_2\text{O}_2]_0 = 2.31 \text{ M}$ Bath = $24.0^\circ\text{C}$		
Thermocouple Number	Position (m)	Temperature $^\circ\text{C}$
Inlet	-	19.06
1	0.0	19.74
2	0.299	26.71
3	0.598	30.14
4	0.897	35.30
5	1.196	38.76
6	1.496	42.80
7	1.795	46.93
8	2.094	49.00
9	2.393	47.41
10	2.692	46.05
11	2.992	43.37
12	3.291	40.20
13	3.590	37.53

Data plotted in Figure 6.3

TABLE C.6		PARAMETRIC SENSITIVITY EXPERIMENT E3
Flow = 380 ml/min $[\text{Na}_2\text{SO}_3]_0 = 0.88 \text{ M}$ $[\text{H}_2\text{O}_2]_0 = 2.31 \text{ M}$ Bath = 24.0°C		
Thermocouple Number	Position (m)	Temperature °C
Inlet	-	24.19
1	0.0	25.86
2	0.299	31.59
3	0.598	35.67
4	0.897	41.19
5	1.196	46.19
6	1.496	50.22
7	1.795	52.42
8	2.094	52.85
9	2.393	47.90
10	2.692	45.57
11	2.992	42.72
12	3.291	39.44
13	3.590	36.72

Data plotted in Figure 6.3

TABLE C.7		PARAMETRIC SENSITIVITY EXPERIMENT E4
Flow = 380 ml/min $[\text{Na}_2\text{SO}_3]_0 = 0.88 \text{ M}$ $[\text{H}_2\text{O}_2]_0 = 2.31 \text{ M}$ Bath = 24.0°C		
Thermocouple Number	Position (m)	Temperature °C
Inlet	-	29.98
1	0.0	31.82
2	0.299	39.02
3	0.598	44.84
4	0.897	53.30
5	1.196	58.95
6	1.496	58.78
7	1.795	54.15
8	2.094	50.03
9	2.393	44.53
10	2.692	41.60
11	2.992	38.49
12	3.291	35.61
13	3.590	33.51

Data plotted in Figure 6.3

TABLE C.8		PARAMETRIC SENSITIVITY EXPERIMENT R1
Flow = 380 ml/min $[\text{Na}_2\text{SO}_3]_0 = 0.88 \text{ M}$ $[\text{H}_2\text{O}_2]_0 = 2.31 \text{ M}$ Bath = 24.0°C		
Thermocouple Number	Position (m)	Temperature °C
Inlet	-	33.69
1	0.0	34.45
2	0.299	45.35
3	0.598	53.64
4	0.897	61.99
5	1.196	61.82
6	1.496	55.41
7	1.795	49.29
8	2.094	46.12
9	2.393	40.97
10	2.692	38.61
11	2.992	35.79
12	3.291	33.58
13	3.590	31.75

Data plotted in Figure 6.3

TABLE C.9		PARAMETRIC SENSITIVITY EXPERIMENT E6
Flow = 380 ml/min $[\text{Na}_2\text{SO}_3]_0 = 0.88 \text{ M}$ $[\text{H}_2\text{O}_2]_0 = 2.31 \text{ M}$ Bath = 24.0°C		
Thermocouple Number	Position (m)	Temperature °C
Inlet	-	41.75
1	0.0	44.47
2	0.299	65.27
3	0.598	83.83
4	0.897	74.31
5	1.196	61.92
6	1.496	50.78
7	1.795	44.23
8	2.094	41.40
9	2.393	36.70
10	2.692	34.71
11	2.992	32.46
12	3.291	30.94
13	3.590	29.34

Data plotted in Figure 6.3

TABLE C.10		PARAMETRIC SENSITIVITY EXPERIMENT E9
Flow = 380 ml/min $[\text{Na}_2\text{SO}_3]_0 = 0.88 \text{ M}$ $[\text{H}_2\text{O}_2]_0 = 2.31 \text{ M}$ Bath = 24.0°C		
Thermocouple Number	Position (m)	Temperature °C
Inlet	-	45.06
1	0.0	46.60
1A	0.149	63.93
2	0.299	77.18
2A	0.448	89.97
3	0.598	86.72
4	0.897	68.66
5	1.196	56.21
6	1.496	46.50
7	1.795	41.24
8	2.094	38.77
9	2.393	34.87
10	2.692	33.15
11	2.992	31.26
12	3.291	29.64
13	3.590	28.46

Data plotted in Figure 6.3



TABLE C.11                      PARAMETRIC SENSITIVITY EXPERIMENT E10		
Flow = 380 ml/min $[\text{Na}_2\text{SO}_3]_0 = 0.88 \text{ M}$ $[\text{H}_2\text{O}_2]_0 = 2.31 \text{ M}$ Bath = 24.0°C		
Thermocouple Number	Position (m)	Temperature °C
Inlet	-	48.71
1	0.0	50.61
1A	0.149	72.38
2	0.299	93.21
2A	0.448	95.06
3	0.598	85.18
4	0.897	67.22
5	1.196	65.30
6	1.496	45.98
7	1.795	40.85
8	2.094	38.68
9	2.393	34.68
10	2.692	33.17
11	2.992	31.26
12	3.291	29.68
13	3.590	28.44

Data plotted in Figure 6.3

TABLE C.12		PARAMETRIC SENSITIVITY EXPERIMENT F1
Flow = 380 ml/min $[\text{Na}_2\text{SO}_3]_0 = 0.88 \text{ M}$ $[\text{H}_2\text{O}_2]_0 = 2.31 \text{ M}$ Bath = $34.0^\circ\text{C}$		
Thermocouple Number	Position (m)	Temperature $^\circ\text{C}$
Inlet	-	10.74
1	0.0	13.25
2	0.299	20.54
3	0.598	26.83
4	0.897	33.74
5	1.196	41.61
6	1.496	51.76
7	1.795	62.80
8	2.094	67.55
9	2.393	62.14
10	2.692	57.98
11	2.992	53.09
12	3.291	49.03
13	3.590	45.56

Data plotted in Figure 6.5

TABLE C.13		PARAMETRIC SENSITIVITY EXPERIMENT F2
Flow = 380 ml/min $[\text{Na}_2\text{SO}_3]_0 = 0.88 \text{ M}$ $[\text{H}_2\text{O}_2]_0 = 2.31 \text{ M}$ Bath = $34.0^\circ\text{C}$		
Thermocouple Number	Position (m)	Temperature $^\circ\text{C}$
Inlet	-	18.16
1	0.0	19.82
2	0.299	28.18
3	0.598	34.98
4	0.897	43.78
5	1.196	54.86
6	1.496	65.58
7	1.795	67.18
8	2.094	64.22
9	2.393	56.30
10	2.692	52.41
11	2.992	48.51
12	3.291	45.28
13	3.590	42.75

Data plotted in Figure 6.5

TABLE C.14		PARAMETRIC SENSITIVITY EXPERIMENT F3
Flow = 380 ml/min $[\text{Na}_2\text{SO}_3]_0 = 0.88 \text{ M}$ $[\text{H}_2\text{O}_2]_0 = 2.31 \text{ M}$ Bath = $34.0^\circ\text{C}$		
Thermocouple Number	Position (m)	Temperature $^\circ\text{C}$
Inlet	-	23.68
1	0.0	25.24
2	0.299	34.43
3	0.598	42.03
4	0.897	53.84
5	1.196	66.58
6	1.496	70.25
7	1.795	63.98
8	2.094	59.56
9	2.393	52.62
10	2.692	49.31
11	2.992	45.97
12	3.291	43.25
13	3.590	41.12

Data plotted in Figure 6.5

TABLE C.15		PARAMETRIC SENSITIVITY EXPERIMENT F4
Flow = 380 ml/min $[\text{Na}_2\text{SO}_3]_0 = 0.88 \text{ M}$ $[\text{H}_2\text{O}_2]_0 = 2.31 \text{ M}$ Bath = $34.0^\circ\text{C}$		
Thermocouple Number	Position (m)	Temperature $^\circ\text{C}$
Inlet	-	31.20
1	0.0	34.42
2	0.299	46.82
3	0.598	61.67
4	0.897	80.46
5	1.196	73.10
6	1.496	62.02
7	1.795	54.73
8	2.094	51.41
9	2.393	46.58
10	2.692	44.45
11	2.992	42.20
12	3.291	40.57
13	3.590	39.10

Data plotted in Figure 6.5

TABLE C.16		PARAMETRIC SENSITIVITY EXPERIMENT F8
Flow = 380 ml/min $[\text{Na}_2\text{SO}_3]_0 = 0.88 \text{ M}$ $[\text{H}_2\text{O}_2]_0 = 2.31 \text{ M}$ Bath = $34.0^\circ\text{C}$		
Thermocouple Number	Position (m)	Temperature $^\circ\text{C}$
Inlet	-	34.43
1	0.0	36.52
1A	0.149	48.13
2	0.299	52.52
2A	0.448	58.53
3	0.598	69.99
4	0.897	80.69
5	1.196	71.36
6	1.496	60.63
7	1.795	54.00
8	2.094	51.41
9	2.393	46.47
10	2.692	44.67
11	2.992	42.29
12	3.291	40.44
13	3.590	39.04

Data plotted in Figure 6.5

TABLE C.17		PARAMETRIC SENSITIVITY EXPERIMENT F9
Flow = 380 ml/min $[\text{Na}_2\text{SO}_3]_0 = 0.88 \text{ M}$ $[\text{H}_2\text{O}_2]_0 = 2.31 \text{ M}$ Bath = $34.0^\circ\text{C}$		
Thermocouple Number	Position (m)	Temperature $^\circ\text{C}$
Inlet	-	40.37
1	0.0	41.05
1A	0.149	58.83
2	0.299	69.00
2A	0.448	83.22
3	0.598	92.13
4	0.897	77.22
5	1.196	64.79
6	1.496	55.27
7	1.795	49.87
8	2.094	47.99
9	2.393	44.02
10	2.692	42.57
11	2.992	40.73
12	3.291	39.26
13	3.590	38.13

Data plotted in Figure 6.5

TABLE C.18		PARAMETRIC SENSITIVITY EXPERIMENT S1
Flow = 380 ml/min $[\text{Na}_2\text{SO}_3]_0 = 0.88 \text{ M}$ $[\text{H}_2\text{O}_2]_0 = 2.31 \text{ M}$ Bath = 34.0°C		
Thermocouple Number	Position (m)	Temperature °C
Inlet	-	46.70
1	0.0	50.25
1A	0.149	69.86
2	0.299	92.21
2A	0.448	98.36
3	0.598	88.87
4	0.897	73.00
5	1.196	61.81
6	1.496	52.79
7	1.795	47.91
8	2.094	45.70
9	2.393	42.55
10	2.692	41.13
11	2.992	39.51
12	3.291	38.26
13	3.590	37.19

Data plotted in Figure 6.5



TABLE C.19		PARAMETRIC SENSITIVITY EXPERIMENT G1
Flow = 380 ml/min $[\text{Na}_2\text{SO}_3]_0 = 0.88 \text{ M}$ $[\text{H}_2\text{O}_2]_0 = 2.31 \text{ M}$ Bath = 44.0°C		
Thermocouple Number	Position (m)	Temperature °C
Inlet	-	11.95
1	0.0	15.66
2	0.299	25.39
3	0.598	34.29
4	0.897	45.61
5	1.196	61.10
6	1.496	76.54
7	1.795	73.56
8	2.094	69.31
9	2.393	62.19
10	2.692	58.80
11	2.992	55.36
12	3.291	53.00
13	3.590	50.75

Data plotted in Figure 6.6

TABLE C.20		PARAMETRIC SENSITIVITY EXPERIMENT G2
Flow = 380 ml/min $[\text{Na}_2\text{SO}_3]_0 = 0.88 \text{ M}$ $[\text{H}_2\text{O}_2]_0 = 2.31 \text{ M}$ Bath = 44.0°C		
Thermocouple Number	Position (m)	Temperature °C
Inlet	-	19.16
1	0.0	22.10
2	0.299	33.29
3	0.598	43.37
4	0.897	59.23
5	1.196	77.40
6	1.496	76.47
7	1.795	68.38
8	2.094	64.56
9	2.393	58.56
10	2.692	55.82
11	2.992	53.13
12	3.291	51.23
13	3.590	49.46

Data plotted in Figure 6.6

TABLE C.21		PARAMETRIC SENSITIVITY EXPERIMENT G3
Flow = 380 ml/min $[\text{Na}_2\text{SO}_3]_0 = 0.88 \text{ M}$ $[\text{H}_2\text{O}_2]_0 = 2.31 \text{ M}$ Bath = 44.0°C		
Thermocouple Number	Position (m)	Temperature °C
Inlet	-	25.44
1	0.0	28.64
2	0.299	41.16
3	0.598	54.85
4	0.897	77.71
5	1.196	80.92
6	1.496	70.96
7	1.795	63.81
8	2.094	60.59
9	2.393	55.75
10	2.692	53.63
11	2.992	51.34
12	3.291	49.90
13	3.590	48.49

Data plotted in Figure 6.6

TABLE C.22		PARAMETRIC SENSITIVITY EXPERIMENT G4
Flow = 380 ml/min $[\text{Na}_2\text{SO}_3]_0 = 0.88 \text{ M}$ $[\text{H}_2\text{O}_2]_0 = 2.31 \text{ M}$ Bath = 44.0°C		
Thermocouple Number	Position (m)	Temperature °C
Inlet	-	29.69
1	0.0	32.53
2	0.299	48.12
3	0.598	67.52
4	0.897	85.82
5	1.196	76.43
6	1.496	66.87
7	1.795	60.58
8	2.094	57.90
9	2.393	53.91
10	2.692	52.01
11	2.992	50.18
12	3.291	48.22
13	3.590	47.69

Data plotted in Figure 6.6

TABLE C.23		PARAMETRIC SENSITIVITY EXPERIMENT G7
Flow = 380 ml/min $[\text{Na}_2\text{SO}_3]_0 = 0.88 \text{ M}$ $[\text{H}_2\text{O}_2]_0 = 2.31 \text{ M}$ Bath = 44.0°C		
Thermocouple Number	Position (m)	Temperature °C
Inlet	-	33.21
1	0.0	35.20
1A	0.149	51.09
2	0.299	56.56
2A	0.448	66.93
3	0.598	87.93
4	0.897	86.13
5	1.196	74.35
6	1.496	64.95
7	1.795	59.38
8	2.094	57.51
9	2.393	53.67
10	2.692	51.91
11	2.992	50.05
12	3.291	48.71
13	3.590	47.49

Data plotted in Figure 6.6

TABLE C.24		PARAMETRIC SENSITIVITY EXPERIMENT G8
Flow = 380 ml/min $[\text{Na}_2\text{SO}_3]_0 = 0.88 \text{ M}$ $[\text{H}_2\text{O}_2]_0 = 2.31 \text{ M}$ Bath = 44.0°C		
Thermocouple Number	Position (m)	Temperature °C
Inlet	-	39.74
1	0.0	41.22
1A	0.149	62.20
2	0.299	75.50
2A	0.448	96.07
3	0.598	98.77
4	0.897	83.39
5	1.196	72.22
6	1.496	63.47
7	1.795	58.19
8	2.094	56.55
9	2.393	52.76
10	2.692	50.90
11	2.992	49.52
12	3.291	48.29
13	3.590	47.18

Data is plotted in Figure 6.6

TABLE C.25		PARAMETRIC SENSITIVITY EXPERIMENT H1
Flow = 380 ml/min $[\text{Na}_2\text{SO}_3]_0 = 0.88 \text{ M}$ $[\text{H}_2\text{O}_2]_0 = 2.31 \text{ M}$ Bath = 29.0°C		
Thermocouple Number	Position (m)	Temperature °C
Inlet	-	17.40
1	0.0	18.67
1A	0.149	24.43
2	0.299	26.24
2A	0.448	27.86
3	0.598	30.86
4	0.897	36.15
5	1.196	42.01
6	1.496	48.20
7	1.795	53.66
8	2.094	57.69
9	2.393	55.10
10	2.692	53.72
11	2.992	50.08
12	3.291	46.57
13	3.590	42.88

Data plotted in Figure 6.7

TABLE C.26		PARAMETRIC SENSITIVITY EXPERIMENT H2
Flow = 380 ml/min $[\text{Na}_2\text{SO}_3]_0 = 0.88 \text{ M}$ $[\text{H}_2\text{O}_2]_0 = 2.31 \text{ M}$ Bath = 29.0°C		
Thermocouple Number	Position (m)	Temperature °C
Inlet	-	24.25
1	0.0	25.34
1A	0.149	31.78
2	0.299	33.66
2A	0.448	35.49
3	0.598	38.93
4	0.897	45.58
5	1.196	52.33
6	1.496	57.34
7	1.795	58.19
8	2.094	57.98
9	2.393	52.20
10	2.692	49.65
11	2.992	45.82
12	3.291	42.81
13	3.590	39.80

Data plotted in Figure 6.7



TABLE C.27		PARAMETRIC SENSITIVITY EXPERIMENT H3
Flow = 380 ml/min $[\text{Na}_2\text{SO}_3]_0 = 0.88 \text{ M}$ $[\text{H}_2\text{O}_2]_0 = 2.31 \text{ M}$ Bath = 29.0°C		
Thermocouple Number	Position (m)	Temperature °C
Inlet	-	29.96
1	0.0	30.90
1A	0.149	38.70
2	0.299	41.60
2A	0.448	44.28
3	0.598	49.52
4	0.897	59.30
5	1.196	65.13
6	1.496	61.30
7	1.795	55.05
8	2.094	52.65
9	2.393	46.41
10	2.692	43.80
11	2.992	40.73
12	3.291	38.35
13	3.590	36.34

Data plotted in Figure 6.7

TABLE C.28		PARAMETRIC SENSITIVITY EXPERIMENT H4
Flow = 380 ml/min $[\text{Na}_2\text{SO}_3]_0 = 0.88 \text{ M}$ $[\text{H}_2\text{O}_2]_0 = 2.31 \text{ M}$ Bath = 29.0°C		
Thermocouple Number	Position (m)	Temperature °C
Inlet	-	11.08
1	0.0	12.59
1A	0.149	17.33
2	0.299	19.55
2A	0.448	21.39
3	0.598	24.15
4	0.897	28.97
5	1.196	33.90
6	1.496	39.10
7	1.795	45.17
8	2.094	50.11
9	2.393	52.33
10	2.692	53.52
11	2.992	53.45
12	3.291	50.59
13	3.590	46.73

Data plotted in Figure 6.7

TABLE C.29		PARAMETRIC SENSITIVITY EXPERIMENT I1
Flow = 380 ml/min $[\text{Na}_2\text{SO}_3]_0 = 0.88 \text{ M}$ $[\text{H}_2\text{O}_2]_0 = 2.31 \text{ M}$ Bath = 19.0°C		
Thermocouple Number	Position (m)	Temperature °C
Inlet	-	10.38
1	0.0	11.60
1A	0.149	14.59
2	0.299	15.59
2A	0.448	16.53
3	0.598	17.91
4	0.897	20.03
5	1.196	22.30
6	1.496	23.86
7	1.795	25.91
8	2.094	27.62
9	2.393	28.42
10	2.692	29.71
11	2.992	32.11
12	3.291	32.42
13	3.590	32.55

Data plotted in Figure 6.4

TABLE C.30		PARAMETRIC SENSITIVITY EXPERIMENT 12
Flow = 380 ml/min $[\text{Na}_2\text{SO}_3]_0 = 0.88 \text{ M}$ $[\text{H}_2\text{O}_2]_0 = 2.31 \text{ M}$ Bath = 19.0°C		
Thermocouple Number	Position (m)	Temperature °C
Inlet	-	17.42
1	0.0	18.08
1A	0.149	20.96
2	0.299	22.42
2A	0.448	22.90
3	0.598	24.32
4	0.897	26.40
5	1.196	27.86
6	1.496	29.06
7	1.795	31.08
8	2.094	32.48
9	2.393	32.72
10	2.692	33.70
11	2.992	35.14
12	3.291	34.71
13	3.590	33.89

Data plotted in Figure 6.4

TABLE C.31                      PARAMETRIC SENSITIVITY EXPERIMENT 13		
Flow = 380 ml/min $[\text{Na}_2\text{SO}_3]_0 = 0.88 \text{ M}$ $[\text{H}_2\text{O}_2]_0 = 2.31 \text{ M}$ Bath = 19.0°C		
Thermocouple Number	Position (m)	Temperature °C
Inlet	-	24.54
1	0.0	25.39
1A	0.149	27.71
2	0.299	30.51
2A	0.448	31.08
3	0.598	32.34
4	0.897	35.55
5	1.196	36.90
6	1.496	37.89
7	1.795	39.67
8	2.094	40.57
9	2.393	38.93
10	2.692	38.50
11	2.992	37.26
12	3.291	35.25
13	3.590	33.11

Data plotted in Figure 6.4

TABLE C.32		PARAMETRIC SENSITIVITY EXPERIMENT 14
Flow = 380 ml/min $[\text{Na}_2\text{SO}_3]_0 = 0.88 \text{ M}$ $[\text{H}_2\text{O}_2]_0 = 2.31 \text{ M}$ Bath = 19.0°C		
Thermocouple Number	Position (m)	Temperature °C
Inlet	-	30.74
1	0.0	31.43
1A	0.149	34.30
2	0.299	37.83
2A	0.448	38.67
3	0.598	40.67
4	0.897	44.33
5	1.196	45.43
6	1.496	44.21
7	1.795	43.81
8	2.094	43.18
9	2.393	39.15
10	2.692	37.43
11	2.992	35.07
12	3.291	32.57
13	3.590	30.44

Data plotted in Figure 6.4

TABLE C.33		PARAMETRIC SENSITIVITY EXPERIMENT 15
Flow = 380 ml/min $[\text{Na}_2\text{SO}_3]_0 = 0.88 \text{ M}$ $[\text{H}_2\text{O}_2]_0 = 2.31 \text{ M}$ Bath = 19.0°C		
Thermocouple Number	Position (m)	Temperature °C
Inlet	-	34.19
1	0.0	34.54
1A	0.149	38.57
2	0.299	42.75
2A	0.448	44.24
3	0.598	46.58
4	0.897	50.71
5	1.196	50.89
6	1.496	47.15
7	1.795	41.63
8	2.094	38.79
9	2.393	34.08
10	2.692	32.10
11	2.992	29.44
12	3.291	27.64
13	3.590	25.93

Data plotted in Figure 6.4

TABLE C.34		PARAMETRIC SENSITIVITY EXPERIMENT I6
Flow = 380 ml/min $[\text{Na}_2\text{SO}_3]_0 = 0.88 \text{ M}$ $[\text{H}_2\text{O}_2]_0 = 2.31 \text{ M}$ Bath = 19.0°C		
Thermocouple Number	Position (m)	Temperature °C
Inlet	-	40.52
1	0.0	40.82
1A	0.149	48.35
2	0.299	55.53
2A	0.448	60.49
3	0.598	65.96
4	0.897	66.73
5	1.196	57.80
6	1.496	47.15
7	1.795	41.63
8	2.094	38.79
9	2.393	34.08
10	2.692	32.10
11	2.992	29.44
12	3.291	27.64
13	3.590	25.93

Data plotted in Figure 6.4



TABLE C.35		PARAMETRIC SENSITIVITY EXPERIMENT I7
Flow = 380 ml/min $[\text{Na}_2\text{SO}_3]_0 = 0.88 \text{ M}$ $[\text{H}_2\text{O}_2]_0 = 2.31 \text{ M}$ Bath = 19.0°C		
Thermocouple Number	Position (m)	Temperature °C
Inlet	-	45.06
1	0.0	45.12
1A	0.149	56.49
2	0.299	68.67
2A	0.448	77.88
3	0.598	80.08
4	0.897	67.56
5	1.196	55.24
6	1.496	44.09
7	1.795	38.88
8	2.094	36.22
9	2.393	32.05
10	2.692	30.32
11	2.992	27.91
12	3.291	26.22
13	3.590	24.71

Data plotted in Figure 6.4

TABLE C.36		PARAMETRIC SENSITIVITY EXPERIMENT 18
Flow = 380 ml/min $[\text{Na}_2\text{SO}_3]_0 = 0.88 \text{ M}$ $[\text{H}_2\text{O}_2]_0 = 2.31 \text{ M}$ Bath = 19.0°C		
Thermocouple Number	Position (m)	Temperature °C
Inlet	-	49.08
1	0.0	50.88
1A	0.149	66.71
2	0.299	87.26
2A	0.448	93.76
3	0.598	84.02
4	0.897	68.89
5	1.196	54.18
6	1.496	43.43
7	1.795	38.00
8	2.094	35.82
9	2.393	31.38
10	2.692	29.46
11	2.992	27.41
12	3.291	25.81
13	3.590	24.27

Data plotted in Figure 6.4

TABLE C.37		PARAMETRIC SENSITIVITY EXPERIMENT J1
Flow = 380 ml/min $[\text{Na}_2\text{SO}_3]_0 = 0.88 \text{ M}$ $[\text{H}_2\text{O}_2]_0 = 2.31 \text{ M}$ Bath = 49.0°C		
Thermocouple Number	Position (m)	Temperature °C
Inlet	-	12.33
1	0.0	16.75
1A	0.14°	24.28
2	0.29°	30.05
2A	0.448	33.76
3	0.598	40.87
4	0.897	58.49
5	1.196	80.26
6	1.496	79.09
7	1.795	71.41
8	2.094	67.69
9	2.393	62.19
10	2.692	59.30
11	2.992	56.72
12	3.291	54.85
13	3.590	53.18

Data plotted in Figure 6.8

TABLE C.38		PARAMETRIC SENSITIVITY EXPERIMENT J2
Flow = 380 ml/min $[\text{Na}_2\text{SO}_3]_0 = 0.88 \text{ M}$ $[\text{H}_2\text{O}_2]_0 = 2.31 \text{ M}$ Bath = 49.0°C		
Thermocouple Number	Position (m)	Temperature °C
Inlet	-	18.19
1	0.0	20.14
1A	0.149	30.08
2	0.299	36.47
2A	0.448	41.26
3	0.598	51.00
4	0.897	77.63
5	1.196	82.22
6	1.496	72.54
7	1.795	66.26
8	2.094	64.15
9	2.393	59.76
10	2.692	57.62
11	2.992	55.17
12	3.291	53.53
13	3.590	52.46

Data plotted in Figure 6.8

TABLE C.39		PARAMETRIC SENSITIVITY EXPERIMENT J3
Flow = 380 ml/min $[\text{Na}_2\text{SO}_3]_0 = 0.88 \text{ M}$ $[\text{H}_2\text{O}_2]_0 = 2.31 \text{ M}$ Bath = 49.0°C		
Thermocouple Number	Position (m)	Temperature °C
Inlet	-	25.35
1	0.0	27.76
1A	0.149	37.07
2	0.299	44.79
2A	0.448	50.54
3	0.598	63.83
4	0.897	87.32
5	1.196	79.20
6	1.496	69.97
7	1.795	64.41
8	2.094	61.97
9	2.393	58.19
10	2.692	56.64
11	2.992	54.67
12	3.291	53.40
13	3.590	52.33

Data plotted in Figure 6.8

TABLE C. 40		PARAMETRIC SENSITIVITY EXPERIMENT J4
Flow = 380 ml/min $[\text{Na}_2\text{SO}_3]_c = 0.88 \text{ M}$ $[\text{H}_2\text{O}_2]_0 = 2.31 \text{ M}$ Bath = 49.0°C		
Thermocouple Number	Position (m)	Temperature °C
Inlet	-	30.59
1	0.0	33.37
1A	0.149	44.63
2	0.299	54.07
2A	0.448	63.45
3	0.598	81.89
4	0.897	86.70
5	1.196	75.57
6	1.496	67.35
7	1.795	62.43
8	2.094	60.57
9	2.393	57.15
10	2.692	55.82
11	2.992	53.59
12	3.291	52.91
13	3.590	51.95

Data plotted in Figure 6.8

TABLE C. 41		PARAMETRIC SENSITIVITY EXPERIMENT K1
Flow = 380 ml/min $[\text{Na}_2\text{SO}_3]_0 = 0.78 \text{ M}$ $[\text{H}_2\text{O}_2]_0 = 2.31 \text{ M}$ Bath = 24.0°C		
Thermocouple Number	Position (m)	Temperature °C
Inlet	-	48.40
1	0.0	50.89
1A	0.149	65.16
2	0.299	82.33
2A	0.448	86.68
3	0.598	79.14
4	0.897	63.71
5	1.196	52.71
6	1.496	43.94
7	1.795	39.18
8	2.094	37.27
9	2.393	33.96
10	2.692	32.65
11	2.992	30.82
12	3.291	29.35
13	3.590	28.31

Data plotted in Figure 6.12

TABLE C.42		PARAMETRIC SENSITIVITY EXPERIMENT K2
Flow = 380 ml/min $[\text{Na}_2\text{SO}_3]_0 = 0.78 \text{ M}$ $[\text{H}_2\text{O}_2]_0 = 2.31 \text{ M}$ Bath = $34.0^\circ\text{C}$		
Thermocouple Number	Position (m)	Temperature $^\circ\text{C}$
Inlet	-	46.00
1	0.0	48.89
1A	0.149	63.20
2	0.299	79.38
2A	0.448	88.85
3	0.598	84.84
4	0.897	70.76
5	1.196	60.63
6	1.496	52.81
7	1.795	48.11
8	2.094	46.41
9	2.393	42.06
10	2.692	41.82
11	2.992	40.02
12	3.291	38.89
13	3.590	37.90

Data plotted in Figure 6.14



TABLE C. 43		PARAMETRIC SENSITIVITY EXPERIMENT K3
Flow = 380 ml/min $[\text{Na}_2\text{SO}_3]_0 = 0.78 \text{ M}$ $[\text{H}_2\text{O}_2]_0 = 2.31 \text{ M}$ Bath = 44.0°C		
Thermocouple Number	Position (m)	Temperature °C
Inlet	-	39.08
1	0.0	42.42
1A	0.149	54.14
2	0.299	66.62
2A	0.448	78.30
3	0.598	87.38
4	0.897	78.31
5	1.196	68.29
6	1.496	61.00
7	1.795	56.32
8	2.094	54.77
9	2.393	51.71
10	2.692	50.56
11	2.992	48.94
12	3.291	47.83
13	3.590	46.97

Data plotted in Fig 6.13

TABLE C. 44		PARAMETRIC SENSITIVITY EXPERIMENT L1
Flow = 380 ml/min $[\text{Na}_2\text{SO}_3]_0 = 0.68 \text{ M}$ $[\text{H}_2\text{O}_2]_0 = 2.31 \text{ M}$ Bath = 24.0°C		
Thermocouple Number	Position (m)	Temperature °C
Inlet	-	47.90
1	0.0	48.91
1A	0.149	57.81
2	0.299	64.69
2A	0.448	68.46
3	0.598	69.22
4	0.897	61.73
5	1.196	52.83
6	1.496	45.05
7	1.795	40.38
8	2.094	38.59
9	2.393	35.12
10	2.692	33.75
11	2.992	31.78
12	3.291	30.57
13	3.590	29.15

Data plotted in Figure 6.12

TABLE C.45		PARAMETRIC SENSITIVITY EXPERIMENT L2
Flow = 380 ml/min $[\text{Na}_2\text{SO}_3]_0 = 0.68 \text{ M}$ $[\text{H}_2\text{O}_2]_0 = 2.31 \text{ M}$ Bath = $34.0^\circ\text{C}$		
Thermocouple Number	Position (m)	Temperature $^\circ\text{C}$
Inlet	-	45.76
1	0.0	47.82
1A	0.149	57.67
2	0.299	66.73
2A	0.448	72.72
3	0.598	75.62
4	0.897	68.51
5	1.196	59.85
6	1.496	52.07
7	1.795	47.69
8	2.094	45.90
9	2.393	42.80
10	2.692	41.35
11	2.992	39.76
12	3.291	38.48
13	3.590	37.52

Data plotted in Figure 6.14

TABLE C. 46		PARAMETRIC SENSITIVITY EXPERIMENT L3
Flow = 380 ml/min $[\text{Na}_2\text{SO}_3]_0 = 0.68 \text{ M}$ $[\text{H}_2\text{O}_2]_0 = 2.31 \text{ M}$ Bath = 44.0°C		
Thermocouple Number	Position (m)	Temperature °C
Inlet	-	39.52
1	0.0	44.01
1A	0.149	51.59
2	0.299	60.44
2A	0.448	67.16
3	0.598	75.52
4	0.897	74.61
5	1.196	67.19
6	1.496	60.35
7	1.795	56.09
8	2.094	54.34
9	2.393	51.62
10	2.692	50.46
11	2.992	48.85
12	3.291	47.74
13	3.590	46.84

Data plotted in Figure 6.14

TABLE C. 47		PARAMETRIC SENSITIVITY EXPERIMENT M1
Flow = 380 ml/min $[\text{Na}_2\text{SO}_3]_0 = 0.58 \text{ M}$ $[\text{H}_2\text{O}_2]_0 = 2.31 \text{ M}$ Bath = 24.0°C		
Thermocouple Number	Position (m)	Temperature °C
Inlet	-	48.08
1	0.0	48.73
1A	0.149	54.06
2	0.299	58.14
2A	0.448	59.53
3	0.598	59.75
4	0.897	55.61
5	1.196	50.05
6	1.496	43.46
7	1.795	39.86
8	2.094	38.43
9	2.393	35.17
10	2.692	33.94
11	2.992	32.18
12	3.291	31.04
13	3.590	29.69

Data plotted in Figure 6.12

TABLE C.48		PARAMETRIC SENSITIVITY EXPERIMENT M2
Flow = 380 ml/min $[\text{Na}_2\text{SO}_3]_0 = 0.58 \text{ M}$ $[\text{H}_2\text{O}_2]_0 = 2.31 \text{ M}$ Bath = $34.0^\circ\text{C}$		
Thermocouple Number	Position (m)	Temperature $^\circ\text{C}$
Inlet	-	46.27
1	0.0	48.13
1A	0.149	55.09
2	0.299	61.29
2A	0.448	64.59
3	0.598	66.83
4	0.897	63.80
5	1.196	57.46
6	1.496	51.54
7	1.795	47.69
8	2.094	46.27
9	2.393	43.19
10	2.692	42.00
11	2.992	40.34
12	3.291	39.22
13	3.590	38.15

Data plotted in Figure 6.14

TABLE C.49		PARAMETRIC SENSITIVITY EXPERIMENT M3
Flow = 380 ml/min $[\text{Na}_2\text{SO}_3]_0 = 0.58 \text{ M}$ $[\text{H}_2\text{O}_2]_0 = 2.31 \text{ M}$ Bath = 44.0°C		
Thermocouple Number	Position (m)	Temperature °C
Inlet	-	39.44
1	0.0	41.00
1A	0.149	48.71
2	0.299	54.51
2A	0.448	58.68
3	0.598	64.34
4	0.897	68.59
5	1.196	66.07
6	1.496	60.97
7	1.795	57.03
8	2.094	55.48
9	2.393	52.53
10	2.692	51.32
11	2.992	49.68
12	3.291	48.42
13	3.590	47.56

Data plotted in Figure 6.13

TABLE C.50      PARAMETRIC SENSITIVITY EXPERIMENT N1		
Flow = 380 ml/min $[\text{Na}_2\text{SO}_3]_0 = 0.48 \text{ M}$ $[\text{H}_2\text{O}_2]_0 = 2.31 \text{ M}$ Bath = $24.0^\circ\text{C}$		
Thermocouple Number	Position (m)	Temperature $^\circ\text{C}$
Inlet	-	47.93
1	0.0	48.18
1A	0.149	51.91
2	0.299	53.82
2A	0.448	54.13
3	0.598	53.82
4	0.897	50.36
5	1.196	45.92
6	1.496	41.13
7	1.795	38.46
8	2.094	37.18
9	2.393	34.57
10	2.692	33.55
11	2.992	32.00
12	3.291	30.86
13	3.590	29.62

Data plotted in Figure 6.12



TABLE C.51		PARAMETRIC SENSITIVITY EXPERIMENT N2
Flow = 380 ml/min $[\text{Na}_2\text{SO}_3]_0 = 0.48 \text{ M}$ $[\text{H}_2\text{O}_2]_0 = 2.31 \text{ M}$ Bath = 34.0°C		
Thermocouple Number	Position (m)	Temperature °C
Inlet	-	45.78
1	0.0	47.02
1A	0.149	52.23
2	0.299	55.67
2A	0.448	57.41
3	0.598	58.90
4	0.897	57.85
5	1.196	54.25
6	1.496	49.87
7	1.795	47.18
8	2.094	45.90
9	2.393	43.17
10	2.692	42.13
11	2.992	40.64
12	3.291	39.46
13	3.590	38.40

Data plotted in Figure 6.14

TABLE C.52		PARAMETRIC SENSITIVITY EXPERIMENT N3
Flow = 380 ml/min $[\text{Na}_2\text{SO}_3]_0 = 0.48 \text{ M}$ $[\text{H}_2\text{O}_2]_0 = 2.31 \text{ M}$ Bath = 44.0°C		
Thermocouple Number	Position (m)	Temperature °C
Inlet	-	39.81
1	0.0	40.78
1A	0.149	47.51
2	0.299	51.99
2A	0.448	54.72
3	0.598	58.62
4	0.897	62.41
5	1.196	61.46
6	1.496	58.40
7	1.795	55.81
8	2.094	54.52
9	2.393	51.94
10	2.692	50.85
11	2.992	49.41
12	3.291	48.32
13	3.590	47.35

Data plotted in Figure 6.13

TABLE C.53		PARAMETRIC SENSITIVITY EXPERIMENT Q2
Flow = 380 ml/min $[\text{Na}_2\text{SO}_3]_0 = 0.88 \text{ M}$ $[\text{H}_2\text{O}_2]_0 = 2.31 \text{ M}$ Bath = $24.0^\circ\text{C}$		
Thermocouple Number	Position (m)	Temperature $^\circ\text{C}$
Inlet	-	18.45
1	0.0	19.36
2	0.299	25.68
3	0.598	29.35
4	0.897	35.22
5	1.196	39.96
6	1.496	47.41
7	1.795	56.12
8	2.094	61.64
9	2.393	61.14
10	2.692	58.89
11	2.992	54.02
12	3.291	49.98
13	3.590	46.17

Stirrer Speed #0

Data plotted in Figure 6.15

TABLE C.54		PARAMETRIC SENSITIVITY EXPERIMENT Q3
Flow = 380 ml/min $[\text{Na}_2\text{SO}_3]_0 = 0.88 \text{ M}$ $[\text{H}_2\text{O}_2]_0 = 2.31 \text{ M}$ Bath = $24.0^\circ\text{C}$		
Thermocouple Number	Position (m)	Temperature $^\circ\text{C}$
Inlet	-	18.21
1	0.0	19.41
2	0.299	25.15
3	0.598	28.51
4	0.897	32.19
5	1.196	35.44
6	1.496	38.29
7	1.795	41.56
8	2.094	43.76
9	2.393	43.79
10	2.692	44.27
11	2.992	43.88
12	3.291	41.47
13	3.590	39.10

Stirrer Speed #10

Data plotted in Figure 6.15

TABLE C.55		PARAMETRIC SENSITIVITY EXPERIMENT Q2A
Flow = 380 ml/min $[\text{Na}_2\text{SO}_3]_0 = 0.88 \text{ M}$ $[\text{H}_2\text{O}_2]_0 = 2.31 \text{ M}$ Bath = 24.0°C		
Thermocouple Number	Position (m)	Temperature °C
Inlet	-	18.58
1	0.0	19.67
1A	0.149	22.97
2	0.299	25.81
2A	0.448	26.89
3	0.598	29.20
4	0.897	34.01
5	1.196	37.47
6	1.496	41.40
7	1.795	46.00
8	2.094	49.73
9	2.393	49.52
10	2.692	49.25
11	2.992	47.69
12	3.291	44.63
13	3.590	41.11

Stirrer Speed #3

Data plotted in Figure 6.15

TABLE C.56		PARAMETRIC SENSITIVITY EXPERIMENT R2
Flow = 380 ml/min $[\text{Na}_2\text{SO}_3]_0 = 0.88 \text{ M}$ $[\text{H}_2\text{O}_2]_0 = 2.31 \text{ M}$ Bath = 24.0°C		
Thermocouple Number	Position (m)	Temperature °C
Inlet	-	33.80
1	0.0	34.76
2	0.299	48.67
3	0.598	64.96
4	0.897	81.95
5	1.196	74.77
6	1.496	64.69
7	1.795	57.47
8	2.094	54.32
9	2.393	49.06
10	2.692	46.48
11	2.992	43.12
12	3.291	40.66
13	3.590	38.31

Stirrer Speed #0

Data plotted in Figure 6.16

TABLE C.57		PARAMETRIC SENSITIVITY EXPERIMENT R3
Flow = 380 ml/min $[\text{Na}_2\text{SO}_3]_0 = 0.88 \text{ M}$ $[\text{H}_2\text{O}_2]_0 = 2.31 \text{ M}$ Bath = 24.0°C		
Thermocouple Number	Position (m)	Temperature °C
Inlet	-	33.12
1	0.0	33.86
2	0.299	44.31
3	0.598	51.75
4	0.897	59.97
5	1.196	61.12
6	1.496	55.33
7	1.795	49.58
8	2.094	46.76
9	2.393	41.48
10	2.692	39.06
11	2.992	36.39
12	3.291	33.96
13	3.590	32.14

Stirrer Speed #10

Data plotted in Figure 6.16

TABLE C.58		PARAMETRIC SENSITIVITY EXPERIMENT R2A
Flow = 380 ml/min $[\text{Na}_2\text{SO}_3]_0 = 0.88 \text{ M}$ $[\text{H}_2\text{O}_2]_0 = 2.31 \text{ M}$ Bath = 24.0°C		
Thermocouple Number	Position (m)	Temperature °C
Inlet	-	33.38
1	0.0	34.16
1A	0.149	40.15
2	0.299	44.81
2A	0.448	47.60
3	0.598	53.65
4	0.897	64.78
5	1.196	67.81
6	1.496	59.23
7	1.795	52.67
8	2.094	49.44
9	2.393	43.60
10	2.692	40.70
11	2.992	37.35
12	3.291	35.14
13	3.590	33.09

Stirrer Speed #3

Data plotted in Figure 6.16



TABLE C.59		PARAMETRIC SENSITIVITY EXPERIMENT S2
Flow = 380 ml/min $[\text{Na}_2\text{SO}_3]_0 = 0.88 \text{ M}$ $[\text{H}_2\text{O}_2]_0 = 2.31 \text{ M}$ Bath = $34.0^\circ\text{C}$		
Thermocouple Number	Position (m)	Temperature $^\circ\text{C}$
Inlet	-	45.76
1	0.0	50.81
1A	0.149	74.53
2	0.299	104.71
2A	0.448	102.38
3	0.598	94.45
4	0.897	82.48
5	1.196	72.65
6	1.496	63.07
7	1.795	57.43
8	2.094	55.22
9	2.393	50.76
10	2.692	48.82
11	2.992	46.31
12	3.291	44.70
13	3.590	42.84

Stirrer Speed #0

Data plotted in Figure 6.17

TABLE C.60		PARAMETRIC SENSITIVITY EXPERIMENT S4
Flow = 380 ml/min $[\text{Na}_2\text{SO}_3]_0 = 0.88 \text{ M}$ $[\text{H}_2\text{O}_2]_0 = 2.31 \text{ M}$ Bath = $34.0^\circ\text{C}$		
Thermocouple Number	Position (m)	Temperature $^\circ\text{C}$
Inlet	-	44.80
1	0.0	47.97
1A	0.149	65.09
2	0.299	83.91
2A	0.448	96.46
3	0.598	89.48
4	0.897	73.17
5	1.196	62.48
6	1.496	52.98
7	1.795	48.16
8	2.094	45.96
9	2.393	42.78
10	2.692	41.40
11	2.992	39.78
12	3.291	38.53
13	3.590	37.63

Stirrer Speed #10

Data plotted in Figure 6.17

### C) Transient Data

The transient temperature profiles for Parametric Sensitivity  
Experiment E2 -

TABLE C.61A		PARAMETRIC SENSITIVITY EXPERIMENT Q1
Flow = 380 ml/min $[\text{Na}_2\text{SO}_3]_0 = 0.88 \text{ M}$ $[\text{H}_2\text{O}_2]_0 = 2.31 \text{ M}$ Bath = $24.0^\circ\text{C}$		
Thermocouple Number	Position (m)	Temperature $^\circ\text{C}$
Inlet	-	19.06
1	0.0	19.13
2	0.299	20.22
3	0.598	20.72
4	0.897	21.79
5	1.196	22.90
6	1.496	22.80
7	1.795	23.49
8	2.094	23.41
9	2.393	24.11
10	2.692	23.80
11	2.992	23.29
12	3.291	23.10
13	3.590	23.50

Time = 0 sec

Data plotted in Figure 6.1

TABLE C.61B		PARAMETRIC SENSITIVITY EXPERIMENT Q1
Flow = 380 ml/min $[\text{Na}_2\text{SO}_3]_0 = 0.88 \text{ M}$ $[\text{H}_2\text{O}_2]_0 = 2.31 \text{ M}$ Bath = 24.0°C		
Thermocouple Number	Position (m)	Temperature °C
Inlet	-	19.06
1	0.0	20.25
2	0.299	25.63
3	0.598	27.86
4	0.897	25.71
5	1.196	23.50
6	1.496	22.91
7	1.795	23.80
8	2.094	23.39
9	2.393	24.13
10	2.692	23.76
11	2.992	23.39
12	3.291	23.02
13	3.590	23.58

Time = 1 sec

Data plotted in Figure 6.1

TABLE C.61C		PARAMETRIC SENSITIVITY EXPERIMENT Q1
Flow = 380 ml/min $[\text{Na}_2\text{SO}_3]_0 = 0.88 \text{ M}$ $[\text{H}_2\text{O}_2]_0 = 2.31 \text{ M}$ Bath = 24.0°C		
Thermocouple Number	Position (m)	Temperature °C
Inlet	-	19.06
1	0.0	20.06
2	0.299	26.93
3	0.598	30.28
4	0.897	34.99
5	1.196	37.73
6	1.496	39.70
7	1.795	41.49
8	2.094	42.35
9	2.393	37.84
10	2.692	36.18
11	2.992	34.00
12	3.291	31.46
13	3.590	29.35

Time = 3 sec

Data plotted in Figure 6.1

TABLE C.61D		PARAMETRIC SENSITIVITY EXPERIMENT Q1
Flow = 380 ml/min $[\text{Na}_2\text{SO}_3]_0 = 0.88 \text{ M}$ $[\text{H}_2\text{O}_2]_0 = 2.31 \text{ M}$ Bath = $24.0^\circ\text{C}$		
Thermocouple Number	Position (m)	Temperature $^\circ\text{C}$
Inlet	-	19.06
1	0.0	20.25
2	0.299	27.12
3	0.598	30.91
4	0.897	35.71
5	1.196	39.18
6	1.496	42.06
7	1.795	45.30
8	2.094	47.43
9	2.393	44.50
10	2.692	42.35
11	2.992	39.98
12	3.291	36.90
13	3.590	33.82

Time = 4 sec

Data plotted in Figure 6.1

TABLE C.61E		PARAMETRIC SENSITIVITY EXPERIMENT Q1
Flow = 380 ml/min $[\text{Na}_2\text{SO}_3]_0 = 0.88 \text{ M}$ $[\text{H}_2\text{O}_2]_0 = 2.31 \text{ M}$ Bath = 24.0°C		
Thermocouple Number	Position (m)	Temperature °C
Inlet	-	19.06
1	0.0	20.25
2	0.299	27.12
3	0.598	30.73
4	0.897	35.71
5	1.196	39.18
6	1.496	43.14
7	1.795	46.57
8	2.094	48.33
9	2.393	46.00
10	2.692	44.34
11	2.992	41.43
12	3.291	38.35
13	3.590	35.81

Time = 5 sec

Data plotted in Figure 6.1

TABLE C.61F                      PARAMETRIC SENSITIVITY EXPERIMENT Q1		
Flow = 380 ml/min $[\text{Na}_2\text{SO}_3]_0 = 0.88 \text{ M}$ $[\text{H}_2\text{O}_2]_0 = 2.31 \text{ M}$ Bath = 24.0°C		
Thermocouple Number	Position (m)	Temperature °C
Inlet	-	19.06
1	0.0	20.25
2	0.299	26.93
3	0.598	30.55
4	0.897	35.53
5	1.196	38.81
6	1.496	42.24
7	1.795	46.02
8	2.094	47.97
9	2.393	46.00
10	2.692	44.16
11	2.992	42.16
12	3.291	39.08
13	3.590	36.36

Time = 7 sec

Data plotted in Figure 6.1



TABLE C.61G		PARAMETRIC SENSITIVITY EXPERIMENT Q1
Flow = 380 ml/min $[\text{Na}_2\text{SO}_3]_0 = 0.88 \text{ M}$ $[\text{H}_2\text{O}_2]_0 = 2.31 \text{ M}$ Bath = 24.0°C		
Thermocouple Number	Position (m)	Temperature °C
Inlet	-	19.06
1	0.0	20.25
2	0.299	26.93
3	0.598	30.55
4	0.897	35.71
5	1.196	38.81
6	1.496	42.96
7	1.795	46.93
8	2.094	48.88
9	2.393	46.72
10	2.692	45.25
11	2.992	42.70
12	3.291	39.44
13	3.590	36.90

Time = 8 sec

Data plotted in Figure 6.1

TABLE C. 61H		PARAMETRIC SENSITIVITY EXPERIMENT Q1
Flow = 380 ml/min $[\text{Na}_2\text{SO}_3]_0 = 0.88 \text{ M}$ $[\text{H}_2\text{O}_2]_0 = 2.31 \text{ M}$ Bath = $24.0^\circ\text{C}$		
Thermocouple Number	Position (m)	Temperature $^\circ\text{C}$
Inlet	-	19.06
1	0.0	20.06
2	0.299	26.93
3	0.598	30.55
4	0.897	35.53
5	1.196	39.00
6	1.496	43.14
7	1.795	46.93
8	2.094	49.06
9	2.393	47.27
10	2.692	45.43
11	2.992	42.88
12	3.291	39.80
13	3.590	36.90

Time = 10 sec

Data plotted in Figure 6.1

TABLE C.61I		PARAMETRIC SENSITIVITY EXPERIMENT Q1
Flow = 380 ml/min $[\text{Na}_2\text{SO}_3]_0 = 0.88 \text{ M}$ $[\text{H}_2\text{O}_2]_0 = 2.31 \text{ M}$ Bath = $24.0^\circ\text{C}$		
Thermocouple Number	Position (m)	Temperature $^\circ\text{C}$
Inlet	-	19.06
1	0.0	20.06
2	0.299	27.12
3	0.598	30.55
4	0.897	35.53
5	1.196	39.00
6	1.496	43.14
7	1.795	47.11
8	2.094	49.06
9	2.393	47.63
10	2.692	45.79
11	2.992	42.88
12	3.291	39.62
13	3.590	37.08

Time = 11 sec

Data plotted in Figure 6.1

TABLE C.61J      PARAMETRIC SENSITIVITY EXPERIMENT Q1		
Flow = 380 ml/min $[\text{Na}_2\text{SO}_3]_0 = 0.88 \text{ M}$ $[\text{H}_2\text{O}_2]_0 = 2.31 \text{ M}$ Bath = $24.0^\circ\text{C}$		
Thermocouple Number	Position (m)	Temperature $^\circ\text{C}$
Inlet	-	19.06
1	0.0	20.06
2	0.299	26.93
3	0.598	30.55
4	0.897	35.53
5	1.196	38.81
6	1.496	42.96
7	1.795	47.47
8	2.094	49.78
9	2.393	48.17
10	2.692	46.16
11	2.992	43.25
12	3.291	39.80
13	3.590	37.08

Time = 13 sec

Data plotted in Figure 6.1

TABLE C.61K		PARAMETRIC SENSITIVITY EXPERIMENT Q1
Flow = 380 ml/min $[\text{Na}_2\text{SO}_3]_0 = 0.88 \text{ M}$ $[\text{H}_2\text{O}_2]_0 = 2.31 \text{ M}$ Bath = 24.0°C		
Thermocouple Number	Position (m)	Temperature °C
Inlet	-	19.06
1	0.0	20.06
2	0.299	26.93
3	0.598	30.55
4	0.897	35.35
5	1.196	38.45
6	1.496	42.24
7	1.795	46.57
8	2.094	48.69
9	2.393	47.27
10	2.692	45.43
11	2.992	43.43
12	3.291	39.98
13	3.590	37.26

Time = 14 sec

Data plotted in Figure 6.1

TABLE C.61L		PARAMETRIC SENSITIVITY EXPERIMENT Q1
Flow = 380 ml/min $[\text{Na}_2\text{SO}_3]_0 = 0.88 \text{ M}$ $[\text{H}_2\text{O}_2]_0 = 2.31 \text{ M}$ Bath = 24.0°C		
Thermocouple Number	Position (m)	Temperature °C
Inlet	-	19.06
1	0.0	20.06
2	0.299	26.75
3	0.598	30.55
4	0.897	35.53
5	1.196	38.63
6	1.496	42.24
7	1.795	46.57
8	2.094	48.69
9	2.393	47.27
10	2.692	45.97
11	2.992	43.25
12	3.291	40.16
13	3.590	37.44

Time = 16 sec

Data plotted in Figure 6.1

TABLE C.61M		PARAMETRIC SENSITIVITY EXPERIMENT Q1
Flow = 380 ml/min $[\text{Na}_2\text{SO}_3]_0 = 0.88 \text{ M}$ $[\text{H}_2\text{O}_2]_0 = 2.31 \text{ M}$ Bath = 24.0°C		
Thermocouple Number	Position (m)	Temperature °C
Inlet	-	19.06
1	0.0	19.88
2	0.299	26.93
3	0.598	30.55
4	0.897	35.89
5	1.196	39.18
6	1.496	43.33
7	1.795	47.47
8	2.094	49.42
9	2.393	47.45
10	2.692	45.79
11	2.992	43.06
12	3.291	40.16
13	3.590	37.44

Time = 17 sec

Data plotted in Figure 6.1

TABLE C.61N		PARAMETRIC SENSITIVITY EXPERIMENT Q1
Flow = 380 ml/min $[\text{Na}_2\text{SO}_3]_0 = 0.88 \text{ M}$ $[\text{H}_2\text{O}_2]_0 = 2.31 \text{ M}$ Bath = 24.0°C		
Thermocouple Number	Position (m)	Temperature °C
Inl	-	19.06
1	0.0	20.06
2	0.299	26.75
3	0.598	30.28
4	0.897	35.53
5	1.196	39.00
6	1.496	43.14
7	1.795	47.29
8	2.094	49.06
9	2.393	47.45
10	2.692	45.79
11	2.992	43.06
12	3.291	39.80
13	3.590	37.26

Time = 19 sec

Data plotted in Figure 6.1



## APPENDIX D

### 1) ODPH Model - Computer Program

The ODPH model for the case of no reaction is given by equation 5.1. Ordinarily, this equation can be solved analytically. However, in this instance, in order to account for the change in reactor characteristics at the tubing tees, a different procedure was used.

A standard 4th order Runge-Kutta routine was employed, with the integration broken into segments. Each segment was characterized by the value of the overall heat transfer coefficient for that particular segment. This value of  $U$  was dependent upon the position in the reactor as it was a function of the internal and external diameter of the tubing. The different segments of the reactor are listed in Table D.1. As is evident from the table, there were only three different types of segment. Thus, only 3 different values of  $U$  had to be calculated.

The computer program developed is given at the end of this section. In the program, the inlet conditions, as well as the value for the outside (i.e., the bath side) heat transfer coefficient were initially obtained. Then, the three different values of  $U$  were determined, using the reactor dimensions given in Table D.1 and the outside heat transfer coefficient. Following this, the differential equation was

TABLE D.1				
Reactor Segments for Integration using the ODPH Model				
Segment	Type	Reactor Position	Inner Diameter	Outer Diameter
1	A	0.00 - 0.0096 m	0.00223 m	0.00711 m
2	B	0.0096 - 0.0216 m	0.00175 m	0.0111 m
3	C	0.0216 - 0.2776 m	0.00175 m	0.00318 m
4	B	0.2776 - 0.2896 m	0.00175 m	0.0111 m
5	A	0.2896 - 0.2992 m	0.00223 m	0.00711 m

Segments #1 thru #5 represent one complete section of tubing. The remaining eleven sections each consist of these 5 segments in the order given above (i.e., 0.0096 m of type A, followed by 0.012 m of type B, 0.256 m of type C, etc. ). The total length of the reactor is 3.59 m.

integrated from  $z=0$  to the end of the reactor, with the appropriate value of  $U$  being used for each section.

It is important to note that the value of  $U$  determined here was based on the inside area (i.e.,  $U_i$ ). The correlation used for determining the value of the inside heat transfer coefficient was:

$$Nu = 0.116 \cdot (Re^{2/3} - 125) \cdot Pr^{1/3} \quad (D.1)$$

This correlation was valid for the turbulent transition region (i.e.,  $2100 < Re < 10\,000$ ).

It should be noted that the computer program was written so as to

simplify the extraction of  $h_o$  from  $U$  (eq 5.6 or 5.7). This was done by specifying  $h_o$  as an input parameter. From this value of  $h_o$ , a value for  $U_i$  was determined (using 5.6) and used in the simulation. Thus, every simulated temperature profile had a characteristic  $U_i$  associated with it that was already based on a  $h_o$  value. Thus, when the optimal  $U_i$  value was found, the optimal  $h_o$  was automatically known as well.

The second computer program attached at the end of this section was used for the actual comparison with the experimental data. It differs in the fact that experimental data is required input. This data is displayed, along with the value of the sum of the squares of the temperature differences.

```

C      PROGRAM SULFITE2
C      SIMULATES ODPH MODEL FOR A TUBULAR REACTOR
C      PROGRAM TAKES INTO ACCOUNT CHANGES IN HEAT TRANSFER
C      AT THE TEES
C      DEFINE VARIABLES
C
      REAL K1,K2,K3,K4,L1,L2,L3,L4,TW,PI,CB,DH,HO,QR,UAVG
      REAL CAO,CBO,T,CA,Q,D,PT,V,CP,RO,A,EA,R,MU,KF,KS,Z,DZ
      INTEGER I,J,RP
      REAL DIA,DOA,DIB,DOB,DIC,DOC,UA,UB,UC,REA,REB,REC
      PI = 3.14159
C      SET PHYSICAL CONSTANTS
C
      DIA = 0.00223
      DOA = 0.00711
      DIB = 0.00175
      DOB = 0.0111
      DIC = 0.00175
      DOC = 0.003175
      CP = 4180
      RO = 1000
      MU = 0.001
      KF = 0.637
      R = 8.314
      KS = 16.27
      DH = 372230
      A = 3.56*10**7.0
      EA = 64268
C      INPUT OUTSIDE HEAT TRANSFER COEFFICIENT AND FLOWRATE
C
      WRITE(6,*) 'INPUT OUTSIDE HEAT TRANSFER COEFFICIENT'
      READ(5,*) QR
      WRITE(6,*) 'H OUTSIDE = ',QR
      WRITE(6,*) 'INPUT FLOWRATE'
      READ(5,*) Q
      WRITE(6,*) 'FLOWRATE = ',Q*60000,' L/MIN'
C      CALCULATE OVERALL HEAT TRANSFER COEFFICIENT FOR EACH SEGMENT TYPE
C
      D = DIA
      PT = (DOA-DIA)/2.0
      WRITE(6,*) '***** FOR SECTION A *****'
      U = HEAT(Q,RO,D,MU,CP,KF,KS,PT,QR)
      UA = U
      D = DIB
      PT = DOB-DIB
      PT = PT/2.0
      WRITE(6,*) '***** FOR SECTION B *****'
      U = HEAT(Q,RO,D,MU,CP,KF,KS,PT,QR)

```

```

UB = U
D = DIC
PT = DOC-DIC
PT = PT/2.0
WRITE(6,*) '***** FOR SECTION C *****'
U = HEAT(Q,RO,D,MU,CP,KF,KS,PT,QR)
UC = U
WRITE(6,*) 'UA = ',UA,' UB = ',UB,' UC = ',UC
UAVG=(0.0192*0.00223*UA)+(0.256*0.00175*UC)+(0.024*0.00175*UB)
UAVG = 12*UAVG/0.00639
WRITE(6,*) 'U AVG = ', UAVG

C
C   INPUT INTIAL CONDITIONS
C
222   CONTINUE
      WRITE(6,*) 'INPUT INITIAL CONCENTRATIONS CAO & CBO'
      READ(5,*) CAO,CBO
      WRITE(6,300) CAO/1000.,CBO/1000.
300   FORMAT(1X,'CAO = ',F5.2,' CBO = ',F5.2)
      CA = CAO
      WRITE(6,*) 'INPUT INITIAL TEMPERATURE'
      READ(5,*) T
      WRITE(6,*) 'INITIAL TEMPERATURE = ',T
      WRITE(6,*) 'INPUT BATH TEMPERATURE'
      READ(5,*) TW
      WRITE(6,*) 'BATH TEMPERATURE = ',TW

C
C   PRINT HEADER
C
      WRITE(6,*) '      Z              T              C'
      Z = 0
      CB = CBO
      WRITE(6,100) Z,T-273,CA

C
C   PERFORM INTEGRATION
C
      DO 10 I=1,12
      WRITE(6,*) '*****'
      DO 20 J=1,12

C
C   DETERMINE REGION AND SET U,D,DZ VALUES ACCORDINGLY
C
      IF(J.EQ.1) THEN
        U = UA
        D = DIA
        DZ = 0.0096
      ELSE
        IF(J.EQ.2) THEN

```

```

U = UB
D = DIB
DZ = 0.012
ELSE
IF(J.EQ.11) THEN
U = UB
D = DIB
DZ = 0.012
ELSE
IF(J.EQ.12) THEN
U = UA
D = DIA
DZ = 0.0096
ELSE
U = UC
D = DIC
DZ = 0.032
END IF
END IF
END IF
END IF
K1 = DZ*DTZ(T, CA, CB, D, A, EA, R, CP, RO, Q, TW, DH, U)
L1 = DZ*DCZ(T, CA, CB, D, A, EA, R, CP, RO, Q, TW, DH)
K2 = DZ*DTZ(T+K1/2.0, CA+L1/2.0, CB, D, A, EA, R, CP, RO, Q, TW, DH, U)
L2 = DZ*DCZ(T+K1/2.0, CA+L1/2.0, CB, D, A, EA, R, CP, RO, Q, TW, DH)
K3 = DZ*DTZ(T+K2/2.0, CA+L2/2.0, CB, D, A, EA, R, CP, RO, Q, TW, DH, U)
L3 = DZ*DCZ(T+K2/2.0, CA+L2/2.0, CB, D, A, EA, R, CP, RO, Q, TW, DH)
K4 = DZ*DTZ(T+K3, CA+L3, CB, D, A, EA, R, CP, RO, Q, TW, DH, U)
L4 = DZ*DCZ(T+K3, CA+L3, CB, D, A, EA, R, CP, RO, Q, TW, DH)
T = T + (K1+2.0*K2+2.0*K3+K4)/6.0
CA = CA + (L1+2.0*L2+2.0*L3+L4)/6.0
Z = Z + DZ
CB = CB0 + CA - CA0
IF(I.EQ.1) THEN
WRITE(6,100) Z, T-273, CA
END IF
IF(J.EQ.12) THEN
WRITE(6,100) Z, T-273, CA
END IF
100 FORMAT(1X,F7.4,2X,F15.3,2X,F15.3)
20 CONTINUE
10 CONTINUE
WRITE(6,*) '*****'
C
C DETERMINE IF MORE SIMULATIONS ARE NEEDED
C
WRITE(6,*) 'ANOTHER SIMULATION ? (0=YES)'
READ(5,*) RP

```

```

      IF(RP.EQ.0) GOTO 222
      STOP
      END

C
C
C      FUNCTION TO CALCULATE THE OVERALL HEAT-TRANSFER COEFFICIENT

      FUNCTION HEAT(Q,RO,D,MU,CP,KF,KS,PT,QR)
      REAL HEAT,V,RE,PR,H,HO,PI,MU,KF,KS,DL,PC
      PI = 3.14159
      DL = 2*PT/LOG((D+2*PT)/D)
      WRITE(6,*) 'LOG MEAN DIAMETER = ',DL
      RE = (4.0*Q*RO)/(PI*D*MU)
      WRITE(6,*) 'RE # = ',RE
      PR = CP*MU/KF

C
C
C      USE CORRELATION FOR TRANSITION REGION

      H = 0.116*(RE**(0.667)-125.0)*PR**(0.333)*KF/D
      WRITE(6,*) 'H = ',H
      PC = (KS*DL)/(PT*(D))
      WRITE(6,*) 'PIPE CONTROL = ',PC
      HO=QR
      WRITE(6,*) 'HO = ',HO

C
C
C      CALCULATE U SUB I

      HEAT = 1.0/(1.0/H + 1.0/PC + (D/HO/(D+2.0*PT)))
      RETURN
      END

C
C
C      FUNCTION DT/DZ

      FUNCTION DTZ(T,CA,CB,D,A,EA,R,CP,RO,Q,TW,DH,U)
      REAL PI
      PI = 3.14159
      DTZ = DH*CA*(CB)*PI*D*A*EXP(-1.0*EA/R/T)/(CP*RO*Q*4.0)
      DTZ = DTZ - U*PI*(D)*(T-TW)/(CP*RO*Q)
      RETURN
      END

C
C
C      FUNCTION DC/DZ

      FUNCTION DCZ(T,CA,CB,D,A,EA,R,CP,RO,Q,TW,DH)
      REAL PI
      PI = 3.14159
      DCZ = -1.0*PI*D*D*CA*(CB)*A*EXP(-1.0*EA/R/T)/(4.0*Q)
      RETURN
      END

```

```

C      PROGRAM SULFITE3
C      SIMULATES ODPH REACTOR MODEL
C      PROGRAM TAKES INTO ACCOUNT CHANGES IN HEAT TRANSFER
C      AT THE TEES
C      PROGRAM ALLOWS FOR COMPARISON WITH EXPERIMENTAL DATA
C      DEFINE VARIABLES
C
      REAL K1,K2,K3,K4,L1,L2,L3,L4,TW,PI,CB,DH,HO,QR
      REAL CAO,CBO,T,CA,Q,D,PT,V,CP,RO,A,EA,R,MU,KF,KS,Z,DZ
      INTEGER I,J
      REAL DIA,DOA,DIB,DOB,DIC,DOC,UA,UB,UC,REA,REB,REC
      REAL TEX(13),SUM
      PI = 3.14159
C      SET PHYSICAL CONSTANTS
C
      DIA = 0.00223
      DOA = 0.00711
      DIB = 0.00175
      DOB = 0.0111
      DIC = 0.00175
      DOC = 0.003175
      CP = 4180
      RO = 1000
      MU = 0.001
      KF = 0.637
      R = 8.314
      KS = 16.27
      DH = 372230
      A = 3.97*10**7.0
      EA = 64450
C      INPUT INTIAL CONDITIONS, FLOW, AND PIPE SIZE
C
      WRITE(6,*) 'INPUT INITIAL CONCENTRATIONS CAO & CBO'
      READ(5,*) CAO,CBO
      WRITE(6,300) CAO/1000.,CBO/1000.
300  FORMAT(1X,'CAO = ',F5.2,' CBO = ',F5.2)
      CA = CAO
      WRITE(6,*) 'INPUT FLOWRATE'
      READ(5,*) Q
      WRITE(6,*) 'FLOWRATE = ',Q*60000,' L/MIN'
      WRITE(6,*) 'INPUT INITIAL TEMPERATURE'
      READ(5,*) T
      WRITE(6,*) 'INITIAL TEMPERATURE = ',T
      WRITE(6,*) 'INPUT BATH TEMPERATURE'
      READ(5,*) TW
      WRITE(6,*) 'BATH TEMPERATURE = ',TW
      WRITE(6,*) 'INPUT OUTSIDE HEAT TRANSFER COEFFICIENT'
      READ(5,*) QR

```



```

WRITE(6,*) 'H OUTSIDE = ',QR
C READ IN EXPERIMENTAL TEMPERATURES
C
WRITE(6,*) 'INPUT EXPERIMENTAL TEMPERATURES'
DO 33 I=1,13
READ (5,*) TEX(I)
33 CONTINUE
C CALCULATE OVERALL HEAT TRANSFER COEFFICIENT FOR EACH SECTION
C
D = DIA
PT = (DOA-DIA)/2.0
WRITE(6,*) '***** FOR SECTION A *****'
U = HEAT(Q,RO,D,MU,CP,KF,KS,PT,QR)
UA = U
D = DIB
PT = DOB-DIB
PT = PT/2.0
WRITE(6,*) '***** FOR SECTION B *****'
U = HEAT(Q,RO,D,MU,CP,KF,KS,PT,QR)
UB = U
D = DIC
PT = DOC-DIC
PT = PT/2.0
WRITE(6,*) '***** FOR SECTION C *****'
U = HEAT(Q,RO,D,MU,CP,KF,KS,PT,QR)
UC = U
WRITE(6,*) 'UA = ',UA,' UB = ',UB,' UC = ',UC
PRINT HEADER
C
C
WRITE(6,*) '      Z              T              C'
Z = 0
CB = CBO
WRITE(6,100) Z,T-273,CA
WRITE(6,*) 'T EXP = ',TEX(1)
SUM = 0.0
C PERFORM INTEGRATION
C
DO 10 I=2,13
WRITE(6,*) '*****'
DO 20 J=1,12
C DETERMINE REGION AND SET U,D,DZ VALUES ACCORDINGLY
C
IF(J.EQ.1) THEN
U = UA
D = DIA
DZ = 0.0096
ELSE
IF(J.EQ.2) THEN

```

```

      U = UB
      D = DIB
      DZ = 0.012
    ELSE
      IF(J.EQ.11) THEN
        U = UB
        D = DIB
        DZ = 0.012
      ELSE
        IF(J.EQ.12) THEN
          U = UA
          D = DIA
          DZ = 0.0096
        ELSE
          U = UC
          D = DIC
          DZ = 0.032
        END IF
      END IF
    END IF
    K1 = DZ*DTZ(T, CA, CB, D, A, EA, R, CP, RO, Q, TW, DH, U)
    L1 = DZ*DCZ(T, CA, CB, D, A, EA, R, CP, RO, Q, TW, DH)
    K2 = DZ*DTZ(T+K1/2.0, CA+L1/2.0, CB, D, A, EA, R, CP, RO, Q, TW, DH, U)
    L2 = DZ*DCZ(T+K1/2.0, CA+L1/2.0, CB, D, A, EA, R, CP, RO, Q, TW, DH)
    K3 = DZ*DTZ(T+K2/2.0, CA+L2/2.0, CB, D, A, EA, R, CP, RO, Q, TW, DH, U)
    L3 = DZ*DCZ(T+K2/2.0, CA+L2/2.0, CB, D, A, EA, R, CP, RO, Q, TW, DH)
    K4 = DZ*DTZ(T+K3, CA+L3, CB, D, A, EA, R, CP, RO, Q, TW, DH, U)
    L4 = DZ*DCZ(T+K3, CA+L3, CB, D, A, EA, R, CP, RO, Q, TW, DH)
    T = T + (K1+2.0*K2+2.0*K3+K4)/6.0
    CA = CA + (L1+2.0*L2+2.0*L3+L4)/6.0
    Z = Z + DZ
    CB = CBO + CA - CAO
    IF(J.EQ.12) THEN
      WRITE(6,100) Z, T-273, CA
    END IF
100  FORMAT(1X,F7.4,2X,F15.3,2X,F15.3)
20   CONTINUE
C
C   FIND SUM OF DELTA T'S
C
      WRITE(6,*) 'TEXP = ', TEX(I)
      IF(TEX(I).EQ.0.0) THEN
        GOTO 578
      END IF
      SUM = SUM + (ABS(TEX(I)-(T-273)))**2.0)
578  CONTINUE
10   CONTINUE

```

```

C      PRINTOUT SUM OF DELTA T'S
C
C      WRITE(6,*) 'SUM = OF DELTA T S SQUARED = ',SUM
C      WRITE(6,*) 'H OUTSIDE = ',QR
C      STOP
C      END
C      FUNCTION TO CALCULATE THE OVERALL HEAT-TRANSFER COEFFICIENT
C
C      FUNCTION HEAT(Q,RO,D,MU,CP,KF,KS,PT,QR)
C      REAL HEAT,V,RE,PR,H,HO,PI,MU,KF,KS,DL,PC
C      PI = 3.14159
C      DL = 2*PT/LOG((D+2*PT)/D)
C      WRITE(6,*) 'LOG MEAN DIAMETER = ',DL
C      RE = (4.0*Q*RO)/(PI*D*MU)
C      WRITE(6,*) 'RE # = ',RE
C      PR = CP*MU/KF
C      USE CORRELATION FOR TRANSITION REGION
C
C      H = 0.116*(RE**(0.667)-125.0)*PR**(0.333)*KF/D
C      WRITE(6,*) 'H = ',H
C      PC = (KS*DL)/(PT*(D))
C      WRITE(6,*) 'PIPE CONTROL = ',PC
C      HO=QR
C      WRITE(6,*) 'HO = ',HO
C      CALCULATE U SUB I
C
C      HEAT = 1.0/(1.0/H + 1.0/PC + (D/HO/(D+2.0*PT)))
C      RETURN
C      END
C      FUNCTION DT/DZ
C
C      FUNCTION DTZ(T,CA,CB,D,A,EA,R,CP,RO,Q,TW,DH,U)
C      REAL PI
C      PI = 3.14159
C      DTZ = DH*CA*(CB)*PI*D*D*A*EXP(-1.0*EA/R/T)/(CP*RO*Q*4.0)
C      DTZ = DTZ - U*PI*(D)*(T-TW)/(CP*RO*Q)
C      RETURN
C      END
C      FUNCTION DC/DZ
C
C      FUNCTION DCZ(T,CA,CB,D,A,EA,R,CP,RO,Q,TW,DH)
C      REAL PI
C      PI = 3.14159
C      DCZ = -1.0*PI*D*D*CA*(CB)*A*EXP(-1.0*EA/R/T)/(4.0*Q)
C      RETURN
C      END

```

## 2) TDPH Model - Computer Program

The TDPH model, once simplified, is described by equation 5.5. As mentioned in section 5.1,  $C_A(z) = C_{Ao}$  in this case.

$$\frac{\partial^2 T}{\partial z^2} + \frac{\partial^2 T}{\partial r^2} + \frac{1}{r} \cdot \frac{\partial T}{\partial r} - \frac{u \cdot \rho \cdot C_p}{k_f} \cdot \frac{\partial T}{\partial z} = 0 \quad (5.5)$$

The boundary conditions are :

$$\left. \frac{\partial T}{\partial r} \right|_{r=0} = 0 \quad (5.5a)$$

$$-k_f \cdot \pi \cdot D_i \cdot \left. \frac{\partial T}{\partial r} \right|_{r=D_i/2} = U_o \cdot \pi \cdot D_o \cdot (T - T_c) \Big|_{r=D_i/2} \quad (5.5b)$$

$$\left. \frac{\partial T}{\partial z} \right|_{z=L} = 0 \quad (5.5c)$$

$$u \cdot \rho \cdot C_p \cdot (T_o - T) \Big|_{z=0} = -k_f \cdot \left. \frac{\partial T}{\partial z} \right|_{z=0} \quad (5.5d)$$

Equations 5.5 through 5.5d can be solved numerically using a finite difference method. If a forward difference formula is used for the axial first derivative and a central difference formula is used for the remaining derivatives, an explicit difference equation can be formulated. Thus,

$$\frac{\partial T}{\partial z} = \frac{T_{i,j+1} - T_{i,j}}{\Delta z} \quad (D.2)$$

$$\frac{\partial^2 T}{\partial z^2} = \frac{T_{i,j+1} - 2 \cdot T_{i,j} + T_{i,j-1}}{\Delta z^2} \quad (D.3)$$

$$\frac{\partial T}{\partial r} = \frac{T_{i+1,j} - T_{i-1,j}}{\Delta r} \quad (D.4)$$

$$\frac{\partial^2 T}{\partial r^2} = \frac{T_{i+1,j} - 2 \cdot T_{i,j} + T_{i-1,j}}{\Delta r^2} \quad (D.5)$$

$$\frac{\partial C_A}{\partial z} = \frac{C_{Ai,j+1} - C_{Ai,j}}{\Delta z}$$

where  $i$ ; and  $j$ ; refer to the radial and axial grid coordinates respectively and  $\Delta r$  and  $\Delta z$  are the step sizes

The radial boundary conditions become

$$T_{2,j} = T_{0,j} \quad (\text{for 5.5a}) \quad (\text{D.6})$$

$$-k_f \cdot (T_{I+1,j} - T_{I-1,j}) = U \cdot 2 \cdot \Delta r \cdot (T_{I,j} - T_c) \quad (\text{for 5.5b}) \quad (\text{D.7})$$

(if U is based on the outside area then the term  $D_o/D_i$  appears on the RHS of the equation)

The axial boundary conditions become

$$T_{i,J} = T_{i,J-1} \quad \text{at } j=J \text{ for all } i \quad (\text{for 5.5c}) \quad (\text{D.8})$$

$$u \cdot \rho \cdot C_p \cdot (T_o - T_{1,1}) = -k_f \cdot (T_{1,2} - T_{1,1}) / \Delta z \quad (\text{for 5.5d}) \quad (\text{D.9})$$

where I; and J; refer to the values of the final radial and axial grid coordinates respectively

The program used to solve the resulting finite difference equations is given at the end of the section. Due to the nature of boundary condition 5.5d, the solution is an iterative one. That is, an initial radial temperature profile must be assumed. After the integration is complete, the inlet boundary condition is checked for compliance. If the boundary condition is not met, then the procedure must be repeated. After a few simulations, however, it was determined that assuming a uniform radial profile with  $T = T_o$  and ignoring the iterations did not introduce any significant error into the solution. Thus all simulations were based on an inlet temperature profile of  $T(r) = T_o$  for all r.

The overall heat transfer coefficient used in this program was based on the outside area (i.e.,  $U_o$ ). Only one value for the overall heat transfer coefficient was used throughout the integration. The effect of the change in tubing dimensions at the tees was taken into account by adjusting the  $D_o/D_i$  parameter in the boundary condition at the wall (equation 5.5b). In addition, the amount of heat transferred through the walls of the reactor, as well as the amount of energy entering and leaving the reactor (in the fluid) was calculated.

The final feature of the program to be noted is the temperature averaging at the tees. The program was designed so that, once the fluid reached the position of the thermocouple in the tee, the radial temperature (and concentration) profile became uniform (i.e., the temperature at each radial position was set equal to the average temperature). This was done because, as the fluid passes through tee, it also passes through an abrupt  $90^\circ$  change in flow direction. In addition, the fluid also flows through a restriction due to the presence of the thermocouple. Because of this, it was felt that the fluid would become mixed as it travelled through the tee. Thus, the radial gradients would be lost and the profile would become uniform.

```

C      PROGRAM URAD3.TEMP
C      SOLVES 2-D HOMOGENEOUS TUBULAR REACTOR MODEL
C      PROGRAM CALCULATES AXIAL AND RADIAL TEMPERATURE PROFILES FOR
C A TUBULAR REACTOR ASSUMING NO AXIAL MIXING OR RADIAL MIXING OF MASS
C      PROGRAM INVOLVES TEMPERATURE AND CONCENTRATION AVERAGING AT TEES
C      AS WELL AS ACCOUNTING FOR CHANGE IN HEAT TRANSFER AREA AT TEES
C      PROGRAM ALLOWS FOR INPUT OF EXPERIMENTAL DATA AND CALCULATES
C      THE SUM OF THE SQUARES OF THE TEMPERATURE DIFFERENCES BETWEEN
C      THE MODEL AND THE EXPERIMENTAL VALUES
C      PROGRAM ALSO CALCULATES THE ENERGY BALANCE FOR THE REACTOR
C
C      DEFINE VARIABLES
C
C      REAL*8 TO, TEMP1, TEMP2, TEMP3, TEMP4, TEMP5
C      REAL*8 T(37,2000), C(37,2000), KF, RO, CP, Q, D, DH, A, EA
C      REAL*8 CAO, CBO, DZ, DR, U, HW, TC, PI, R, RD, AR, FG(36)
C      REAL*8 TEMP(200), TAV(2000), CAV(2000)
C      REAL*8 DZ1, DZ2, AR1, AR2
C      REAL*8 SUM1, SUM2, SUM
C      INTEGER I, J, II, JJ, K, KK
C
C      SET PHYSICAL PARAMETERS
C
C      PI = 3.14159
C      R = 8.314
C      DR = 0.000025
C      HW = 3955
C      DH = -372230
C      RO = 1000
C      CP = 4180
C      D = 0.00175
C      EA = 64268
C      A = 3.56*10**7.0
C      KF = 0.637
C      RD = 0.000875
C      AR1 = 1.81
C      AR2 = 4.40
C      DZ1 = 0.002
C      DZ2 = 0.0012
C
C      INPUT INITIAL CONDITIONS
C
C      WRITE(6,*) 'INPUT CAO,CBO,Q,TO,TC'
C      READ (5,*) CAO,CBO,Q,TO,TC
C      U = Q/(PI*D*D/4)
C      WRITE(6,*) 'COMPUTING'
C
C      READ EXPERIMENTAL TEMPERATURES

```



```

C      DO 50 I=1,12
      READ(5,*) TEXP(I)
50     CONTINUE
C
C      READ U AND INTIAL TEMPERATURE PROFILE
C
      READ(5,*) HW
      READ(5,*) (FG(I),I=1,36)
C
C      SET TEMPERATURE AND CONCENTRATION PROFILES AT Z=0
C
      DO 10 I=1,36
      T(I,1) = T0+FG(I)
      C(I,1) = CA0
10     CONTINUE
C
C      PERFORM INTEGRATION AT J=1 FOR 2ND LEVEL
C
      DZ = DZ2
      AR = AR2
      J = 1
      TAV(J+1) = 0.0
      CAV(J+1) = 0.0
      DO 201 I=1,36
      IF (I.EQ.1) THEN
      T(I,J+1) = DH/KF*A*EXP(-EA/R/T(I,J))*C(I,J)*(C(I,J)+CB0-CA0)
      TEMP1 = (2*T(2,J)-2*T(1,J))/DR/DR
      TEMP2 = (2*T(1,J)-2*T0)/DZ/DZ
      TEMP3 = (1/DZ/DZ - (U*RO*CP/KF/DZ))
      T(I,J+1) = (T(I,J+1)-TEMP1+TEMP2-(U*RO*CP/KF/DZ*T(1,J)))/TEMP3
      TAV(J+1) = T(I,J+1)*DR*(I-1)
      GOTO 151
      END IF
      IF(I.EQ.36) THEN
      TEMP1 = DH/KF*A*EXP(-EA/R/T(I,J))*C(I,J)*(C(I,J)+CB0-CA0)
      TEMP2 = (-2*HW*AR*DR/KF*(T(I,J)-TC))/(2*DR*RD)
      TEMP3 = (2*T(I-1,J)-2*T(I,J)-2*HW*AR*DR/KF*(T(I,J)-TC))/DR/DR
      TEMP4 = (2*T(I,J)-T0)/DZ/DZ
      TEMP5 = (1/DZ/DZ-(U*RO*CP/KF/DZ))
      T(I,J+1)=(TEMP1-TEMP2-TEMP3+TEMP4-(U*RO*CP*T(I,J)/KF/DZ))/TEMP5
      TAV(J+1) = TAV(J+1) + T(I,J+1)*DR*(I-1)
      GOTO 151
      END IF
      TEMP1 = DH*A/KF*EXP(-EA/R/T(I,J))*C(I,J)*(C(I,J)+CB0-CA0)
      TEMP2 = (T(I+1,J)-T(I-1,J))/2/DR/((I-1)*DR)
      TEMP3 = (T(I+1,J)-2*T(I,J)+T(I-1,J))/DR/DR
      TEMP4 = (2*T(I,J)-T0)/DZ/DZ

```

```

      TEMP5 = (1/DZ/DZ-(U*RO*CP/KF/DZ))
      T(I,J+1) = (TEMP1-TEMP2-TEMP3+TEMP4-(U*RO*CP*T(I,J)/KF/DZ))/TEMP5
      TAV(J+1)=TAV(J+1) + 2.0*T(I,J+1)*DR*(I-1)
151  CONTINUE
      C(I,J+1)= -A/U*EXP(-EA/R/T(I,J))*C(I,J)*(C(I,J)+CB0-CA0)*DZ
      C(I,J+1) = C(I,J+1) + C(I,J)
      CAV(J+1) = CAV(J+1) + 2.0*C(I,J+1)*DR*(I-1)
201  CONTINUE
      CAV(J+1) = CAV(J+1) - C(36,J+1)*DR*35
      CAV(J+1) = CAV(J+1)*DR/2.0*2.0/D/D*4.0
      TAV(J+1)= TAV(J+1)*DR/2.0*2.0/D/D*4.0

C
C
C
      DO 100 J=2,1967
      K = INT((J+17)/164)
      IF (ABS((K*164)-J).LE.18) THEN
      AR = AR2
      DZ = DZ2
      ELSE
      AR = AR1
      DZ = DZ1
      END IF
      IF (REAL(J/164).EQ. (J/164.0)) THEN
      WRITE(6,*) 'TAV = ',TAV(J)-273
      DO 7 II=1,36
      T(II,J) = TAV(J)
      C(II,J) = CAV(J)
7  CONTINUE
      END IF
      TAV(J+1) = 0.0
      CAV(J+1) = 0.0
      DO 200 I=1,36
      IF (I.EQ.1) THEN
      T(I,J+1) = DH/KF*A*EXP(-EA/R/T(I,J))*C(I,J)*(C(I,J)+CB0-CA0)
      TEMP1 = (2*T(2,J)-2*T(1,J))/DR/DR
      TEMP2 = (2*T(1,J)-2*T(1,J-1))/DZ/DZ
      TEMP3 = (1/DZ/DZ - (U*RO*CP/KF/DZ))
      T(I,J+1)=(T(I,J+1)-TEMP1+TEMP2-(U*RO*CP/KF/DZ*T(1,J)))/TEMP3
      TAV(J+1) = T(I,J+1)*DR*(I-1)
      GOTO 150
      END IF
      IF(I.EQ.36) THEN
      TEMP1 = DH/KF*A*EXP(-EA/R/T(I,J))*C(I,J)*(C(I,J)+CB0-CA0)
      TEMP2 = (-2*HW*AR*DR/KF*(T(I,J)-TC))/(2*DR*RD)
      TEMP3 = (2*T(I-1,J)-2*T(I,J)-2*HW*AR*DR/KF*(T(I,J)-TC))/DR/DR
      TEMP4 = (2*T(I,J)-T(I,J-1))/DZ/DZ
      TEMP5 = (1/DZ/DZ-(U*RO*CP/KF/DZ))

```

```

T(I,J+1)=(TEMP1-TEMP2-TEMP3+TEMP4-(U*RO*CP*T(I,J)/KF/DZ))/TEMP5
TAV(J+1)=TAV(J+1) + T(I,J+1)*DR*(I-1)
GOTO 150
END IF
TEMP1 = DH*A/KF*EXP(-EA/R/T(I,J))*C(I,J)*(C(I,J)+CBO-CAO)
TEMP2 = (T(I+1,J)-T(I-1,J))/2/DR/((I-1)*DR)
TEMP3 = (T(I+1,J)-2*T(I,J)+T(I-1,J))/DR/DR
TEMP4 = (2*T(I,J)-T(I,J-1))/DZ/DZ
TEMP5 = (1/DZ/DZ-(U*RO*CP/KF/DZ))
T(I,J+1)=(TEMP1-TEMP2-TEMP3+TEMP4-(U*RO*CP*T(I,J)/KF/DZ))/TEMP5
TAV(J+1)=TAV(J+1) + 2.0*T(I,J+1)*DR*(I-1)
150 CONTINUE
C(I,J+1)= -A/U*EXP(-EA/R/T(I,J))*C(I,J)*(C(I,J)+CBO-CAO)*DZ
C(I,J+1) = C(I,J+1) + C(I,J)
CAV(J+1) = CAV(J+1) + 2.0*C(I,J+1)*DR*(I-1)
200 CONTINUE
TAV(J+1) = TAV(J+1)*DR/2.0*2.0/D/D*4.0
CAV(J+1) = CAV(J+1) - C(36,J+1)*DR*35
CAV(J+1) = CAV(J+1)*DR/2.0*2.0/D/D*4.0
100 CONTINUE
C
C CHECK ON INITIAL BOUNDARY CONDITION
C
DO 77 I=1,36
WRITE(6,101)
101 FORMAT(1X)
WRITE(6,*) 'UROCP TERM ',U*RO*CP*(TO-T(I,1))
WRITE(6,*) 'KDT/DZ TERM ', -1.0*KF*(T(I,2)-T(I,1))/DZ
77 CONTINUE
C
C CALCULATE SUM OF THE SQUARES OF THE TEMP DIFFERENCES
C
SUM = 0
DO 300 I=1,12
T1 = TAV(I*164)-273.0
WRITE(6,*) 'T EXP ', ' T MODEL'
WRITE(6,*) TEXP(I), ' ', T1
WRITE(6,*) CAV(I*164)
IF(TEXP(I).NE.0) THEN
SUM = SUM + (ABS(TEXP(I)-TAV(I*164)+273)**2.0)
END IF
300 CONTINUE
WRITE(6,*) 'SUM OF DELTA T = ',SUM
C
C CALCULATE HEAT BALANCE
C ***** REMEMBER TEMPERATURE MEASUREMENTS ARE NOT EQUALLY SPACED
C ***** AND HEAT TRANSFER AREA VARIES
C

```

```

SUM1 = 0.0
SUM2 = 0.0
DO 405 I=1,12
K1 = 164*(I-1)+1
K2 = 164*(I-1)+18
DO 410 II=K1,K2
SUM2 = SUM2 + 2.0*T(36,II) - 2.0*TC
410 CONTINUE
SUM2 = SUM2 - T(36,K1) - T(36,K2)
SUM2 = SUM2 + 2.0*TC
K1 = 164*(I-1)+147
K2 = 164*(I-1)+164
DO 411 II=K1,K2
SUM2 = SUM2 + 2.0*T(36,II) - 2.0*TC
411 CONTINUE
SUM2 = SUM2 - T(36,K1) - T(36,K2)
SUM2 = SUM2 + 2.0*TC
K1 = 164*(I-1) + 19
K2 = 164*(I-1) + 163
DO 412 II=K1,K2
SUM1 = SUM1 + 2.0*T(36,II) - 2.0*TC
412 CONTINUE
SUM1 = SUM1 - T(36,K1) - T(36,K2)
SUM1 = SUM1 + 2.0*TC
405 CONTINUE
SUM1 = SUM1*DZ1/2.0
SUM2 = SUM2*DZ2/2.0
SUM1 = SUM1*HW*PI*AR1*D
SUM2 = SUM2*HW*PI*AR2*D
SUM = SUM1+SUM2
WRITE(6,*) 'HW =',HW
WRITE(6,*) 'HEAT TRANSFERRED OUT = ',SUM
WRITE(6,*) 'HEAT IN =',Q*RO*CP*TO
WRITE(6,*) 'HEAT OUT =',Q*RO*CP*TAV(1967)
STOP
END

```

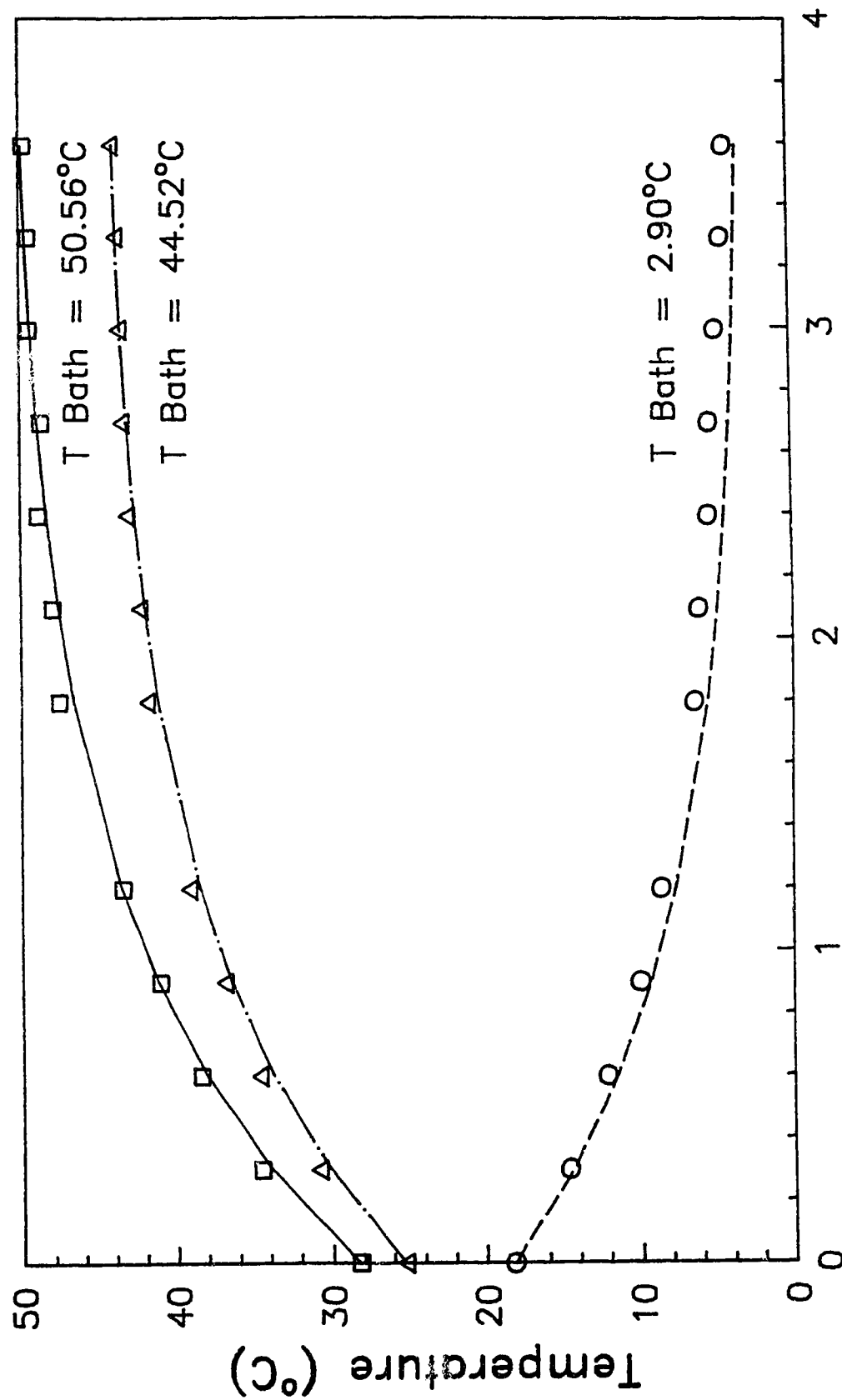
### 3) ODPH and TDPH Model Simulations

In this section are presented the results obtained using the ODPH and TDPH models. The computer programs discussed in the two previous sections were used to obtain the simulated temperature profiles. These profiles can be seen throughout section 5.1. Table D.2 is a summary of all the results obtained, illustrating convergence on the optimal heat transfer coefficient for each set of experimental data.

Figure D.1 illustrates how well the ODPH model describes all the experimental data. The simulations shown use the average value of the experimentally determined bath side heat transfer coefficient.

TABLE D.2			
Experimental Data and Model Comparisons			
Experiment	Model	U (W/(m <sup>2</sup> ·K))	$\Sigma_i (T(\text{model}) - T(\text{exp}))^2$
2	TDPH	4 000	4.53
		5 000	0.99
		5 500	0.48
		6 000	0.389
		6 500	0.55
		7 000	0.87
3	TDPH	2 000	5.39
		2 500	1.703
		2 750	1.87
		3 000	2.68
		4 000	8.34
1	TDPH	3 000	14.25
		4 000	2.96
		4 500	1.66
		5 000	1.59
		5 500	2.17
		6 000	3.12
		7 000	5.44

TABLE D.2 CONTINUED				
Experimental Data and Model Comparisons				
Experiment	Model	$h_o$ W/(m <sup>2</sup> ·K)	U W/(m <sup>2</sup> ·K)	$\Sigma_1 (T(\text{model})-T(\text{exp}))^2$
2	ODPH	2 900	3 034	23.69
		3 900	3 501	6.07
		4 900	3 858	1.03
		5 400	4 006	0.41
		5 600	4 061	0.36
		5 700	4 088	0.37
		5 900	4 139	0.45
3	ODPH	2 400	2 741	2.59
		2 600	2 864	1.78
		2 700	2 923	1.66
		2 800	2 979	1.70
		2 900	3 034	1.86
		3 400	3 284	3.94
		3 900	3 501	7.15
1	ODPH	3 000	3 087	18.34
		4 000	3 541	3.43
		4 500	3 726	1.67
		4 800	3 826	1.50
		4 900	3 858	1.55
		5 000	3 889	1.64



**Axial Coordinate (m)**

Figure D.1 Experimental Heat Transfer Data and ODPH  
Model Simulations with  $H_o = 4,367 \text{ W/(m}^2\cdot\text{K)}$



## APPENDIX E

### 1) ODPH and TDPH Models - Computer Programs

The programs use to simulate the ODPH and TDPH models for the case of a reaction occurring were essentially the same as those illustrated in Appendix D. This is because the programs were initially designed to handle the case of a reaction occurring. (If the initial concentration of one of the reactants was set to 0, then the solution became the same as that for no reaction occurring. Thus the same program could handle both situations.) The program used for the ODPH model was the same one described in Appendix D (SULFITE2).

The program for the TDPH model is given at the end of this section (URAD4.TEMP). It differs from the program URAD3.TEMP listed in Appendix D in that there is no energy balance calculation. In addition, because there is reaction occurring, eq 5.4 no longer simplifies to  $C_A(z) = C_{A0}$ . Rather, equation 5.4 now becomes:

$$\frac{-dC_A}{dz} = \frac{R_A}{u} \quad (E.1)$$

Therefore, a finite difference expression must also be used for this derivative. This is given by:

$$\frac{\partial C_A}{\partial z} = \frac{C_{A1,j+1} - C_{A1,j}}{\Delta z} \quad (E.2)$$

Of course, the boundary condition is still

$$C_A(z=0) = C_{Ao} \quad (E.3)$$

```

C      PROGRAM URAD4.TEMP
C      SOLVES 2-D HOMOGENEOUS TUBULAR REACTOR MODEL
C      PROGRAM CALCULATES AXIAL AND RADIAL TEMPERATURE PROFILES FOR
C      A TUBULAR REACTOR ASSUMING NO AXIAL MIXING OR RADIAL MIXING OF MASS
C
C      PROGRAM INVOLVES TEMPERATURE AND CONCENTRATION AVERAGING AT TEES
C      AS WELL AS ACCOUNTING FOR CHANGE IN HEAT TRANSFER AREA AT TEES
C      PROGRAM ALLOWS FOR INPUT OF EXPERIMENTAL DATA AND CALCULATES
C      THE SUM OF THE SQUARES OF THE TEMPERATURE DIFFERENCES BETWEEN
C      THE MODEL AND THE EXPERIMENTAL VALUES
C
C      DEFINE VARIABLES
C
C      REAL*8 TO, TEMP1, TEMP2, TEMP3, TEMP4, TEMP5
C      REAL*8 T(37,2000), C(37,2000), KF, RO, CP, Q, D, DH, A, EA
C      REAL*8 CAO, CBO, DZ, DR, U, HW, TC, PI, R, RD, AR, FG(36)
C      REAL*8 TEXP(20), TAV(2000), CAV(2000)
C      REAL*8 DZ1, DZ2, AR1, AR2
C      REAL*8 SUM1, SUM2, SUM
C      INTEGER I, J, II, JJ, K, KK
C
C      SET PHYSICAL PARAMETERS
C
C      PI = 3.14159
C      R = 8.314
C      DR = 0.000025
C      HW = 3955
C      DH = -372230
C      RO = 1000
C      CP = 4180
C      D = 0.00175
C      EA = 64268
C      A = 3.56*10**7.0
C      KF = 0.637
C      RD = 0.000875
C      AR1 = 1.81
C      AR2 = 4.40
C      DZ1 = 0.002
C      DZ2 = 0.0012
C
C      INPUT INITIAL CONDITIIONS
C
C      WRITE(6,*) ' INPUT CAO,CBO,Q,TO,TC'
C      READ (5,*) CAO,CBO,Q,TO,TC
C      U = Q/(PI*D*D/4)
C      WRITE(6,*) 'TO = ',TO
C      WRITE(6,*) 'T BATH = ',TC

```

```

WRITE(6,*) 'COMPUTING'
C
C READ EXPERIMENTAL TEMPERATURES
C
DO 50 I=1,12
READ(5,*) TEXP(I)
50 CONTINUE
C
C READ U AND INITIAL TEMPERATURE PROFILE
C
READ(5,*) HW
WRITE(6,*) 'U = ',HW
READ(5,*) (FG(I),I=1,36)
C
C SET TEMPERATURE AND CONCENTRATION PROFILES AT Z=0
C
DO 10 I=1,36
T(I,1) = T0+FG(I)
C(I,1) = CAO
10 CONTINUE
C
C PERFORM INTEGRATION AT J=1 FOR 2ND LEVEL
C
DZ = DZ2
AR = AR2
J = 1
TAV(J+1) = 0.0
CAV(J+1) = 0.0
DO 201 I=1,36
IF (I.EQ.1) THEN
T(I,J+1) = DH/KF*A*EXP(-EA/R/T(I,J))*C(I,J)*(C(I,J)+CBO-CAO)
TEMP1 = (2*T(2,J)-2*T(1,J))/DR/DR
TEMP2 = (2*T(1,J)-2*T0)/DZ/DZ
TEMP3 = (1/DZ/DZ - (U*RO*CP/KF/DZ))
T(I,J+1) = (T(I,J+1)-TEMP1+TEMP2-(U*RO*CP/KF/DZ*T(1,J)))/TEMP3
TAV(J+1) = T(I,J+1)*DR*(I-1)
GOTO 151
END IF
IF(I.EQ.36) THEN
TEMP1 = DH/KF*A*EXP(-EA/R/T(I,J))*C(I,J)*(C(I,J)+CBO-CAO)
TEMP2 = (-2*HW*AR*DR/KF*(T(I,J)-TC))/(2*DR*RD)
TEMP3 = (2*T(I-1,J)-2*T(I,J)-2*HW*AR*DR/KF*(T(I,J)-TC))/DR/DR
TEMP4 = (2*T(I,J)-T0)/DZ/DZ
TEMP5 = (1/DZ/DZ-(U*RO*CP/KF/DZ))
T(I,J+1)=(TEMP1-TEMP2-TEMP3+TEMP4-(U*RO*CP*T(I,J)/KF/DZ))/TEMP5
TAV(J+1) = TAV(J+1) + T(I,J+1)*DR*(I-1)
GOTO 151
END IF

```

```

TEMP1 = DH*A/KF*EXP(-EA/R/T(I,J))*C(I,J)*(C(I,J)+CB0-CA0)
TEMP2 = (T(I+1,J)-T(I-1,J))/2/DR/((I-1)*DR)
TEMP3 = (T(I+1,J)-2*T(I,J)+T(I-1,J))/DR/DR
TEMP4 = (2*T(I,J)-T0)/DZ/DZ
TEMP5 = (1/DZ/DZ-(U*RO*CP/KF/DZ))
T(I,J+1) = (TEMP1-TEMP2-TEMP3+TEMP4-(U*RO*CP*T(I,J)/KF/DZ))/TEMP5
TAV(J+1)=TAV(J+1) + 2.0*T(I,J+1)*DR*(I-1)
151  CONTINUE
C(I,J+1)= -A/U*EXP(-EA/R/T(I,J))*C(I,J)*(C(I,J)+CB0-CA0)*LZ
C(I,J+1) = C(I,J+1) + C(I,J)
CAV(J+1) = CAV(J+1) + 2.0*C(I,J+1)*DR*(I-1)
201  CONTINUE
CAV(J+1) = CAV(J+1) - C(36,J+1)*DR*35
CAV(J+1) = CAV(J+1)*DR/2.0*2.0/D/D*4.0
TAV(J+1)= TAV(J+1)*DR/2.0*2.0/D/D*4.0

C
C
C
DO 100 J=2,1967
K = INT((J+17)/164)
IF(ABS((K*164)-J).LE.18) THEN
AR = AR2
DZ = DZ2
ELSE
AR = AR1
DZ = DZ1
END IF
IF(REAL(J/164).EQ.(J/164.0)) THEN
C
WRITE(6,*) 'TAV = ',TAV(J)-273
DO 7 II=1,36
T(II,J) = TAV(J)
C(II,J) = CAV(J)
7  CONTINUE
END IF
TAV(J+1) = 0.0
CAV(J+1) = 0.0
DO 200 I=1,36
IF (I.EQ.1) THEN
T(I,J+1) = DH/KF*A*EXP(-EA/R/T(I,J))*C(I,J)*(C(I,J)+CB0-CA0)
TEMP1 = (2*T(2,J)-2*T(1,J))/DR/DR
TEMP2 = (2*T(1,J)-2*T(1,J-1))/DZ/DZ
TEMP3 = (1/DZ/DZ - (U*RO*CP/KF/DZ))
T(I,J+1)=(T(I,J+1)-TEMP1+TEMP2-(U*RO*CP/KF/DZ*T(1,J)))/TEMP3
TAV(J+1) = T(I,J+1)*DR*(I-1)
GOTO 150
END IF
IF(I.EQ.36) THEN
TEMP1 = DH/KF*A*EXP(-EA/R/T(I,J))*C(I,J)*(C(I,J)+CB0-CA0)

```

```

TEMP2 = (-2*HW*AR*DR/KF*(T(I,J)-TC))/(2*DR*RD)
TEMP3 = (2*T(I-1,J)-2*T(I,J)-2*HW*AR*DR/KF*(T(I,J)-TC))/DR/DR
TEMP4 = (2*T(I,J)-T(I,J-1))/DZ/DZ
TEMP5 = (1/DZ/DZ-(U*RO*CP/KF/DZ))
T(I,J+1)=(TEMP1-TEMP2-TEMP3+TEMP4-(U*RO*CP*T(I,J)/KF/DZ))/TEMP5
TAV(J+1)=TAV(J+1) + T(I,J+1)*DR*(I-1)
GOTO 150
END IF
TEMP1 = DH*A/KF*EXP(-EA/R/T(I,J))*C(I,J)*(C(I,J)+CBO-CA0)
TEMP2 = (T(I+1,J)-T(I-1,J))/2/DR/((I-1)*DR)
TEMP3 = (T(I+1,J)-2*T(I,J)+T(I-1,J))/DR/DR
TEMP4 = (2*T(I,J)-T(I,J-1))/DZ/DZ
TEMP5 = (1/DZ/DZ-(U*RO*CP/KF/DZ))
T(I,J+1)=(TEMP1-TEMP2-TEMP3+TEMP4-(U*RO*CP*T(I,J)/KF/DZ))/TEMP5
TAV(J+1)=TAV(J+1) + 2.0*T(I,J+1)*DR*(I-1)
150 CONTINUE
C(I,J+1)= -A/U*EXP(-EA/R/T(I,J))*C(I,J)*(C(I,J)+CBO-CA0)*DZ
C(I,J+1) = C(I,J+1) + C(I,J)
CAV(J+1) = CAV(J+1) + 2.0*C(I,J+1)*DR*(I-1)
200 CONTINUE
TAV(J+1) = TAV(J+1)*DR/2.0*2.0/D/D*4.0
CAV(J+1) = CAV(J+1) - C(36,J+1)*DR*35
CAV(J+1) = CAV(J+1)*DR/2.0*2.0/D/D*4.0
100 CONTINUE
C
C CALCULATE SUM OF THE SQUARES OF THE TEMP DIFFERENCES
C
SUM = 0
DO 300 I=1,12
T1 = TAV(I*164)-273.0
WRITE(6,*) 'T EXP ', 'T MODEL'
WRITE(6,*) TEXP(I), ' ', T1
WRITE(6,*) 'CA = ', CAV(I*164)
IF(TEXP(I).NE.0) THEN
SUM = SUM + (ABS(TEXP(I)-TAV(I*164)+273)**2.0)
END IF
300 CONTINUE
WRITE(6,*) 'SUM OF DELTA T = ', SUM
STOP
END

```

## 2) ODPH and TDPH Model Simulations

The results of the simulations are illustrated in figure form throughout chapter 7.

### 3) Evaluation of the "fine-tuned" Arrhenius Parameters

From Figure 7.22 the error sum of squares can be calculated. This can be compared to the error sum of squares obtained from the linear regression of figure A.2.

$$\text{Error Sum of Squares (ESS)} = \sum_1 (\hat{Y} - Y)^2 \quad (\text{E.4})$$

where  $\hat{Y}$  is the predicted value

and  $Y$  is the measured (or actual) value

From Figure 7.22, ESS = 0.785

From Figure A.2, ESS = 0.428

If the ratio of these two numbers is within the value of the F distribution (for the number of degrees of freedom used in the regression and at a 95 % confidence level), then the "fine-tuned" parameters can be said to be statistically valid. This is because the line drawn through the data using the "fine-tuned" parameters, is within the 95 % confidence level of the "proper" regression as illustrated in figure A.2.

Therefore, the ratio =  $0.785/0.428 = 1.83$ . The corresponding F value for (33,33) degrees of freedom at a 95 % confidence level is 1.77. Thus, the ratio indicates that the new parameters are not strictly speaking statistically valid. However, for practical purposes, they



can be considered as being statistically valid.

## APPENDIX F

### 1) Extraction of Critical Data ---

Tables F.1 through F.14 are a list of the maximum temperature vs inlet temperature (or bath temperature or inlet concentration) data. Each set of data was fit to a third order polynomial. This was carried out using the statistical package MINITAB (a program listing is attached at the end of this section). The results obtained and the critical conditions extracted are shown as well.

TABLE F.1 Bath Temperature = 19°C [Na <sub>2</sub> SO <sub>3</sub> ] = 0.88 M	
Maximum Temperature (°C)	Inlet Temperature (°C)
32.55	10.99
35.14	18.29
40.57	24.56
45.43	30.59
50.89	33.96
66.73	40.75
80.08	45.70
93.76	47.71

TABLE F.2 Bath Temperature = 24°C [Na <sub>2</sub> SO <sub>3</sub> ] = 0.88 M	
Maximum Temperature (°C)	Inlet Temperature (°C)
47.51	10.99
48.5	18.29
52.85	24.56
58.95	30.59
68.47	33.96
83.83	40.75
89.97	45.70
95.06	47.71

TABLE F.3 Bath Temperature = 29°C [Na <sub>2</sub> SO <sub>3</sub> ] = 0.88 M	
Maximum Temperature (°C)	Inlet Temperature (°C)
53.45	10.99
57.69	18.29
58.19	24.56
65.13	30.59

TABLE F.4 Bath Temperature = 34°C [Na <sub>2</sub> SO <sub>3</sub> ] = 0.88 M	
Maximum Temperature (°C)	Inlet Temperature (°C)
67.55	10.99
67.18	18.29
70.25	24.56
80.46	30.59
80.69	33.96
92.13	40.75
100.46	45.70

TABLE F.5 Bath Temperature = 44°C [Na <sub>2</sub> SO <sub>3</sub> ] = 0.88 M	
Maximum Temperature (°C)	Inlet Temperature (°C)
76.54	10.99
77.4	18.29
80.92	24.56
85.82	30.59
87.93	33.96
98.77	40.75

TABLE F.6 Inlet Temperature = 10.99°C [Na <sub>2</sub> SO <sub>3</sub> ] = 0.88 M	
Maximum Temperature (°C)	Bath Temperature (°C)
32.55	19.0
47.51	24.0
53.52	29.0
67.55	34.0
76.54	44.0
80.26	49.0

TABLE F.7 Inlet Temperature = 18.29°C [Na <sub>2</sub> SO <sub>3</sub> ] = 0.88 M	
Maximum Temperature (°C)	Bath Temperature (°C)
35.14	19.0
48.50	24.0
57.69	29.0
67.18	34.0
77.4	44.0
82.22	49.0

TABLE F.8 Inlet Temperature = 24.56°C [Na <sub>2</sub> SO <sub>3</sub> ] = 0.88 M	
Maximum Temperature (°C)	Bath Temperature (°C)
40.57	19.0
52.85	24.0
58.19	29.0
70.25	34.0
80.92	44.0
87.37	49.0

TABLE F.9 Inlet Temperature = 30.59°C [Na <sub>2</sub> SO <sub>3</sub> ] = 0.88 M	
Maximum Temperature (°C)	Bath Temperature (°C)
45.43	19.0
58.95	24.0
65.13	29.0
80.46	34.0
85.82	44.0
86.70	49.0

TABLE F.10 Inlet Temperature = 33.96°C [Na <sub>2</sub> SO <sub>3</sub> ] = 0.88 M	
Maximum Temperature (°C)	Bath Temperature (°C)
50.89	19.0
68.47	24.0
80.69	34.0
87.93	44.0

TABLE F.11 Inlet Temperature = 40.75°C [Na <sub>2</sub> SO <sub>3</sub> ] = 0.88 M	
Maximum Temperature (°C)	Bath Temperature (°C)
66.73	19.0
83.83	24.0
92.13	34.0
98.77	44.0

TABLE F.12 Inlet Temperature = 39°C Bath Temperature = 44°C	
Maximum Temperature (°C)	[Na <sub>2</sub> SO <sub>3</sub> ] <sub>o</sub> (M)
98.77	0.88
87.38	0.78
75.52	0.68
68.59	0.58
62.41	0.48

TABLE F.13 Inlet Temperature = 48°C Bath Temperature = 24°C	
Maximum Temperature (°C)	[Na <sub>2</sub> SO <sub>3</sub> ] <sub>o</sub> (M)
95.06	0.88
86.68	0.78
69.22	0.68
59.75	0.58
54.13	0.48

TABLE F.14 Inlet Temperature = 46°C Bath Temperature = 34°C	
Maximum Temperature (°C)	[Na <sub>2</sub> SO <sub>3</sub> ] <sub>o</sub> (M)
100.46	0.88
88.85	0.78
75.62	0.68
66.83	0.58
58.90	0.48

The regression results are as follows :

Bath Temperature = 19.0°C; [Na<sub>2</sub>SO<sub>3</sub>] = 0.88 M

$$T_{\max} = 19.5 + 1.82 \cdot T_{\text{in}} - 0.0767 \cdot T_{\text{in}}^2 + 0.00147 \cdot T_{\text{in}}^3$$

$$T_{\text{inlet critical}} = 28.19 \text{ }^{\circ}\text{C}$$

Bath Temperature = 24.0°C; [Na<sub>2</sub>SO<sub>3</sub>] = 0.88 M

$$T_{\max} = 48.5 - 0.228 \cdot T_{\text{in}} + 0.000665 \cdot T_{\text{in}}^3$$

$$T_{\text{inlet critical}} = 24.81 \text{ }^{\circ}\text{C}$$

Bath Temperature = 34.0°C; [Na<sub>2</sub>SO<sub>3</sub>] = 0.88 M

$$T_{\max} = 30.7 - 2.05 \cdot T_{\text{in}} + 0.0834 \cdot T_{\text{in}}^2 - 0.000641 \cdot T_{\text{in}}^3$$

$$T_{\text{inlet critical}} = 26.20 \text{ }^{\circ}\text{C}$$



Bath Temperature = 44.0°C; [Na<sub>2</sub>SO<sub>3</sub>]<sub>o</sub> = 0.88 M

$$T_{\max} = 76.1 + 0.011 \cdot T_{\text{in}} - 0.0025 \cdot T_{\text{in}}^2 + 0.000387 \cdot T_{\text{in}}^3$$

$$T_{\text{inlet critical}} = 31.42 \text{ }^{\circ}\text{C}$$

Bath Temperature = 29.0°C; [Na<sub>2</sub>SO<sub>3</sub>] = 0.88 M

$$T_{\max} = 52.3 + 0.107 \cdot T_{\text{in}} + 0.000317 \cdot T_{\text{in}}^3$$

$$T_{\text{inlet critical}} = 30.64 \text{ }^{\circ}\text{C}$$

Inlet Temperature = 10.99°C; [Na<sub>2</sub>SO<sub>3</sub>]<sub>o</sub> = 0.88 M

$$T_{\max} = -34.0 + 4.28 \cdot T_{\text{bath}} - 0.0398 \cdot T_{\text{bath}}^3$$

$$T_{\text{bath critical}} = 41.21 \text{ }^{\circ}\text{C}$$

Inlet Temperature = 18.29°C; [Na<sub>2</sub>SO<sub>3</sub>]<sub>o</sub> = 0.88 M

$$T_{\max} = -15.2 + 2.82 \cdot T_{\text{bath}} - 0.000351 \cdot T_{\text{bath}}^3$$

$$T_{\text{bath critical}} = 41.57 \text{ }^{\circ}\text{C}$$

Inlet Temperature = 24.56°C; [Na<sub>2</sub>SO<sub>3</sub>]<sub>o</sub> = 0.88 M

$$T_{\max} = -0.41 + 2.26 \cdot T_{\text{bath}} - 0.000201 \cdot T_{\text{bath}}^3$$

$$T_{\text{bath critical}} = 45.71 \text{ }^{\circ}\text{C}$$

Inlet Temperature = 30.59°C; [Na<sub>2</sub>SO<sub>3</sub>]<sub>o</sub> = 0.88 M

$$T_{\max} = -12.6 + 3.23 \cdot T_{\text{bath}} - 0.000502 \cdot T_{\text{bath}}^3$$

$$T_{\text{bath critical}} = 38.48 \text{ }^{\circ}\text{C}$$

Inlet Temperature = 33.96°C;  $[\text{Na}_2\text{SO}_3]_0 = 0.88\text{M}$

$$T_{\max} = -6.6 + 3.35 \cdot T_{\text{bath}} - 0.000628 \cdot T_{\text{bath}}^3$$

$$T_{\text{bath critical}} = 35.3^\circ\text{C}$$

Inlet Temperature = 40.75°C;  $[\text{Na}_2\text{SO}_3]_0 = 0.88\text{ M}$

$$T_{\max} = 17.6 + 2.91 \cdot T_{\text{bath}} - 0.000557 \cdot T_{\text{bath}}^3$$

$$T_{\text{bath critical}} = 33.81^\circ\text{C}$$

For the following regressions, the inlet concentration was adjusted to  $C^* = 89 \cdot C_{\text{Ao}}$  so that the critical condition was defined by  $dT_m/dC^* = 1.0$

Inlet Temperature = 39°C; Bath Temperature = 44°C

$$T_{\max} = 63.3 - 0.604 \cdot C^* + 0.0135 \cdot C^{*2}$$

$$C_{\text{Ao critical}} = 0.667\text{ M}$$

Inlet Temperature = 48°C; Bath Temperature = 24°C

$$T_{\max} = 41.7 - 0.25 \cdot C^* + 0.0122 \cdot C^{*2}$$

$$C_{\text{Ao critical}} = 0.576\text{ M}$$

Inlet Temperature = 46°C; Bath Temperature = 34°C

$$T_{\max} = 43.9 - 0.107 \cdot C^* + 0.0106 \cdot C^{*2}$$

$$C_{\text{Ao critical}} = 0.587\text{ M}$$

NOTE  
 NOTE DETERMINING CRITICAL CONDITIONS  
 NOTE  
 NAME C1 'IN TEMP'  
 READ INTO C1  
 18.29  
 24.56  
 30.39  
 33.96  
 40.75  
 READ INTO C2  
 77.4  
 80.92  
 85.82  
 87.93  
 98.77  
 NAME C2 'MAX TEMP'  
 NAME C5 'IN SQ'  
 NAME C6 'IN CUB'  
 LET C5 = C1\*C1  
 LET C6 = C1\*C1\*C1  
 REGRESS C2 ON 3 C1 C5 C6 AND STORE ST.RESIDUALS IN C10 AND PRED Y  
 IN C11  
 PRINT C1 C5 C6 C2 C11 C10  
 REGRESS C2 ON 2 C1 C5 AND STORE ST.RESIDUALS IN C12 AND PRED IN C13  
 PRINT C1 C5 C2 C13 C12  
 STOP

## 2) Evaluation of the Criterion of Barkelew (1959)

Barkelew developed a sensitivity diagram based the following groupings.

$$N/S = \frac{4 \cdot U \cdot R \cdot T_c^2}{D \cdot \Delta H \cdot C_{Ao} \cdot C_{Bo} \cdot A \cdot \exp(-E_A / (R \cdot T_c)) \cdot E_A} \quad (F.1)$$

$$S = \frac{\Delta H \cdot C_{Ao} \cdot E_A}{C_p \cdot \rho \cdot R \cdot T_c^2} \quad (F.2)$$

The sensitivity diagrams were given in terms of N/S and S with  $\alpha$  and  $\tau_o$  as parameters. These parameters are:

$$\alpha = \frac{C_{Ao}}{C_{Bo}} = \frac{[Na_2SO_3]_o}{[H_2O_2]_o} \quad (F.3)$$

$$\tau_o = \frac{E_A \cdot (T_o - T_c)}{R \cdot T_c^2} \quad (F.4)$$

The only usable stability diagrams were for  $\tau_o = 0$ , thus the only conditions that could be studied were those where the inlet temperature was equal to the bath temperature. There were five such conditions ( $T = 19, 24, 29, 34$  and  $44^\circ\text{C}$ ). A sample calculation follows. A summary of the results is given in Table F.15.

### Sample Calculation

For  $T_{\text{inlet}} = T_{\text{bath}} = 19^{\circ}\text{C}$  and  $[\text{Na}_2\text{SO}_3]_o = 0.88 \text{ M}$  ( $[\text{H}_2\text{O}_2]_o = 2.31 \text{ M}$ )

$$\alpha = 0.88/2.31 = 0.38$$

$$\tau_o = 0$$

$$N/S = 1.31$$

$$S = 7.07$$

From the sensitivity diagram, the critical S value for  $N/S = 1.31$  is  $S = 15$ . Therefore, the prediction is that the system will be insensitive.

TABLE F.15 SUMMARY OF BARKELEW CRITERION ANALYSIS				
Inlet Conditions ( $T_o = T_c$ )	N/S	S	Barkelew's Prediction	Observed Figure 8.12
$T = 19^{\circ}\text{C}$ $[\text{Na}_2\text{SO}_3]_o = 0.88 \text{ M}$	1.31	7.07	Insensitive	Insensitive
$T = 24^{\circ}\text{C}$ $[\text{Na}_2\text{SO}_3]_o = 0.88 \text{ M}$	0.87	6.84	Sensitive	Insensitive
$T = 29^{\circ}\text{C}$ $[\text{Na}_2\text{SO}_3]_o = 0.88 \text{ M}$	0.59	6.61	Sensitive	Sensitive
$T = 34^{\circ}\text{C}$ $[\text{Na}_2\text{SO}_3]_o = 0.88 \text{ M}$	0.39	6.40	Sensitive	Sensitive
$T = 44^{\circ}\text{C}$ $[\text{Na}_2\text{SO}_3]_o = 0.88 \text{ M}$	0.19	6.00	Sensitive	Sensitive

2a) Barkelew's Criterion with  $T_o \neq T_c$  using the diagram of Butt (1960)

The parameter groupings remain the same, only the areas of sensitivity and insensitivity on the stability plots change. Also, an average value of the peroxide concentration must be used as the stability plot

is only valid for first order reactions.

$$\begin{aligned}\text{Thus the value of } C_B \text{ to be used for calculation} &= \sqrt{C_{Bo} \cdot C_{Bf}} \\ &= \sqrt{2.31 \cdot (2.31 - 0.88)} \\ &= 1.82 \text{ M}\end{aligned}$$

This value will of course change depending on the inlet sulfite concentration.

The results obtained are illustrated in Table F.16

TABLE F.16 SUMMARY OF BARKELEW CRITERION WITH $T_c \neq T_o$						
Inlet (°C)	Bath (°C)	$[\text{Na}_2\text{SO}_3]_o$ (M)	N/S	S	Prediction	Observed Figure 8.12
24.56	19.0	0.88	1.66	7.07	Insensitive	Insensitive
30.59	19.0	0.88	1.66	7.07	Sensitive	Sensitive
18.29	24.0	0.88	1.10	6.84	Sensitive	Insensitive
30.59	24.0	0.88	1.10	6.84	Sensitive	Sensitive
33.96	24.0	0.88	1.10	6.84	Sensitive	Sensitive
24.25	29.0	0.88	0.75	6.61	Sensitive	Insensitive
30.59	34.0	0.88	0.50	6.40	Sensitive	Sensitive
40.75	34.0	0.88	0.50	6.40	Sensitive	Sensitive
45.70	34.0	0.88	0.50	6.40	Sensitive	Sensitive
40.75	44.0	0.88	0.24	6.00	Sensitive	Sensitive
46.0	34.0	0.58	0.70	4.21	Sensitive	Insensitive
46.0	34.0	0.68	0.62	4.94	Sensitive	Sensitive
39.0	44.0	0.58	0.34	3.95	Sensitive	Insensitive
39.0	44.0	0.68	0.3	4.63	Sensitive	Sensitive

### 3) Evaluation of the Criteria of Van Welsenaere and Froment (1970)

A method was developed by Van Welsenaere and Froment to determine the maximum allowable inlet concentration (for insensitivity) for a given set of operating conditions. This method was only applicable for the case of  $T_o = T_c$ . In addition, this method was based on pseudo-first-order-kinetics. Since the conditions of the sulfite reaction were not pseudo-first-order, the concentration of the peroxide was assumed to be constant (at a value equal to the geometric mean of its initial and final values) for calculation purposes. A sample calculation and a summary of the results follows.

#### Sample Calculation

$$\begin{aligned}\text{Value of } C_B \text{ to be used for calculation} &= \sqrt{C_{Bo} \cdot C_{Bf}} \\ &= \sqrt{2.31 \cdot (2.31 - 0.88)} \\ &= 1.82 \text{ M}\end{aligned}$$

Defined groupings are

$$A = C_{Bo} \quad (F.5)$$

$$B = (\Delta H \cdot C_{Bo}) / (C_p \cdot \rho) \quad (F.6)$$

$$C = (2 \cdot U) / (C_p \cdot \rho \cdot r) \quad (F.7)$$

$$a = -E_A / R \quad (F.8)$$

$$b = \ln(A) \quad (F.9)$$



Maximum allowable  $C_{Ao}$  is the geometric mean of the following

$$(C_{Ao})_l = \frac{C \cdot T_{cr} \cdot T_{cr}}{a \cdot B \cdot \exp(-a/T_{cr} + b)} + \frac{A}{B} \cdot (T_{cr} - T_c) \quad (F.10)$$

$$(C_{Ao})_u = \frac{A}{B} \cdot (T_{cr} - T_c) \cdot \left( \left( \frac{A}{C} \cdot \exp(-a/T_{cr} + b) \right)^{-0.5} + 1 \right)^2 \quad (F.11)$$

$$\text{where } T_{cr} = 0.5 \cdot (a - \sqrt{a \cdot (a - 4T_c)}) \quad (F.12)$$

For  $T_c = 292$  ( $19^\circ\text{C}$ )

$T_{cr} = 304$  K (from F.12)

$(C_{Ao})_l = 698$  mol/m<sup>3</sup> (from F.10)

$(C_{Ao})_u = 1248$  mol/m<sup>3</sup> (from F.11)

Therefore, maximum allowable  $C_{Ao} = (698 \cdot 1248)^{0.5} = 933$  mol/m<sup>3</sup>

This then means that an inlet concentration of 0.88 M (880 mol/m<sup>3</sup>) would be insensitive

TABLE F.17 SUMMARY OF VAN WELSENARE AND FROMENT CRITERION ANALYSIS			
Inlet Conditions $T_o = T_c$	Maximum $C_{Ao}$ VanWelsenare	Prediction for $C_A = 0.88$ M	Observed From Fig 8.12
$T = 19^\circ\text{C}$	0.93 M	Insensitive	Insensitive
$T = 24^\circ\text{C}$	0.71 M	Sensitive	Insensitive
$T = 29^\circ\text{C}$	0.56 M	Sensitive	Sensitive
$T = 34^\circ\text{C}$	0.45 M	Sensitive	Sensitive
$T = 44^\circ\text{C}$	0.34 M	Sensitive	Sensitive

3a) Criterion of Van Welsenaere and Froment as applied to any kinetics and any set of inlet/bath temperatures

As defined by Van Welsenaere and Froment (1970), the critical trajectory is that which intersects the maxima curve at its maximum. Therefore, the maximum of the maxima curve must be found.

The equation describing the experimental plug flow reactor (based on the ODPH Model) is

$$\frac{dT}{dz} = B \cdot C_A \cdot (C_{Bo} - C_{Ao} + C_A) \cdot \exp(-E_A/(R \cdot T)) + D \cdot (T_c - T) \quad (F.13)$$

where

$$B = (\pi \cdot D_1^2 \cdot \Delta H \cdot A) / (4 \cdot Q \cdot \rho \cdot Cp) \quad (F.14)$$

and

$$D = (U \cdot \pi \cdot D_1) / (Q \cdot \rho \cdot Cp) \quad (F.15)$$

Thus, the maxima curve is defined by those points where

$$\frac{dT}{dz} = 0$$

or, from F.13

$$D \cdot (T_c - T_m) = -B \cdot C_{Am} \cdot (C_{Bo} - C_{Ao} + C_{Am}) \cdot \exp(-E_A/(R \cdot T_m)) \quad (F.16)$$

Solving for  $C_{Am}$  yields

$$C_{Am} = \frac{(C_{Ao} - C_{Bo})}{2} \pm \frac{[(C_{Bo} - C_{Ao})^2 - 4 \cdot D \cdot (T_c - T_m) \cdot \exp(-E_A/(R \cdot T_m)) / B]^{0.5}}{2} \quad (F.17)$$

The maximum of this curve occurs at  $dC_{Am}/dT_m = 0$ , therefore from F.17 the following is obtained:

$$T_{cr} = [a - \sqrt{a^2 - 4 \cdot a \cdot T_c}] / 2 \quad (F.18)$$

where  $a = -E_A/R$  as before

This is the same results as F.12.

The critical inlet concentration can be determined by assuming an adiabatic trajectory from the inlet of the reactor to the hot-spot.

The adiabatic relationship is given by

$$\Delta H \cdot (C_{Ao} - C_{Am}) / (C_p \cdot \rho) = (T_{cr} - T_o) \quad (F.19)$$

$C_{Am}$  can be substituted for using F.17 with  $T_m = T_{cr}$ . Upon substitution and rearranging of F.19, an explicit equation for  $C_{Ao}$ (critical) is obtained:

$$C_{Ao}(\text{critical}) = \frac{C_{Bo}^2 - K^{*2} - 4 \cdot D \cdot (T_c - T_{cr}) \cdot \exp(-E_A / (R \cdot T_{cr})) / B}{2 \cdot C_{Bo} - 2 \cdot K^*} \quad (F.20)$$

$$\text{where } K^* = 2 \cdot C_p \cdot \rho \cdot (T_{cr} - T_o) - C_{Bo} \quad (F.21)$$

Thus, for any given operating condition defined by  $\{T_o, T_c, C_{Bo}\}$ , equations F.18, F.20 and F.21 can be used to find  $C_{Ao}$ (critical).

### Sample Calculation

For  $T_c = 297$  K,  $T_o = 300$  K,  $C_{Bo} = 2.31$  M

$T_{cr} = 309$  K from F.18

From F.20 and F.21,  $C_{Ao}(\text{critical}) = 0.41 \text{ M}$

A list of the results obtained for all the experimental operating conditions can be found in Table F.18.

TABLE F.18 SUMMARY OF RESULTS USING VAN WELSENAERE AND FROMENT CRITERION AS APPLIED TO ALL EXPERIMENTAL OPERATING CONDITIONS				
Inlet (°C)	Bath (°C)	Critical $C_{Ao}$ (M)	Prediction for $C_A=0.88$ M	Observed Figure 8.12
10.99	19.0	0.72	Sensitive	Insensitive
18.29	19.0	0.61	Sensitive	Insensitive
24.56	19.0	0.53	Sensitive	Insensitive
30.59	19.0	0.45	Sensitive	Sensitive
33.96	19.0	0.40	Sensitive	Sensitive
40.75	19.0	0.31	Sensitive	Sensitive
45.70	19.0	0.25	Sensitive	Sensitive
47.71	19.0	0.22	Sensitive	Sensitive
10.99	24.0	0.62	Sensitive	Insensitive
18.29	24.0	0.53	Sensitive	Insensitive
24.56	24.0	0.45	Sensitive	Insensitive
30.59	24.0	0.37	Sensitive	Sensitive
33.96	24.0	0.33	Sensitive	Sensitive
40.75	24.0	0.24	Sensitive	Sensitive
45.70	24.0	0.18	Sensitive	Sensitive
47.71	24.0	0.15	Sensitive	Sensitive
11.08	29.0	0.57	Sensitive	Insensitive
17.4	29.0	0.5	Sensitive	Insensitive
24.25	29.0	0.41	Sensitive	Insensitive

**TABLE F.18 SUMMARY OF RESULTS USING VAN WELSENAERE AND FROMENT  
CRITERION (CONTINUED)**

<b>Inlet (°C)</b>	<b>Bath (°C)</b>	<b>Critical <math>C_{Ao}</math> (M)</b>	<b>Prediction for <math>C_A=0.88</math> M</b>	<b>Observed Figure 8.12</b>
29.96	29.0	0.35	Sensitive	Sensitive
10.99	34.0	0.57	Sensitive	Insensitive
18.29	34.0	0.48	Sensitive	Insensitive
24.56	34.0	0.41	Sensitive	Insensitive
30.59	34.0	0.34	Sensitive	Sensitive
33.96	34.0	0.29	Sensitive	Sensitive
40.75	34.0	0.21	Sensitive	Sensitive
45.70	34.0	0.15	Sensitive	Sensitive
10.99	44.0	0.62	Sensitive	Insensitive
18.29	44.0	0.53	Sensitive	Insensitive
24.56	44.0	0.46	Sensitive	Insensitive
30.59	44.0	0.39	Sensitive	Sensitive
33.96	44.0	0.35	Sensitive	Sensitive
40.75	44.0	0.27	Sensitive	Sensitive
12.33	49.0	0.64	Sensitive	Insensitive
18.19	49.0	0.57	Sensitive	Insensitive
25.35	49.0	0.49	Sensitive	Sensitive
30.59	49.0	0.43	Sensitive	Sensitive
48.4	24.0	0.14	Sensitive	Sensitive

TABLE F.18 SUMMARY OF RESULTS USING VAN WELSENAERE AND FROMENT CRITERION (CONTINUED)				
Inlet (°C)	Bath (°C)	Critical $C_{Ao}$ (M)	Prediction for $C_A=0.88$ M	Observed Figure 8.12
46.0	34.0	0.15	Sensitive	Sensitive
39.08	44.0	0.29	Sensitive	Sensitive

#### 4) Evaluation of the Criterion of Oroskar and Stern (1979)

The criteria developed by Oroskar and Stern was illustrated in the form of a sensitivity diagram. The parameter groupings were similar to those of Barkelew. However, the criteria was only valid for a 1st order reaction with  $T_o = T_c$ . Thus, a suitable value for the concentration of peroxide was needed for calculation purposes and, only those experiments with  $T_o = T_c$  could be examined. A sample calculation and summary of results follows.

##### Sample Calculation

Using the approximation applied previously

$$C_B = \text{constant} = (2.31 \cdot 1.43)^{0.5} = 1.82 \text{ M}$$

Since  $C_{Bo}$  does not appear explicitly in the parameter groupings, it will be factored in with the pre-exponential factor.

Defined groupings are

$$\alpha = \frac{\Delta H \cdot C_{Ao} \cdot E_A}{C_p \cdot \rho \cdot R \cdot T_c^2} \quad (\text{F.22})$$

$$\beta = \frac{4 \cdot U}{C_p \cdot \rho \cdot D \cdot A \cdot \exp(-E_A / (R \cdot T_c))} \quad (\text{F.23})$$

For the case of  $T_o = T_c = 292 \text{ K } (19^\circ\text{C})$

$\alpha = 7.07$  (from eq F.22)

$\beta = 11.79$  (from eq F.23)



from sensitivity d'agram, critical  $\alpha$  value for  $\beta = 11.79$  is 9.34.

Thus, these conditions are insensitive.

TABLE F.17 SUMMARY OF OROSKAR AND STERN CRITERION ANALYSIS				
Inlet Conditions ( $T_o = T_c$ )	$\alpha$	$\beta$	Prediction	Observed Figure 8.12
$T = 19^\circ\text{C}$ $[\text{Na}_2\text{SO}_3]_o = 0.88 \text{ M}$	7.07	11.8	Insensitive	Insensitive
$T = 24^\circ\text{C}$ $[\text{Na}_2\text{SO}_3]_o = 0.88 \text{ M}$	6.84	7.56	Insensitive	Insensitive
$T = 29^\circ\text{C}$ $[\text{Na}_2\text{SO}_3]_o = 0.88 \text{ M}$	6.61	4.93	Sensitive	Sensitive
$T = 34^\circ\text{C}$ $[\text{Na}_2\text{SO}_3]_o = 0.88 \text{ M}$	6.40	3.25	Sensitive	Sensitive
$T = 44^\circ\text{C}$ $[\text{Na}_2\text{SO}_3]_o = 0.88 \text{ M}$	6.00	1.47	Sensitive	Sensitive

### 5) Evaluation of the Criterion of Morbidelli and Varma (1982)

Morbidelli and Varma developed sensitivity diagrams with essentially the same parameter groupings as Oroskar and Stern. However, Morbidelli and Varma developed diagrams for various reaction orders, activation energies and dimensionless inlet temperatures. Unfortunately, the only diagrams available were for  $T_o = T_c$ , so once again the comparisons were limited to the experimental conditions where  $T_o = T_c$ . A sample calculation and a summary of the results follow.

#### Sample Calculation

Defined groupings are

$$\alpha = \frac{\Delta H \cdot C_{Ao} \cdot E_A}{C_p \cdot \rho \cdot R \cdot T_c^2} \quad (F.24)$$

$$\beta = \frac{4 \cdot U}{C_p \cdot \rho \cdot D \cdot A \cdot \exp(-E_A / (R \cdot T_c)) \cdot C_{Ao}^{n-1}} \quad (F.25)$$

$$\gamma = E_A / (R \cdot T_c) \quad (F.26)$$

$$\tau = (T - T_c) / (T_c \cdot \gamma) \quad (F.27)$$

However, the rate law is defined in the following way.

$$R_A = k \cdot C_{Ao} \cdot (1-X)^n \quad (F.28)$$

where  $X$  = conversion of  $A$

For the sulfite reaction the rate law is given by

$$R_A = k \cdot C_{Ao} \cdot C_{Bo} \cdot (1-X) \cdot (1-KX) \quad (F.29)$$

$$\text{where } K = C_{A0}/C_{B0} \quad (\text{F.30})$$

Therefore, an "average" reaction order must be used for calculation purposes. This can be found in the following fashion.

Set  $(1-X) \cdot (1-KX) = (1-X)^n$  and solve for  $n$  for various values of  $X$ .

For  $K=0.38$

X	n
0.01	1.38
0.2	1.35
0.4	1.32
0.6	1.28
0.8	1.22
0.99	1.10

Therefore, an average reaction order is

$$\frac{(1.38)+(1.35)+(1.32)+(1.28)+(1.22)+(1.10)}{6} = 1.28$$

For  $T_o=T_c = 292 \text{ K } (19^\circ\text{C})$

$\gamma = 26.36$  (from eq F.26)

$\alpha = 7.07$  (from eq F.24)

$\beta = 1.77$  (from eq F.25)

Unfortunately, diagrams only exist for  $\gamma=20$  and  $\gamma=\infty$ . Thus, we must interpolate between diagrams.

From the diagram, the critical  $\alpha = 6$  for  $\gamma=20$  and the critical  $\alpha = 5.5$  for  $\gamma=100$ .

Therefore, for  $\gamma=26.4$ , the prediction is that system will be sensitive.

TABLE F.18 SUMMARY OF MUFFIDELLI AND VARMA CRITERION ANALYSIS					
Inlet Conditions $T_o = T_c$	$\gamma$	$\alpha$	$\beta$	Prediction	Observed From Fig 8.12
$T=19^{\circ}\text{C}$ $[\text{Na}_2\text{SO}_3]_o=0.88$	26.4	7.07	1.77	Sensitive	Insensitive
$T=24^{\circ}\text{C}$ $[\text{Na}_2\text{SO}_3]_o=0.88$	25.9	6.84	1.13	Sensitive	Insensitive
$T=29^{\circ}\text{C}$ $[\text{Na}_2\text{SO}_3]_o=0.88$	25.4	6.61	0.74	Sensitive	Sensitive
$T=34^{\circ}\text{C}$ $[\text{Na}_2\text{SO}_3]_o=0.88$	25.1	6.40	0.48	Sensitive	Sensitive
$T=44^{\circ}\text{C}$ $[\text{Na}_2\text{SO}_3]_o=0.88$	24.3	6.00	0.22	Sensitive	Sensitive

## 6) Evaluation of the Criterion of Akella and Lee (1983)

Akella and Lee developed a method of analyzing parametric sensitivity in a reactor with the coolant flowing counter-currently (as in a tube and shell heat exchanger). This method, referred to as a "phase-plane analysis", involves constructing a diagram (inlet reactor temperature vs inlet coolant temperature) where the regions of insensitivity and sensitivity are marked out. The construction of such a diagram for the system under study is as follows.

Akella and Lee defined the following parameters

$$a_1 = \frac{\pi \cdot D^2 \cdot L}{4 \cdot Q \cdot C_{Ao}} \quad (F.31)$$

$$a_2 = \frac{\pi \cdot D^2 \cdot L \cdot \Delta H}{4 \cdot \rho \cdot C_p \cdot Q} \quad (F.32)$$

$$a_3 = \frac{\pi \cdot D \cdot L \cdot U}{Q \cdot \rho \cdot C_p} \quad (F.33)$$

$$a_4 = \frac{\pi \cdot D \cdot L \cdot U}{Q_c \cdot \rho_c \cdot C_{p_c}} \quad (F.34)$$

For the experimental conditions (with  $C_{Ao} = 0.88$  M;  $C_{Bo} = 1.82$  M (i.e., assuming an average value for pseudo-first-order approximation)) these become

$$a_1 = 1.61 \cdot 10^{-3} \quad (\text{from eq F.31})$$

$$a_2 = 0.125 \quad (\text{from eq F.32})$$

$$a_3 = 3.12 \quad (\text{from eq F.33})$$

$$a_4 = 0 \quad (\text{from eq F.34}) \quad \text{because coolant is isothermal}$$

Construction of diagram consists of four lines

- i) Feed Quench Line
- ii) Coolant Quench Line
- iii) Lateral Ignition Line
- iv) Upper Ignition Line

#### i) Feed Quench Line

This is an arbitrarily set value. Here it will be set at  $0^\circ\text{C}$  which is the minimum feed temperature (in order for the feed to still be liquid) possible.

Therefore  $T_o = 273 \text{ K}$

#### ii) Coolant Quench Line

The equation of this line is given by

$$T_f = T_o \cdot \exp(-a_3) + T_c \cdot (1 - \exp(-a_3)) \quad (\text{F.35})$$

where  $T_f$  is such that

$$a_1 \cdot C_{Ao} \cdot C_{Bo} \cdot A \cdot \exp(-E_A / (R \cdot T_f)) = 0.01 \quad (\text{F.36})$$

from eq F.36,  $T_f = 260.5$

Therefore from eq F.35  $T_c = 272.3 - 0.046 T_o \text{ K}$

#### iii) Lateral Ignition Line

This is given by

$$T_c = T^* - [a_2/a_3 \cdot A \cdot C_{Ao} \cdot C_{Bo} \cdot \exp(-E_A/(R \cdot T^*))] \quad (F.37)$$

such that

$$\frac{dT_c}{dT^*} = 0 \quad (F.38)$$

therefore, from eq F.37

$$\frac{dT_c}{dT^*} = 1 - d[a_2/a_3 \cdot A \cdot C_{Ao} \cdot C_{Bo} \cdot \exp(-E_A/(R \cdot T^*))]/dT^* \quad (F.39)$$

so, combining F.38 and F.39

$$A \cdot C_{Ao} \cdot C_{Bo} \cdot \exp(-E_A/(R \cdot T^*)) \cdot E_A/T^{*2} = a_3/a_2 \quad (F.40)$$

trial and error solution of F.40 yields  $T^* = 299$

therefore, from F.37

$T_c = 286.9 \text{ K}$

#### iv) Upper Ignition Line

This is defined by the set of points  $(T_c, T_o)$  such that

$$\left. \frac{dT}{dz} \right|_{z=0} > 0 \quad (F.41)$$

and

$$\left. \frac{d^2T}{dz^2} \right|_{z=0} > 0 \quad (F.42)$$

thus, for the system

$$a_2 \cdot A \cdot C_{Ao} \cdot C_{Bo} \cdot \exp(-E_A/(R \cdot T_o)) - a_3 \cdot (T_o - T_c) > 0 \quad \text{from eq F.41} \quad (F.43)$$

and

$$a_2 \cdot d[A \cdot C_{A0} \cdot C_{B0} \cdot \exp(-E_A/(R \cdot T_o))]/dz - a_3 \cdot dT_o/dz > 0 \text{ from eq F.42 (F.44)}$$

upon simplification and substitution these become

$$5.75 \cdot 10^{12} \cdot \exp(-7698/T_o) - 3.12 \cdot (T_o - T_c) > 0 \quad (\text{F.43a})$$

$$\{4.43 \cdot 10^{16}/T_o^2 \cdot \exp(-7698/T_o) - 3.12\} \cdot dT_o/dz > 0 \quad (\text{F.44a})$$

Equations F.43a and F.44a can be solved by assuming a value for  $T_c$  and finding the minimum value of  $T_o$  that satisfies both equations.

By trial and error, for  $T_c = 265$ ,  $T_o = 317$  K. Similarly

for  $T_c = 280$      $T_o = 310$

for  $T_c = 286.8$      $T_o = 300$

and for  $T_c = 258$      $T_o = 319$

Upper Ignition Line Defined By

$$(T_c, T_o) = \{ (258, 319), (265, 317), (280, 310), (286.8, 300) \}$$



## APPENDIX G

### Computer Programs for Data Acquisition

The programs used for the data acquisition (both parametric sensitivity experiments and adiabatic batch reactor experiments) are listed in this section.

```

C      PROGRAM TEMP3.FTN
C      PROGRAM USED FOR DATA ACQUISITION
C      DURING PARAMETRIC SENSITIVITY EXPERIMENTS
C      TIME INTERVAL OF SAMPLING IS APPROX 30 SECONDS
FTN7X
$FILES(4,4)
      PROGRAM TEMP3
      INTEGER TrimLen
      INTEGER CNVRTERR
      INTEGER DATA(32)
      INTEGER CHANIN(2)
      INTEGER IOS
      INTEGER*4 TimeNow
      LOGICAL IFBRK
      REAL TP
      REAL TC(22,10)
      REAL FG(22)
      CHARACTER*12 Out
      CHARACTER*100 IN2
      CHARACTER*28 TimeBuff
      CHARACTER*100 In
      CHARACTER*84 IN1
      CHARACTER*4 CHANREADING
      INTEGER*2 OutBuf(6), InBuff(40), OptoLu
      EQUIVALENCE (OutBuf(1), Out), (InBuff(1), In)
      EQUIVALENCE (CHANIN(1), CHANREADING)
      FG(1) = -0.16
      FG(2) = 0.00
      FG(3) = 0.18
      FG(4) = 0.08
      FG(5) = -0.08
      FG(6) = 0.26
      FG(7) = 0.00
      FG(8) = 0.00
      FG(9) = 1.30
      FG(10) = 0.37
      FG(11) = 0.18
      FG(12) = 0.00
      FG(13) = 0.00
      FG(14) = 0.55
      FG(15) = 0.18
      FG(16) = 1.00
      FG(17) = 1.00
      FG(18) = 0.00
      FG(19) = 0.78
      FG(20) = 0.37
      OPEN(6, FILE='OPT1')
      OPEN(7, FILE='OPT3')

```

```

      OptoLu = 23
C     OPEN(5,FILE='OPTODATA')
      Out = '>FEA'
      CALL CheckSum(Out,4,Out)
      Len = TrimLen(Out)
C     CALL DayTime(TimeNow(),TimeBuff)
      CALL EXEC(2,OptoLu + 100B,OutBuf,-Len)
D     CALL EXEC(2,1 + 100B,OutBuf,-Len)
D     WRITE(1,*)Out
100    FORMAT(A6)
      READ(OptoLu,'(A80)',iostat=IOS,ERR=77) In
      77    WRITE(1,100) In
      IF(IOS .NE. 0) WRITE(1,*) 'Error ',ios
C     Len = TrimLen(In)
C     IF(Len .GT. 2) Len = Len - 2
C     IF(len .EQ. 1) THEN
C       WRITE(1,*) In,' ',TimeBuff
C     ELSE
C       WRITE(1,*)In(2:Len),' ',TimeBuff
C     ENDIF
      CALL WAIT(15,1,Ierr)
      OUT = '>FFA'
      CALL CHECKSUM(OUT,4,OUT)
      LEN = TRIMLEN(OUT)
      CALL EXEC(2,OPTOLU + 100B,OUTBUF,-LEN)
      READ(OPTOLU,'(A80)',iostat=ios,err=177) IN
177    WRITE(1,100) IN
      IF(IOS .NE. 0) WRITE(1,*) 'Error ',ios
      CALL WAIT(15,1,IERR)
      OUT = '>FFHFFFF'
      CALL CHECKSUM(OUT,8,OUT)
      LEN = TRIMLEN(OUT)
      CALL DAYTIME(TIMENOW(),TIMEBUFF)
      CALL EXEC(2,OPTOLU + 100B,OUTBUF,-LEN)
      READ(OPTOLU,'(A80)',iostat=ios,err=277) IN
277    LEN = TRIMLEN(IN)
      IF(IOS .NE. 0) WRITE(1,*) 'Error ',ios
      IF(LEN.GT.2) LEN = LEN - 2
      IF(LEN.EQ.1) THEN
        WRITE(1,*) IN,' ',TIMEBUFF
      ELSE
        WRITE(1,*) IN(2:LEN),' ',TIMEBUFF
      END IF
      CALL WAIT(15,1,IERR)
      Out = '>FEHFFFF'
      CALL CheckSum(Out,8,Out)
      Len = TrimLen(Out)
      CALL DayTime(TimeNow(),TimeBuff)

```

```

        CALL EXEC(2,OptoLu + 100B,OutBuf,-Len)
D      CALL EXEC(2,1 + 100B,OutBuf,-Len)
D      WRITE(1,*)Out
      READ(OptoLu,'(A80)',iostat=ios,err=377) In
377   Len = TrimLen(In)
      IF(IOS .NE. 0) WRITE(1,*) 'Error ',ios
      IF(Len .GT. 2) Len = Len - 2
      IF(len .EQ. 1) THEN
        WRITE(1,*) In,' ',TimeBuff
      ELSE
        WRITE(1,*)In(2:Len),' ',TimeBuff
      ENDIF
      CALL WAIT(15,1,Ierr)
      WRITE(6,301)
301   FORMAT(1X,'THERMOCOUPLES 1-11')
302   FORMAT(1X,'THERMOCOUPLES 12-22')
      WRITE(7,302)
      DO 10 j=1,360
      CALL WAIT(5,2,IERR)
      IF(IFBRK()) GOTO 200
      Out = '>FELFFFF'
      CALL CheckSum(Out,4,Out)
      Len = TrimLen(Out)
      CALL DayTime(TimeNow(),TimeBuff)
      CALL EXEC(2,OptoLu + 100B,OutBuf,-Len)
D      CALL EXEC(2,1 + 100B,OutBuf,-Len)
D      WRITE(1,*)Out
      READ(OptoLu,'(A80)',iostat=ios,err=477) In
477   Len = TrimLen(In)
      IF(IOS .NE. 0) WRITE(1,*) 'Error ',ios
      LEN = LEN - 2
C      CLOSE(5)
      OUT= '>FFL003F'
      CALL CHECKSUM(OUT,4,OUT)
      LEN1=TRIMLEN(OUT)
      CALL EXEC(2,OPTOLU+100B,OUTBUF,-LEN1)
      READ(OPTOLU,'(A80)',iostat=ios,err=577) IN1
577   LEN1 = TRIMLEN(IN1)
      IF(IOS .NE. 0) WRITE(1,*) 'Error ',ios
      LEN1 = LEN1 - 2
      IN2 = IN1(42:65) // IN(2:65)
      WRITE(1,*)
      WRITE(1,*) TIMEBUFF
      DO 99 I = 1,88,4
        CHANREADING = IN2(I:I+3)
        IF (CHANREADING(1:1).EQ.'1') THEN
          CHANREADING(1:1) = '0'
        CALL HEXI(CHANIN,DATA((I/4)+1),4,CNVRTERR)

```

```

END IF
TP = REAL(DATA((I/4)+1))
IF(TP.GT.3901) THEN
  TP = (TP-3901)/194.*30. + 670.1
  ELSE IF(TP.GT.3743) THEN
    TP = (TP-3743)/59.*25 + 645.17
    ELSE IF(TP.GT.3464) THEN
      TP = (TP-3464)/279.*45. + 600.2
      ELSE IF(TP.GT.3191) THEN
        TP = (TP-3191)/272.*45. + 555.1
        ELSE IF(TP.GT.2895) THEN
          TP = (TP-2895)/296.*50. + 505.1
          ELSE IF(TP.GT.2546) THEN
            TP = (TP-2546)/349.*60. + 445.05
            ELSE IF(TP.GT.1766) THEN
              TP = (TP-1766)/780.*135. + 310.
              ELSE IF(TP.GT.867) THEN
                TP = (TP-867)/899.*155 + 155.1
                ELSE IF(TP.GT.551) THEN
                  TP = (TP-551)/316.*55 + 100.15
                  ELSE IF(TP.GT.354) THEN
                    TP = (TP-354)/197.*35. + 65.1
                    ELSE IF(TP.GT.161) THEN
                      TP = (TP-161)/193.*35. + 30.19
                      ELSE IF(TP.GT.0) THEN
                        TP = TP/161*30. + 0.1
                        ELSE TP = (TP-104)/140.*20. + 20.15
          ENDIF
NT = 23 - ((I/4)+1)
TC(NT,8) = TP + FG(NT)
99  CONTINUE
DO 50 II = 1,22
WRITE(1,500) II,(TC(II,JJ) , JJ=8,1,-1)
500  FORMAT(1X,'TC ',I2,' ',8F7.2)
50  CONTINUE
DO 55 II = 1,22
DO 56 JJ = 1,7
TC(II,JJ) = TC(II,JJ+1)
56  CONTINUE
55  CONTINUE
WRITE(6,300) (TC(JJ,8) , JJ=1,11)
300  FORMAT(1X,11F7.2)
WRITE(7,300) (TC(JJ,8) , JJ=12,22)
RIN = ((305.0*TC(17,8))+(75.0*TC(16,8)))/380.0
WRITE(1,*) 'BATH TEMP= ',TC(18,8),' AVG INLET = ',RIN
10  CONTINUE
200 CLOSE(6)
CLOSE(7)
END

```

```

C      PROGRAM TEMP4.FTN
C      PROGRAM USED FOR DATA ACQUISITION
C      DURING ADIABATIC BATCH REACTOR EXPERIMENTS
C      SAMPLING INTERVAL IS ONE SECOND

```

FTN7X

\$FILES(4,4)

```

PROGRAM TEMP4
INTEGER TrimLen
INTEGER CNVRTERR
INTEGER DATA(32)
INTEGER CHANIN(2)
INTEGER IOS
integer iyear
integer itimes(5)
INTEGER*4 TimeNow
LOGICAL IFBRK
REAL TP
REAL TC(22,10)
REAL FG(22)
CHARACTER*12 Out
CHARACTER*100 IN2
CHARACTER*28 TimeBuff
CHARACTER*100 In
CHARACTER*84 IN1
CHARACTER*4 CHANREADING
INTEGER*2 OutBuf(6), InBuff(40), OptoLu
EQUIVALENCE (OutBuf(1),Out),(InBuff(1),In)
EQUIVALENCE (CHANIN(1),CHANREADING)
FG(1) = -0.16
FG(2) = 0.00
FG(3) = 0.18
FG(4) = 0.08
FG(5) = -0.08
FG(6) = 0.26
FG(7) = 0.00
FG(8) = 0.00
FG(9) = 1.30
FG(10) = 0.37
FG(11) = 0.18
FG(12) = 0.00
FG(13) = 0.00
FG(14) = 0.55
FG(15) = 0.18
FG(16) = 1.00
FG(17) = 1.00
FG(18) = 0.00
FG(19) = 0.78
FG(20) = 0.37

```

```

OPEN(6, FILE='OPT1')
OPEN(7, FILE='OPT3')
OptoLu = 23
C OPEN(5, FILE='OPTODATA')
  Out = '>FEA'
  CALL CheckSum(Out, 4, Out)
  Len = TrimLen(Out)
C CALL DayTime(TimeNow(), TimeBuff)
  CALL EXEC(2, OptoLu + 100B, OutBuf, -Len)
D CALL EXEC(2, 1 + 100B, OutBuf, -Len)
D WRITE(1, *) Out
100 FORMAT(A6)
  READ(OptoLu, '(A80)', iostat=IOS, ERR=77) In
  77 WRITE(1, 100) In
    IF(IOS .NE. 0) WRITE(1, *) 'Error ', ios
    CALL WAIT(15, 1, IERR)
    OUT = '>FFA'
    CALL CHECKSUM(OUT, 4, OUT)
    LEN = TRIMLEN(OUT)
    CALL EXEC(2, OPTOLU + 100B, OUTBUF, -LEN)
    READ(OPTOLU, '(A80)', iostat=ios, err=177) IN
  177 WRITE(1, 100) IN
    IF(IOS .NE. 0) WRITE(1, *) 'Error ', ios
    CALL WAIT(15, 1, IERR)
    OUT = '>FFHFFFF'
    CALL CHECKSUM(OUT, 8, OUT)
    LEN = TRIMLEN(OUT)
    CALL DAYTIME(TIMENOW(), TIMEBUFF)
    CALL EXEC(2, OPTOLU + 100B, OUTBUF, -LEN)
    READ(OPTOLU, '(A80)', iostat=ios, err=277) IN
  277 LEN = TRIMLEN(IN)
    IF(IOS .NE. 0) WRITE(1, *) 'Error ', ios
    IF(LEN.GT.2) LEN = LEN - 2
    IF(LEN.EQ.1) THEN
      WRITE(1, *) IN, ' ', TIMEBUFF
    ELSE
      WRITE(1, *) IN(2:LEN), ' ', TIMEBUFF
    END IF
    CALL WAIT(15, 1, IERR)
    Out = '>FEHFFFF'
    CALL CheckSum(Out, 8, Out)
    Len = TrimLen(Out)
    CALL DayTime(TimeNow(), TimeBuff)
    CALL EXEC(2, OptoLu + 100B, OutBuf, -Len)
D CALL EXEC(2, 1 + 100B, OutBuf, -Len)
D WRITE(1, *) Out
  READ(OptoLu, '(A80)', iostat=ios, err=377) In
  377 Len = TrimLen(In)

```

```

IF(IOS .NE. 0) WRITE(1,*) 'Error ',ios
IF(Len .GT. 2) Len = Len - 2
IF(len .EQ. 1) THEN
  WRITE(1,*) In,' ',TimeBuff
ELSE
  WRITE(1,*)In(2:Len),' ',TimeBuff
ENDIF
CALL WAIT(15,1,Ierr)
WRITE(6,301)
301 FORMAT(1X,'THERMOCOUPLES 1-11')
302 FORMAT(1X,'THERMOCOUPLES 12-22')
WRITE(7,302)
DO 10 J=1,3600
  call exec(11,itimes,iyear)
  write(6,910) iyear,(itimes(nn),nn=5,1,-1)
910 format(' Time ',14,':',13,3(':',12),'.',12)
  CALL WAIT(500,1,IERR)
  IF(IFBRK()) GOTO 200
  Out = '>FELFFFF'
  CALL CheckSum(Out,4,Out)
  Len = TrimLen(Out)
  CALL DayTime(TimeNow(),TimeBuff)
  CALL EXEC(2,OptoLu + 100B,OutBuf,-Len)
D   CALL EXEC(2,1 + 100B,OutBuf,-Len)
D   WRITE(1,*)Out
  READ(OptoLu,'(A80)',iostat=ios,err=477) In
477 Len = TrimLen(In)
  IF(IOS .NE. 0) WRITE(1,*) 'Error ',ios
  LEN = LEN - 2
C   CLOSE(5)
  OUT= '>FFL003F'
  CALL CHECKSUM(OUT,4,OUT)
  LEN1=TRIMLEN(OUT)
  CALL EXEC(2,OPTOLU+100B,OUTBUF,-LEN1)
  READ(OPTOLU,'(A80)',iostat=ios,err=577) IN1
577 LEN1 = TRIMLEN(IN1)
  IF(IOS .NE. 0) WRITE(1,*) 'Error ',ios
  LEN1 = LEN1 - 2
  IN2 = IN1(42:65) // IN(2:65)
  DO 99 I = 1,88,4
    CHANREADING = IN2(I:I+3)
    IF (CHANREADING(1:1).EQ.'1') THEN
      CHANREADING(1:1) = '0'
    CALL HEXI(CHANIN,DATA((I/4)+1),4,CNVRTERR)
  END IF
  TP = REAL(DATA((I/4)+1))
  IF(TP.GT.3901) THEN
    TP = (TP-3901)/194.*30. + 670.1

```



```

ELSE IF(TP.GT.3743) THEN
  TP = (TP-3743)/59.*25 + 645.17
ELSE IF(TP.GT.3464) THEN
  TP = (TP-3464)/279.*45. + 600.2
ELSE IF(TP.GT.3191) THEN
  TP = (TP-3191)/272.*45. + 555.1
ELSE IF(TP.GT.2895) THEN
  TP = (TP-2895)/296.*50. + 505.1
ELSE IF(TP.GT.2546) THEN
  TP = (TP-2546)/349.*60. + 445.05
ELSE IF(TP.GT.1766) THEN
  TP = (TP-1766)/780.*135. + 310.
ELSE IF(TP.GT.867) THEN
  TP = (TP-867)/899.*155 + 155.1
ELSE IF(TP.GT.551) THEN
  TP = (TP-551)/316.*55 + 100.15
ELSE IF(TP.GT.354) THEN
  TP = (TP-354)/197.*35. + 65.1
ELSE IF(TP.GT.161) THEN
  TP = (TP-161)/193.*35. + 30.19
ELSE IF(TP.GT.0) THEN
  TP = TP/161*30. + 0.1
ELSE TP = (TP-104)/140.*20. + 20.15
ENDIF
NT = 23 - ((I/4)+1)
TC(NT,8) = TP + FG(NT)
99  CONTINUE
    GOTO 51
    DO 50 II = 1,22
      WRITE(1,500) II,(TC(II,JJ) , JJ=8,1,-1)
500  FORMAT(1X,'TC ',I2,' ',8F7.2)
50  CONTINUE
51  CONTINUE
    DO 55 II = 1,22
      DO 56 JJ = 1,7
        TC(II,JJ) = TC(II,JJ+1)
56  CONTINUE
55  CONTINUE
      WRITE(6,300) (TC(JJ,8) , JJ=1,11)
300  FORMAT(1X,11F7.2)
      WRITE(7,300) (TC(JJ,8) , JJ=12,22)
      RIN = ((305.0*TC(17,8))+(75.0*TC(16,8)))/380.0
C   WRITE(1,*) 'BATH TEMP= ',TC(18,8),' AVG INLET = ',RIN
      WRITE(1,*) TC(13,8)
10  CONTINUE
200 CLOSE(6)
    CLOSE(7)
    END

```